

INFORMATION TO USERS

The most advanced technology has been used to photograph and reproduce this manuscript from the microfilm master. UMI films the text directly from the original or copy submitted. Thus, some thesis and dissertation copies are in typewriter face, while others may be from any type of computer printer.

The quality of this reproduction is dependent upon the quality of the copy submitted. Broken or indistinct print, colored or poor quality illustrations and photographs, print bleedthrough, substandard margins, and improper alignment can adversely affect reproduction.

In the unlikely event that the author did not send UMI a complete manuscript and there are missing pages, these will be noted. Also, if unauthorized copyright material had to be removed, a note will indicate the deletion.

Oversize materials (e.g., maps, drawings, charts) are reproduced by sectioning the original, beginning at the upper left-hand corner and continuing from left to right in equal sections with small overlaps. Each original is also photographed in one exposure and is included in reduced form at the back of the book. These are also available as one exposure on a standard 35mm slide or as a 17" x 23" black and white photographic print for an additional charge.

Photographs included in the original manuscript have been reproduced xerographically in this copy. Higher quality 6" x 9" black and white photographic prints are available for any photographs or illustrations appearing in this copy for an additional charge. Contact UMI directly to order.

U·M·I

University Microfilms International
A Bell & Howell Information Company
300 North Zeeb Road, Ann Arbor, MI 48106-1346 USA
313/761-4700 800/521-0600

Order Number 9012807

**Sedimentology and structural geology of the Endicott Mountains
allochthon, central Brooks Range, Alaska**

Handschy, James William, Ph.D.

Rice University, 1989

U·M·I

**300 N. Zeeb Rd.
Ann Arbor, MI 48106**

RICE UNIVERSITY

SEDIMENTOLOGY AND STRUCTURAL GEOLOGY OF THE
ENDICOTT MOUNTAINS ALLOCHTHON,
CENTRAL BROOKS RANGE, ALASKA

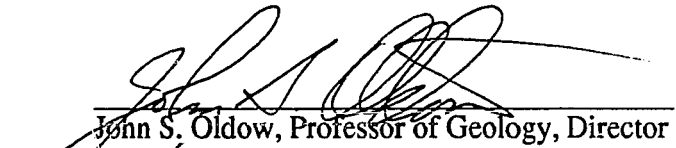
by

JAMES WILLIAM HANDSCHY

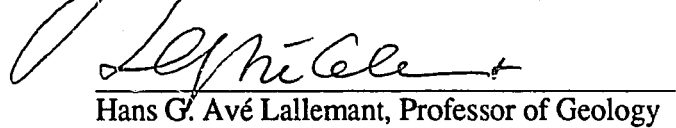
A THESIS SUBMITTED
IN PARTIAL FULFILLMENT OF THE
REQUIREMENTS FOR THE DEGREE

DOCTOR OF PHILOSOPHY


APPROVED, THESIS COMMITTEE:



John S. Oldow, Professor of Geology, Director



Hans G. Avé Lallemant, Professor of Geology



Rex B. McLellan, Professor of Material Science



Albert W. Bally, Professor of Geology

Houston, Texas

June, 1988

ABSTRACT

Sedimentology and structural geology of the Endicott Mountains allochthon,
central Brooks Range, Alaska

by

James W. Handschy

The Endicott Mountains allochthon is an east-west striking stack of north-northwest vergent thrust sheets which were emplaced during late Mesozoic and Cenozoic (Brookian) orogenesis. Thrust sheets in the allochthon are composed of clastic and carbonate rocks which track the progressive evolution of a Late Devonian and Early Carboniferous continental margin. Sedimentary facies in lower Upper Devonian rocks of the Beaucoup Formation delimit a volcanically active depositional basin. Volcaniclastic sediments within the Beaucoup were apparently derived from the south; whereas siliciclastic sediments were derived from the north. By the late Late Devonian, the Beaucoup depositional basin had developed into a south-facing continental margin. Southwestward progradation of the Kanayut-Hunt Fork delta system deposited thick conglomerates, sandstones, and shales on the margin and created a lithofacies pattern in which the Kanayut Conglomerate is thicker in the north and the Hunt Fork Shale is thicker in the south. Transgression of the Lower Mississippian Kayak Shale over the Kanayut Conglomerate occurred as sea level rose during the Early Mississippian. Subsequent transgressive-regressive cycles in carbonates of the Lisburne Group indicate that the margin had evolved into a stable passive margin by the middle Mississippian.

The style of Brookian structures in the Endicott Mountains allochthon changes from imbricate thrust sheets and large single-phase folds in the north to a thick, variably strained thrust nappe in the south. Strain variation in the southern nappe is evidenced by a progressive change from single-phase folds at the top of the nappe to polyphase folds at the bottom. First phase fold axes change from strike-parallel at the top of the nappe to dip-parallel at the bottom, and the angle between first phase axial planes and the basal

thrust decreases with depth. The change from thrust imbrication in the north to heterogeneous intranappe strain in the south apparently was controlled by the distribution of sedimentary facies and the extent of tectonic burial. The greater thickness of Kanayut Conglomerate and lack of a superjacent thrust sheet favored thrust imbrication in the north; whereas the greater proportion of shale and tectonic burial beneath the Skajit allochthon favored heterogeneous intranappe deformation in the south. Changes in fold orientation, the number of superposed fold phases, and measured strain in the southern nappe indicate that deformation was facilitated by a combination of layer parallel shortening and simple shear in a collapsing shear zone.

ACKNOWLEDGEMENTS

This study is part of a geologic transect through the central Brooks Range which was funded by the U.S. Department of Energy, grant number DE-AS05-83ER13124, the National Science Foundation, grant number EAR-8517384, and the Rice University Alaska Industrial Associates Program. Members of the Alaska Industrial Associates are: Amoco Production Company, Arco Exploration Company, Chevron, U.S.A. Inc., Gulf Oil Company, Mobil Exploration and Producing Services, Inc., and Standard Production Company. The Alyeska Pipeline Company provided helicopter and logistical support.

Discussions with John S. Oldow, Hans Avé Lallemant, A.W. Bally, Mike Seidensticker, Betsy Julian, Jim Phelps, Rick Gottschalk, Kent Boler, Wes Wallace (University of Alaska at Fairbanks and John Dillon (Alaska Department of Geological and Geophysical Surveys) greatly improved my understanding of Brooks Range geology. Larry Guth wrote many of the computer programs used to process data for this thesis. Hans Avé Lallemant and Larry Guth also provided insights about the relationships between folding and strain. Bob Guthrie and Ken Hewlett assisted with field work. David Stone and Lorraine Wolf (both at the University of Alaska at Fairbanks) helped with logistical problems.

Special thanks go to John S. Oldow for the criticism, guidance, and inspiration that I often needed during this study. Most of all, I thank my wife, Karen, and my parents for their constant support and encouragement during all of my geologic endeavors.

	TABLE OF CONTENTS	iv
Abstract		i
Acknowledgements		iii
Table of Contents		iv
List of Figures		vii
List of Tables		viii
List of Plates		ix
Preface		x
Chapter 1	Late Devonian and Early Mississippian sedimentology of the Endicott Mountains allochthon, central Brooks Range, Alaska	1
	Abstract	1
	Introduction	1
	Regional stratigraphy and previous work	2
	Structural setting	4
	Stratigraphy and depositional environments	8
	Kayak Shale and Kekiktuk Conglomerate	8
	Kanayut Conglomerate and Hunt Fork Shale	19
	Beaucoup Formation	31
	Sequence stratigraphy	34
	Provenance	39
	Paleogeographic Implications	43
	Conclusions	53
Chapter 2	Strain Variation in the Endicott Mountains allochthon, central Brooks Range, Alaska, U.S.A.	54
	Abstract	54
	Introduction	55
	Stratigraphy	56

	v
Beaucoup Formation	57
Kanayut Conglomerate and Hunt Fork Shale	57
Structural relations	62
Structural domains	62
Fold style and cleavage	71
Thrust faults	74
Boudinage	77
Strain indicators	78
Structural analysis	85
Controls on structural style	85
Relative timing of intranappe deformation	87
Strain factorization	91
Discussion	102
Fold reorientation and strain	102
Implications for cross section balancing	103
Lateral strain variations	107
Conclusions	108
References	110
Appendix 1 Measured stratigraphic sections	120
Appendix 2 Point count data	135
Appendix 3 Lower-hemisphere stereographic plots of structural data	138
Appendix 4 Strain analysis	157

LIST OF FIGURES

Figure 1.1	Location map	3
Figure 1.2	Tectonostratigraphic map and balanced cross section, central Brooks Range	5
Figure 1.3	General stratigraphy of the Endicott Mountains allochthon	9
Figure 1.4	Stratigraphy of the Kayak Shale and Kekiktuk Conglomerate	10
Figure 1.5	Facies map and cross sections, southern Endicott Mountains allochthon	12
Figure 1.6	Stratigraphy of the Kanayut Conglomerate	20
Figure 1.7	Block diagram showing depositional facies in the Kanayut-Hunt Fork delta system	22
Figure 1.8	Paleocurrent directions	26
Figure 1.9	Stratigraphy of the Hunt Fork Shale	27
Figure 1.10	Stratigraphy of the upper Beaucoup Formation	33
Figure 1.11	Unconformities	35
Figure 1.12	Late Devonian sea level curves	37
Figure 1.13	Sandstone compositions	40
Figure 1.14	Plate tectonic cross sections	44
Figure 1.15	Paleogeography of the Kanayut - Hunt Fork delta system	46
Figure 2.1	Geologic maps and cross sections	
	a) Map of southern Endicott Mountains allochthon	59
	b) Cross sections	60
	c) Map and cross section of the northern Endicott Mountains allochthon	61
Figure 2.2	Structural domains of the Endicott Mountains allochthon	
	a) Domain map	63
	b) Stereographic plots of structural data	65
Figure 2.3	Cross section showing D1 fold style	67
Figure 2.4	Photos and sketches of structural relations	69

Figure 2.5	Regional map of the Amawk thrust along the margins of the Doonerak duplex	76
Figure 2.6	Stereographic plot of stretching lineations	79
Figure 2.7	Volume changes	83
Figure 2.8	Graphs of depth related changes in fold orientation and style	88
Figure 2.9	Fold axis reorientation	
	a) Contoured stereographic plots of D1 fold axes	89
	b) K-value vs. depth plot	90
Figure 2-10	Relations between shear angle, the orientation of the strain ellipse, and strain axes	92
Figure 2.11	Palinspastic reconstructions illustrating the sequence of deformation of the Endicott Mountains allochthon	95
Figure 2.12	Geometric models for polyphase folding	97
Figure 2.13	R_s vs. θ' plot	98
Figure 2.14	Schematic vertical section through the southern nappe of the Endicott Mountains allochthon	100
Figure 2.15	Spatial and temporal relations of deformational phases	101
Figure 2.16	Deformation by a combination of simple shear and pure shear	105
Figure 2.17	Balanced cross section model incorporating intranappe strain	106

LIST OF TABLES

Table 1.1	Fossils identified in the Hunt Fork Shale and Beaucoup Formation	14
Table 1.2	Lithofacies codes for the Kanayut Conglomerate	21
Table 1.3	Grain parameters	41
Table 2.1	Fold characteristics	72
Table 2.2	Measured and estimated strain	81

LIST OF PLATES

- | | |
|---------|--|
| Plate 1 | Facies map and fossil localities, southern Endicott Mountains allochthon |
| Plate 2 | Geologic map of the Southern Endicott Mountains Allochthon |
| Plate 3 | Near-surface cross sections, southern Endicott Mountains allochthon |
| Plate 4 | Geologic map and near-surface cross sections, northern Endicott Mountains allochthon |
-

PREFACE

This thesis is written in the form of two publication ready manuscripts. Each manuscript is a separate chapter. Although each manuscript is unique and covers a different topic, this format necessitates some redundancy of introductory material. Data, which is summarized graphically in the text, is presented in the appendices. The folded plates are full-size versions of maps presented in reduced form in the text.

Chapter 1

Sedimentology and stratigraphy of Upper Devonian and Lower Mississippian clastic rocks, Endicott Mountains allochthon, central Brooks Range, Alaska

ABSTRACT

Upper Devonian and Lower Mississippian rocks exposed in the Endicott Mountains allochthon of the central Brooks Range track the progressive evolution of a Late Devonian and Early Carboniferous continental margin. Sedimentary facies in lower Upper Devonian rocks of the Beaucoup Formation delimit a volcanically active depositional basin, possibly related to a convergent arc system or an active rift. Volcaniclastic sediments within the Beaucoup Formation were apparently derived from the south; whereas nonvolcanic sediments were derived from the north. By the late Late Devonian, the Beaucoup depositional basin had developed into a south-facing continental margin. Southwestward progradation of the Upper Devonian Kanayut Conglomerate - Hunt Fork Shale deltaic system deposited thick conglomerates, sandstones, and shales on the margin and created a lithofacies pattern in which the Kanayut Conglomerate is thicker in the north and the Hunt Fork Shale is thicker in the south. Transgression of the Lower Mississippian Kayak Shale over the Kanayut Conglomerate occurred during the first major rise in Mississippian sea level. Subsequent transgressive-regressive cycles in carbonates of the Lisburne Group indicate that the margin had evolved into a stable passive margin by the middle Mississippian.

INTRODUCTION

The Endicott Mountains allochthon is part of a large structural sheet that constitutes

much of the northern, non-metamorphic, part of the late Mesozoic and Cenozoic Brooks Range fold-thrust belt in Arctic Alaska (Fig. 1.1). The allochthon is comprised of an east-west striking stack of north-northwest vergent thrust sheets composed predominantly of Upper Devonian and Lower Carboniferous clastic and carbonate rocks of the Endicott and Lisburne Groups (Brosge et al., 1962; Tailleux et al., 1967; Brosge et al., 1979, etc.). Typically, thrust nappes in the allochthon only expose the upper part of the Endicott Group and the lower part of the Lisburne Group. However, in the central Brooks Range, uplift and folding of the Endicott Mountains allochthon by the Doonerak duplex (Oldow et al., 1987; Mull et al., 1987) has exposed the entire Endicott Group and a significant part of the underlying Beaucoup Formation.

Regional Stratigraphy and Previous Work

The Endicott Group was named for exposures in the Endicott Mountains of the central Brooks Range and, in its type area, includes the Kayak Shale, Kanayut Conglomerate, and Hunt Fork Shale (Tailleux et al., 1967). Bowsher and Dutro (1957) described the type sections of the Kanayut Conglomerate and Kayak Shale at Shainin Lake (Fig. 1.1) and Chapman et al. (1964) defined the type section of the Hunt Fork Shale 100 km farther west near the Killik river. In the western Brooks Range, and locally in the central Brooks Range, the Endicott Group also includes the Noatak Sandstone which lies between the Hunt Fork and Kanayut (Tailleux et al., 1967). In the northeastern Brooks Range and along the margins of the Doonerak window, where the Kanayut Conglomerate and Hunt Fork Shale are absent due to non-deposition, the Endicott Group is composed of the Kekiktuk Conglomerate and the Kayak Shale (Armstrong et al., 1976; Brosge et al., 1962).

The basal contact of the Endicott Group is a disconformity(?) which separates the Hunt Fork Shale from mixed clastics and carbonates of the Beaucoup Formation (Tailleux et al., 1967). The type section of the Beaucoup Formation is located on the northeast side of

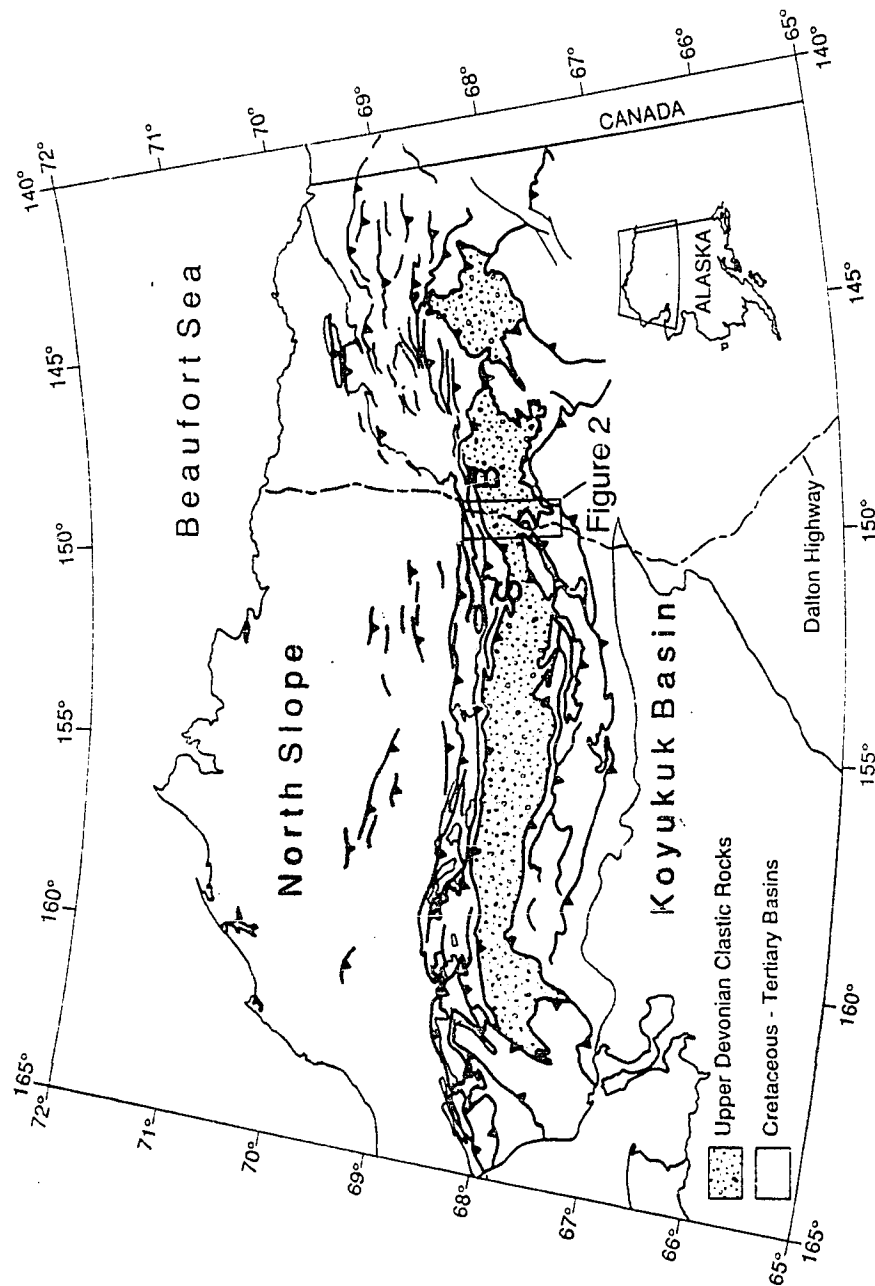


Figure 1.1 - Location map of northern Alaska showing the Brooks Range fold-thrust belt, the distribution of Devonian clastic rocks of the Endicott Mountains and equivalent allochthons, Cretaceous syntectonic basins, and the location of Figure 1.2. The Dalton Highway, Shainin Lake (S), and Beaucoup Creek (B) are shown for reference.

Beaucoup Creek approximately 100 km east of the study area (Fig. 1.1; Dutro et al., 1979). The contact between Kayak Shale, at the top of the Endicott Group, and the basal limestone of the Lisburne Group is gradational (Armstrong and Mamet, 1978).

Aside from the preliminary work listed above, the only detailed study of Late Devonian stratigraphy in the Brooks Range is a regional analysis of the Kanayut Conglomerate by Nilsen and Moore (1984; Moore and Nilsen, 1984; Nilsen and Moore, 1982a; Nilsen and Moore, 1982b; Nilsen et al., 1982; Nilsen, 1981; Nilsen et al., 1981a; Nilsen et al., 1981b; Nilsen et al., 1980a; Nilsen et al., 1980b). This study compliments the work of Nilsen and Moore by focusing on marine and transitional marine facies distribution in the Kanayut-Hunt Fork clastic wedge, depositional relationships between the Hunt Fork Shale and Beaucoup Formation, and the significance of Upper Devonian and Lower Mississippian sequence boundaries in the central Brooks Range.

Sedimentary facies, paleocurrents, and provenance indicate a northern siliciclastic source for the Kanayut and Hunt Fork. Clastics in the Beaucoup were apparently derived from both a northern siliciclastic source and a southern volcanic source. Age and compositional similarities between the Beaucoup, at the bottom of the Endicott Mountains allochthon, and mixed carbonates and clastics in the superjacent Skajit allochthon (Oldow et al., 1987; Dillon et al., 1987a) provide a tentative stratigraphic tie between the two allochthons. Paleogeographic reconstructions based on these facies relations in the central Brooks Range, balanced cross sections through the central Brooks Range (Oldow et al., 1987), and facies in the western and southern Brooks Range suggest that the tectonic setting of sedimentation changed from a continental or intra-arc rift basin in the early Late Devonian, to a rifted continental margin in the latest Devonian and earliest Mississippian, and eventually to a passive margin by the middle Mississippian.

Structural Setting

The structural geology of the central Brooks Range is dominated by a series of

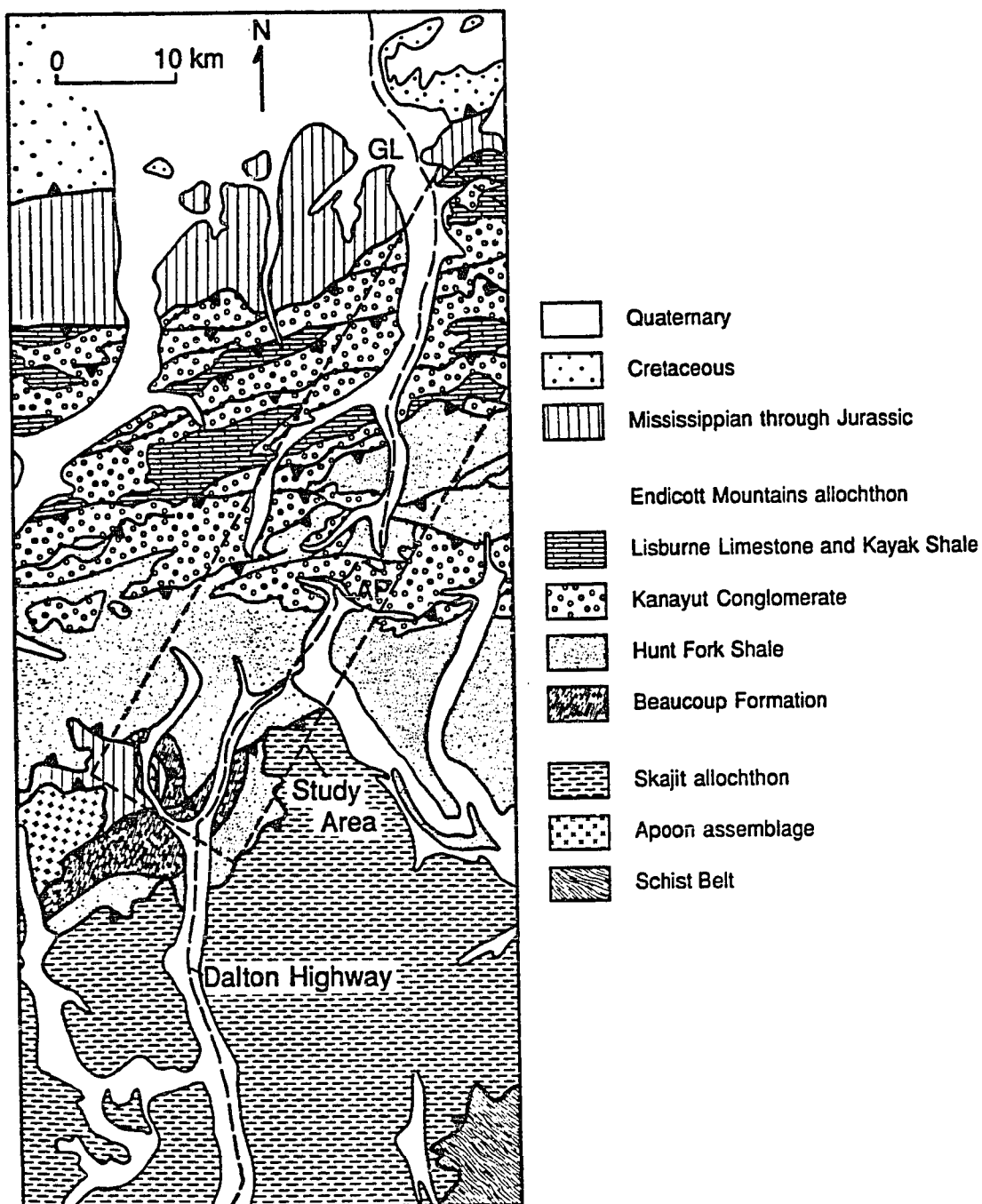
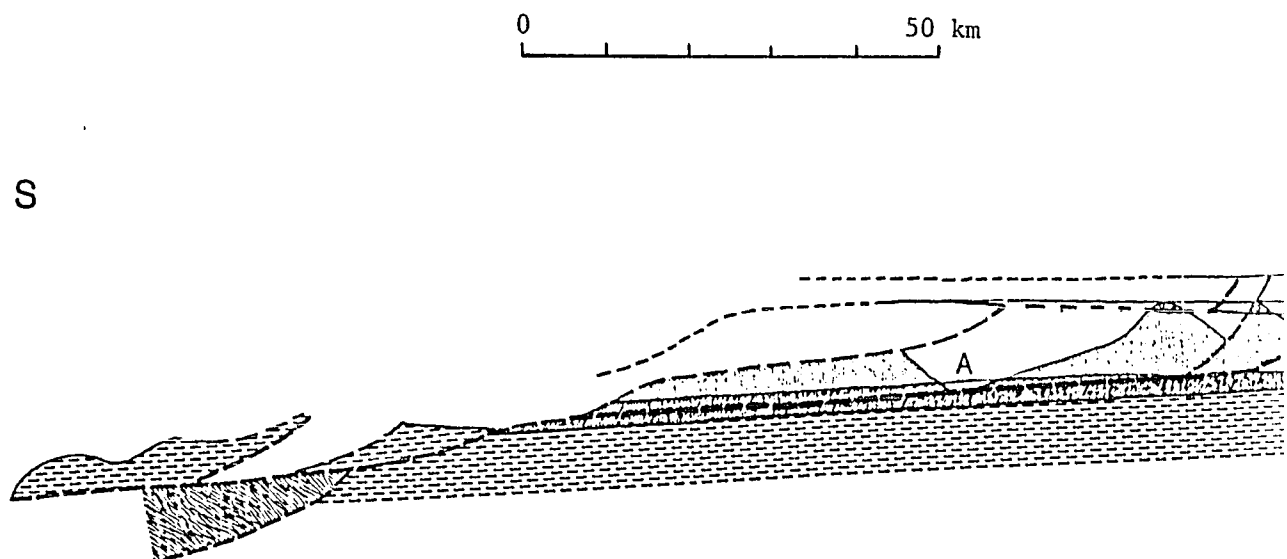
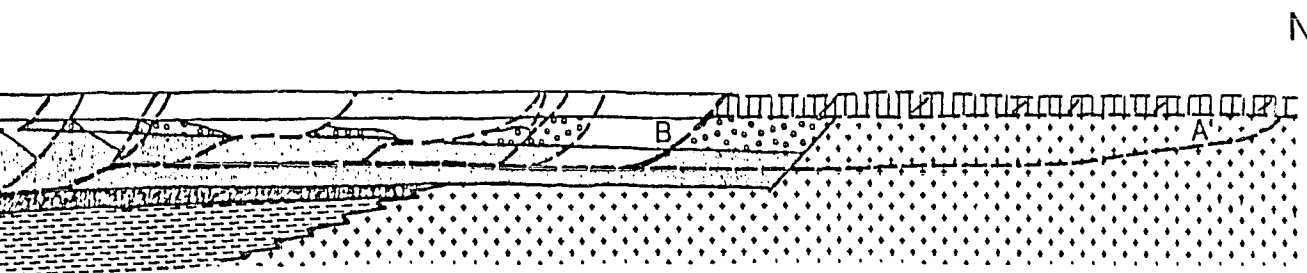
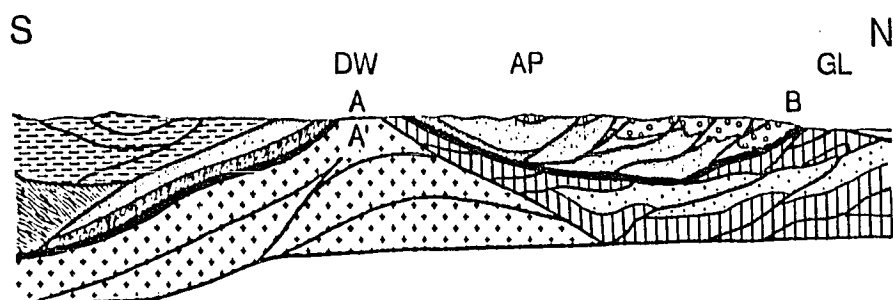


Figure 1.2a - Location map of the study area and the surrounding tectonostratigraphic units in the central Brooks Range. The locations of Galbraith Lakes (GL) and Atigun Pass (AP) are shown for reference.

Figure 1.2b - Balanced cross section through the study area. Structures in the Cretaceous and Carboniferous through Jurassic beneath the Endicott Mountains allochthon, and the structures in the Apoon assemblage are taken from Oldow et al. (1987). A, A', and B are reference points to help the reader understand the reconstruction. *Note:* In the restored section, the part of the section north of the Doonerak window is not shown. Also, only the preserved parts of the section are patterned, material that is missing because of erosion is not patterned.





north-vergent thrust sheets. Adjacent to the study area (Fig. 1.2a), these thrust sheets are grouped into five structural packages on the basis of position, internal stratigraphy, and degree of metamorphism (Oldow et al., 1987). The Endicott Mountains allochthon, which is central to this study, structurally overlies an allochthonous, internally imbricated, sequence of Kayak Shale, Lisburne Group carbonates, and Permian through Jurassic clastics along the front of the Brooks Range and along the northern margin of the Doonerak window (Fig. 1.2a; Oldow et al., 1987; Mull, 1982; Mull et al., 1987; Seidensticker, 1986). At the front of the Brooks Range, the Carboniferous through Jurassic rocks are thrust over Cretaceous foredeep deposits; whereas in the Doonerak window they structurally overlie duplexed phyllitic shales, volcanoclastics, and metavolcanic rocks of the Cambrian through Silurian Apoon assemblage (Fig. 1.2b; Armstrong et al., 1976; Dutro et al., 1976; Julian et al., 1984; Julian, 1986; Oldow et al., 1984; Oldow et al., 1987; Seidensticker, 1986). On the south side of the Doonerak window, the Endicott Mountains allochthon is in thrust contact with the Apoon assemblage, and is structurally overlain by internally imbricated, weakly metamorphosed carbonates and clastics of the Precambrian(?) through Late Devonian Skajit allochthon (Fig. 1.2; Oldow et al., 1987; Phelps 1987). Farther to the southeast, the Endicott Mountains allochthon is structurally overlain by both the Skajit allochthon and rocks of the schist belt (Fig 2; Oldow et al., 1987). The age(s) of the protoliths of the schist belt are poorly constrained, but deformed granitic plutons within the Schist Belt have yielded Devonian ages (Dillon et al., 1980; Dillon et al., 1987).

The present structural position of the Endicott Mountains allochthon is the product of: 1) northward translation of the allochthon, and; 2) duplexing of the Apoon assemblage beneath the allochthon (Fig. 1.2b; Oldow et al., 1987; Mull et al., 1987). Balanced cross sections (Oldow et al., 1987) and facies reconstructions (Mull et al., 1987) indicate that

the Endicott Mountains allochthon was originally located south of the Apoon assemblage (Fig. 1.2b). North-directed thrusting of the Endicott Mountains allochthon placed Upper Devonian rocks at the base of the allochthon over the Carboniferous through Jurassic sequence which overlies the Apoon assemblage in the Doonerak window (Dutro et al., 1976; Mull, 1982). Duplexing of the Apoon assemblage beneath the Carboniferous through Jurassic sequence was accompanied by detachment of the Carboniferous section from the Apoon (Seidensticker, 1976; Seidensticker et al., 1987; Oldow et al., 1987), and folded the overlying stack of thrust sheets into an anticlinorium (Fig. 1.2b).

Most of this study is based on detailed examination of outcrops in the southern Endicott Mountains allochthon on the north flank of the Doonerak duplex (Fig. 1.5) and reconnaissance work in the northern thrust imbricates of the allochthon (Fig. 1.2).

STRATIGRAPHY AND DEPOSITIONAL ENVIRONMENTS

Five stratigraphic units are exposed in thrust sheets of the Endicott Mountains allochthon adjacent to the Dalton Highway between the northeastern corner of the Doonerak duplex and Galbraith Lakes (Fig. 1.2a). From top to bottom, these five units represent three depositional sequences: 1) transgressive sandstones and shales, and progradational carbonates of the Lower Mississippian Kayak Shale and middle Mississippian through Lower Pennsylvanian Lisburne Limestone; 2) progradational shales, sandstones, and conglomerates of the Upper Devonian and lowest Mississippian(?) Kanayut Conglomerate and Hunt Fork Shale, and; 3) mixed carbonates and clastics of the Upper Devonian Beaucoup Formation (Fig. 1.3).

Kayak Shale and Kekiktuk Conglomerate

The Mississippian Kayak Shale is exposed beneath the Endicott Mountains allochthon along the flanks of the Doonerak duplex (Fig. 1.5), at the top of the southern thrust nappe of the Endicott Mountains allochthon (Fig. 1.5), and in several thrust sheets in the northern part of the allochthon. Balanced cross sections through the central Brooks Range

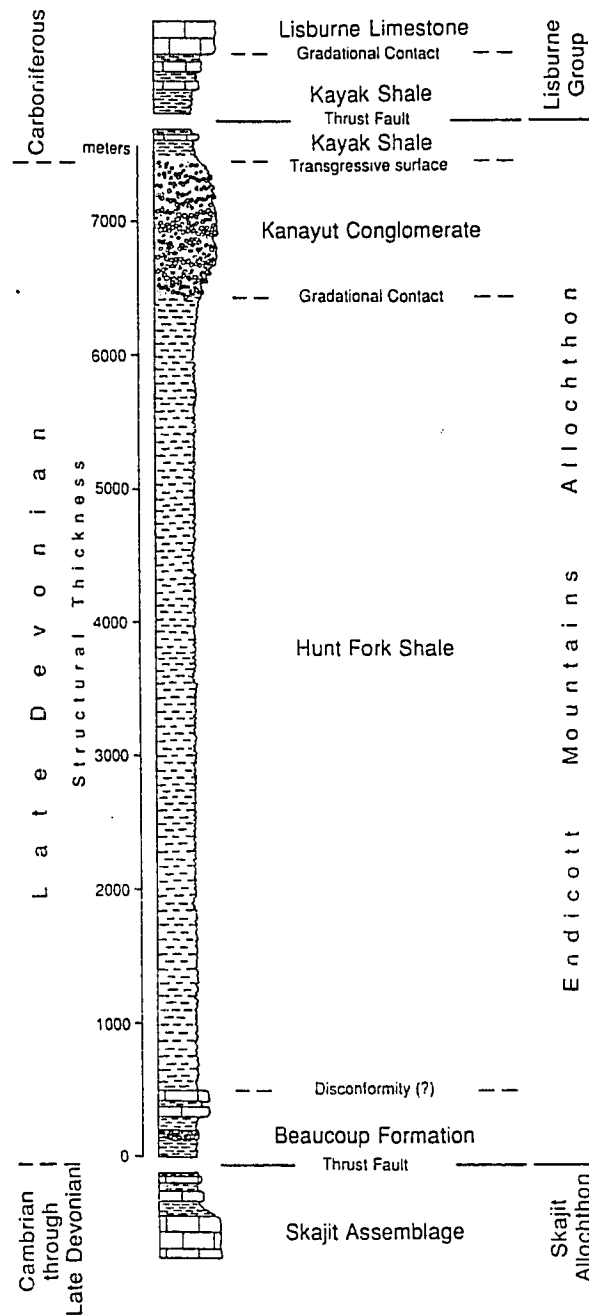


Figure 1.3 - General stratigraphy of the the Endicott Mountains allochthon. Note that the vertical scale is tectonic thickness. The Hunt Fork and Beaucoup are internally deformed and their stratigraphic thicknesses are unknown. The stratigraphic thickness of the Kanayut varies from 1 km in the southern thrust nappe (illustrated) to over 2.6 km in the northern imbricates of the allochthon.

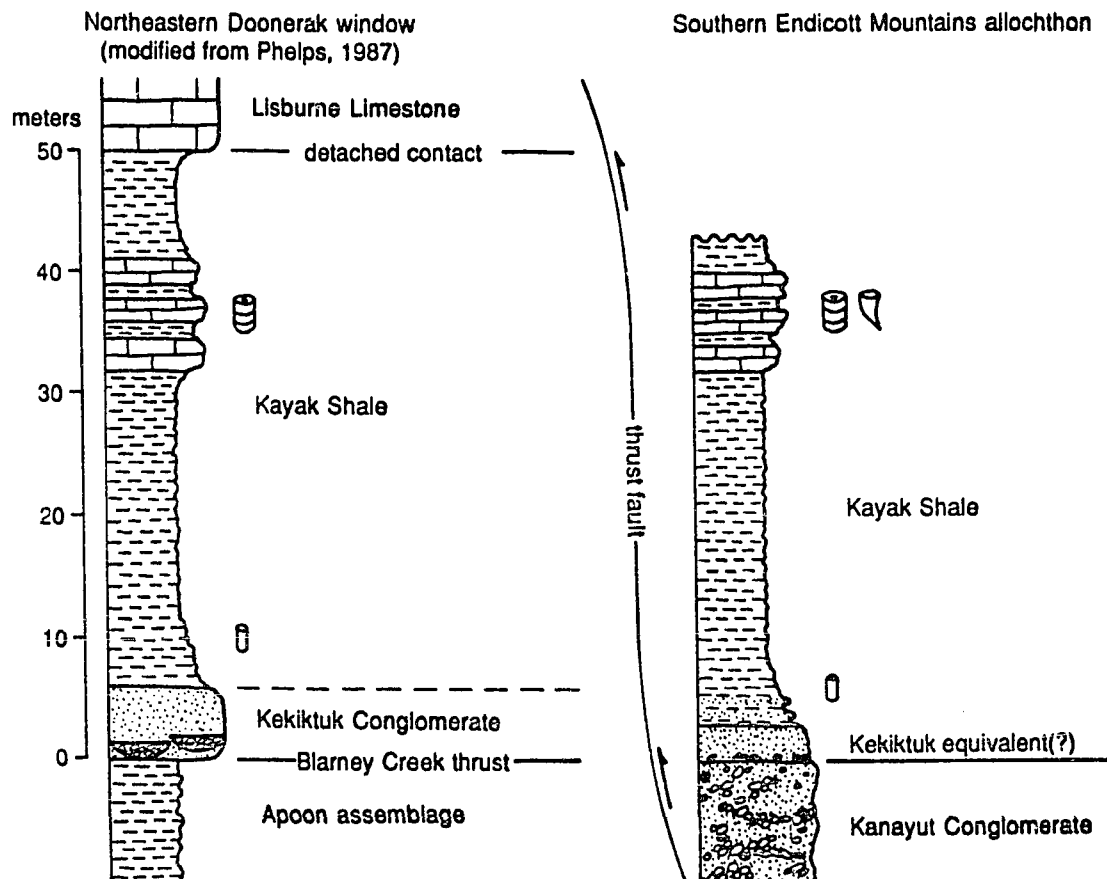


Figure 1.4 - Stratigraphy of the Kayak Shale and Kekiktuk Conglomerate. a) Northeastern Doonerak window (modified from Phelps, 1987). b) Southern Endicott Mountains allochthon. Section locations shown on Figure 1.5.

(Fig. 1.2b; Oldow et al., 1987) indicate that the original distribution of the Kayak Shale was such that the section in the northeastern Doonerak window was located approximately 150 km north of the southern Endicott Mountains allochthon section, with the northern Endicott Mountains sections located at intermediate positions. Despite this initial separation, the sections in the Doonerak window and the southern Endicott Mountains are very similar.

In the northeastern Doonerak window, the Kayak Shale is gradationally underlain by the Kekiktuk Conglomerate and is overlain by the Lisburne Limestone (Fig. 1.4a). Its age is constrained by early Viséan (Late Mississippian) microfossils at the base of the Lisburne Limestone on Mount Doonerak, 30 km west of the study area, and by middle Tournaisian (Early Mississippian) microfossils 1 m above the base of the Kayak Shale exposed along Amawk Creek, 15 km west of the study area (Armstrong et al., 1976).

In the section measured along Kuyuktuvuk Creek (Figs. 4a and 5), disharmonic folds across the contact between the Kekiktuk Conglomerate and phyllites of the underlying Apoon assemblage (Julian et al., 1984; Julian, 1986; Phelps, 1987) indicate that the two units are separated by a detachment surface (Fig. 1.4a). The age of the Apoon assemblage is inferred to be Cambrian through Silurian on the basis of Middle Cambrian trilobites in the western part of the Doonerak duplex (Dutro et al., 1984; Palmer et al., 1984), correlation to the Neruokpuk Formation in the northeastern Brooks Range (Dutro et al., 1976; Moore and Churkin, 1984), and correlation to lower Paleozoic rocks beneath the Skajit Limestone in the south-central Brooks Range (Dillon et al., 1987a).

Massive to trough cross-stratified chert pebble conglomerate at the base of the Kekiktuk grades upward into massive, moderate- to well-sorted, coarse- to fine-grained quartz arenite immediately below the Kayak Shale (Fig. 1.4a). The basal part of the Kayak is composed of interlayered sandstone, siltstone, and mottled shale (Phelps, 1987). Above the mottled shale, the Kayak is dominated by black shale. The transition into the

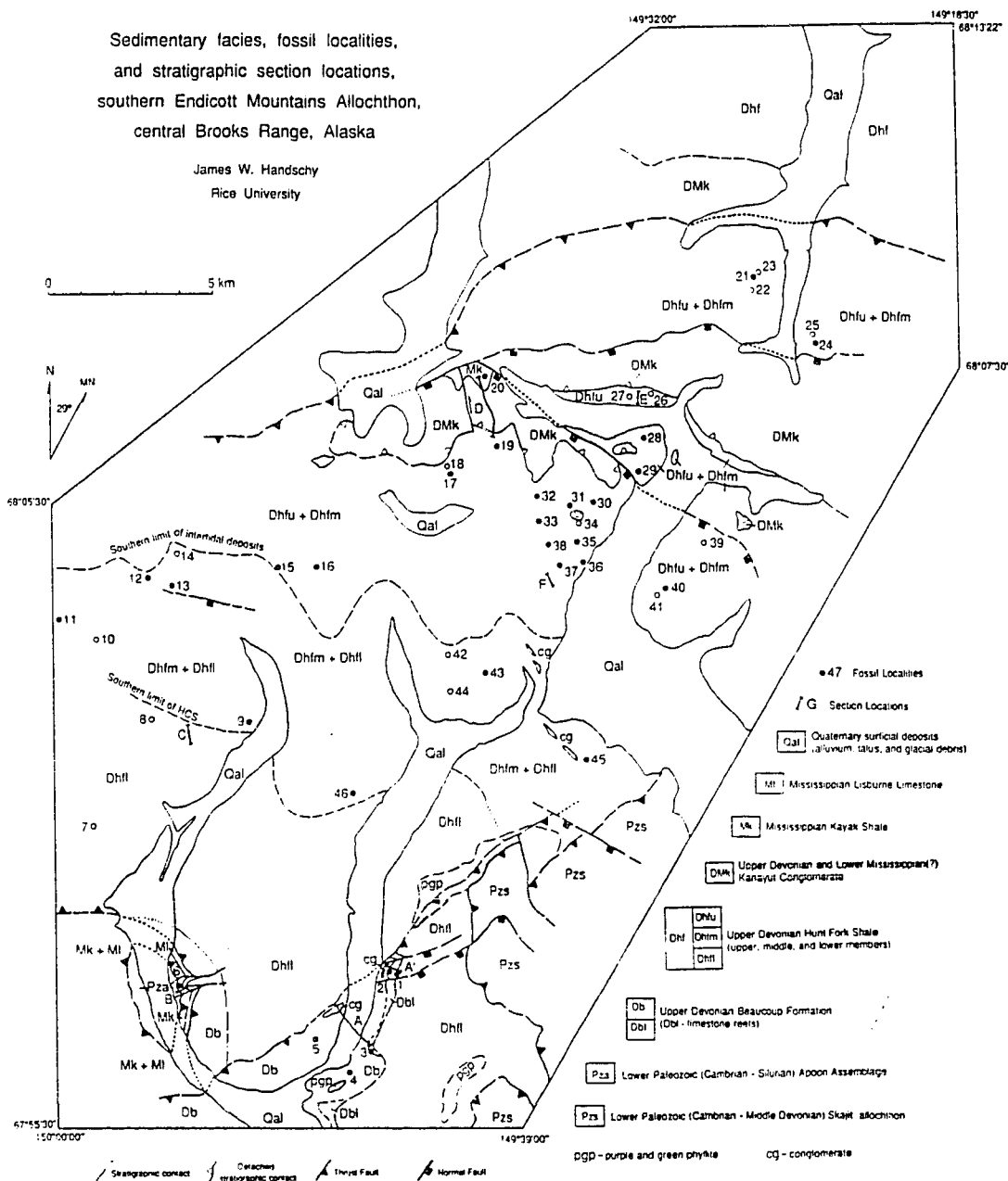


Figure 1.5a - Geologic map of the southern Endicott Mountains allochthon showing fossil localities and the locations of measured stratigraphic sections. Fossils are listed by locality number in Table 1.1. Stratigraphic section locations: A and A' - Beaucoup Formation (Fig. 1.10), B - Kayak Shale (Fig. 1.4a); C - lower Hunt Fork Shale (Fig. 1.9); D - Kayak Shale (Fig. 1.4b) and Kanayut Conglomerate (Fig. 1.6a); E - upper Hunt Fork Shale (Fig. 1.9); F - middle Hunt Fork Shale (Fig. 1.9).

Table 1.1 - Fossil assemblages in the southern Endicott Mountains allochthon. Localities correspond to Figure 1.5. All fossils in this table were collected and identified by the author. Three localities, #1, #9 and #40 are near fossil localities identified by other authors. Dbl* near Middle to early Late Devonian Phacelloid rugose coral locality (Dillon et al., 1987, location 24). Dhfm† near Frasnian (early Late Devonian) brachiopod and coral localities (Brosgé et al., 1979, locations 147, 148, 163). References used for fossil identification: Moore (1953; 1956; 1965); Moore, Lalicker, and Fischer (1952); Shimer and Shrock (1944); Tasch (1980); Warren and Stelck (1956).

Location	Unit	Brachiopods	Corals	Bryozoans	Miscellaneous	Trace Fossils
1	Db1*		Syringopora sp. Hexagonaria sp.(?) Tabulophyllum sp.(?) unidentified zaphrentids (colonial and solitary)	Fenestrellina sp.(?)		
2	Db1		Syringopora sp. unidentified zaphrentids (colonial and solitary)		stromatoporoids(?) crinoids	
3	Db1		Syringopora sp.			
4	Db (shale)	unidentified spirifer fragments				
5	Db (shale)	unidentified spirifer fragments				
6	Mk				crinoid fragments	
7	Dh1l					Planolites
8	Dn1l					Chondrites
9	Dh1m†					
10	Dh1m		unidentified rugose fragments			Skolithos Ichnofacies
11	Dh1m	unidentified spirifer fragments	Favosites sp.			
12	Dh1m	Cryptospirifer sp. Eleutherokomma sp.(?) Atrypa sp.				Chondrites
13	Dh1m				Manticoceras sp.(?) ammonite	
14	Dh1m					plant impressions
15	Dh1u	Centronella sp.(?) and/or Gypidula sp.(?) terebratulids				
16	Dh1m	Regelia sp.	Coenites sp.			
17	Dh1u	unidentified terebratulid fragments			algal rip-up clasts	
18	Dh1u					Skolithos Ichnofacies

19	Dhfm(?)	unidentified spirifer fragments			
20	Mk		unidentified rugose corals	crinoid fragments	
21	Dhfm(?)	unidentified spirifer fragments	Favosites sp.	Fenestrellina sp.	algal rip-up clasts and oncolites
22	Dhfu				Skolithos Ichnofacies
23	Dhfu				Cruziana Ichnofacies
24	Dhfm	unidentified spirifer fragments			Skolithos Ichnofacies
25	Dhfu(?)				Skolithos Ichnofacies
26	Dhfu				Skolithos Ichnofacies
27	Dhfu				Skolithos Ichnofacies
28	Dhfm	Theodossia sp. (?) Productella sp.(?) fragments Atrypa sp.			Cruziana Ichnofacies
29	Dhfm				Chondrites
30	Dhfm	Eleutherokomma sp. Cryptospirifer sp.(?)	Coenites sp. Favosites sp.	Berenicea sp. Fenestrella sp.	algal rip-up clasts and oncolites crinoid fragments planispiral gastropod fragments
31	Dhfm	Atrypa sp.(?) fragments Schizophoria sp.(?) fragments			
32	Dhfm	Atrypa sp. Cryptospirifer sp.	Favosites sp. Coenites sp.	Acanthoclema sp.	algal rip-up clasts and oncolites
33	Dhfm	Cryptospirifer sp.	Favosites sp.		algal rip-up clasts and oncolites crinoid fragments
34	Dhfm				plant impressions
35	Dhfm	Atrypa sp. Cryptospirifer sp.	Favosites sp. Coenites sp.	Acanthoclema sp.	algal rip-up clasts and oncolites
36	Dhfm	Cryptospirifer sp.	Favosites sp.		algal rip-up clasts planispiral and turreted gastropods
37	Dhfm	Atrypa sp. Eleutherokomma sp.(?)	Favosites sp.	Fenestrellina sp.	turreted gastropods oncolites

38	Dh/m	Atrypa sp. Cryptospirifer sp.	Favosites sp.	algal rip-up clasts and oncolites
39	Dh/m			Skolithos Ichnofacies
40	Dh/m†	unidentified spirifer fragments	Coenites sp.	Skolithos Ichnofacies
41	Dh/m			Chondrites
42	Dh/m			
43	Dh/m		Zaphrentis sp(?)	Cruziana Ichnofacies
44	Dh/m			
45	Dh/m	unidentified spirifer fragments		Planolites

overlying Lisburne Limestone is marked by the appearance of crinoidal limestone beds approximately 30 m above the uppermost Kekiktuk sandstone bed.

The Kayak Shale in the southern Endicott Mountains allochthon differs from that of the northeastern Doonerak window in that it overlies the Upper Devonian and Lower Mississippian(?) Kanayut Conglomerate instead of the Mississippian Kekiktuk Conglomerate and lower Paleozoic Apoon assemblage (Fig. 1.4). Famennian (late Late Devonian) brachiopods and Early Mississippian(?) plant fossils in the upper Kanayut (Moore and Nilsen, 1984), and Tournaisian foraminifera in the basal Lisburne Limestone (Armstrong et al., 1970) restrict the age of the Kayak in the Endicott Mountains allochthon to Tournaisian.

At the base of the Kayak, a 2 m thick interval of massive, horizontally laminated and ripple cross-laminated, well-sorted, fine-grained quartz arenite depositionally overlies a thin (<10 cm) pebble lag that appears to be reworked from the underlying Kanayut Conglomerate. This quartz arenite interfingers with thinly-laminated, bioturbated black shale. The highest sandstone bed (>1 cm) is located approximately 4.5 m above the top of the Kanayut Conglomerate. Black shales dominate the next 22.5 m of section. 27.0 m above the top of the Kanayut, black shale is interbedded with a 7.5 m thick interval of medium- to dark-gray argillaceous limestone containing abundant crinoid fragments and rugose corals. These limestone beds are, in turn, overlain by 5.0 m of thinly laminated black shale (Fig. 1.4). The uppermost Kayak is missing due to erosion.

Both the Kekiktuk Conglomerate in the northeastern Doonerak window and the quartz arenite at the base of the Kayak Shale in the southern Endicott Mountains allochthon appear to be transgressive beach deposits. Poorly sorted, trough cross-stratified fluvial and paralic(?) conglomerates are overlain by thin, horizontally laminated to ripple cross-laminated, well-sorted, quartz-rich sandstones which, in turn, grade upward into shallow marine shales and carbonates. The disappearance of sandstone interbeds in the

overlying Kayak Shale indicates continued deepening and a transition to off-shore deposition. Cyclical shale and limestone interbeds in the upper Kayak Shale and lower Lisburne Limestone indicate changes in the relative amounts of carbonate production and terrigenous sediment influx and may reflect high frequency sea level fluctuations and/or variations in clastic sediment influx.

Kanayut Conglomerate and Hunt Fork Shale

The Kanayut Conglomerate and Hunt Fork Shale are, respectively, the fluvial and marine parts of a large Late Devonian through Early Mississippian(?) fluvio-deltaic depositional system which is exposed in thrust sheets of the Endicott Mountains and related allochthons for approximately 950 km along the crest of the Brooks Range (Fig. 1.1; see also, Moore and Nilsen, 1984). Measured stratigraphic thicknesses of Kanayut in the study area vary from approximately 1 km in the southern nappe to over 2.6 km in the northern thrust imbricates (Fig. 1.6), reflecting southwestward thinning of the Kanayut Conglomerate over the Hunt Fork Shale (Fig. 1.7). The age of the Kanayut-Hunt Fork system is constrained by Famennian brachiopods and Early Mississippian(?) plant fragments in the upper Kanayut (Moore and Nilsen, 1984), and Frasnian (early Late Devonian) brachiopods and corals in the lower Hunt Fork (Dutro et al., 1979; Brosgé et al., 1979).

Regionally, the Kanayut is divided into the Ear Peak, Shainin Lake, and Stuver Members, in ascending order (Fig. 1.6). The Stuver and Ear Peak Members generally consist of multiple fining-upward cycles and, at a regional scale, are interpreted as meandering river deposits by Nilsen and Moore (1984; Moore and Nilsen, 1984). The intervening Shainin Lake Member is more conglomeratic than the other two members and is interpreted as a braided river deposit (Moore and Nilsen, 1984). In the study area, all three members are dominated by conglomerate and sandstone beds, and appear to have been deposited primarily by braided river systems. Where all three members can be distinguished, maximum and average clast sizes are larger in the Shainin Lake Member, and

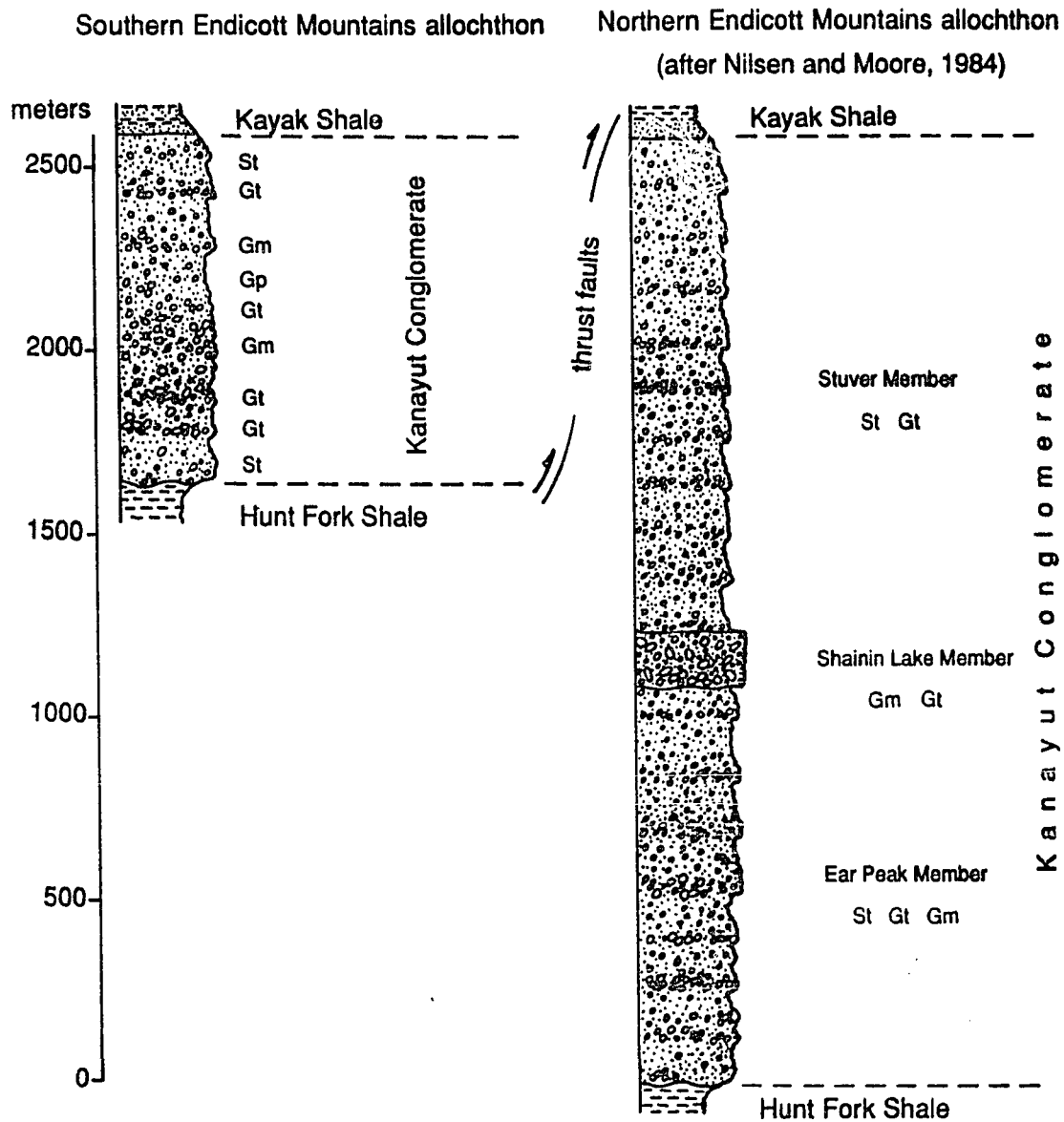


Figure 1.6 - Stratigraphy of the Kanayut Conglomerate. a) Southern Endicott Mountains allochthon. b) Northern thrust imbricates of the allochthon (after Nilsen and Moore, 1984). Lithofacies are from Table 1.2.

Facies Code	Lithofacies	Sedimentary Structures	Interpretation
Gm (organized)	clast supported, poorly-sorted, pebble-cobble conglomerate	massive	longitudinal gravel bars
Gt	clast-supported, poorly-sorted, pebble-cobble conglomerate	trough x-strata	large 3D ripples and scour fills
Gp	clast-supported, poorly-sorted, pebble-cobble conglomerate	planar x-strata	large 2D ripples and late-stage modification of gravel bars
St	poorly- to moderately-sorted sandstone and pebbly sandstone	trough x-strata	large 3D ripples
Sp	poorly- to moderately-sorted sandstone and pebbly sandstone	planar x-strata	2D ripples and lateral accretion on bar margins during waning flow
Sh	moderately-sorted sandstone	horizontal lamination	planar bed flow
Fm	mudstone	massive	overbank and waning flow; sometimes pedogenically altered
Fl	mudstone	horizontal lamination	overbank and waning flow

Table 1.2 - Summary of Kanayut conglomerate lithofacies. Modified from Miall (1981) and Graham et al. (1986).

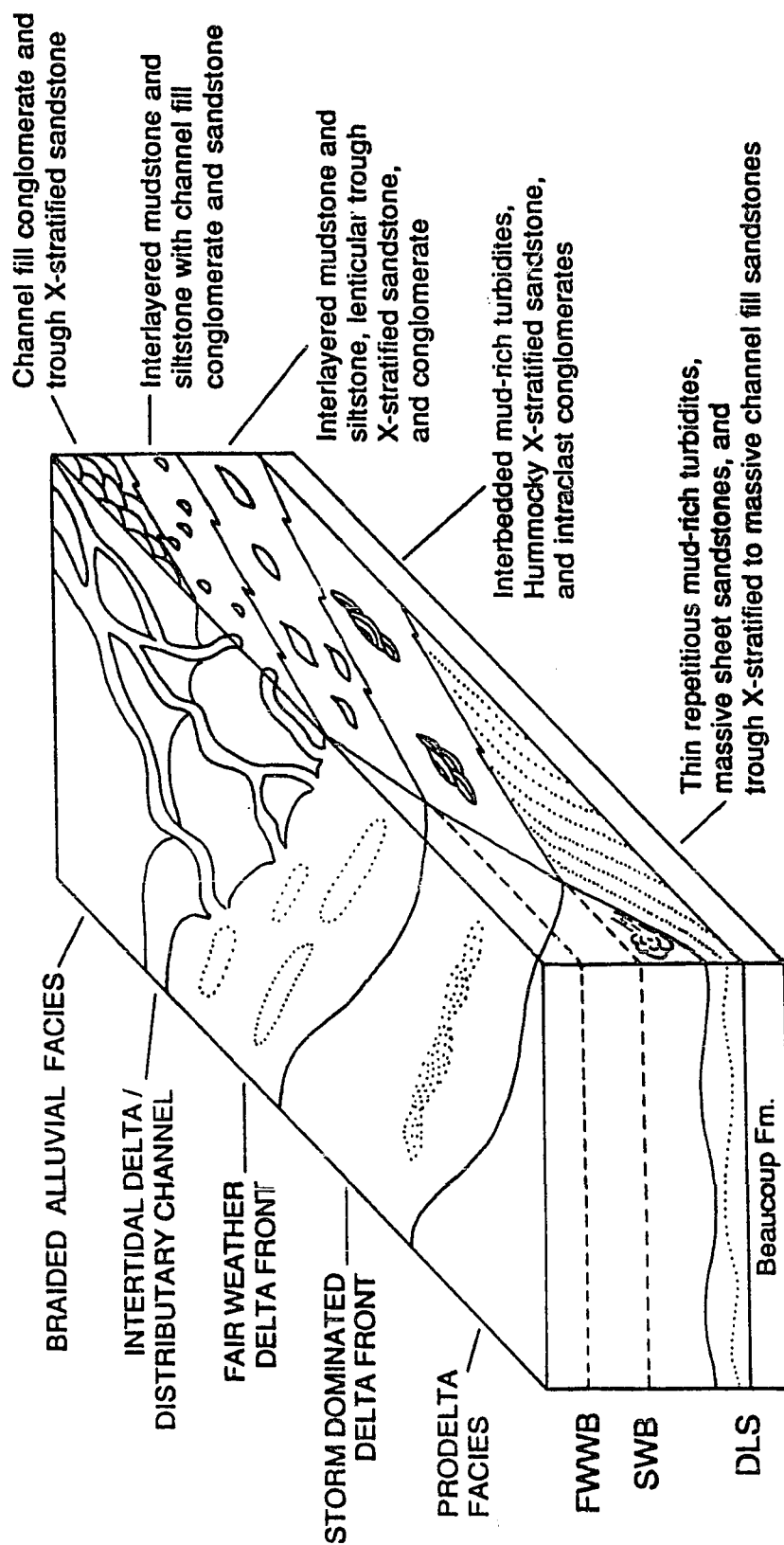


Figure 1.7 - Block diagram showing the distribution of facies in the Kanayut-Hunt Fork delta system.

sandstone/conglomerate ratios are higher in the Ear Peak and Stuver Members.

Conglomerates in the Kanayut are light gray to grayish orange, organized, and clast-supported. They generally have a bimodal clast distribution, with either pebble- to cobble-size framework clasts and a medium-grained sand to granule matrix, or granule- to pebble-size clasts and a fine- to coarse-grained sand matrix. Three distinct conglomerate lithofacies are recognized on the basis of sedimentary structures (Table 1.2). Large-scale trough cross-stratified conglomerate (Gt) is the most common lithofacies in the study area. Individual troughs range from 1 m to 5 m wide and 0.2 m to 1.5 m deep. Trough cross-stratified conglomerate beds are laterally continuous or form broadly lenticular bodies from 50 m to over 500 m wide. Occasionally, individual troughs and trough cross-stratified beds are normally graded. Massive to crudely horizontally stratified conglomerate (Gm), the second most common conglomerate lithofacies in the Kanayut, occurs as single channel fill deposits or thick (> 1 m) laterally continuous beds with erosional lower boundaries. Some Gm beds and channels are normally graded, but grain-size trends are usually absent. Minor occurrences of planar cross-stratified conglomerate (Gp) are also found in the Kanayut. Where they occur, planar cross-stratified conglomerate beds are associated with trough cross-stratified conglomerates. Stratification in all three conglomerate lithofacies is defined by sandy layers and/or alignment of oblate pebbles. Imbricated clasts are present in Gm and Gt lithofacies.

Sandstone lithofacies compose approximately 40% of the Kanayut in both the northern and southern Endicott Mountains allochthon. Sandstone occurs in small lenses and channel fill deposits within amalgamated conglomerate bodies, in the upper parts of fining upward cycles, and as laterally continuous, tabular to broadly lenticular bodies. Light olive gray to grayish yellow, trough cross-stratified, sometimes pebbly, very coarse- to fine-grained sandstone (St) is the most common sandstone lithofacies in both sections.

Troughs are generally 0.5 m to 3 m wide and 0.1 m to 1.0 m deep. Pebbles are concentrated in the lower third of the troughs or, less commonly, scattered throughout the troughs. Horizontally laminated (Sh) and planar cross-stratified (Sp) sandstones are present, but uncommon.

Reddish brown mudstone lithofacies constitute less than 10% of the northern Endicott Mountains section and less than 5% of the southern Endicott Mountains section. Massive (Fm) and horizontally laminated (Fl) siltstone, sandy mudstone, and mudstone are the only fine-grained lithofacies recognized. Some Fm beds are mottled, suggesting that they are burrowed or pedogenically altered. Fine-grained lithofacies occur as lenses within amalgamated sandstone and conglomerate beds, and as broadly lenticular sheets 100 m to over 500 m wide and up to 1 m thick. These laterally extensive sheets frequently contain channelized conglomerate and sandstone and are truncated by sub-conglomerate erosion surfaces.

The dominance of Gt, Gm, and St lithofacies in both sections, and in all three members of the northern section, is indicative of deposition by braided river systems. Lithofacies Gt is produced by migration of large three-dimensional gravel ripples in braided channels and by incision of channels into bars during flood stages (Rust, 1972; Miall, 1978). Lithofacies Gm is generally interpreted to represent longitudinal bars (Miall, 1977). Lithofacies St is the sandy braided river equivalent of lithofacies Gt, and is deposited by migration of sinuous dunes (Cant, 1978; Miall, 1981). Subordinate amounts of Gp and Sp lithofacies formed by accretion of gravel on the margins of longitudinal bars during waning flow and by the migration of gravelly and sandy transverse bars (Smith, 1974; Hein and Walker, 1977; Rust, 1978). Laterally extensive fine-grained lithofacies represent overbank muds deposited during waning flow (Williams and Rust, 1969); whereas mudstone lenses in amalgamated conglomerate and sandstone beds are probably remnants of mud drapes deposited during waning flow within channels or abandonment of

channels.

The combination of lithofacies in the Kanayut (Table 1.2) and the overall percentage of conglomerate (50% to 55%) are characteristic of braided rivers with well defined active channels, elevated partially active to inactive channels, and abundant sand and gravel bedload (Donjek type braided rivers; Miall, 1978; 1981). Fining upward cycles, similar to the ones described in the Ear Peak and Stuver Members by Nilsen et al. (1982), are common in Donjek type braided rivers (Williams and Rust, 1969). The absence of disorganized Gm and Gms lithofacies in the northernmost exposures also suggests that proximal alluvial fan environments are not represented in the study area.

Paleocurrents in the Kanayut of the southern Endicott Mountains allochthon are unimodal and indicate flow toward the south-southwest (Fig. 1.8a). This is consistent with paleocurrent data from the Atigun River valley in the northern Endicott Mountains allochthon and paleocurrents from the Kanayut in general (Moore and Nilsen, 1984). Maximum clast size decreases from 30 cm in the northernmost exposures of Kanayut in the Atigun River valley to 8 cm in the southern Endicott Mountains allochthon.

The contact between the Hunt Fork Shale and the Kanayut Conglomerate is gradational. Channel fill conglomerates and sandstones, which cut into and are interbedded with intertidal shales, siltstones, and calcareous mudstones of the upper Hunt Fork, can be traced laterally into amalgamated conglomerate and sandstone beds in the Kanayut.

Sedimentary structures and fossil assemblages allow the Hunt Fork to be subdivided into upper, middle, and lower members (Fig. 1.9). The upper Hunt Fork is composed of olive gray to black, thinly laminated mudstone and siltstone, channelized grayish yellow quartz- and chert-rich sandstone and conglomerate, and olive gray quartz-rich sheet sandstones. Thin (<10 cm) grayish orange calcareous shales are locally present. Mudcracks, wrinkle marks, ripples, algal mats, oncolites, brachiopods, *Skolithos* and

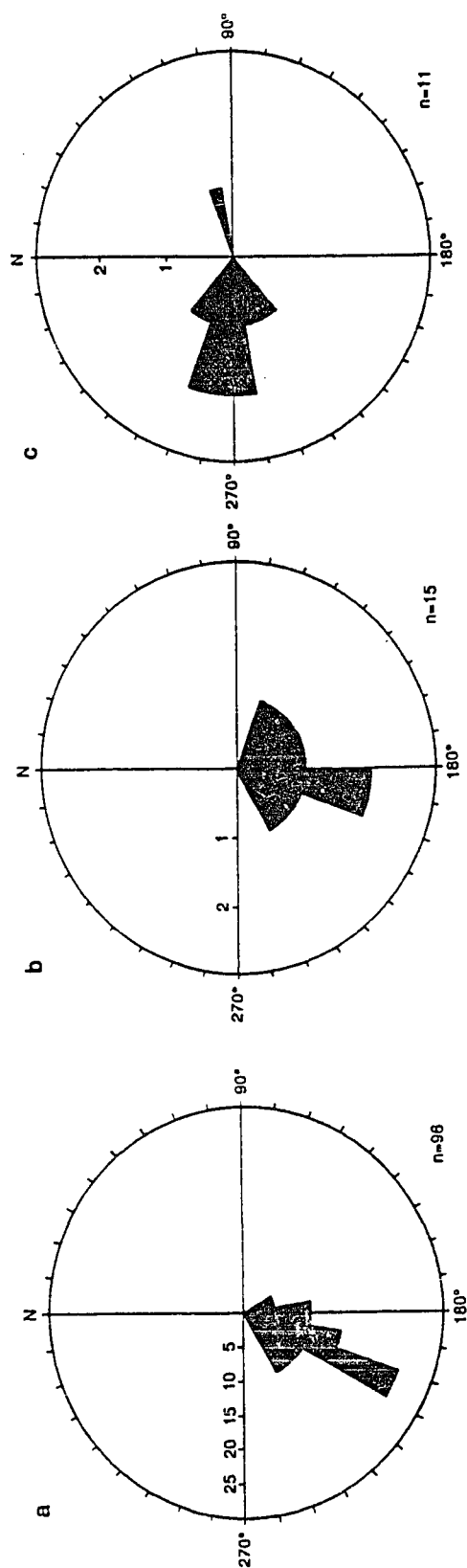


Figure 1.8 - Paleocurrent directions, southern Endicott Mountains allochthon. a) Kanayut Conglomerate. b) Upper Hunt Fork Shale distributary channels. c) Middle Hunt Fork off-shore bars.

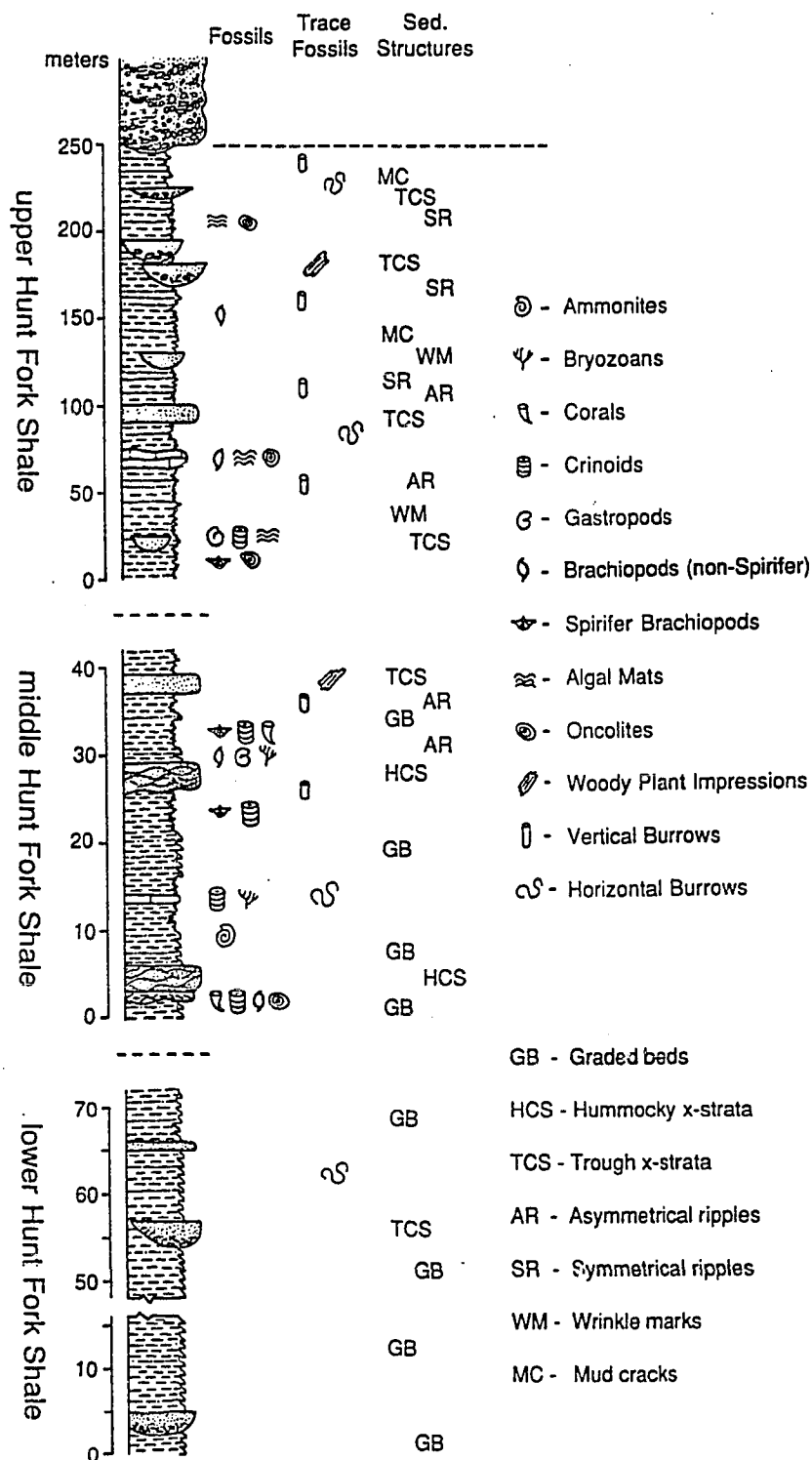


Figure 1.9 - Representative stratigraphic sections for the upper, middle, and lower Hunt Fork Shale in the southern Endicott Mountains allochthon. Section locations shown on Figure 1.5.

Cruziana ichnofacies trace fossils, and rip-up breccias indicate deposition in an intertidal environment. Channels which cut into these intertidal shales are filled with trough cross-stratified fine- to coarse-grained sandstones and/or pebble conglomerates. Paleocurrents in upper Hunt Fork channels are more variable than paleocurrents in the Kanayut, possibly indicating greater channel sinuosity. Mean flow in both units, however, was approximately parallel (Fig. 1.8). Sheet sandstones are fine- to medium-grained and massive or trough cross-stratified.

The middle Hunt Fork is composed mostly of olive gray to black, thinly laminated mud- and silt-shale, but also contains: lenticular, trough cross-stratified, fine-grained sandstone; massive fine- to medium-grained sheet sandstones; fine- to coarse-grained hummocky cross-stratified sandstones, and; thin graded beds (Fig. 1.9). All sandstones are composed mostly of quartz and chert grains, and have a grayish yellow to light olive gray color. Light olive gray to medium gray channelized chert-pebble conglomerates occur locally along discontinuous horizons (Fig. 1.5). Faunal assemblages in the middle Hunt Fork are more diverse than in the upper Hunt Fork and include rugose corals, tabulate corals, crinoids, bryozoans, gastropods, ammonites, and several types of brachiopods (Table 1.1). Rip-up breccias and allogenic fossils are commonly present at the bases of hummocky cross-stratified units. Lenticular, east-west trending, trough cross-stratified, fine- to medium-grained sandstones with east-west trending paleocurrents (Fig. 1.8c) appear to be longitudinal off-shore bar deposits. Allogenic rugose corals and crinoid fragments in lenticular carbonate beds suggest that small patch reefs were locally present in the middle Hunt Fork. *Skolithos* and *Cruziana* ichnofacies trace fossils occur in some interbedded sandstone and shale intervals.

The absence of hummocky cross-stratified units, longitudinal bar deposits, and fossils distinguishes the lower Hunt Fork from the middle Hunt Fork (Fig. 1.9). Most of the lower Hunt Fork is composed of dark greenish gray to black, thin (0.5 to 4 cm),

repetitious graded beds. Individual graded beds fine upward from siltstone or very fine-grained sandstone to clay-shale. Planolites and Chondrites are the only trace fossils present in the lower Hunt Fork. Locally, graded sequences are interrupted by laterally continuous, massive, light olive gray, fine-grained sandstones up to 2 m thick. These sandstones have sharp upper and lower contacts, but do not appear to scour into the underlying shales. Less frequently, lower Hunt Fork shales are cut by asymmetric channels up to 3 m deep and 10 m wide. Channels are filled with medium gray to greenish gray, massive or trough cross-stratified, fine- to medium-grained sandstone and rip-up clast conglomerates. Phelps (1987) also reports chert pebble conglomerates in some lower Hunt Fork channels farther to the west.

Deformation of the Hunt Fork makes it impossible to accurately measure a complete stratigraphic section in the study area. The tectonic thickness of the Hunt Fork in the southern nappe, where both the top and bottom of the formation are exposed, is approximately 6 km (Fig. 1.3). Despite the intense intraformational deformation, the distribution of facies in the Hunt Fork is in a normal stratigraphic order. Prodelta slope deposits of the Lower Hunt Fork are overlain by shelf facies of the middle Hunt Fork, these shelfal deposits are in turn overlain by intertidal deposits of the upper Hunt Fork which grade laterally and vertically into fluvial deposits of the Kanayut (Figs. 5 and 6).

Lithofacies, unimodal paleocurrents, and the areal extent of the Kanayut classify the Kanayut-Hunt Fork delta as a braid-delta (McPherson et al., 1987). The distribution of sedimentary facies in the Hunt Fork, however, differs from previously described coarse-grained deltas in that turbidites are the only sediment-gravity flow structures recognized. Debris flows and slumps, which are common in the subaqueous parts of many coarse-grained deltas (Postma, 1984), are uncommon in the Hunt Fork. Massive sheet sandstones in the lower Hunt Fork may be grain flow deposits or, alternatively, they may be well-sorted, sand-rich turbidites deposited by unchannelized sheet flow down the

delta front. The dearth of gravity induced sedimentation suggests that the Kanayut-Hunt Fork delta front had a relatively shallow depositional dip.

Shoreline and subaqueous deposition in the Hunt Fork was controlled by sediment influx rates, tidal range, wave energy, and wave direction. Intertidal deposits in the upper Hunt Fork are cut by channelized sandstones and conglomerates suggesting that tidal flats developed between distributary channels. Sedimentary structures and paleocurrents in distributary channels, however, indicate unidirectional flow toward the south-southwest (Fig. 1.8b) discounting significant tidal influence within the channels. Variable flow rates are evidenced by fining-upward trends within single channels and by conglomerates in some channels and fine- to medium-grained sand in other channels. Laterally continuous siltstone and sandstone layers within the upper Hunt Fork were deposited by sheet flood of interdistributary areas when flow rates exceeded channel capacity and/or channels were clogged by high sediment loads.

Juxtaposition of intertidal/distributary channel deposits against delta-front shales without intervening beach and upper shoreface deposits suggests that fair-weather wave energy was low. East-west trending offshore bars in the middle Hunt Fork indicate that wave convergence was oblique to the shore line and created longshore currents. Paleocurrents in the middle Hunt Fork of the study area (Fig. 1.8c) and thickening of upper shoreface and beach sandstones in the Noatak Sandstone farther to the west (Moore and Nilsen, 1984) suggest that longshore drift was from east to west. This combination of relatively high sediment influx, relatively low tidal influence, and low wave energy typifies modern fluvial dominated deltas (Galloway, 1975).

Hummocky cross-stratification and rip-up breccias, such as the ones preserved in the middle Hunt Fork, are indicative of storm wave reworking of delta front deposits below fair weather wave base (Chan and Dott, 1986). However, since fair weather wave energy was apparently low, hummocky cross-stratified units could have been generated by small

storms at shallow depths. This is supported by intertidal units in close proximity to hummocky cross-stratified units and by interbedded hummocky cross-stratified units and trough cross-stratified longitudinal bar deposits in the middle Hunt Fork.

Deposition of the lower Hunt Fork occurred below storm wave base, primarily by turbidity currents. The absence of *Zoophycos* and *Nerites* ichnofacies suggests that the lower Hunt Fork was deposited in the sub-littoral zone (< 200 m; Crimes, 1975; Frey and Pemberton, 1984). However, since the *Planolites* and *Chondrites* trace fossils found in the lower Hunt Fork are also common bathal deposits (Chamberlain, 1978) the maximum depth of deposition cannot be constrained.

Beaucoup Formation

Regionally, the contact between the Hunt Fork and the underlying Beaucoup Formation is interpreted as an unconformity (Tailleur et al., 1967). Dutro et al. (1979), however, report that "the Beaucoup Formation at its type section is conformably overlain by the Hunt Fork Shale". In the study area, the lower Hunt Fork is in depositional contact with different Beaucoup lithologies, possibly indicating the presence of a disconformity, but there is no evidence for an angular unconformity between the two units.

The top of the Beaucoup is defined as the top of the uppermost reef or, in the absence of reefs, by the contact between the Hunt Fork and brown to yellow weathering sandstone, shale, and calcareous shale "directly beneath the darker Hunt Fork Shale" (Dutro et al., 1979). Based on these criteria, Dutro et al. (1979) assigned the unnamed Upper Devonian brown calcareous clastic rocks in the Phillip Smith Mountains quadrangle (Brosgé et al., 1979) to the Beaucoup Formation. In the vicinity of the Dalton Highway, however, rocks mapped as the brown shale member of the unnamed unit (Brosgé et al., 1979) include all three Hunt Fork facies (Fig. 1.9) and can be traced laterally into the Hunt Fork Shale as it is mapped by Brosgé et al. (1979). The actual Hunt Fork-Beaucoup contact is south of the contact between the Hunt Fork Shale and the unnamed brown shale

mapped by Brosgé et al. (1979).

The Beaucoup Formation of the southern Endicott Mountains allochthon is a 0 to 1.5 km thick sequence of interlayered shales, calcareous shales, sandstones, conglomerates, volcaniclastics, limestone reefs, and their low-grade metamorphic equivalents. Bedding varies from less than 1 mm in shales and phyllites to greater than 5 m in massive reef limestones and amalgamated sandstones. Most of the lithologies are thinly layered and strongly deformed. Limestone reefs and sandstone units greater than 2 m thick are relatively undeformed.

Adjacent to the Dalton Highway (Fig. 1.5), the Beaucoup has a minimum tectonic thickness of 347 m (Fig. 1.10). The top of the Beaucoup at this locality is a 5 m thick medium dark gray limestone reef containing colonial and solitary rugose corals, tabulate corals, and bryozoans (Table 1.1). The upper reef is separated from a thinner (4 m thick) coral, crinoid, stromatoporoid, and bryozoan reef (Table 1.2) by 8 m of intensely deformed yellowish gray to olive-black shale. Below the second reef, the section consists of 330 m of poorly exposed, intensely deformed, olive gray to olive black shale, yellowish gray to light gray calcareous silt-shale, and mottled grayish red to greenish gray shale. A discontinuous grayish yellow to medium gray chert- and quartz-granule conglomerate interrupts this shaley sequence 20 m below the base of the lower reef. A 2 m thick interval of reddish brown volcaniclastic breccia, medium light gray chert pebble conglomerate, and grayish yellow fine-grained quartz arenite is located approximately 30 m above the lower fault contact (Fig. 1.10).

Intense deformation in the shales of the Beaucoup makes it difficult to interpret all of the depositional environments represented. Where sedimentary structures are preserved, shales are horizontal- to wavy-laminated and composed of silt or mud; graded beds are rare. Detrital components in both calcareous and non-calcareous shales are petrographically similar, with the exception of carbonate grains in the calcareous shales.

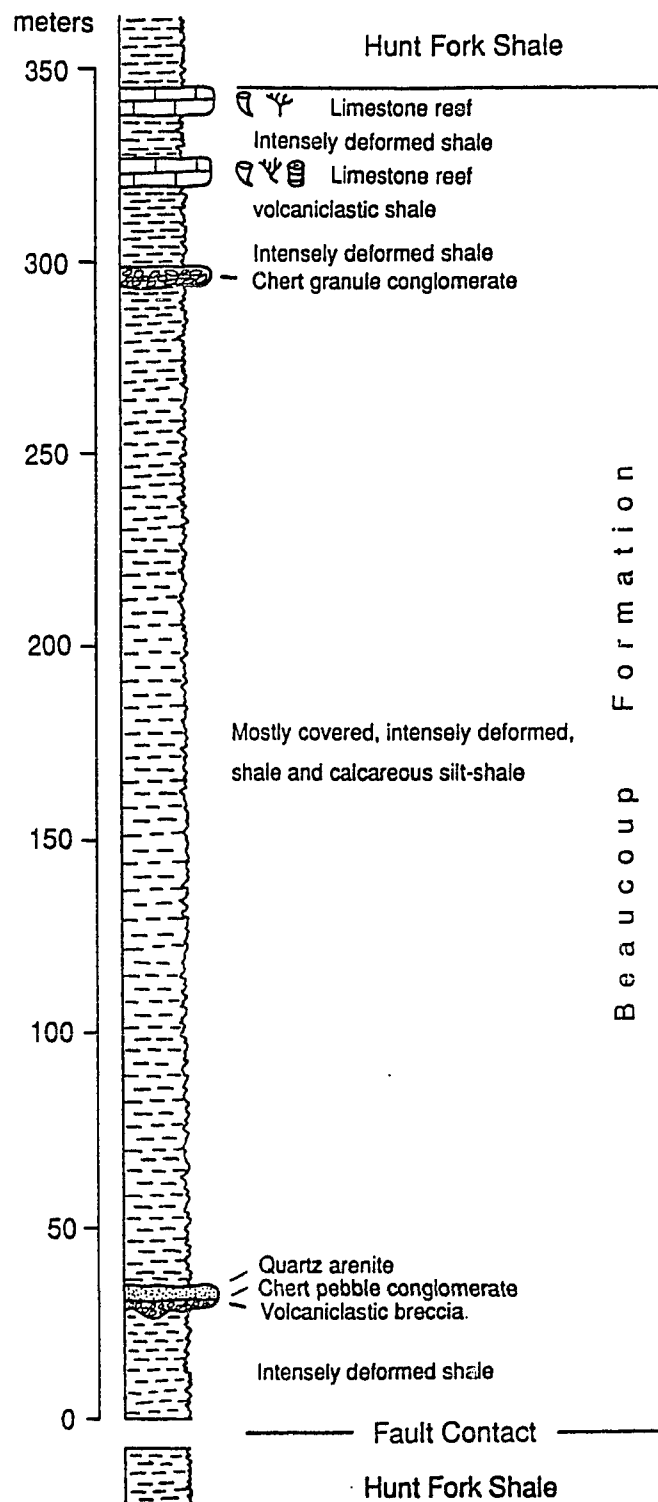


Figure 1.10 - Schematic stratigraphic section for the upper Beaucoup Formation in the southern Endicott Mountains allochthon. Section location shown on Figure 1.5.

Shales containing volcanoclastic detritus can be distinguished in the field because of their mottled reddish brown and greenish gray color. Corals, crinoids, and other marine fossils (Table 1.1) collected from the carbonate reefs and some calcareous shales indicate deposition in a relatively shallow marine environment. Amalgamated, channelized sandstones and conglomerates occur at several stratigraphic levels in the Beaucoup. Channel-fill pebble conglomerates are usually massive and composed of subrounded to subangular, light gray to dark gray chert and white quartz clasts. Medium gray carbonate clasts and reddish brown volcanic clasts are locally abundant. Beaucoup sandstones are massive to trough cross-stratified, fine- to very coarse-grained, poorly- to moderately-sorted, quartz-rich to lithic-rich wackestones and arenites.

The age of the Beaucoup is restricted to the early Frasnian by corals and brachiopods at the type section (Dutro et al., 1979). Age equivalent corals, stromatoporoids, and conodonts have also been recovered from the Beaucoup in the Chandalar and Wiseman quadrangles (Dillon et al., 1987a).

SEQUENCE STRATIGRAPHY

In the southeastern part of the study area, east of the Dalton Highway, prodelta turbidites of the lower Hunt Fork overlie fossiliferous reefs in the upper Beaucoup (Fig. 1.10). Since the lower Hunt Fork was deposited below storm wave base and rugose coral-tabulate coral-stromatoporoid reefs grew within the influence of surface waves (Tasch, 1980, p.181), the Hunt Fork-Beaucoup contact is interpreted to indicate that there was an increase in water depth between Beaucoup deposition and deposition of the overlying Hunt Fork Shale. If the contact is an unconformity, as postulated by Tailleux et al. (1967), the two formations were deposited in temporally separate depositional systems (Fig. 1.11b). An alternative depositional model, proposed by Phelps (1987) and Handschy et al. (1987), considers the Beaucoup as a transitional facies between the Hunt Fork Shale and the Skajit Limestone. In this interpretation, quartz- and chert-rich

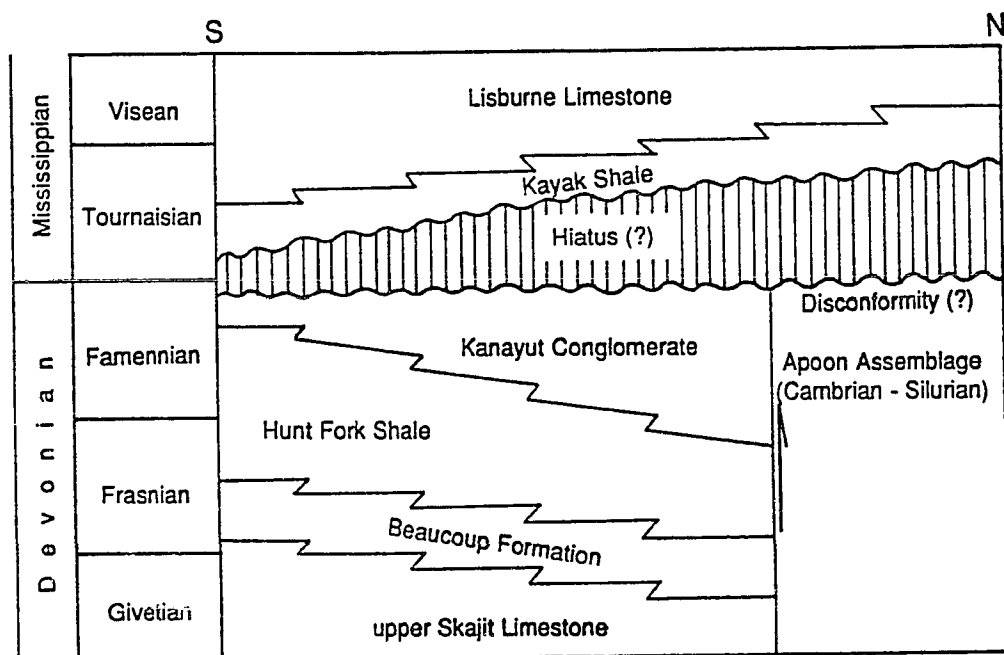
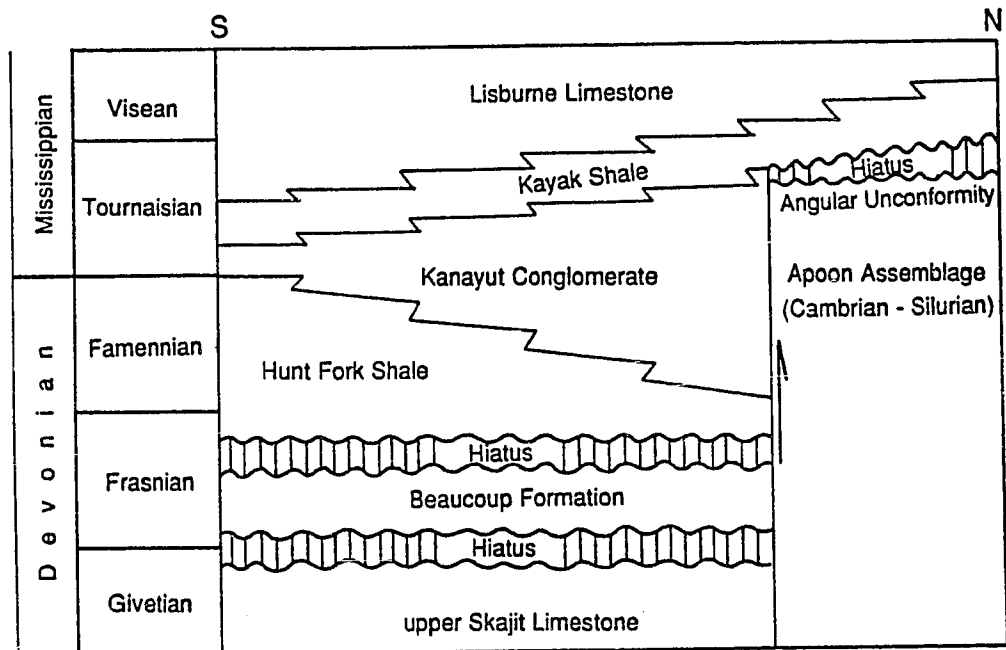


Figure 1.11 - Unconformities and facies changes in the central Brooks Range. a) Stated or implied by Tailleux et al. (1967), Armstrong et al. (1976), Dutro et al. (1979), and/or Moore and Nilsen (1984). b) Interpreted from known fossil ranges and sedimentary facies relations in the central Brooks Range (modified from Handschy et al., 1987; Phelps, 1987; Oldow et al., 1984).

conglomerate, sandstone, and shale in the Beaucoup are inferred to be distal Hunt Fork equivalents which interfinger with carbonates and volcanoclastics of the Skajit Limestone and Whiteface Mountain volcanics (terminology of Dillon et al., 1986). The Hunt Fork-Beaucoup contact is interpreted as a downlap surface formed as terrigenous clastics of the Kanayut-Hunt Fork delta prograded over the Beaucoup (Fig. 1.11a).

Neither field relations nor paleontological control are adequate to conclusively resolve these alternative depositional models. Dutro et al. (1979) report Frasnian ages for both the Beaucoup and lower Hunt Fork, and infer an early Frasnian age for the Beaucoup on the basis of the brachiopod *Warrenella*. Thus, if an unconformity is present, the hiatus it represents is relatively short ($\ll 7$ Ma). Similarly, it is unclear whether there is an unconformity between the Beaucoup and the underlying Skajit Limestone since both units have yielded fossils with Middle and early Late Devonian age ranges (Dillon et al., 1987a).

The influx of coarse- and fine-grained terrigenous clastics during deposition of the Kanayut-Hunt Fork delta system requires uplift of a northern source area and suggests that deepening across the Beaucoup-Hunt Fork contact may be due to subsidence. Alternatively, Devonian sea level curves (Johnson et al., 1985) show two deepening events in the Frasnian that could also account for the increase in water depth across the Beaucoup-Hunt Fork contact (Fig. 1.12). As before, field relations and paleontology do not adequately resolve these options, but, if the Beaucoup and Hunt Fork are separated by an unconformity, the apparent absence of falls in eustatic sea level during the Frasnian (Fig. 1.12; Johnson et al., 1985) requires a tectonic origin for the unconformity.

Prograding and retrograding sequences in the Kanayut (Moore and Nilsen, 1984) follow the overall Famennian pattern of regression (progradation) in the lower part of the sequence and transgression (retrogradation) in the upper part of the sequence (Fig. 1.12). They do not, however, reflect the high-frequency fluctuations in the Famennian sea level

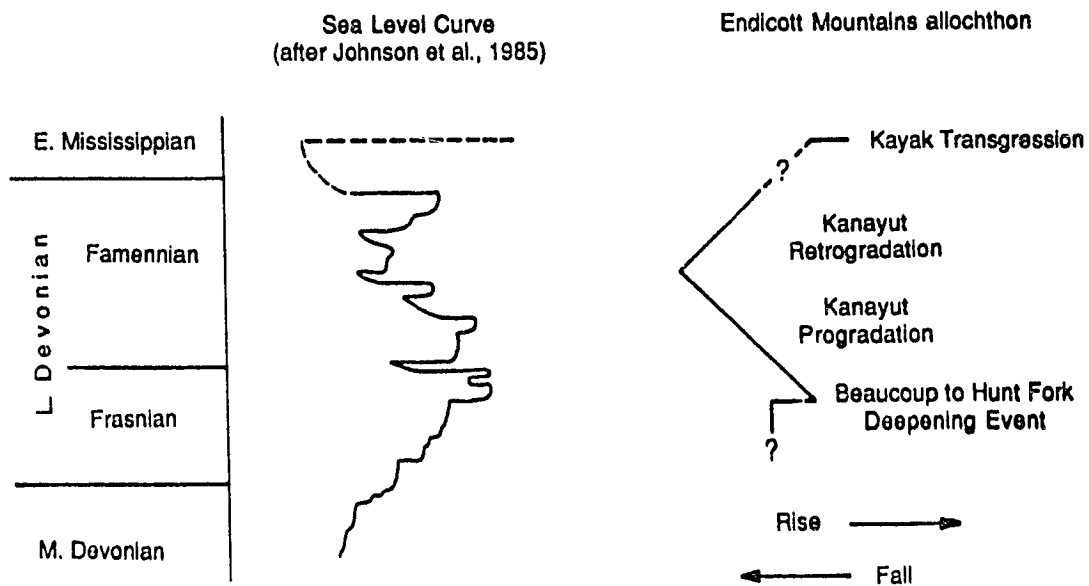


Figure 1.12 - Eustatic sea level during the Late Devonian and earliest Mississippian (after Johnson et al, 1985; Krebs, 1979) and relative sea level fluctuations in the Endicott Group and Beaucoup Formation (inferred from facies changes).

curve (Fig. 1.12). The biggest discrepancy between the sea level curves and depositional patterns in the Kanayut-Hunt Fork occurs in the latest Famennian and Early Mississippian. Nilsen and Moore (1984) report a possible Early Mississippian age for the uppermost Kanayut and show the retrograde cycle in the upper Kanayut to be continuous into the Kayak Shale; whereas the sea level curves indicate a major regression in the latest Famennian (Fig. 1.12). This regression should have been accompanied by progradation of paralic and fluvial facies. Continued retrogradation of the Kanayut may indicate that the rate of basin subsidence was equal to or greater than the rate of sea level fall, that the sediment supply was decreasing faster than sea level was falling, or that the upper Kanayut is Famennian in age and is separated from the Kayak Shale by a disconformity. The youngest fossils collected from the Hunt Fork Shale and Noatak Sandstone, which occurs between the Hunt Fork Shale and Kanayut Conglomerate in the western Brooks Range, are Famennian in age (Nilsen and Moore, 1984), so paleontology cannot resolve these options.

The implications of these alternative depositional models are important for interpreting the significance of tectonism during the latest Devonian. If the Kanayut-Hunt Fork basin subsided at a rate equal to, or faster than, sea level was falling, then the basin must have been tectonically active during the latest Devonian. In contrast, decreasing sediment influx could indicate that topography, and possibly tectonic activity, in the source terrane was decreasing. Unfortunately, the data currently available does not adequately define the type or age of the contact at the top of the Kanayut.

Younger-to-the-north onlap of the of the Kekiktuk Conglomerate and Kayak Shale over the Kanayut Conglomerate and Apoon assemblage reflects a marine transgression during the Early Mississippian (Fig. 1.12). Subsequent transgressive-regressive cycles in the upper Kayak Shale and in carbonates of the Lisburne Group have been tentatively

correlated to Mississippian and Pennsylvanian sea level fluctuations (Carlson and Watts, 1987; K.F. Watts, 1987, personal comm.), and suggest that the Lisburne carbonate platform was deposited in a tectonically quiet setting.

PROVENANCE

Chert is the principal conglomerate clast lithology in all of the formations in the Endicott Mountains allochthon. Pebbles in the Kekiktuk Conglomerate are composed of white and gray chert, mudstone, and milky quartz. Cobbles and pebbles in the Kanayut Conglomerate include: gray, white, green, red, and black chert; milky and clear quartz; quartzite; mudstone; argillite; slate; and, rarely, granite. Hunt Fork conglomerates contain mudstone rip-up intraclasts, and black, gray, white and green chert clasts. Conglomerates in the Beaucoup are chert- and quartz-rich, carbonate-rich, or volcanic-rich. Chert pebble conglomerates and volcanoclastic conglomerates are occasionally interbedded, but chert and volcanic clasts are never mixed in the same channels.

The overwhelming abundance of chert in most Kanayut, Hunt Fork, and Beaucoup conglomerates makes it difficult to evaluate the compositions of the respective source terranes on the basis of conglomerate clasts alone, because chert is the most resistant lithology present and is preferentially concentrated in coarser deposits. Provenance studies in other coarse-grained clastic wedges have shown that conglomerate clast compositions strongly reflect clast durability (Graham et al., 1986), and that accurate provenance analysis of conglomerates should include petrography of finer-grained components which contain the more labile lithologies (Ingersoll et al., 1987).

One significant problem for interpreting detrital modes in sandstones is destruction of labile grains during reworking in high-energy, especially near-shore, environments (Mack, 1978). Because they were deposited in relatively high-energy depositional environments, quartz arenites and quartz-chert arenites in the Kekiktuk Conglomerate and lower Kayak Shale provide little information about the source of the detritus. Sandstones

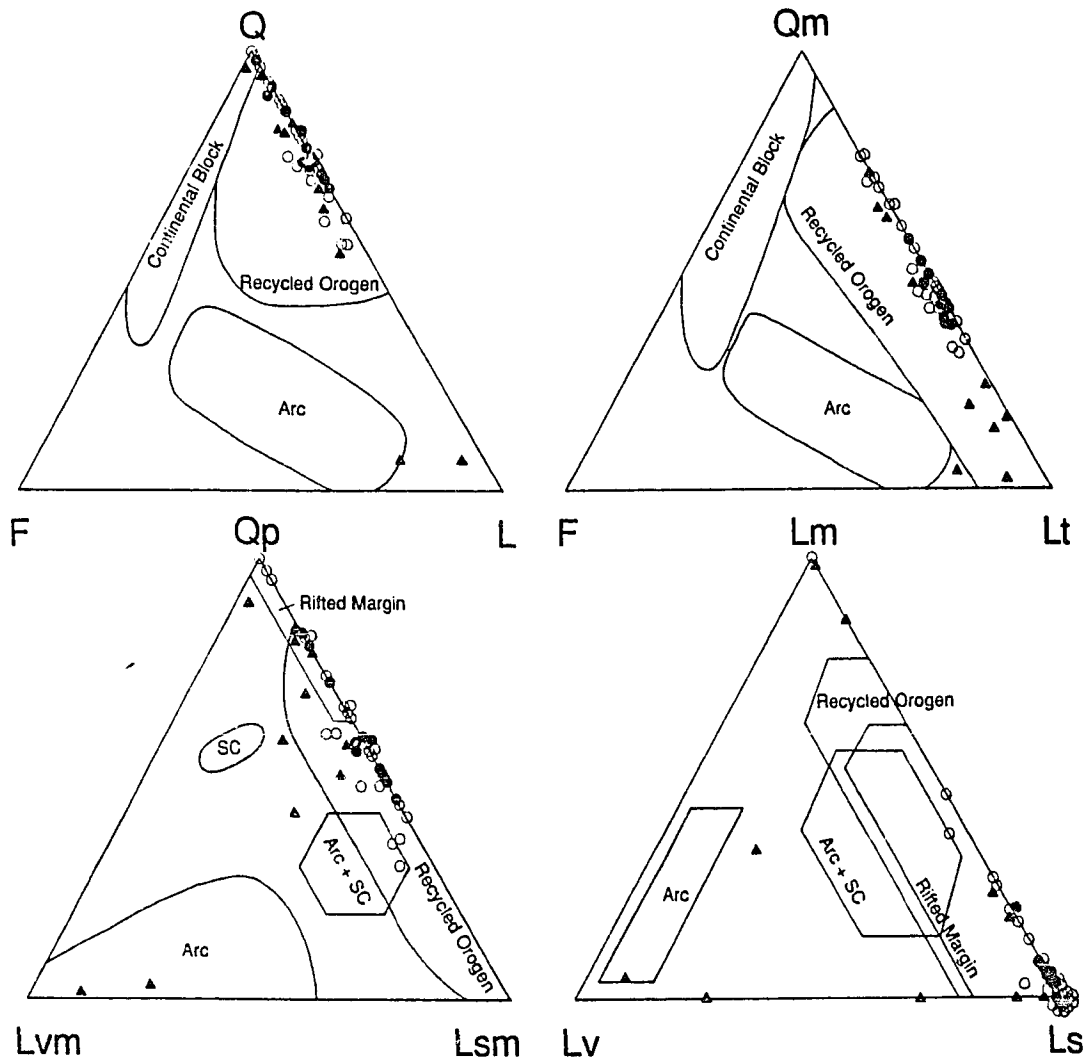


Figure 1.13 - Plots of sandstone compositions in the Kanayut (solid circles; 13 samples), Hunt Fork (open circles; 23 samples), and Beaucoup (solid triangles; 10 samples). a) QFL plot. b) QmFLt plot. c) LmLvLs plot. d) QpLvmLsm plot. Grain type parameters are defined in Table 1.3. Tectonic fields are from Dickinson and Suczek (1979) and Ingersoll and Suczek (1979).

$Q = Q_m + Q_p$	where	<p>Q = total quartzose grains</p> <p>Q_m = monocrystalline quartz grains</p> <p>Q_p = polycrystalline quartz and chert grains</p>
$F = P + K$	where	<p>F = total feldspar grains</p> <p>P = plagioclase feldspar grains</p> <p>K = potassium-feldspar grains</p>
$L = L_m + L_v + L_s$	where	<p>L = total lithic grains (exclusive of chert and polycrystalline quartz)</p> <p>L_m = metamorphic rock fragments</p> <p>L_v = volcanic rock fragments</p> <p>L_s = sedimentary rock fragments</p>
$L = L_{vm} + L_{sm}$ fragments	where	<p>L_{vm} = volcanic and metavolcanic rock</p> <p>L_{sm} = sedimentary and metasedimentary rock fragments</p>
$L_t = L + Q_p$		

Table 1.3 - Grain type parameters. After Ingersoll et al., 1987.

in the Kanayut, Hunt Fork, and Beaucoup are compositionally much less mature than sandstones in the Kekiktuk and Kayak and do not appear to be significantly effected by reworking in high-energy environments.

Sandstone compositions in the Kanayut and Hunt Fork reflect a mixed sedimentary, low-grade metamorphic, and igneous source terrane. Quartz is the most common constituent in both units (Fig. 1.13a). Chert and silicified argillite are the most common lithic fragments. Low-grade metamorphic rock fragments usually comprise less than 5% of the total lithics (Fig. 1.13c), but quartz instability indices (Young, 1976; Basu et al., 1975) for undeformed medium-grained sandstone samples from the upper Kanayut suggest that 10% to 20% of the quartz grains also had a low-grade metamorphic source. Metamorphic rock fragments include quartz-muscovite schist, ribbon quartz, and slate. Chert petrography indicates that 20% to 50% of the chert in the Kanayut had an argillite or mudstone protolith. The bulk of the chert is pure SiO_2 or contains scattered clay inclusions, suggesting deposition from a siliceous ooze or diagenetic precipitation from a non-argillaceous protolith. Chert clasts occasionally contain radiolarians (Anderson, 1987). Less than 5% of the chert was deformed and/or metamorphosed before deposition of the Kanayut. Plagioclase is the most common feldspar, with trace amounts (<1%) of perthite, orthoclase and microcline present in some samples. Granitic rock fragments, mafic igneous rock fragments, and volcanic quartz (Folk, 1980) are present, but rare (<<1%), in samples from the northern Endicott Mountains allochthon.

The provenance of Beaucoup sandstones is much more complex. Some Beaucoup sandstones are petrographically indistinguishable from Hunt Fork and Kanayut sandstones; whereas others have an exclusively volcanic source (Fig. 1.13). Quartz and chert are the most common detrital grains in non-volcanic arenites and wackestones. Small percentages of plagioclase, biotite, muscovite, mudrock fragments, metamorphic rock fragments, carbonate rock fragments, and/or volcanic rock fragments are also present

in many Beaucoup wackestones.

The mixture of compositionally distinct sandstones and conglomerates indicates that the clastics in the Beaucoup were derived from multiple sources. Although no paleocurrent data are available, compositional similarities between some of the Beaucoup, Hunt Fork and Kanayut sandstones, and the apparent absence of volcanoclastics farther to the northeast, in the type section of the Beaucoup (Dutro et al., 1979), suggest that quartz and chert rich clastics in the Beaucoup were sourced in the north. Similarly, the increasing abundance of volcanoclastics in the Beaucoup and equivalent units southwest of the study area, and in the superjacent Skajit allochthon suggests that the volcanic source may have been to the south and/or southwest (J.T. Dillon, 1986, personal comm.). Mixing of volcanoclastic and siliciclastic grains in wackestones and mudstones of the Beaucoup indicate that material from both sources was entering the basin simultaneously.

PALEOGEOGRAPHIC IMPLICATIONS

Provenance of the Beaucoup Formation unquestionably reflects mixing of volcanic and siliciclastic sources. This mixing could have occurred in several tectonic settings, such as a back-arc basin, a strike-slip system that juxtaposed different source terranes (Suczek, 1987), a rift setting which exposed an older volcanic arc (Mack, 1984), a volcanically active rift basin, or a volcanically active strike-slip system. Volcanic flows and pillow basalts in the Beaucoup of the southern Phillip Smith Mountains quadrangle (Dutro et al., 1979), first-cycle volcanoclastics in Upper Devonian mixed carbonates and clastics in the Skajit allochthon (Hammond terrane; Anderson, 1987), and volcanic flows in the Skajit allochthon and the schist belt (Dillon et al., 1986; 1987b) provide evidence for active volcanism within the depositional basin, eliminating tectonic settings in which the volcanic detritus is reworked. This restricts the probable tectonic setting to a back-arc basin, an active rift, or possibly a volcanically active transtensional-fault system (Fig. 1.14). Uncertainties about the depositional setting of the Skajit carbonate platform (passive

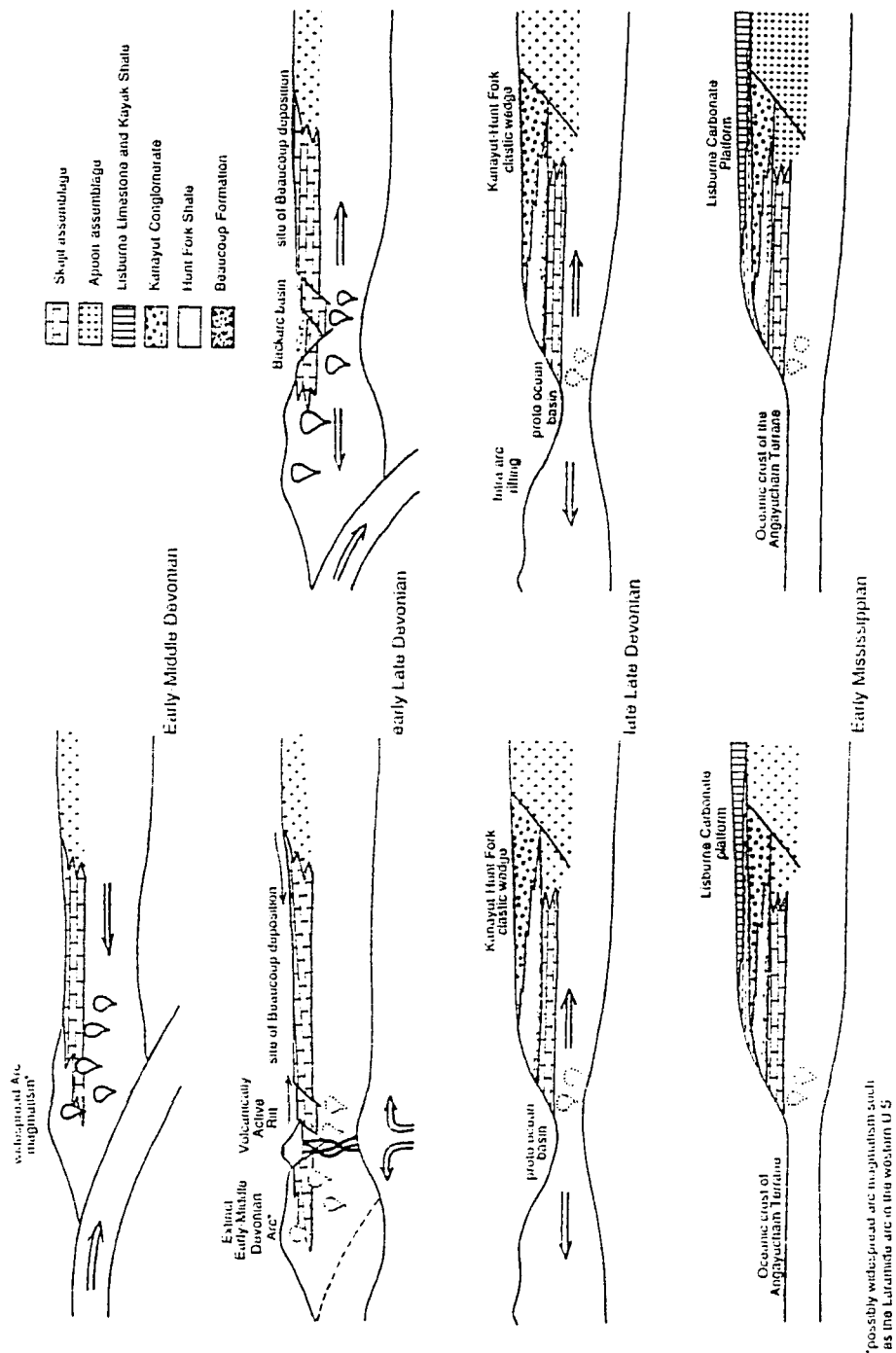


Figure 1.14 - Conceptual models for the plate tectonic setting of Late Devonian and Early Mississippian sedimentation in northern Alaska. *Note:* Strike-slip tectonics during the Late Devonian is mentioned as a possibility in the text, but not illustrated in these simplistic cross sections.

margin vs. intracratonic basin) and the tectonic affinities of the volcanics (arc vs. intracratonic rift) make it impossible to definitively distinguish between these options.

Upper Devonian volcanoclastics in the Skajit allochthon, which restore to a position south of the Beaucoup (Fig. 1.2b; Oldow et al., 1987), are age equivalent (Dillon et al., 1987a) and compositionally similar to volcanoclastics in the Beaucoup, suggesting that parts of the Skajit allochthon were laterally equivalent to the Beaucoup prior to Brookian thrusting. Peraluminous two-mica granitic plutons in the schist belt (Dillon et al., 1987b), which restore to positions south of and/or below the Skajit allochthon (Fig. 1.2b; Oldow et al., 1987), have yielded late Early to early Late Devonian zircons (Dillon et al., 1980; Dillon et al., 1987b). If these plutons are the intrusive equivalents of volcanics in the Beaucoup Formation and the Skajit allochthon, as postulated by Dillon et al. (1987b), then they may be remnants of a marginal volcanic arc. If, however, the volcanics in the Beaucoup are not the extrusive equivalents of the plutons, then the two igneous systems may represent different tectonic settings and the volcanics could be rift related (Moore, 1986). An intracratonic rift setting is unlikely for the peraluminous Devonian plutons in the southern Brooks Range because igneous activity in continental rifts is dominantly alkaline or peralkaline (Barberi et al., 1982).

Since the northern margin of the Kanayut-Hunt Fork basin is not exposed, it is difficult to assess the width or orientation (in present coordinates) of the basin. The present-day east-west distribution of the Kanayut Conglomerate and Hunt Fork Shale along the crest of the Brooks Range suggests that the Late Devonian through earliest Carboniferous shoreline may have had an east-west strike (Moore and Nilsen, 1984), but these units have been displaced a minimum of 150 km to the north during late Mesozoic and Cenozoic (Brookian) thrusting (Fig. 1.2b; Oldow et al., 1987; Mull et al., 1987) and may not accurately reflect the pre-thrust orientation of the basin. Because of the lateral continuity and apparently constant strike of the Kanayut (Fig. 1.1), it is assumed that

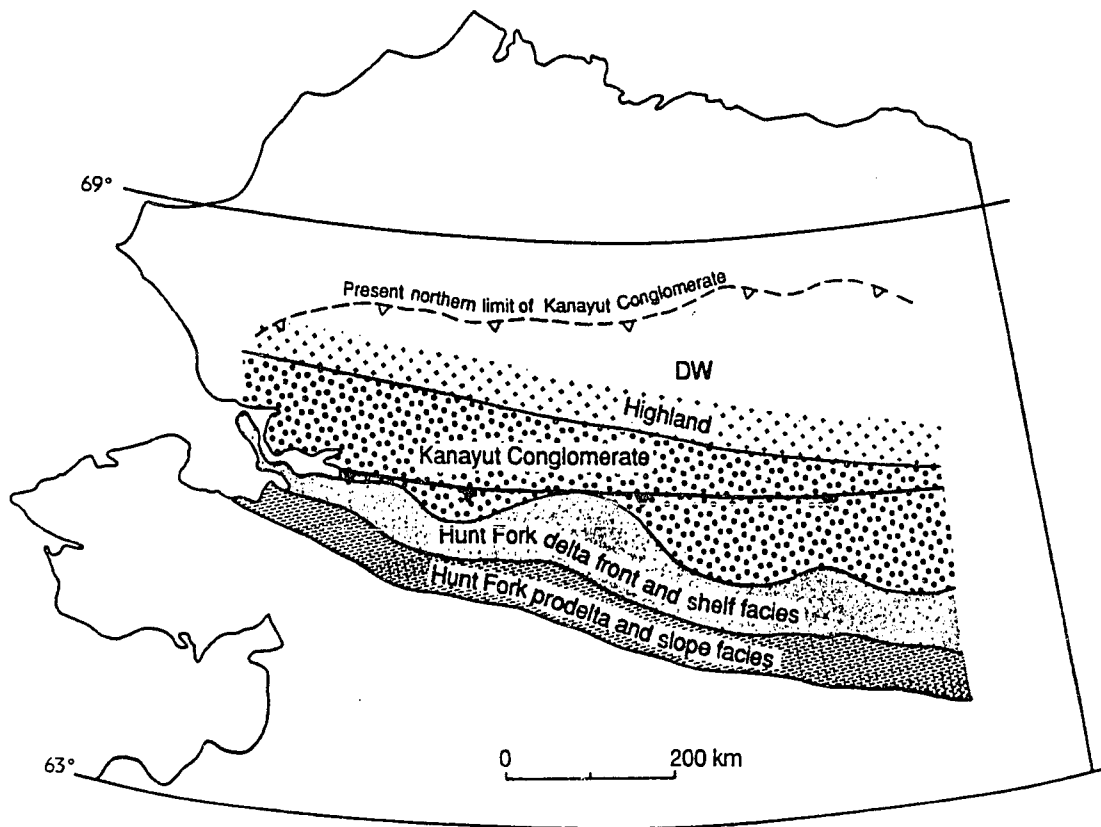


Figure 1.15 - Hypothetical paleogeographic map of the distribution of facies in the Kanayut-Hunt Fork system (modified from Morre and Nilsen, 1984). The present (allochthonous) northern edge of the Kanayut conglomerate is shown as a dashed thrust; whereas the postulated pre-thrust location of the same Kanayut beds is shown as a solid thrust. The location of the Doonerak window is shown for reference.
Note: The restored positions of facies boundaries do not account for an unknown amount of shortening in the Apoon assemblage by the Doonerak duplex. Shortening in the Doonerak duplex (Julian et al., 1984; Oldow et al. 1984) necessitates that the Kanayut and Hunt Fork restore even farther south than shown (Oldow et al., 1987).

thrust sheets were not rotated significantly during emplacement. However, regionally consistent south-southwest directed paleocurrents and a southwestward decrease in clast size in the Kanayut (Moore and Nilsen, 1984) suggest that the margin of Kanayut-Hunt Fork basin had a west-northwest strike instead of an east-west strike (Fig. 1.15). If the Late Devonian and earliest Mississippian shore line did trend west-northwest, then the paucity of Kanayut Conglomerate in the western Brooks Range may be the product of oblique truncation of facies boundaries in the Kanayut-Hunt Fork system by east-west striking Brookian thrusts (Fig. 1.15), and not related westward decreasing relief in the source area as implied by Moore and Nilsen (1984). Across-strike, balanced cross sections (e.g. Fig. 1.2b; Oldow et al., 1987) allow the relative location and minimum width of the Kanayut-Hunt Fork basin to be estimated. In the central Brooks Range, the absence of the Beaucoup, Hunt Fork, and Kanayut between the Apoon assemblage and the Kekiktuk-Kayak transgressional sequence along the margins of the Doonerak window indicates that the Kanayut-Hunt Fork clastic wedge has been thrust past the northern margin of its own depositional basin (Fig. 1.2b). In addition, the dearth of proximal alluvial fan environments in the Kanayut of the central Brooks Range may indicate that part of the Kanayut-Hunt Fork system was left on the lower plate during thrusting (Fig. 1.2b). The southward prograded wedge geometry of the Kanayut-Hunt Fork delta system (Fig. 1.7) and southward thinning of the Kanayut (Fig. 1.6) suggests that the southern most Hunt Fork shelf edge was located immediately south of the study area.

Compositional plots for the Kanayut and Hunt Fork indicate that these units were derived from a recycled orogenic belt (Fig. 1.13). The exact tectonic setting of deposition is less certain, however, since the age of the orogenic belt is unknown. The most common interpretation of the tectonic setting of the Kanayut-Hunt Fork system is that it was deposited in a foredeep adjacent to a fold-thrust belt (Nilsen, 1981; Nilsen, 1984; Moore, 1986). The primary evidence cited for a foredeep setting includes: the lateral

continuity of the Kanayut; the distribution of sedimentary facies (alluvial in the north and marine in the south); provenance of the Kanayut (Nilsen et al., 1981); and the presence of pre-Mississippian folds in the lower Paleozoic rocks exposed in the Doonerak window (Dutro et al., 1976).

Of these criteria, only the existence of pre-Mississippian folds in the Doonerak window provide evidence for a Late(?) Devonian compressional orogenic belt in the central Brooks Range. Recent structural analysis in the Doonerak window, however, has shown that all of the fold phases in the lower Paleozoic Apoon assemblage are related to late Mesozoic and Cenozoic (Brookian) orogenesis (Julian et al., 1984; Oldow et al., 1984; Seidensticker et al., 1987). Duplexing of the Apoon assemblage beneath the Mississippian Kekiktuk Conglomerate and Kayak Shale has produced an angular relationship across the roof thrust of the duplex (Seidensticker, 1986), but no evidence for a pre-Mississippian folding event has been found (Oldow et al., 1984). The lack of pre-Mississippian structures in the Doonerak window presents a significant problem for the foredeep model. Regional balanced cross sections indicate that the Kanayut-Hunt Fork depositional basin restores to a position south of the Apoon assemblage (Fig. 1.2b; Oldow et al., 1987). Thus, deposition in a foredeep would require the coarse clastics of the Kanayut to be transported from the fold-thrust belt, across the apparently undeformed Apoon assemblage, to a distant foreland basin.

Foreland basins associated with both modern (Andes, Himalayas, Taiwan, etc.) and ancient (Alps, Appalachian-Ouachita, Canadian Rocky Mountains, etc.) fold-thrust belts are developed immediately adjacent to fold-thrust belt, and syntectonic sediments deposited in the foreland basin are often involved in deformation along the leading edge of the thrust belt. Thus, separation of the foreland basin from the foldbelt by an undeformed region, as required for the Kanayut-Hunt Fork system, is atypical of foreland basins. From an analytical perspective, separation of a fold-thrust belt from its associated foreland

is impossible because foreland basins (as presently interpreted) are the product of thrust sheet and syntectonic sediment loading (Beaumont et al., 1982) and must be located immediately adjacent to the fold-thrust belt.

A second depositional setting which is compatible with the distribution of facies and along strike continuity of the Kanayut and Hunt Fork is a rift setting. Rift systems (e.g. East Africa, Rio Grande, Rhine Graben) are often continuous for hundreds to thousands of kilometers and filled with thick clastic wedges (Ramberg and Morgan, 1984). Clastics which fill rift basins are derived from rocks that are exposed during extensional faulting and, as such, their compositions often plot in tectonic fields (as defined by Dickinson and Suczek, 1979; and Ingersoll and Suczek, 1979) which do not accurately represent the tectonic setting of the depositional basin (Mack, 1984). Since the age of the orogenic belt which was recycled into the Kanayut-Hunt Fork delta is unknown, it is possible that the clastics in these units were derived from an exhumed pre-Late Devonian orogenic belt instead of a syndepositional orogenic belt. The topography required to generate cobbles in the Kanayut Conglomerate could have been produced by down-to-the-south normal faults along the northern margin of the rift basin. Similar down-to-the-south normal faults, which bound pre-Mississippian extensional basins beneath the north slope, are visible on seismic lines from the National Petroleum Reserve (Mauch, 1985; Oldow et al., 1987).

Since rift-fill sediments are derived primarily from erosion of uplifted areas along the margins of the rift basin, an extensional setting for Kanayut-Hunt Fork deposition does not require coarse clastics to be transported from a northern fold-thrust belt, past the undeformed Apoon assemblage, to a southern foreland basin. Extensional disaggregation of a fold-thrust belt could easily explain why Kanayut and Hunt Fork sandstones plot in the recycled orogen field (Fig. 1.13), and it does not require the an angular unconformity between the Apoon assemblage and the overlying Kekiktuk Conglomerate and Kayak Shale.

The distribution of facies in the Kanayut and Hunt Fork (Fig. 1.7), the across-strike width of the delta system (> 100 km; Fig. 1.2b), and regionally consistent paleocurrents in the Kanayut (Moore and Nilsen, 1984) are fairly typical of both foredeep clastic wedges and rift-phase continental margin clastic wedges. They are atypical of narrower continental rifts in which flow is perpendicular to the rift axis near the margins of the basin, but parallel to the rift axis in the center of the basin (Potter, 1978). As outlined above, a foredeep setting is not compatible with the apparent absence of pre-Mississippian folds in the Apoon assemblage. Deposition in a rift setting fits all of the data currently available, but requires a significant amount of extension prior to southward progradation of the Kanayut-Hunt Fork system.

Stratigraphic relations in the Lisburne Limestone and obducted Mississippian through Jurassic ophiolites in the southern Brooks Range (Patton, 1973; Roeder and Mull, 1978; Siblering and Jones, 1984) suggest that the rift-phase margin, on which the Kanayut-Hunt Fork delta system was deposited, had evolved into a drift-phase margin by the middle Mississippian. The spatial extent (300+ km wide and 1000+ km long) and distribution of sedimentary facies (restricted environment in the north and open marine in the south; Armstrong, 1974) in the late Early Mississippian through Pennsylvanian Lisburne Limestone are typical of passive margin carbonate platforms. Progressive, younger-to-the-north onlap of the Kayak Shale and Lisburne Limestone (Armstrong et al., 1976), and glacio-eustatic(?) transgressive-regressive cycles in the Lisburne (Carlson and Watts, 1987) also suggest that tectonic influences on sedimentation had diminished by the middle Mississippian. Mississippian through Jurassic ophiolites in the Angayucham terrane (Patton, 1973; Roeder and Mull, 1978; Siblering and Jones, 1984; Wirth et al., 1986), which restore to positions south of the Skagit allochthon (Oldow et al., 1987) indicate the presence of an ocean basin south of the Lisburne shelf edge from Carboniferous to Jurassic (Fig. 1.14; Churkin et al., 1979).

At a broader scale, the Paleozoic evolution of depositional systems in the central Brooks Range is similar to other parts of the cordilleran miogeocline. Cambrian through Devonian carbonate/shale platform deposits, analogous to some of the rocks in the Skagit allochthon, are common along the cordillera from Mexico to northern Canada (Cook and Bally, 1975). In western Canada, the miogeocline was disrupted by extensional or transtensional faulting and igneous activity during the Late Devonian and Early Mississippian (Abbott, 1986; Gordey et al., 1987). At several localities in the Yukon and British Columbia, chert-rich conglomerates, sandstones, and shales of the Earn sequence overlie or are intercalated with mafic to felsic igneous rocks, and are inferred to represent deposition on a rifted continental margin and/or in smaller transtensional basins (Gordey et al., 1987; Templeman-Kluit, 1979; Eisbacher, 1983).

Farther to the south, the miogeocline is disrupted by the Late Devonian and Early Mississippian Antler orogeny (Roberts et al., 1958), and by early Late Mississippian to Permian extension or transtension (Miller et al., 1984; Little, 1987). Within the Late Devonian through Permian Schoonover sequences of Nevada, volcanoclastics derived from a western source are intercalated with siliciclastic sediments derived from the Antler orogenic belt to the east (Miller et al., 1984). Late Mississippian basalt flows in the Schoonover sequences are coeval with basaltic volcanism and subsidence in the "overlap sequence" which unconformably overlies the Roberts Mountain allochthon (Little, 1987), and are interpreted to signal extensional disaggregation of the Antler orogenic belt (Little, 1987; Miller et al., 1984).

Intermediate between the Earn sequence of northwestern Canada and the Schoonover sequences of Nevada, pre-Mississippian deformation in rocks of the Kootenay arc is evidenced by foliated clasts in the Mississippian through Lower Pennsylvanian Milford Group which unconformably overlies the internally imbricated Lardeau Group (Kelpacki and Wheeler, 1985; Gehrels and Smith, 1987). Gehrels and Smith (1987) have

interpreted this angular unconformity and Ordovician through Devonian plutons within the Kootenay arc (Okulitch, 1985) to indicate that Antler orogenic belt extends at least as far north as southern British Columbia. Stratigraphic similarities between the Milford Group (Kelpacki and Wheeler, 1985; Gehrels and Smith, 1987) and the Late Mississippian "overlap sequence" in Nevada (Little, 1987) may also indicate that post-Antler extension extended into British Columbia.

Clearly, there are correlation problems between the Beaucoup-Hunt Fork-Kanayut sequence in the Brooks Range, the Earn sequence and Milford Group of western Canada, and the Schoonover sequences of Nevada. First, coarse clastics in the Earn group were derived from the west (Gordey et al., 1987); whereas, the Kanayut and Hunt Fork were derived from the north and northeast. Second, extension apparently began in the Late Devonian in the Brooks Range, in the latest Devonian and/or Early Mississippian in northwestern Canada, and in the middle Mississippian in Nevada. Despite these problems, Late Devonian through Early Mississippian sedimentation in the central Brooks Range is similar to Late Devonian through Late Mississippian sedimentation in British Columbia and Nevada, in that convergent tectonics (an arc system in the Brooks Range and an arc system plus fold-thrust belt in British Columbia and Nevada) is apparently followed by extension (Kanayut-Hunt Fork system in the Brooks Range, Schoonover and "overlap" sequences in Nevada, and possibly the Milford Group in British Columbia). It is unclear whether there was a Late Devonian convergent margin in northwestern Canada. Because of these similarities and the absence of an angular unconformity in the Doonerak window (Oldow et al., 1984), the Late Devonian through Early Mississippian depositional history of rocks in the Endicott Mountains allochthon seems more compatible with tectonics along the western margin of North America than with foredeep deposits in either northwestern Canada (Norris and Yorath, 1981) or north of the Greenland foldbelt (Nilsen, 1981) which were folded shortly after deposition, but have previously

been correlated with the Kanayut and Hunt Fork (Nilsen, 1981; 1984).

CONCLUSIONS

Upper Devonian and Lower Mississippian clastics in the Endicott Mountains allochthon form three depositional sequences. Each sequence is characterized by specific depositional environments, facies distributions, provenance, and tectonic setting. Mixed carbonates and clastics of the Upper Devonian Beaucoup Formation were deposited in a volcanically active, probably back-arc or rift, basin. Facies distribution and detrital modes indicate that volcanoclastics were derived from the south, and terrigenous clastics were derived from the north (Fig. 1.14).

The laterally extensive Late Devonian and Early Mississippian(?) Kanayut-Hunt Fork delta system was apparently deposited on a south facing rifted continental margin (Fig. 1.14). Southward progradation of the Kanayut Conglomerate over the Hunt Fork Shale produced a lithofacies pattern in which the Kanayut is thickest in the north and the Hunt Fork is thickest in the south (Fig. 1.7). Coarse-grained lithofacies in the Kanayut define the Kanayut-Hunt Fork delta as a braid delta; whereas, the distribution of sedimentary structures and fossil assemblages in the Hunt Fork delineate intertidal and storm influenced portions of the delta front and a turbidite dominated prodelta. Sedimentation rates in the Kanayut-Hunt Fork system apparently overwhelmed high-frequency sea level cycles in the Upper Devonian, but larger eustatic fluctuations are represented by deepening across the Hunt Fork-Beaucoup contact, and by progradational and retrogradational cycles in the Kanayut Conglomerate (Fig. 1.12).

Transgression of the Kekiktuk Conglomerate and Kayak Shale over the Kanayut-Hunt Fork delta and the lower Paleozoic Apoon assemblage reflects a sea level rise in the Early Mississippian (Fig. 1.12). Carbonate facies in the Lisburne Limestone (Armstrong, 1974) and oceanic crust in the Angayucham terrane suggest that the latest Devonian rifted continental margin had evolved into a passive margin by the middle Mississippian.

Chapter 2

**Strain variation in the Endicott Mountains allochthon,
central Brooks Range, Alaska**

ABSTRACT

The Endicott Mountains allochthon in the central Brooks Range of northern Alaska is an east-west striking stack of north-northwest vergent thrust sheets. It is composed of mid-Paleozoic clastic and carbonate rocks that were deformed during late Mesozoic and early Cenozoic (Brookian) orogenesis. Fundamental differences in structural style within the allochthon are related to the original distribution of lithostratigraphic units, the rheologies of the units, and the structural depth at which deformation occurred. In the north, the allochthon is characterized by imbricate thrust sheets and large single-phase folds. In the south, it is composed of an 8 km thick thrust nappe which exhibits a vertical strain gradient. Strain variation is most readily evidenced by a progressive change from single-phase folds at the top of the nappe to polyphase folds at the bottom. First phase fold axes change from strike-parallel at the top of the southern nappe to dip-parallel at the bottom, and the angle between first phase axial planes and the inferred attitude of the basal thrust decreases from approximately 70° at the top of the nappe to less than 10° near the base. The change in structural style from thrust imbrication in the north to heterogeneous intranappe strain in the south apparently was controlled by the original distribution of coarse- and fine-grained sedimentary rocks in the Endicott Mountains allochthon and the extent of tectonic burial by a thick (10+ km) superjacent allochthon. The distribution of

sedimentary facies in the Upper Devonian clastic wedge, which constitutes the majority of the Endicott Mountains allochthon, produced a lithofacies pattern in which a thick (2.5 km), well cemented conglomerate unit in the north is replaced by shale in the south. The relative rigidity of the thick conglomerate and lack of an overriding thrust sheet favored thrust imbrication in the north; whereas the greater proportion of shale and tectonic burial beneath the overriding allochthon favored heterogeneous intranappe deformation in the south. Changes in fold orientation, the number of superposed folds, and measured strain in the southern nappe are best explained by a combination of layer parallel shortening and simple shear in a collapsing shear zone.

INTRODUCTION

The Endicott Mountains allochthon (Mull, 1982; Oldow et al., 1987) is part of a large structural sheet that constitutes much of the outer, non-metamorphic, part of the late Mesozoic and Cenozoic Brooks Range fold-thrust belt in northern Alaska (Fig. 1.1). Internally, it is comprised of several east-west striking, north-northwest vergent thrust sheets composed of Upper Devonian and Lower Carboniferous clastic and carbonate rocks. Individual thrust sheets attain thicknesses in excess of 8 km and the allochthon is continuous for approximately 50 km across-strike from the southern, metamorphic part of the orogen to the northern limit of the mountain range. Along the front of the Brooks Range, the Endicott Mountains allochthon structurally overlies an imbricate stack of Carboniferous carbonates of the Lisburne Group (Brosagé et al., 1979; Oldow et al., 1987) and, near Galbraith Lakes (Fig. 1.2), is in close proximity to mid-Cretaceous foredeep deposits. Compositional similarities between the Cretaceous foredeep deposits and Upper Devonian and Lower Carboniferous(?) clastic units in the Endicott Mountains allochthon (Appendix 1) suggest that the coarse-grained and ostensibly the fine-grained components of the foredeep succession were derived almost exclusively from the Endicott Mountains allochthon. To the south and east (Fig. 1.2), the Endicott Mountains allochthon is

structurally overlain by lower Paleozoic and Precambrian(?) metasedimentary rocks of the Skagit allochthon (Fig. 1.2) which achieves a thickness of 10 km or more (Oldow et al., 1987).

Thrust faults and folds are well exposed throughout the study area, which is a northeast-southwest transect following the Dalton Highway through the north-central Brooks Range (Fig. 1.2). The basal detachment of the Endicott Mountains allochthon, the Amawk thrust (Mull, 1982), is exposed both in the north and, more importantly, in the south where the base of the allochthon is uplifted and exposed by the late-stage Doonerak duplex (Oldow et al., 1984; Julian et al., 1984). The allochthon extends around the closure of the east-northeast plunging duplex, and the Amawk thrust is exposed both on the northern and southern flanks of the uplift (Mull, 1982; Phelps, 1987). Uplift and erosion of the Endicott Mountains allochthon around the Doonerak duplex offers a unique opportunity to investigate differences in the internal strain of the allochthon over an essentially continuous structural section approximately 8 km thick and to compare vertical strain variations with changes in structural style across strike for a distance of over 50 km.

Models of thrust sheet emplacement generally attribute the commonly observed downward increase in bulk strain to progressive simple shear (Sanderson, 1982). In contrast, our work indicates that the Endicott Mountains allochthon has experienced a more complex strain history involving elements of layer parallel pure shear, simple shear, and layer normal pure shear. Additional controls on structural style and strain state are related to lithologic differences and the presence or absence of an overlying structural sheet during emplacement of the Endicott Mountains allochthon.

STRATIGRAPHY

In the study area, fold-thrust nappes of the Endicott Mountains allochthon are comprised of five stratigraphic units ranging in age from Late Devonian to Early Carboniferous (Fig. 1.3). These five stratigraphic units are divided into three depositional

sequences: 1) mixed carbonates and clastics of the Late Devonian Beaucoup Formation; 2) progradational shales, sandstones, and conglomerates of the Late Devonian and earliest Carboniferous(?) Hunt Fork Shale and Kanayut Conglomerate, and; 3) transgressional shales and progradational carbonates of the Early Carboniferous Kayak Shale and Lisburne Limestone. The Beaucoup Formation, Hunt Fork Shale, and Kanayut Conglomerate make up the bulk of the allochthon. Lithofacies relationships within and between these units are critical to this study, because the different lithologies controlled deformation style within the Endicott Mountains allochthon.

Beaucoup Formation

The Beaucoup Formation (Dutro et al., 1979) exposed in the southern Endicott Mountains allochthon is a sequence of interlayered shales, calcareous shales, sandstones, conglomerates, volcanoclastics, limestone reefs, and their low-grade metamorphic equivalents which achieve a thickness of up to 1.5 km (Phelps, 1987; Chapter 1 of this volume). Bedding varies from less than 1 mm thick in shales and phyllites to greater than 5 m thick in massive reef limestones and amalgamated sandstones. Most of the lithologies are thinly layered and strongly deformed with the notable exception of limestone reefs and sandstone units greater than 2 m thick which are relatively undeformed internally. The top of the Beaucoup is defined as the top of the uppermost reef (Dutro et al., 1979). The bottom of the Beaucoup Formation is not exposed in the Endicott Mountains allochthon.

Kanayut Conglomerate and Hunt Fork Shale

Facies relations in the Kanayut and Hunt Fork reflect deposition in a fluvio-deltaic system (Moore and Nilsen, 1984; Nilsen and Moore, 1984; Chapter 1 of this volume). Due to southwestward progradation of the Kanayut Conglomerate over the Hunt Fork Shale, the Kanayut is thicker in the northeast, and the Hunt Fork is thicker in the southwest (Moore and Nilsen, 1984).

The Kanayut is divided into three members. The upper and lower members consist of

multiple fining-upward cycles interpreted as meandering river deposits (Moore and Nilsen, 1984; Nilsen and Moore, 1984). The middle member is more conglomeratic than the other two and is interpreted as a braided river deposit (Moore and Nilsen, 1984). In the study area, all three members are amalgamated conglomerate and sandstone units that appear to have been deposited primarily by braided river systems. Measured stratigraphic thicknesses of Kanayut vary from approximately 1 km in the southern nappe of the Endicott Mountains allochthon to over 2.5 km in the northern imbricates (Chapter 1 of this volume).

The contact between the Hunt Fork Shale and the Kanayut Conglomerate is gradational. Channel fill conglomerates and sandstones, which cut into and are interbedded with intertidal shales of the upper Hunt Fork, can be traced laterally into amalgamated conglomerate and sandstone beds in the Kanayut.

Sedimentary structures and fossil assemblages allow the Hunt Fork to be divided into upper, middle, and lower members. The upper Hunt Fork is composed of intertidal mudstone, and channelized sandstone and conglomerate. The middle Hunt Fork is composed mostly of thinly laminated shale, but also contains lenticular trough cross-stratified sandstone, massive sheet sandstones, hummocky cross-stratified sandstones, and thin graded beds. Channelized chert-pebble conglomerates occur locally along discontinuous horizons. The lower Hunt Fork is similar to the middle Hunt Fork except that it does not contain hummocky cross-stratified units, graded beds are more common and undisturbed intervals of repetitious graded beds are thicker than in the middle Hunt Fork. Deformation in the Hunt Fork makes it impossible to measure stratigraphic thickness in the study area. The tectonic thickness of the Hunt Fork in the southern nappe, where both the top and bottom of the formation are exposed, is approximately 6 km.

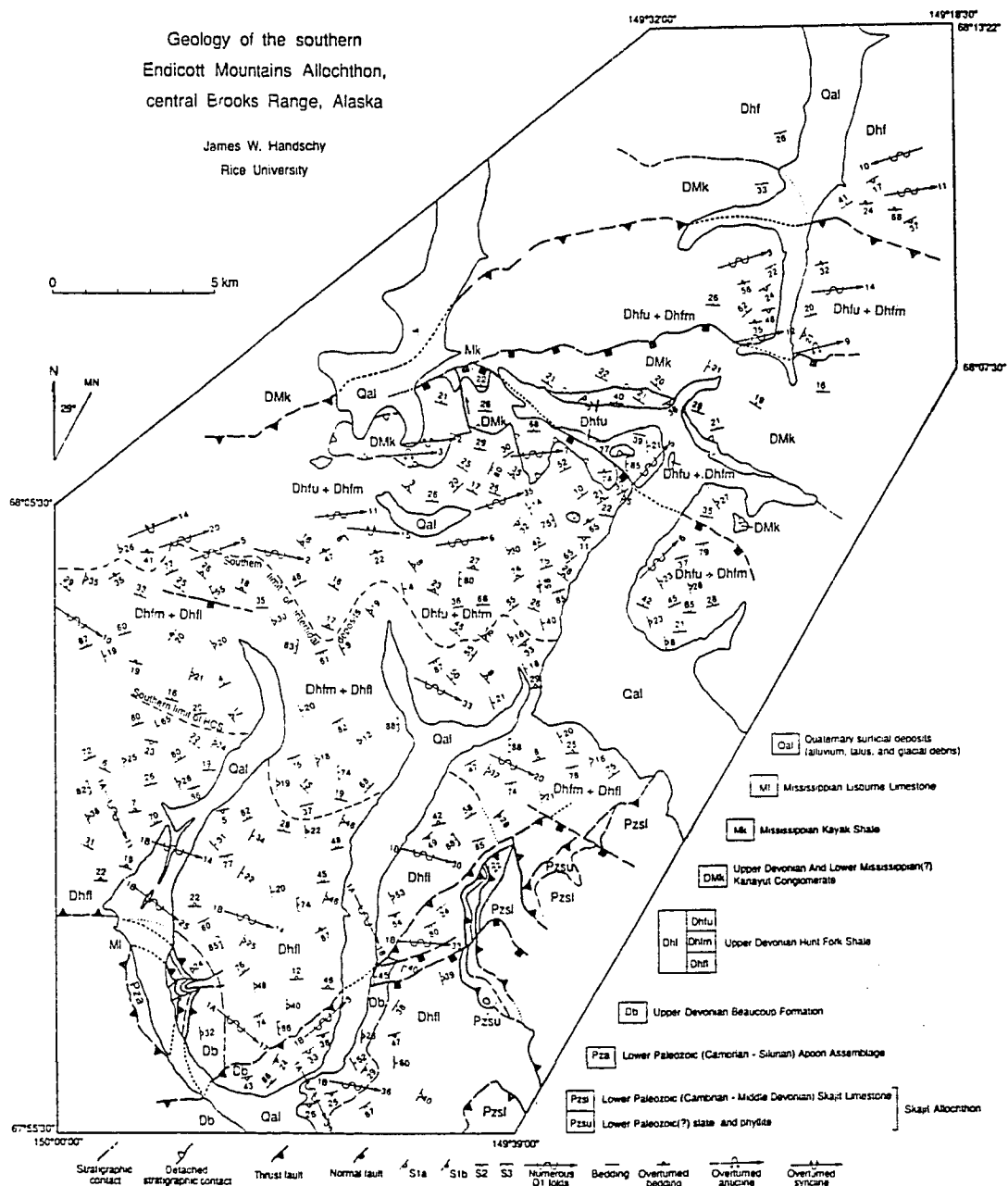
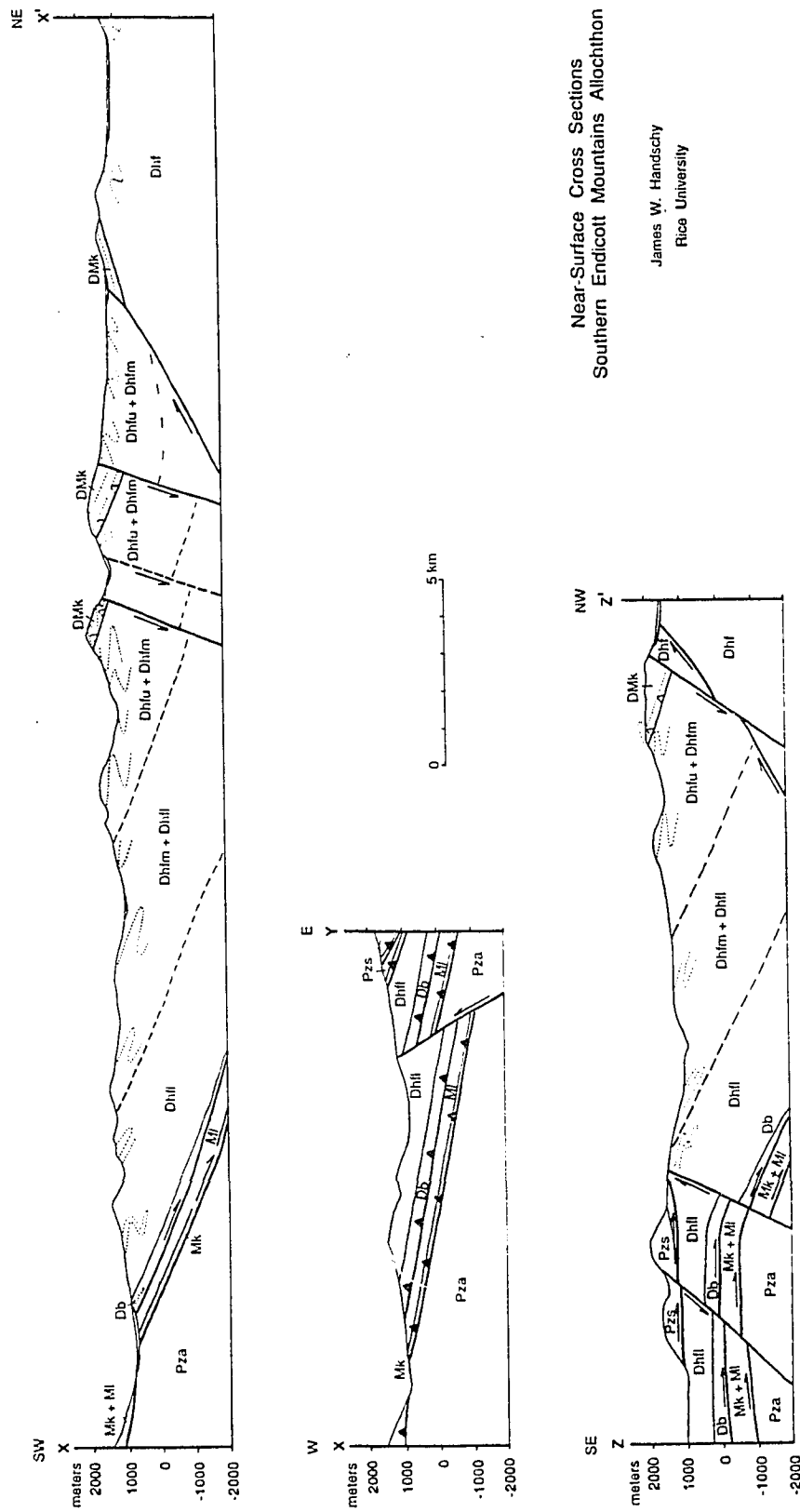


Figure 2.1a - Geologic map of the southern Endicott Mountains allochthon.



Near-Surface Cross Sections
Southern Endicott Mountains Allochthon

James W. Handschy
Rice University

Figure 2.1b - Cross sections X-X', X-Y, and Z-Z' through the southern Endicott Mountains allochthon.

Geologic map and near-surface cross section,
northern Endicott Mountains allochthon,
Brooks Range, Alaska
James W. Handschy

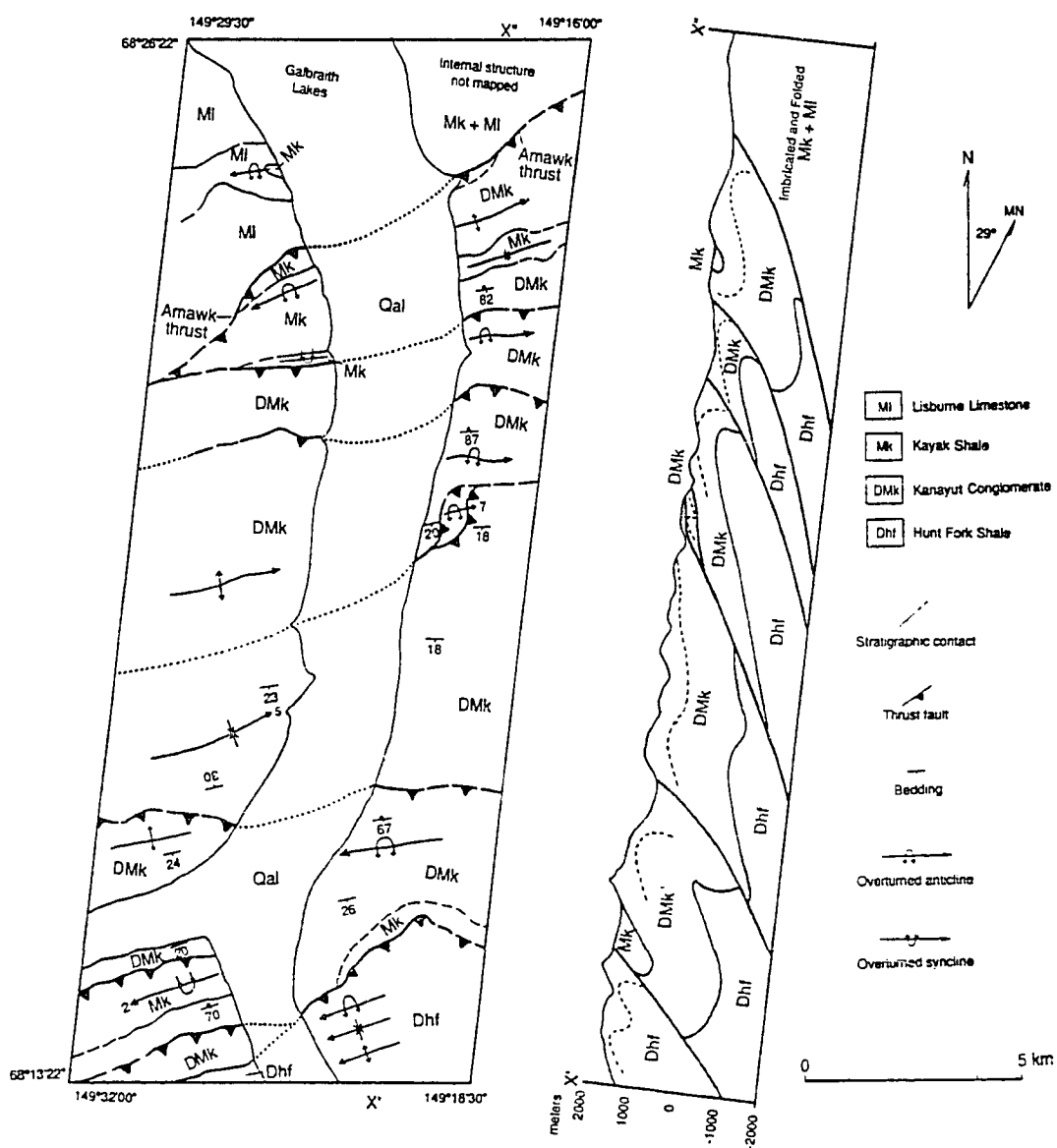


Figure 2.1c - Reconnaissance map and cross section of the northern Endicott Mountains allochthon.

STRUCTURAL RELATIONS

The style and intensity of deformation in the Endicott Mountains allochthon changes with lithology, across-strike position, and depth. Variations in fold style, orientation, and the number of superposed fold phases allow the allochthon to be divided into 5 structural domains (Fig. 2.2a). Domain 1 is the largest and includes the northern thrust imbricates lying between the front of the Brooks Range and the vicinity of Atigun Pass (Fig. 2.2a). Domains 2, 3, 4, and 5 all lie within the southern nappe and their boundaries approximately coincide with lithofacies boundaries within and between the Kanayut Conglomerate, Hunt Fork Shale, and Beaucoup Formation.

Structural domains

Cross-cutting cleavages and fold superposition allow discrimination of four phases of folds in the southern nappe. In domains 1 through 4, where fold vergence can be determined, first phase folds (D1) are north-vergent. In the northern imbricates and the upper part of the southern nappe, D1 is characterized by a single phase of north-vergent inclined folds (Fig. 2.3). In the lower part of the southern nappe, D1 is divided into sequentially superposed structures, D1a and D1b. Superposition of D1b folds on D1a folds occurs where D1a interlimb angles approach 0° and the angle between D1a axial planes and the Amawk thrust is approximately 10° . Upright northeast trending D2 folds and cleavage (S2) are superposed on D1 folds in the Hunt Fork and Beaucoup of the southern nappe. Small D3 folds and a sub-vertical north-northwest to north-northeast striking crenulation cleavage (S3) post-date D2. High-angle south dipping normal faults (Fig. 2.1) also post-date D2 folds, but the temporal relations between D3 and these normal faults is not clear. A dynamic analysis of tension cracks and fault plane lineations (Phelps et al., 1987) suggests that D3 and the high-angle faults are genetically related, but more work is necessary before this contention can be adequately substantiated.

Thrust imbricates in domain 1 (Fig. 2.2a) expose the upper and middle Hunt Fork

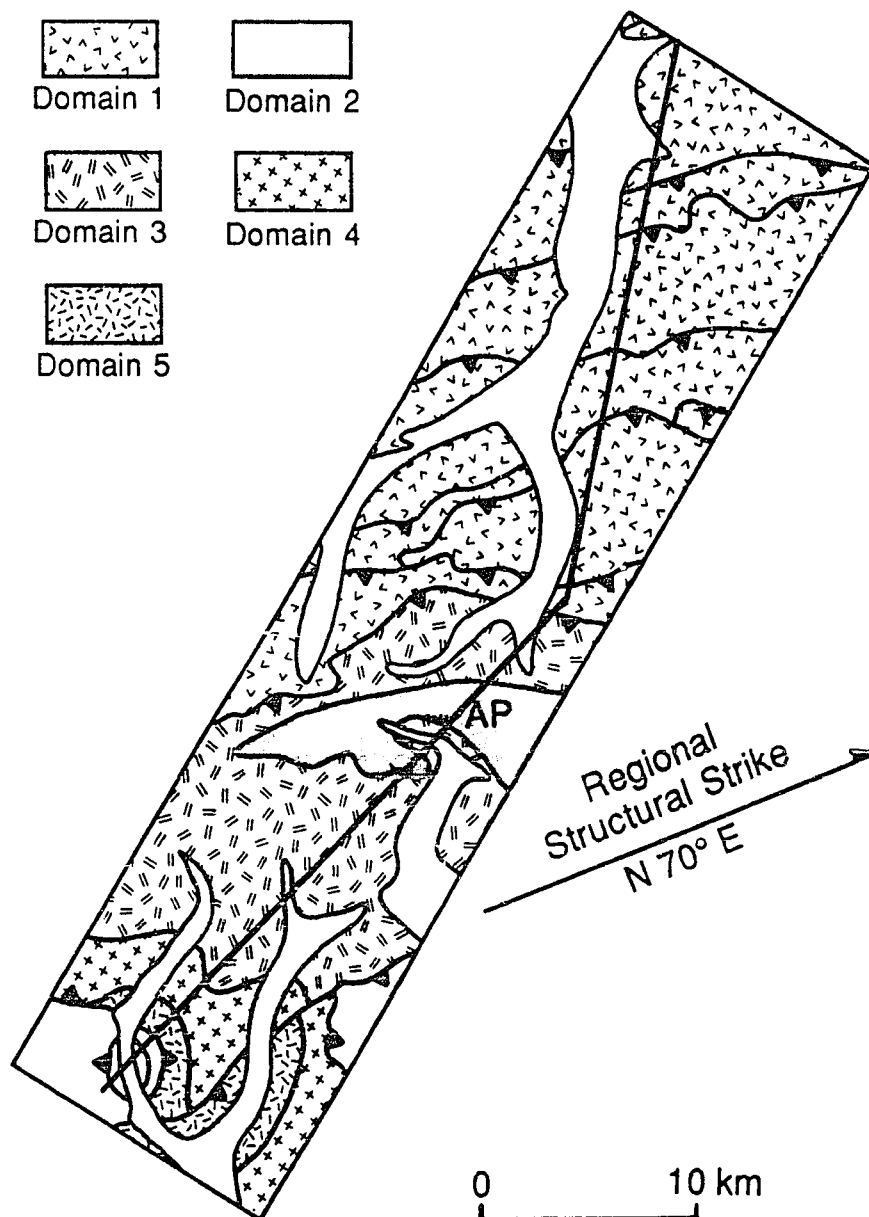
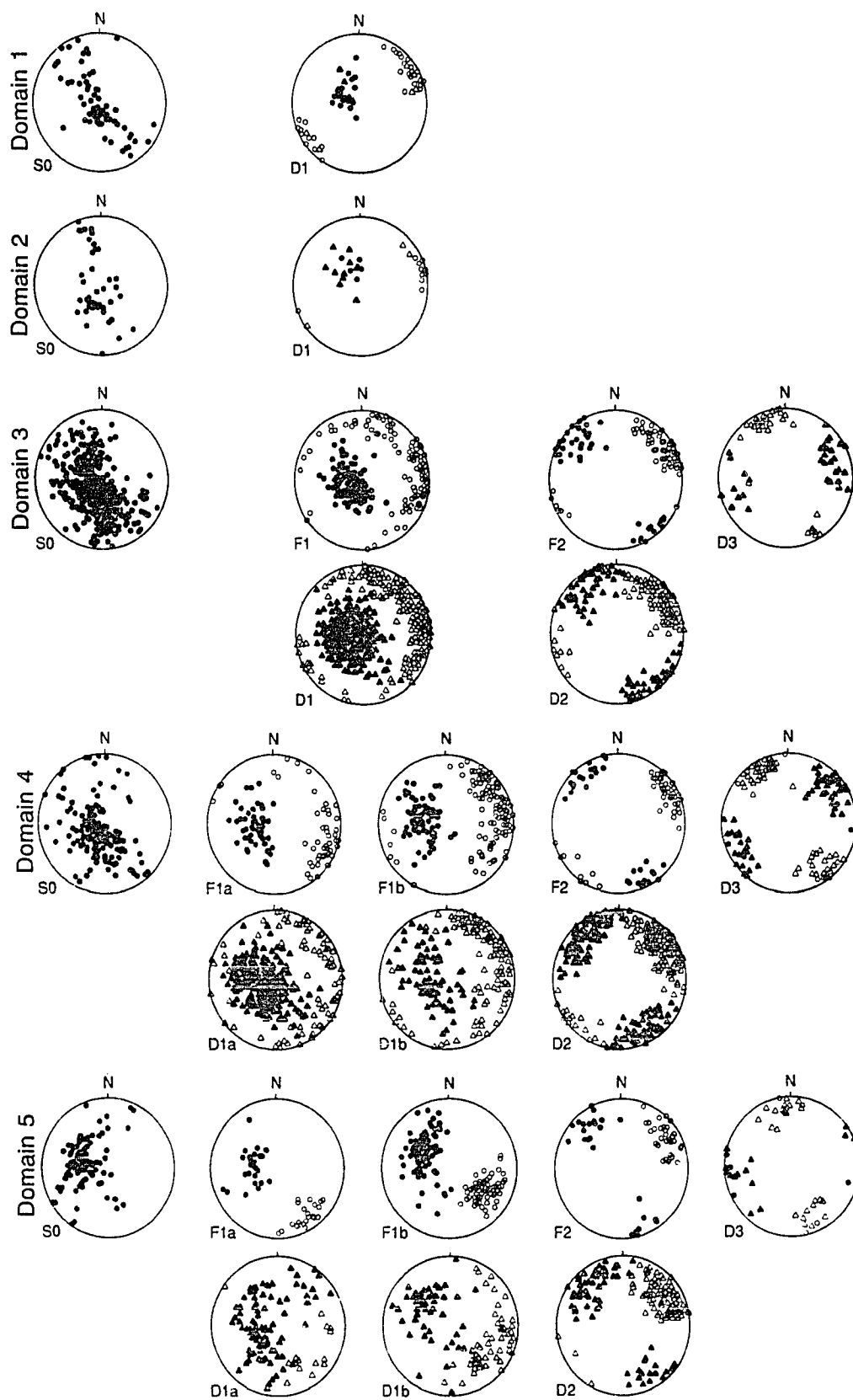


Figure 2.2a - Structural domain map of the study area.

Figure 2.2b - Lower-hemisphere equal-area projections of fold and cleavage data. Solid circles on S0 stereonets are poles to bedding. Open circles are fold axes, solid circles are poles to axial planes, open triangles are intersection lineations, and solid triangles are poles to cleavage on all other stereonets. For D1, D1a, D1b, and D2 in domains 3, 4, and 5 fold data (F) and cleavage data (D) are plotted on separate stereonets.



Shale, Kanayut Conglomerate, Kayak Shale, and part of the Lisburne Limestone.

Exposures of the Hunt Fork are restricted to the southern part of domain 1; whereas the Kayak and Lisburne only crop out in the northern part of the domain. A single phase of open to close (Fleuty, 1964) north-vergent folds characterizes the structure in domain 1. Fold amplitudes range from 0.2 km to 1 km. Fold axes are subhorizontal and trend east-northeast or west-southwest (Fig. 2.2b). Axial planes dip to the south (Fig. 2.2b) and are inclined 30° to 70° relative to the nearest imbricate thrust. Usually all of the stratigraphic units in Domain 1 are folded together, but in the southern part of the domain, the Kanayut is locally detached from the Hunt Fork. Folds in both units have similar amplitudes, wavelengths, and orientations, but the contact between the units is relatively flat.

Domain 2 includes the Kanayut Conglomerate and Kayak Shale exposed at the top of the southern thrust nappe of the Endicott Mountains allochthon (Fig. 2.2a). It is separated from domain 1 by a thrust fault that places Hunt Fork over Kanayut (Fig. 1.2) and from domain 3 by a detachment surface that lies within the transition from Kanayut Conglomerate to Hunt Fork Shale (Fig. 2.4a). As in domain 1, only one phase of north-vergent folds is present in domain 2 (Fig. 2.2b). Fold amplitudes are between 0.5 km and 1 km. Unlike in domain 1, fold axes in domain 2 preferentially plunge to the east-northeast because of their position on the northern flank of the Doonerak duplex. Axial planes dip 20° to 50° toward the south (Fig. 2.2b) and are inclined 40° to 70° relative to the detachment along the Kanayut-Hunt Fork contact which dips 20° toward the north-northeast (Fig. 2.4a). Axial-planar cleavage (S1) is well developed only in the hinges of folds.

The detachment surface along the Kanayut-Hunt Fork contact separates open to close, moderately south dipping asymmetric D1 folds in domain 2 from tight, inclined to recumbent, north-vergent D1 folds with amplitudes of up to 1 km in domain 3 (Fig. 2.4a).

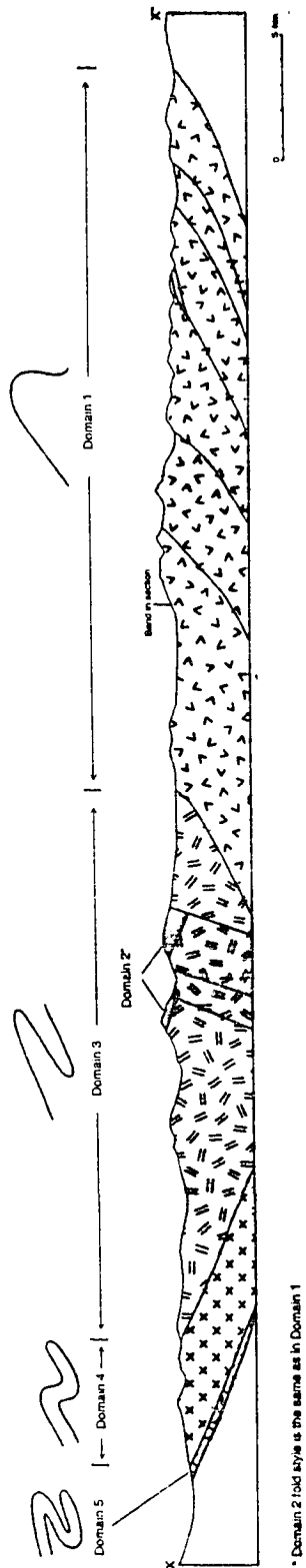
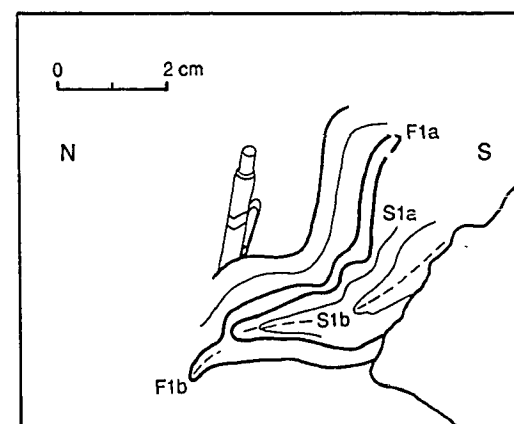
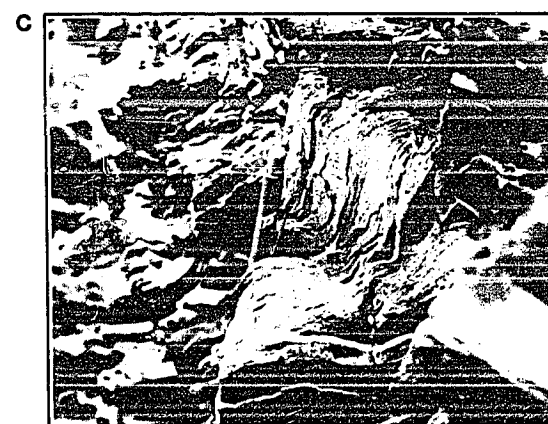
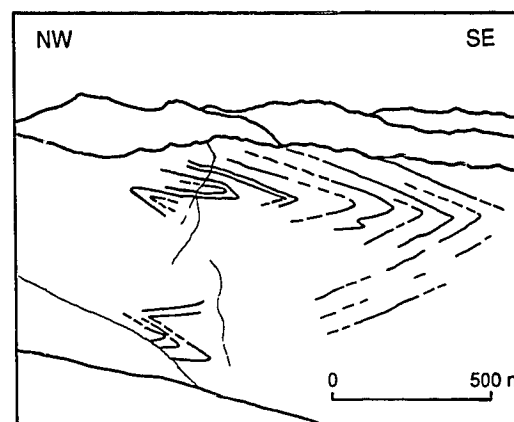
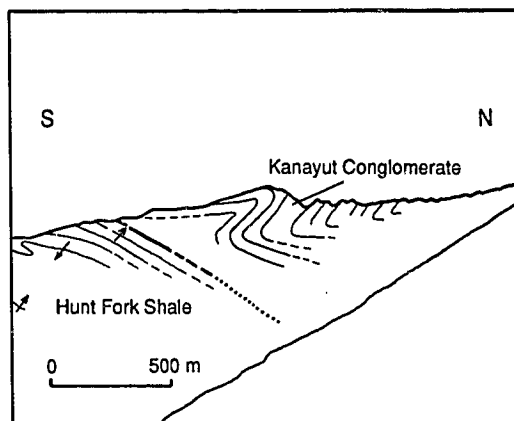
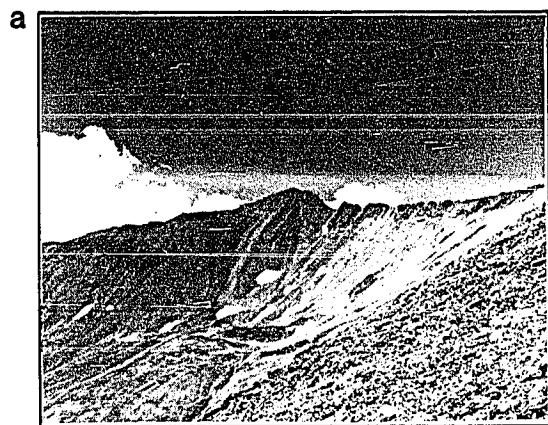


Figure 2.3 - Cross section through the Endicott Mountains allochthon showing spatial distribution of D1 fold style. Location of cross section is shown on Figure 2.1.

Figure 2.4 - Photos and sketches of structural relationships in the Endicott Mountains allochthon: a) Disharmonic folding across the Hunt Fork - Kanayut contact (photo left, sketch right); b) D1 folds in domain 3 (photo left, sketch right); c) D1a and D1b folds in domain 5 (photo left, sketch right).



Superimposed on the D1 folds in domain 3 are small, open, upright northeast trending D2 folds with amplitudes less than 1 m and a crenulation cleavage (S2). Like domain 2, domain 3 is located on the northern flank of the Doonerak duplex. Most D1 axial planes are inclined 10° to 30° relative to the Kanayut-Hunt Fork contact which dips 20° toward the north, and as such have dips between 10° toward the north and 10° toward the south (Fig. 2.2b). Mesoscopic D1 fold axes plunge moderately in various directions, but are concentrated in the northeastern quadrant (Fig. 2.2b). D2 fold axes and macroscopic D1 fold axes plunge toward the east-northeast.

Domain 4 corresponds to the lower Hunt Fork and differs from domain 3 in two important ways. First, the maximum fold amplitudes observed in domain 4 are less than 500 m. Second, D1 structures are divided into two phases, D1a and D1b (Fig. 2.2b). Tight D1a folds have a well developed, closely spaced, axial-planar cleavage (S1a). These D1a structures are folded by open, inclined, north-vergent, asymmetric D1b folds. D1b folds also have an associated cleavage (S1b) which cuts and locally crenulates S1a. Mesoscopic D1a folds measured in domain 4 have amplitudes between 0.5 m and 10 m; whereas D1b folds have amplitudes between 0.5 m and 3 m. Superimposed on D1a and D1b folds are small, open, upright, northeast trending D2 folds and an associated (S2) crenulation cleavage. Domain 4 is folded by the Doonerak duplex, and as such the orientation of structures varies with location. North of the duplex, the boundary between domains 3 and 4 is approximately parallel to both the Amawk thrust and the Kanayut-Hunt Fork contact (Fig. 2.2a). East of the duplex, the strike of D1 structures mimics the strike of the Amawk thrust where it plunges into the subsurface along the northeastern corner of the Doonerak window. Throughout domain 4, D1b axial planes and S1b are inclined 20° to 50° relative to the Amawk thrust and, after the effects of D1b and D2 folding have been removed, D1a axial planes and S1a are inclined approximately 10° relative to the Amawk thrust.

The lower Hunt Fork - Beaucoup contact is the boundary between domains 4 and 5. In domain 5, D1a and D1b folds are tight to isoclinal (Fig. 2.4c). Bedding, S1a, and S1b are all parallel except in the hinges of folds. The largest D1 folds found in domain 5 have amplitudes of less than 100 m. Superimposed on the D1a and D1b folds are open, upright D2 folds with amplitudes less than 1 m and a crenulation cleavage (S2). Like domain 4, domain 5 wraps around the northeastern corner of the Doonerak duplex. D1a and D1b axial planes are inclined between 0° and 10° relative to the Amawk thrust. D1a and D1b fold axes are concentrated in the southeastern quadrant approximately parallel to stretching lineations (Fig. 2.2b). As in all of the domains, D2 fold axes trend east-northeasterly.

Deformation in domain 5 is strongly lithology dependant. When compared to the intensely folded shales which comprise most of the domain, limestone reefs and sandstone/conglomerate beds thicker than 2 m are relatively undeformed. Top indicators, where found, indicate that these competent units are consistently upright. Unit boundaries are either faults or shear zones which exhibit increasing amounts of shear strain into adjacent shaley units.

Fold style and cleavage

Fold style varies with lithology, structural position, and bulk strain within the Endicott Mountains allochthon. In domains 1 and 2, D1 structures are all large, open to close, class 1b folds (Ramsay, 1967, p.357). Parasitic mesoscopic D1 folds are uncommon in the Kanayut Conglomerate and Lisburne Limestone, and are only locally important in the Hunt Fork Shale and Kayak Shale. In the Kanayut, S1 cleavage is developed only in the hinges of folds. In all lithologies, S1 cleavage is zoned (Type C; Gray, 1978). D2 and D3 structures are not developed in domains 1 and 2.

In the Hunt Fork of domain 3, macroscopic D1 folds have approximately the same amplitudes as in domains 1 and 2, but the amplitude/wavelength ratio is higher (Table 2.1). Several orders of parasitic mesoscopic D1 folds are common on the limbs of the

	Fold Class	α	α / λ	Interlimb Angle
Domain 1				
D1	1b	≤ 1 km	0.5 - 1.0	$120^\circ - 45^\circ$
Domain 2				
D1	1b	≤ 1 km	0.5 - 1.0	$120^\circ - 45^\circ$
Domain 3				
D1	1c	≤ 1 km	1.5 - 3.0	$45^\circ - 10^\circ$
D2	1b - 1c	≈ 1 m	0.2 - 0.5	$> 120^\circ$
D3	c.c. only			
Domain 4				
D1a	2	< 500 m	> 5.0	$\leq 10^\circ$
D1b	1c	< 10 m	0.5 - 1.5	$90^\circ - 30^\circ$
D2	1b - 1c	≈ 1 m	0.2 - 0.5	$> 120^\circ$
D3	c.c. only			
Domain 5				
D1a	2 - 3	< 500 m	$< \infty$	$\approx 0^\circ$
D1b	2	< 100 m	> 5.0	$\leq 10^\circ$
D2	1b - 1c	≈ 1 m	0.2 - 0.5	$> 120^\circ$
D3	c.c. only			

Table 2.1 - Fold characteristics in the Endicott Mountains allochthon. Fold classification is from Ramsay, 1967. α is fold amplitude. λ is fold wavelength.

macroscopic folds. Most macroscopic D1 folds are class 1c. The style of mesoscopic D1 folds varies from class 1c to class 3 depending on the lithologies involved and bedding thickness. Beds greater than 1 cm thick and amalgamated packages of siltstone and/or sandstone generally form asymmetric class 1c folds. Siltstone or sandstone beds less than 1 cm thick and flanked by shale often form class 2 or rootless class 3 folds. S1 cleavage is always closely spaced (Type B) and accompanied by syntectonic phyllosilicates.

Macroscopic D1a folds in domain 4 have amplitude/wavelength ratios similar to D1 folds in domain 3, but the maximum amplitude is smaller by a factor of two. D1a folds in Domain 4 are more difficult to identify than D1 structures in domain 3. Most D1a folds in domain 4 are mesoscopic class 1c and class 2 folds with amplitudes less than 100 m. Small rootless class 3 folds are infrequent because discrete, thin sandstone and siltstone beds are rare. D1b folds in domain 4 generally belong to class 1c. S1a cleavage is always closely spaced (Type B) and accompanied by recrystallized phyllosilicates along the cleavage planes. S1b cleavage is variable between closely spaced (Type B) and zoned (Type C). Where zoned, S1b crenulates S1a. Recrystallized phyllosilicates are not as well developed along S1b cleavage planes.

D1a and D1b folds in domain 5 are mesoscopic class 1c and 2 folds with amplitudes less than 100 m. Amplitude/wavelength ratios are very large. S1a and S1b cleavages are equally well developed and only distinguishable in the hinges of D1b folds.

D2 structures are upright to inclined, class 1b folds with amplitudes less than 1m and amplitude/wavelength ratios of approximately 2:3. S2 cleavage is variable from discontinuous (Type A), to closely spaced (Type B), to zoned (Type C) and locally crenulates S1. D2 structures are equally well developed in domains 3 through 5 south of Atigun pass, they decrease northward in domain 3 north of Atigun pass, and they are absent in domains 1 and 2. The lack of D2 structures in the Kanayut of domain 2 is appears to be a function of lithology. Cleavage is rare in the well cemented conglomerate and sandstone

beds which comprise most of the Kanayut, and, possibly because amalgamated packages of beds in the Kanayut are several meters thick, small scale folds with moderate to large ($>1/10$) amplitude/wavelength ratios are not developed. The northward decrease of D2 in domain 3 and the absence of D2 structures in the Hunt Fork of domain 1 is more difficult to explain. Based on cross-cutting relationships between faults and D2 structures adjacent to the roof thrust of the Doonerak duplex, Seidensticker et al. (1987) have presented a model in which the northward decrease in the intensity of D2 is a function of location relative to the frontal culmination of the duplex. In their model (Seidensticker et al., 1987), the frontal culmination of the Doonerak duplex acts as a buttress causing D2 shortening south of the culmination to be accommodated by shortening along conjugate shears, thus explaining the bi-vergent nature of D2 structures in domains 3 through 5, the decrease in the intensity of D2 structures in domain 3, and the absence of D2 structures in domain 1 (C.M. Seidensticker, personal comm., 1988).

D3 is usually a steeply dipping, zoned (Type C) crenulation cleavage, however, inclined D3 folds are locally present in domains 4 and 5. D3 folds are open to close class 1b folds with amplitudes less than 2 m and amplitude/wavelength ratios between 2:3 and 1:1. Axial planes strike north-northwest to north-northeast and dip toward both the east and the west.

Thrust faults

In addition to the Amawk thrust, the basal thrust of the Endicott Mountains allochthon (Mull, 1982), there are six major imbricate thrust faults within the Endicott Mountains allochthon (Fig. 2.1). All of the imbricate thrusts place Hunt Fork over Kanayut, Kanayut over Kanayut, and Kanayut over Kayak and/or Lisburne (Fig 3). Northward displacements along these faults range from greater than 100 km along the Amawk thrust (Oldow et al., 1987; Mull et al., 1987) to less than 5 km along some of the imbricate thrusts (Fig. 1.2). With the exception of the southern thrust nappe, all of the imbricate sheets are in domain 1.

Within the southern thrust nappe, intraformational thrusts and bedding parallel

detachment surfaces are common. The distance between intraformational thrusts in the southern nappe varies from over 1 km to less than 10 m, and the amount of demonstrable displacement along most of the intraformational thrusts is between 1 m and 500 m. Because of the relatively homogeneous nature of shales in the Hunt Fork and Beaucoup, the amount of displacement along some intraformational thrusts cannot be determined and it is often difficult to trace the faults laterally. Although closely spaced faults are present in domain 3, the maximum spacing between intraformational thrusts decreases from greater than 1 km in upper part of domain 3 to less than 500 m in domain 5 and is similar to the depth related decrease in maximum fold size noted in Table 2.1.

Exposures of the Amawk thrust along the flanks of the Doonerak duplex (Oldow et al., 1984, 1987; Julian et al., 1984) and near Galbraith Lakes demonstrate that the Amawk thrust cuts up-section from within the Beaucoup Formation south of the Doonerak window to near the base of the Kanayut Conglomerate beneath the leading edge of the allochthon (Fig. 1.2). Along the southern flank of the Doonerak duplex, approximately 1.5 km of the Beaucoup Formation structurally overlies the lower Paleozoic Apoon assemblage (Phelps, 1987). Seven kilometers to the north, on the northern flank of the duplex, the Amawk thrust lies near the top of the Beaucoup Formation. Along strike, the Amawk thrust also changes stratigraphic position (Fig. 2.5). Immediately adjacent to the Dalton Highway, east of the Doonerak duplex, the Amawk thrust lies at least 1 km beneath the Hunt Fork - Beaucoup contact. Along the northeastern corner of the duplex the Amawk thrust cuts up-section into the lower Hunt Fork Shale (Phelps, 1987). Farther to the west, along the northern margin of the Doonerak duplex, it again cuts down-section into the Beaucoup (Fig. 2.5).

In the structural analysis section, reference is made to the angular relationship between axial planes of D1 folds and the "inferred orientation of the Amawk thrust." The orientation of the Amawk thrust beneath the southern Endicott Mountains allochthon is constrained by:

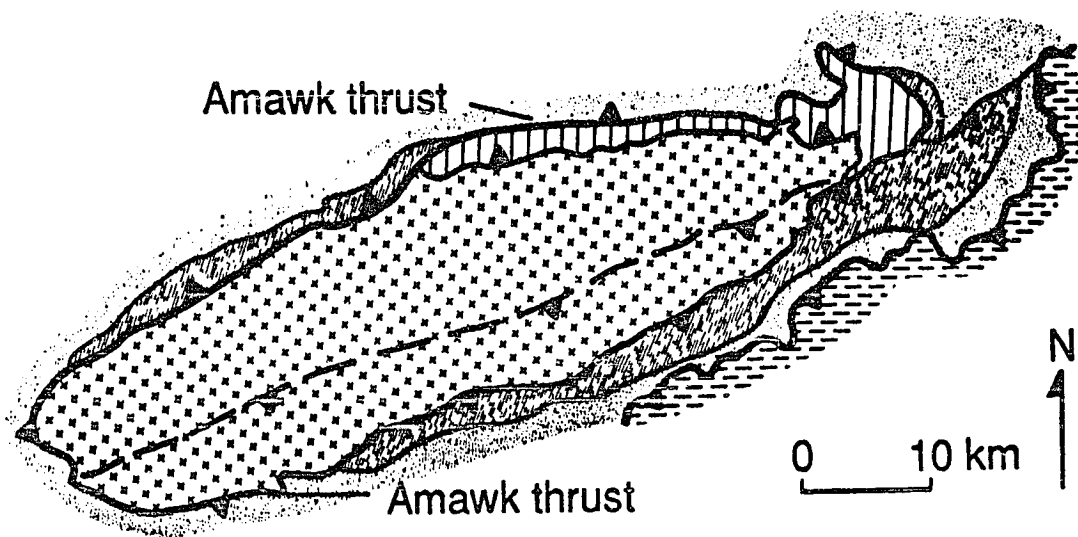


Figure 2.5 - Regional map of the Amawk thrust along the margins of the Doonerak duplex (modified from Oldow et al., 1987). See Figure 1.2 for legend.

- 1) outcrops of the Amawk thrust along the margins of the Doonerak window (Fig. 2.1a);
- 2) the axis of the synclinorium which is located in front of the Doonerak duplex (Fig. 1.2). Clearly, these constraints only provide an approximate orientation for the Amawk thrust in the subsurface.

If the Hunt Fork - Beaucoup contact were a simple stratigraphic contact, this along-strike fault topography might reflect a high-relief unconformity between the two units. Alternative explanations include, folding of the contact before forward propagation of the Amawk thrust, and/or the positions of lateral ramps. Because the Hunt Fork - Beaucoup contact also forms the boundary between domains 4 and 5, which are distinguished on the basis of D1b fold orientation, along-strike truncation of the contact requires a structural origin. Domain 5 structures are only developed in the Beaucoup; they are not present in the lower Hunt Fork where it overlies the Amawk thrust. Progressive refolding of D1a and reorientation of D1b from domain 4 to domain 5 indicates that the two domains were at least partially coupled during D1 folding. The absence of domain 5 structures in the lower Hunt Fork adjacent to the Amawk thrust suggests that the fault ramped into the Hunt Fork during the latest stages of, or following, D1 folding.

The youngest Brookian thrust fault in the study area is a relatively steep south dipping thrust in the southern nappe that places Beaucoup over Hunt Fork (Figs. 4a and 7). This fault cuts the Amawk thrust near the eastern end of the Doonerak duplex and post-dates D1 folding. Oldow et al. (1987) interpret this fault to be an out-of-sequence thrust associated with the late stage of duplex formation beneath the Endicott Mountains allochthon. Rather than merging into the Amawk thrust, this late-stage thrust cut up-section through the duplex, off-setting the Amawk thrust.

Boudinage

Two distinct morphologies of boudinage are exposed in domains 3 and 4. The most conspicuous boudins occur in sandstone beds between 10 cm and 1 m thick. Intermediate

boudin axes are often several meters long and separated by straight to sigmoidal tension cracks which indicate less than 10% extension. These large boudins occur on both limbs of macroscopic folds and have long axes that are approximately parallel to bedding-S1 intersection lineations and D1 fold axes. In domain 3, most boudins trend northeast; whereas in domain 4 they trend east or southeast. Where bedding tops can be determined, the orientation of tension cracks indicates south-over-north shear in upright beds and north-over-south shear in overturned beds.

The second boudin morphology is found in thin sandstone and siltstone layers contained within a shaley matrix. These boudins occur on both upper and lower limbs of mesoscopic folds. Characteristically they are bound on two sides by cleavage planes and have long axes consistently parallel to bedding-S1 intersections. In domain 3, most boudins trend northeast; whereas in domain 4 they trend southeast. The distance between boudins is commonly many times greater than the length of the intermediate boudin axes, indicating several hundred percent extension. In some localities, the intermediate axes of the boudins within an individual bed are parallel to each other; whereas in other locations, the boudins are systematically rotated. Boudin rotation varies with location, but in domain 3 the rotation usually indicates south-over-north shear in the upper limbs and north-over-south shear in the overturned limbs of macroscopic D1 folds. In domains 4 and 5, and adjacent to intraformational thrusts, boudin rotation almost always indicates south-over-north shear.

Strain indicators

Sheared Skolithos burrows, stretched conglomerates, stretched breccia clasts, and deformed fossils provide evidence for the direction of tectonic transport during thrusting (Fig. 2.6). In the upper Hunt Fork of domains 2 and 3, sheared Skolithos burrows are found in two structural settings. Along the contact between the Kanayut and Hunt Fork, immediately west of Atigun Pass (Fig. 1.2), Skolithos burrows in thinly bedded

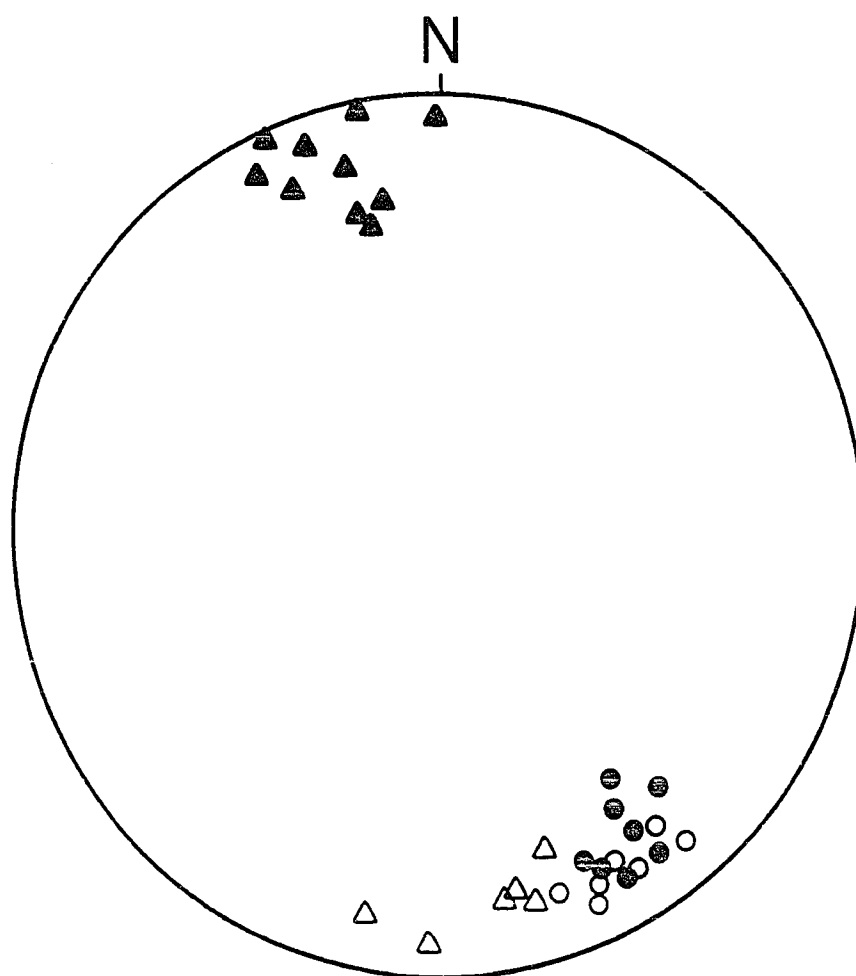


Figure 2.6 - Stretching lineations in the Endicott Mountains allochthon. Lower-hemisphere equal-area projection. Solid triangles are from sheared Skolithos and bedding plane lineations in domain 3, open triangles are sheared corals in domain 5, open circles are stretched breccia clasts in domain 4, and solid circles are stretched pebbles in domain 6.

sandstones are sheared between 45° and 70° toward the north-northwest. Slickenside lineations on bedding planes in the thin shale-partings between the sandstone beds are parallel to the direction of shear, indicating that shear strain locally exceeds $\gamma=2.75$. Below the Kanayut-Hunt Fork contact farther to the southwest, sheared Skolithos burrows are found on both limbs of macroscopic folds. Burrows in the upper limbs are sheared as much as 60° toward the north-northwest; whereas burrows in the overturned limbs are sheared between 42° toward the north-northwest and 55° toward the south-southeast. As elsewhere, slickenside lineations on bedding planes indicate that these angles only provide minimum values for shear strain.

Breccia clasts in domain 4 near the base of the Skajit allochthon, stretched conglomerates in domain 5, and consistently aligned, deformed corals along the bases of limestone reefs in domain 5 also indicate north-northwest or south-southeast stretching (Fig. 2.6). R_f/ϕ analysis indicates that undeformed conglomerate clasts had axial ratios between 1.0 and 1.6 and that there has been up to 400% extension parallel to stretching lineations (Table 2.2).

Cleavage in Hunt Fork and Beaucoup mudrocks is apparently the product of dissolution of relatively soluble minerals (e.g. quartz and chert) and the subsequent concentration and alignment of less soluble phyllosilicates along dissolution planes. Microlithons between cleavage planes contain abundant quartz and chert grains in a phyllosilicate-rich matrix; whereas cleavage planes are composed almost exclusively of phyllosilicates. Contacts between sand- and silt-sized grains within deformed mudrocks are rare, but where present, are irregular and/or sutured, indicating removal of material by pressure solution (Durney, 1972). Grains which are separated from other grains by phyllosilicate-rich cleavage planes are often elongate and their long axes are parallel to the cleavage planes. In some samples, grain boundaries adjacent to cleavage planes are pitted, suggesting dissolution. In other samples, however, there is no evidence for

	ψ	θ	Rs Meso	Rs Micro	α
Domain 1		$50^{\circ} \pm 20^{\circ}$			0.6–0.7
Domain 2		$60^{\circ} \pm 10^{\circ}$			0.6–0.7
Domain 3	$45^{\circ} - 70^{\circ}$	$20^{\circ} \pm 5^{\circ}$	2.9	<1.2	
Domain 4		$10^{\circ} \pm 5^{\circ}$	3.2	1.6	
Domain 5		$8^{\circ} \pm 5^{\circ}$	5.1	2.1	

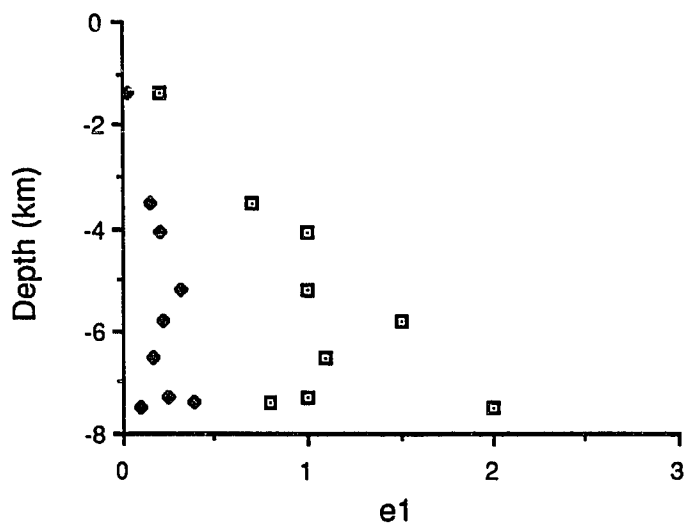
Table 2.2 - Measured and estimated strain in the Endicott Mountains allochthon. ψ is shear strain measured directly from sheared Skolithos burrows. θ is the angle between the Kanayut-Hunt Fork contact and D1 axial planes in domains 1, 2, and 3, and the inferred angle between the Amawk thrust and D1a axial planes in domains 4 and 5. Note: The Kanayut-Hunt Fork contact and the Amawk thrust are approximately parallel on the northern flank of the Doonerak duplex (Fig. 2.1b). Rs meso is the x:z axial ratio of stretched conglomerate and breccia clasts. Rs micro is the x:z axial ratio in deformed mudrocks determined using the Fry technique. α is the amount of shortening by folds in the Kanayut Conglomerate where bed thickness is relatively constant and cleavage is rare.

dissolution along grain boundaries. In these samples, the elongate character of the grains apparently has a detrital origin and alignment of grains parallel to cleavage planes may be the product of grain rotation.

Fry analysis (Ramsay and Huber, 1983) of sand- and silt-grain distributions in cleaved mudrocks from domains 3, 4, and 5 indicate that the principal extension directions ($1+e1$) parallel stretching lineations, and that the principal flattening direction ($1+e3$) is almost always perpendicular to S1 cleavage planes. Axial ratios determined using the Fry method vary with location, but consistently indicate lower strains than stretched pebbles and breccia clasts (Table 2.2). Pressure shadows composed of quartz and, less frequently quartz plus phyllosilicates, are commonly developed on detrital grains within microlithons. Pressure shadow lengths vary from grain to grain and do not always indicate consistent extension within an individual sample. They do, however, usually indicate more extension than measured using the Fry method (Fig. 2.7a).

If deformation was constant volume, both techniques should yield similar values for the amount of extension. If deformation was accompanied by a volume loss, then the Fry technique should indicate greater extension, and, alternatively, if deformation is accompanied by a volume gain, then pressure shadows should indicate greater extension. Because pressure shadows in domains 3 through 5 indicate more extension than estimated by the Fry analysis, two possibilities exist: 1) deformation was accompanied by a volume gain, or; 2) entire grains have been dissolved along cleavage planes and the strain measured using the Fry technique is too low. As noted above, dissolution of grains is evidenced by pitted, irregular, and/or sutured grain boundaries, but it is impossible to evaluate whether entire grains are missing. Likewise, the only evidence for volume gain is that pressure shadows indicate greater extension than estimated using the Fry method (Fig. 2.7a). Since the question of volume loss or volume gain cannot be adequately evaluated on the basis of microfabirc data, other information is needed help constrain volume

a.



b.

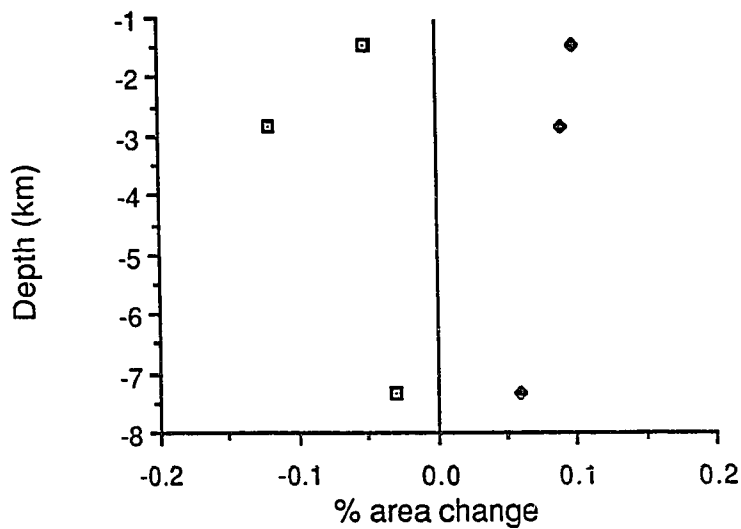


Figure 2.7 - a) Maximum extension (e_1) in the xz plane vs. depth. Open squares are values determined from pressure shadows. Solid diamonds are values determined using Fry analysis. b) Comparison of the amount of material removed by pressure solution (open squares) to the amount of material deposited in syntectonic veins (solid diamonds) in sandstone beds in the Hunt Fork Shale and Beaucoup Formation. Data are two-dimensional (area) and were measured perpendicular to S_1 cleavage.

changes during deformation.

Dissolution in carbonates and some sandstones is evidenced by the presence of stylolites and cleavage planes. Although pressure shadows are infrequent in cleaved Hunt Fork and Beaucoup sandstones, syntectonic veins are fairly common. Compositions of syntectonic veins within the sandstone beds mimic the bulk compositions of the sandstones they are deposited in (i.e. calcite veins in calcareous sandstones and quartz veins in quartz- and chert-rich sandstones), suggesting that the vein material was derived from dissolution of the host rock. Based on the assumption that dissolution of grains in sandstones which exhibit discontinuous (Type A) cleavage is approximately homogeneous, the absence of pressure shadows in Hunt Fork and Beaucoup sandstones allows the amount of dissolution to be evaluated using the Fry method. The amount of dissolution in the sandstone can then be compared to the amount of material filling veins in the same bed. Application of this technique to two Hunt Fork sandstone beds and one Beaucoup sandstone sample shows that the amount of material removed by pressure solution is slightly less than the amount of material precipitated within adjacent veins (Fig. 2.7b).

In limestone reefs, stylolites are oriented at various angles with respect to the reef margins, are usually widely spaced (>10 cm), and have tooth amplitudes of less than 0.5 cm suggesting relatively small amounts of dissolution (Alvarez et al., 1978). Syntectonic veins in the reefs are composed of calcite and may have been sourced by pressure solution along the stylolites. There is no evidence for dissolution within stretched pebble conglomerates.

Despite the ambiguity of mudrock microfabrics, which indicate that there was either a volume gain during deformation or that entire grains have been dissolved and that the Fry technique is unusable in Beaucoup and Hunt Fork mudstones, comparison of dissolution and vein precipitation in sandstones, stylolite spacing in carbonates, and the absence of

cleavage planes in deformed pebble conglomerates all suggest that deformation of the southern Endicott Mountains allochthon was approximately constant volume.

STRUCTURAL ANALYSIS

Seven fundamental observations provide the basis for interpreting deformation in the Endicott Mountains allochthon: 1) the northern imbricates (domain 1) are composed mostly of Kanayut Conglomerate; whereas the southern nappe (domains 2, 3, 4, and 5) is composed mostly of Hunt Fork and Beaucoup; 2) provenance of Albian syntectonic sediments near Galbraith Lakes indicate that the Kanayut was exposed during emplacement of the Endicott Mountains allochthon; 3) the preserved northern limit of the Skajit allochthon does not overlap the frontal imbricates of the Endicott Mountains allochthon; 4) lateral and vertical facies relations indicate that the Kanayut, Hunt Fork, and Beaucoup in the southern Endicott Mountains allochthon are in correct stratigraphic order; 5) within the southern nappe, the number of fold phases and the amplitude/wavelength ratio of D1 folds increases with depth; 6) bedding parallel shear zones are preferentially developed along contacts between mechanically different lithologies and increase in frequency with depth, and; 7) quantitative strain measurements indicate that strain increases with depth.

Controls on structural style

The change in structural style from imbricate thrust sheets and large single-phase folds in domain 1 to heterogeneous intranappe deformation in domains 2 through 5 appears to be the product of mechanical differences between the Kanayut Conglomerate and the underlying shales, the relative thicknesses of the units, the depth of deformation, and the amount of strain. Mechanical differences between the units are evidenced by disharmonic folds across the Kanayut-Hunt Fork contact and, locally, by a decoupling surface between the two units that is characterized by breccia zones and mylonites (Fig. 2.4a). Detachment of the Kanayut from the Hunt Fork is less common and less conspicuous in the northern

imbricates than in the southern nappe because folds in both units have similar geometries and orientations. Locally, however, the contact between folded Kanayut and folded Hunt Fork is flat, indicating slip between the two units. Fold kinematics and small scale kinematic indicators (e.g. Skolithos burrows, mylonites, etc.) along the contact consistently indicate south-over-north shear.

Because of the northward thickening wedge geometry (Fig. 1.2b) and relative rigidity of the Kanayut Conglomerate, shortening in domain 1 is preferentially accommodated by thrust imbrication. If deformation was controlled exclusively by these mechanical differences, however, structures characteristic of the Hunt Fork of domain 3 would be developed in the Hunt Fork of domain 1 as well. The lack of fold reorientation in the Hunt Fork of domain 1 suggests that other factors contributed to the change in structural style from the northern imbricates to the southern nappe. Aside from the relative proportions of Kanayut and Hunt Fork, the most obvious difference between the northern imbricates and the southern nappe is the thickness of overburden during deformation. Syntectonic clastics exposed along the front of the central Brooks Range were derived almost exclusively from the Kanayut Conglomerate, indicating that at least part of the deformation in the northern imbricates occurred at the surface. In contrast, exposures of the Skajit allochthon to the south, east, and northeast of the Doonerak duplex (Fig. 1.2), demonstrate that the southern nappe was partially, or completely, overlain by between 1 km and 10+ km of overburden during deformation.

Throughout the southern nappe, formation contacts, sedimentary facies boundaries, domain boundaries, intraformational thrusts, and the Amawk thrust (Fig. 2.1) are approximately parallel. Sedimentary facies are, for the most part, in normal stratigraphic order despite intranappe deformation. This suggests that the southern nappe deformed in a banded fashion and that the depth related increase in deformation intensity reflects a strain gradient.

Changes in D1 fold style and orientation are the most obvious indicators of strain-depth relationships (Fig. 2.3). As depth increases, the angles between bedding, cleavage, and the inferred orientation of the Amawk thrust decrease (Fig. 2.8). D1 fold axes become increasingly reoriented, changing from a strike parallel point concentration in domain 2, to girdle distributions in domains 3 and 4, and then to a dip parallel point concentration in domain 5 (Fig. 2.9). The rotation of axial planes toward a shear zone boundary (in this case, the Amawk thrust) and the alignment of linear features parallel to the direction of stretching has been well documented in shear zones at many scales (Ramsay and Graham, 1970; Sanderson, 1982; etc.). In the Endicott Mountains allochthon, the systematic decrease in the angle between axial planes and the Amawk thrust from domain 3 to domain 5 is interpreted to indicate that amount of shear strain increases as the distance from the fault decreases. The appearance of D1b folds in domain 4 coincides with very small D1a interlimb angles (Table 2.1; Fig. 2.8b) and increasing alignment of D1a fold axes and stretching lineations, and apparently reflects refolding of D1a folds as they became approximately parallel to the direction of shear.

Relative timing of intranappe deformation

D1 structures in the Endicott Mountains allochthon illustrate that different deformational phases can form concurrently in different parts of the same thrust sheet. Because domains 3, 4, and 5 are not separated by sharp boundaries or major detachment surfaces, but are instead transitional into each other, the systematic, progressive reorientation and tightening of D1 folds and refolding of D1a folds is interpreted to indicate that deformation in these domains was continuous in both space and time. As noted above, strain rotation of D1 folds increases with depth in the southern nappe and superposition of D1b folds on D1a folds occurs in domains 4 and 5 where D1a interlimb angles approach zero and the inferred angle between the Amawk thrust and D1a axial

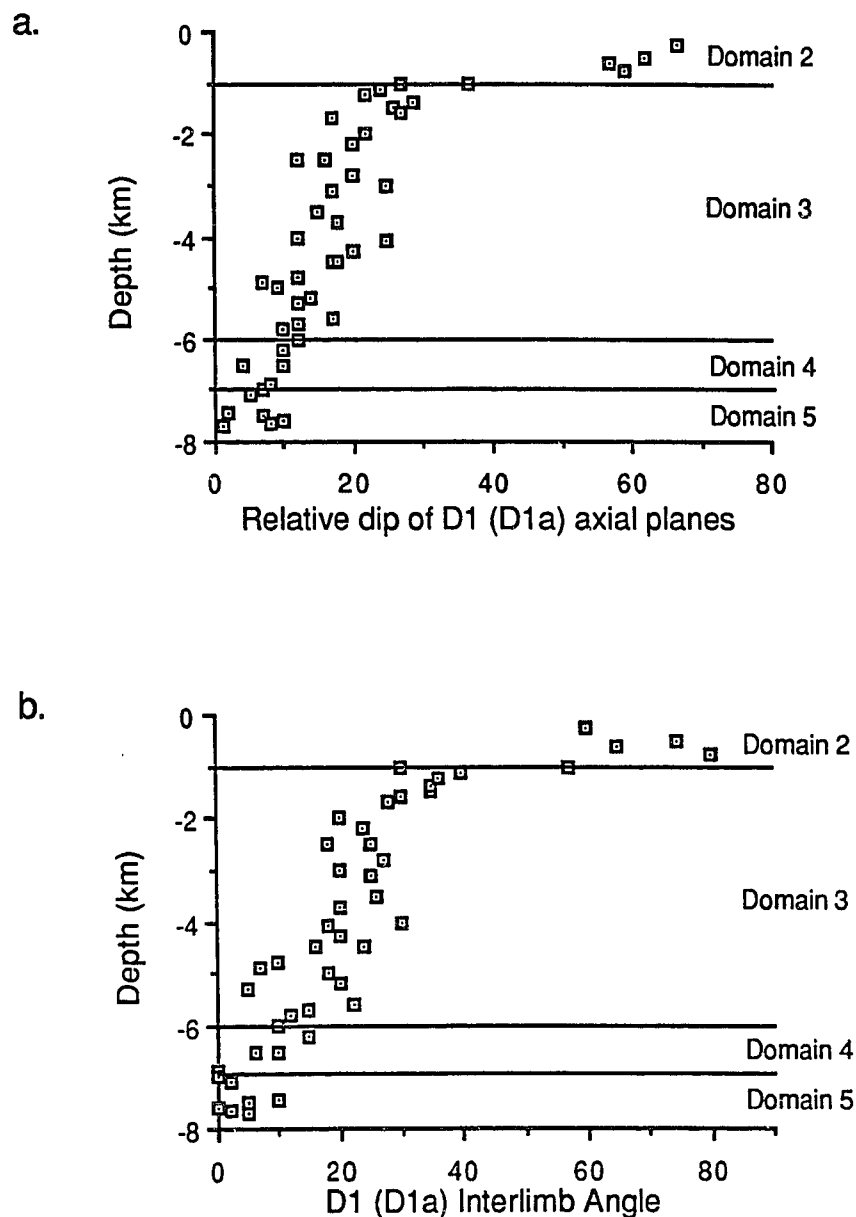


Figure 2.8 - Graphs of depth related changes in D1 fold orientation and tightness in the southern Endicott Mountains allochthon. a) Relative angles between D1 axial planes and the Kanayut-Hunt Fork contact in Domains 2 and 3, and between D1a axial planes and the Amawk thrust in Domains 4 and 5. Note: Along the northern flank of the Doonerak duplex, where both the Amawk thrust and the Kanayut-Hunt Fork contact are exposed, the Amawk thrust is approximately parallel to the Kanayut-Hunt Fork contact (Fig. 2.1). b) D1 interlimb angles. The approximate depths of domain boundaries are plotted for reference.

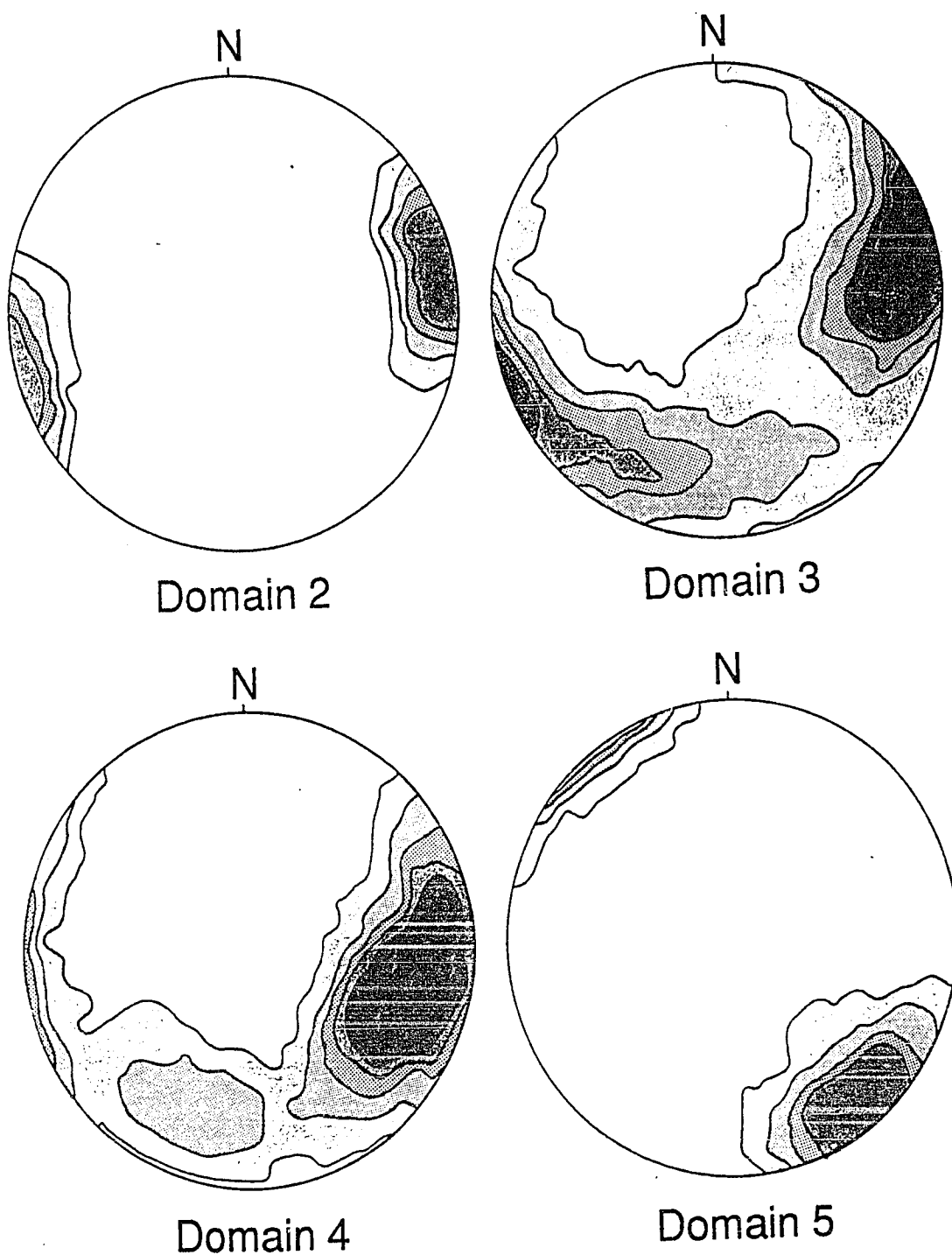


Figure 2.9a - Structurally corrected lower-hemisphere equal-area plots of D1 fold concentrations. The effects of D2 folding have been removed from all domains and D3 folding has been removed from domains 4 and 5. Contours are 5% of data per 5% of area. Dark areas represent greatest concentrations, light areas are smallest concentrations.

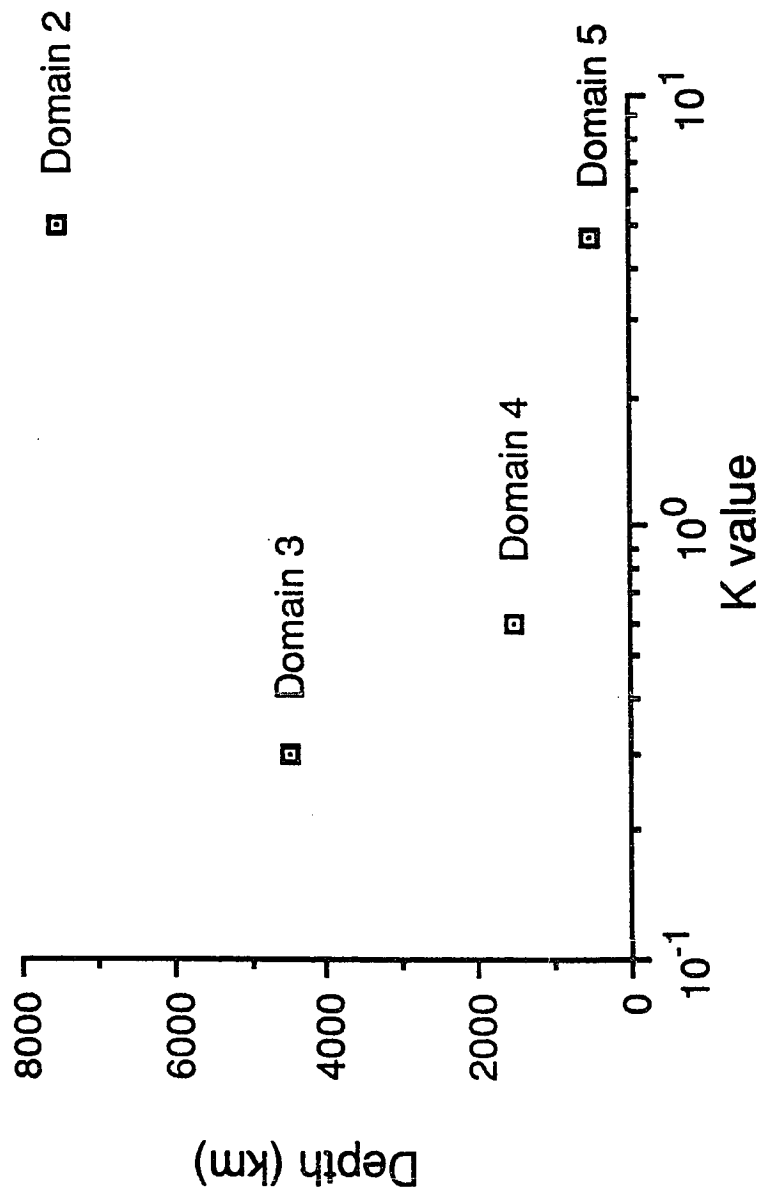


Figure 2.9b - K values (Woodcock, 1977) vs. depth for D1 and D1a fold axes. High K values indicate point concentrations; low K values indicate girdle distributions. Depth values are for domain mid-points.

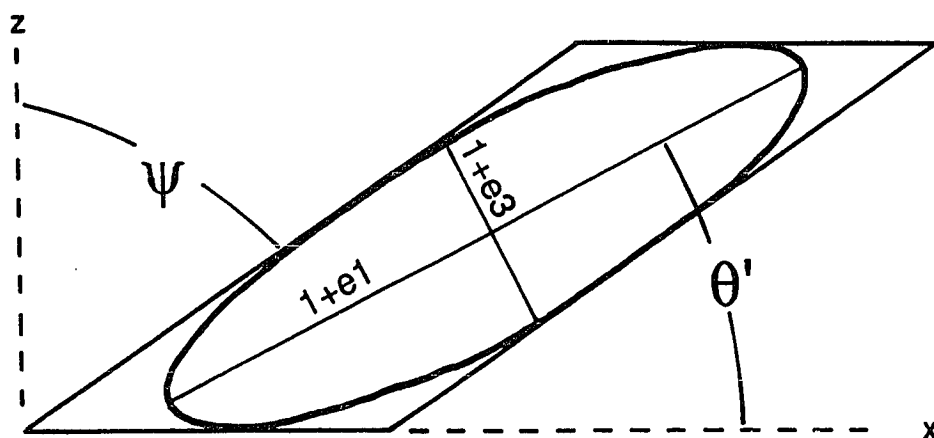
planes is approximately 10° . Like D1 and D1a folds, D1b folds are progressively reoriented from the top of domain 4 to the base of domain 5 (Fig. 2.14). The transitional nature of the domain boundaries between domains 3, 4, and 5 implies that D1 (D1a) folding started at the same time in each domain (Fig. 2.15). As deformation progressed the interlimb angles of the folds decreased and the axial planes were rotated toward the Amawk thrust. As folds were tightened to isoclinal and rotated approximately parallel to the direction of tectonic transport they were refolded. The depth controlled increase in strain caused deeper structures to be rotated faster and, thus, refolded earlier (Fig. 2.15).

The progressive development, rotation, and refolding of D1 folds is interpreted to predate D2 folding throughout the southern Endicott Mountains allochthon because consistently oriented D2 structures are superimposed on D1 folds and cleavage in domain 3 and on both D1a and D1b folds and cleavage in domains 4 and 5. Unlike D1 structures, which are folded by the Doonerak duplex, the attitudes D2 axial planes and cleavage the same on both the northern and southern flanks of the duplex. In all three domains, D2 axial planes and cleavage strike northeast- southwest and S2 x S1 intersection lineations trend northeast (Fig. 2.2b).

Strain factorization

The progressive change from upright to recumbent folds and from strike parallel to dip parallel fold axes is well documented in simple shear zones at many scales (Ramsay and Graham, 1970; Escher and Watterson, 1974; Sanderson, 1979; Mitra and Elliott, 1980) and most studies of strain in thrust sheets (e.g. Carmignani et al., 1978; Coward and Kim, 1981; Ramsay et al., 1983) cite these reorientation parameters as evidence that simple shear was the dominant mechanism during progressive intranappe deformation. If the primary layering in the thrust nappe is inclined in the direction of shear, folding can result from simple shear alone (Ramsay et al., 1983), but if deformation is banded (i.e. macroscopic layering in the thrust sheet remains parallel to the basal thrust during

a



Pure shear (α) >1 if $x>z$, and <1 if $z>x$

b

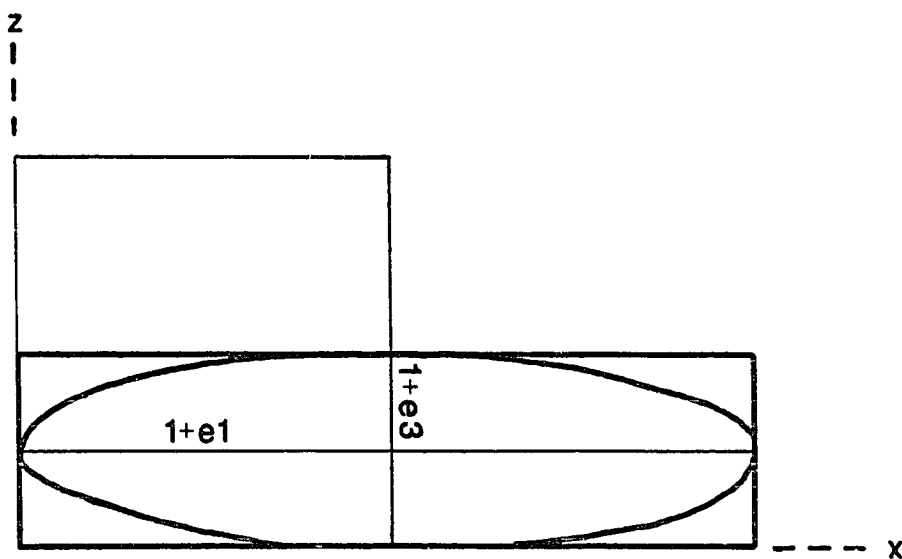


Figure 2.10 - a) Relations between shear angle (ψ), the orientation of the strain ellipse (θ'), and strain axes. $\gamma = \tan(\psi)$. $R_s = (1+e_1)/(1+e_3)$. b) Deformation by pure shear.

deformation), intranappe folding requires boundary parallel pure shear (Sanderson, 1982).

The effects of combined pure and simple shear have been recognized in many thrust sheets and, if the sequence of deformation is known, the total strain can be factored into pure shear (α) and simple shear (γ), or volume change (Δv) and simple shear components by plotting strain ratio (R_s) against the angle (θ') between the x-strain axis and the shear direction (Fig. 2.10; Coward, 1980; Coward and Kim, 1981; Kligfield et al., 1981; Sanderson, 1982). Assuming that volume changes in the Endicott Mountains allochthon are negligible, the relative roles of pure and simple shear can be evaluated.

For the Endicott Mountains allochthon, the sequence of deformation is constrained by the relative timing of deformational phases, regional cross-cutting relationships, and balanced cross sections (Oldow et al., 1987). Four distinct, but partly synchronous, "events" are recognized (Fig. 2.11): 1) emplacement of the Skagit allochthon over the southern portion of the Endicott Mountains allochthon; 2) internal imbrication of the Endicott Mountains allochthon; 3) northward displacement of the Endicott Mountains allochthon, and; 4) duplexing of the Apoon assemblage beneath the Endicott Mountains allochthon (Oldow et al., 1987). Genetic links between D2 and the last stages of duplex formation (Seidensticker et al., 1987) coupled with consistently well developed, uniformly oriented D2 structures in all of the structural sheets above and below the Amawk thrust, indicate that D1 in the southern Endicott Mountains allochthon ended before or during the latest stages of duplex formation (Seidensticker, 1988).

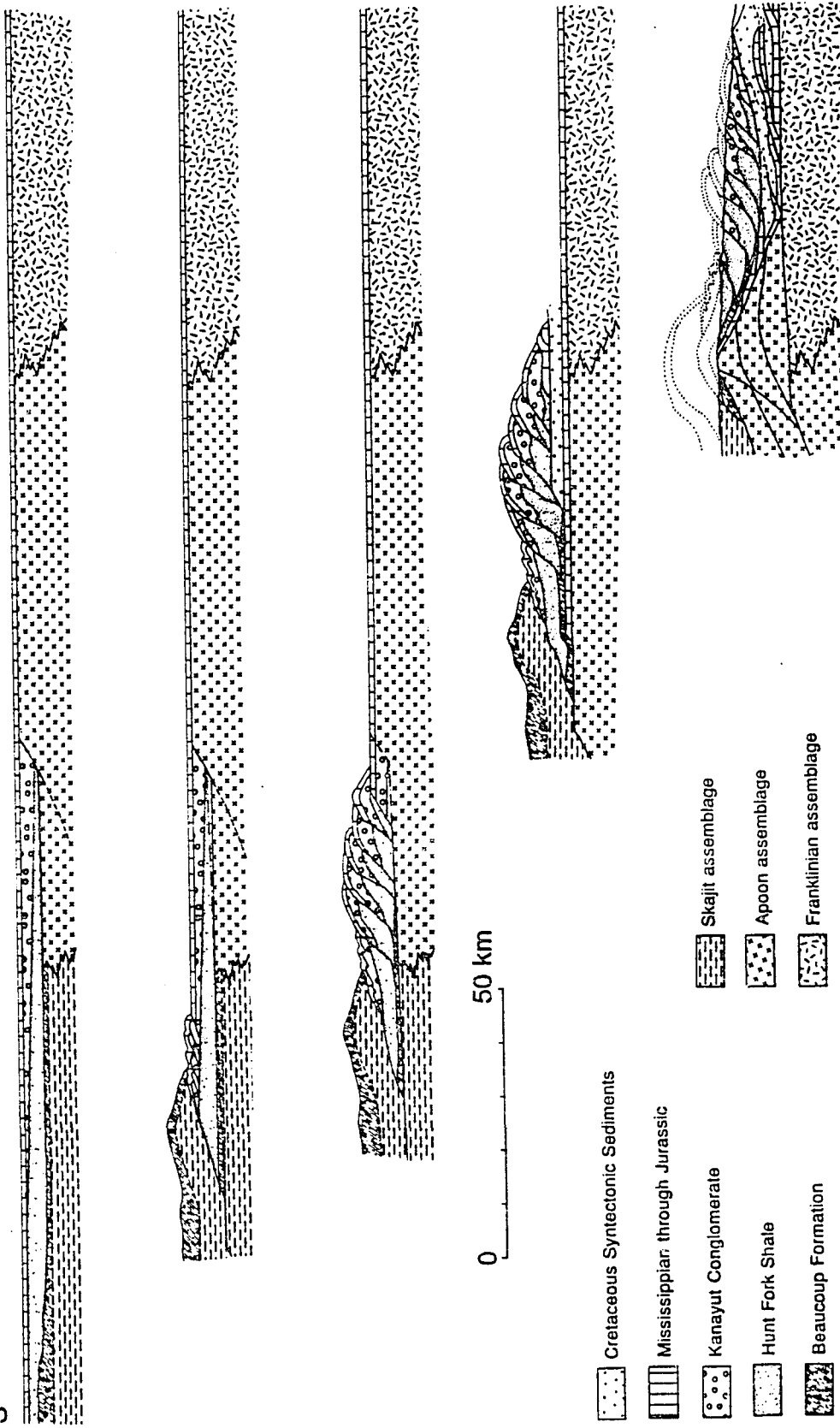
Because deformation was banded, this sequence of events, consisting of the progressive reorientation of D1 folds in domains 3 through 5, and the superposition of D1a and D1b folds in domains 4 and 5 suggests that D1 deformation was facilitated by alternating pure and simple shear in the form:

$$\alpha + \gamma + \alpha + \gamma \dots ,$$

Figure 2.11 - Sequence of events during northward movement of the Endicott Mountains allochthon (D1 and D2): a) emplacement of the Skagit allochthon over the southern portion of the Endicott Mountains allochthon; b) imbrication of the Endicott Mountains allochthon; c) northward translation of the Endicott Mountains allochthon; d) duplexing of the Apoon assemblage beneath the Endicott Mountains allochthon.

N

S



where $\alpha < 1$ (Fig. 2.12a). Ramberg (1975) has shown that the equations for alternating incremental pure and simple shear and synchronous pure and simple shear are the same if the increments are very small, the number of increments is very large, and the strain rate is constant. Figure 2.13 is a R_s vs. θ' diagram with isopleths for α and γ formed during synchronous pure and simple shear. Sanderson (1982) postulated that layer parallel pure shear in a thrust sheet is constant with a value $\alpha < 1$ (i.e. layer parallel shortening) and that the commonly observed depth related decrease in θ' is a function of increasing shear strain. Measured values for R_s and θ' from both mesoscopic and microscopic strain indicators (Table 2.2) deviate substantially from a predicted $\alpha = \text{constant}$ curve and suggest that α is not constant, but varies with depth in the nappe (Fig. 2.13).

Proper interpretation of Figure 2.13 requires detailed understanding of field relationships and the limitations of our strain measurements. The southern nappe of the Endicott Mountains allochthon is not a continuous media because intraformational thrust faults (discontinuities) are common throughout the nappe. The frequency of intraformational thrusts and bedding parallel detachments increases with depth in the nappe, possibly indicating that the amount of fault distributed shear strain also increases with depth. Adjacent to intraformational thrusts, shear strain is heterogeneous. Between faults, different strain indicators often yield different strain values. For example, in domain 3, Skolithos burrows are sheared from 45° to 70° , yielding strain ratios from $R_s \approx 2.6$ to $R_s \approx 9.5$. In the same domain, R_f/ϕ analysis of stretched pebbles and Fry analysis of mudstone microfabrics yield strain ratios less than $R_s = 1.2$. Boudinage in the same domain indicates less than 10% to over 600% stretching. These inconsistencies are partly related to lithology, but also reflect heterogeneous strain distribution within the same lithologies.

Since the preserved finite strain represents superposition of multiple incremental finite strains, the principal uncertainty in this analysis is whether the measured finite strains

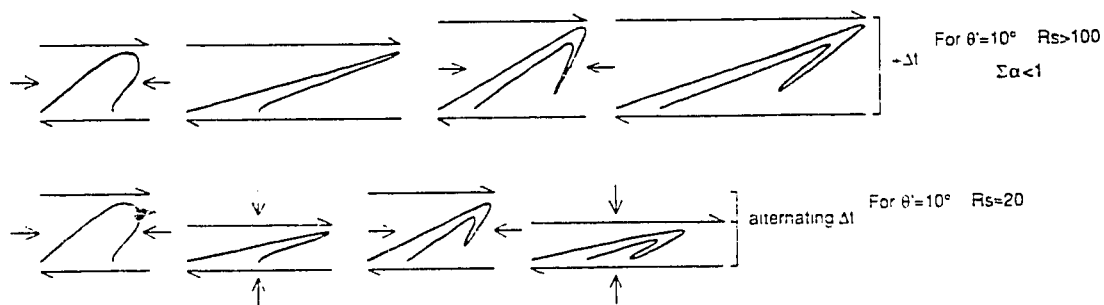


Figure 2.12 - Geometric models for polyphase folding formed by various combinations of pure and simple shear: a) Folds formed by alternating layer parallel shortening ($\alpha < 1$) and simple shear. This model requires an increase in the distance between shear zone boundaries through time; b) Folds formed by alternating layer parallel shortening ($\alpha < 1$), simple shear, and layer parallel lengthening ($\alpha > 1$). In this model the distance between shear zone boundaries increases and decreases through time, but if the net pure shear component is $\alpha > 1$, then the overall spacing of the shear zone boundaries will decrease.

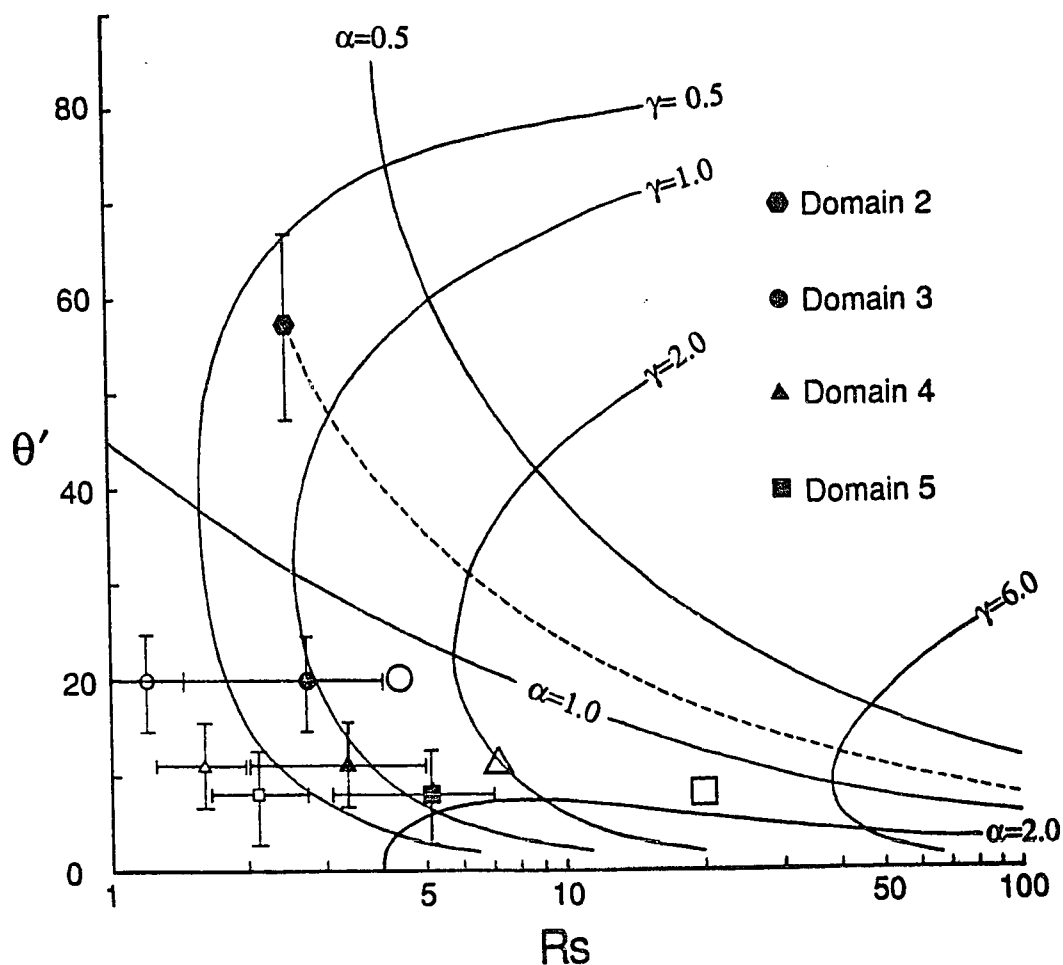


Figure 2.13 - Plot of strain ratio (R_s) vs. angle (θ') between the x-strain axis and the Kanayut-Hunt Fork contact in domains 2 and 3 (and the inferred orientation of the Amawk thrust in domains 4 and 5). Solid lines are isopleths for synchronous pure (α) and simple (γ) shear. The dashed line is the theoretical α -constant path from D1 in domain 2 to $\theta'=8^\circ$ of domain 5. Solid symbols represent mesoscopic strain measurements. Small open symbols represent strain from Fry analysis of microfabrics. Error bars indicate the spread of data. Large open symbols represent modeled strain ratios required to produce the observed fold arcuation K values in domains 3 ($K=0.3$), 4 ($K=0.5$), and 5 ($K=4.8$).

accurately represent the strains required to produce the observed folds. Geometric modeling of fold axis reorientation suggests that mesoscopic strain in domain 3 is adequate to produce the observed fold arcuation (Fig. 2.13). Measured strains in domains 4 and 5, however, are approximately four times smaller than model strains required to produce the observed amounts of fold arcuation (Fig. 2.13). This suggests that, in polyphase terranes, fold arcuation may be a more accurate indicator of strain than finite strain markers.

Both mesoscopic strain indicators and strain ratios required to produce the observed fold axis arcuation imply that α increases with depth and that the total pure shear component changes from $\alpha < 1$ in domain 2 to $\alpha > 1$ in domains 3 through 5. The change from $\alpha < 1$ to $\alpha > 1$ occurs abruptly across a bedding parallel detachment that separates the Kanayut Conglomerate from the Hunt Fork Shale (Fig. 2.4a), and reflects a major change in deformational style across a relatively inconspicuous intraformational discontinuity. Within the Hunt Fork and Beaucoup strain is locally heterogeneous, but it appears to increase systematically with depth.

During banded deformation, initiation of D1a folding and superposition of D1b folds on D1a folds in domains 4 and 5 requires at least two periods of layer parallel shortening (Fig. 2.12a), but the final strain state in these domains is $\Sigma \alpha > 1$. This can be interpreted to mean that the pure shear component changed with time, yielding a deformation sequence in the form:

$$\alpha_1 + \gamma_1 + \alpha_2 + \gamma_2 + \alpha_3 + \gamma_3 \dots,$$

where $\alpha_1 \neq \alpha_2 \neq \alpha_3$ (Fig. 2.12b), or that deformation involved layer parallel shortening and simple shear in a collapsing shear zone (Fig. 2.12c). Because time dependant changes in α violate the constant strain rate assumption (Ramberg, 1975) in the second model (Fig. 2.12b), and the third model (Fig. 2.12c) implies synchronous layer parallel shortening and layer normal flattening, the α and γ isopleths in Figure 2.13 are only approximations of

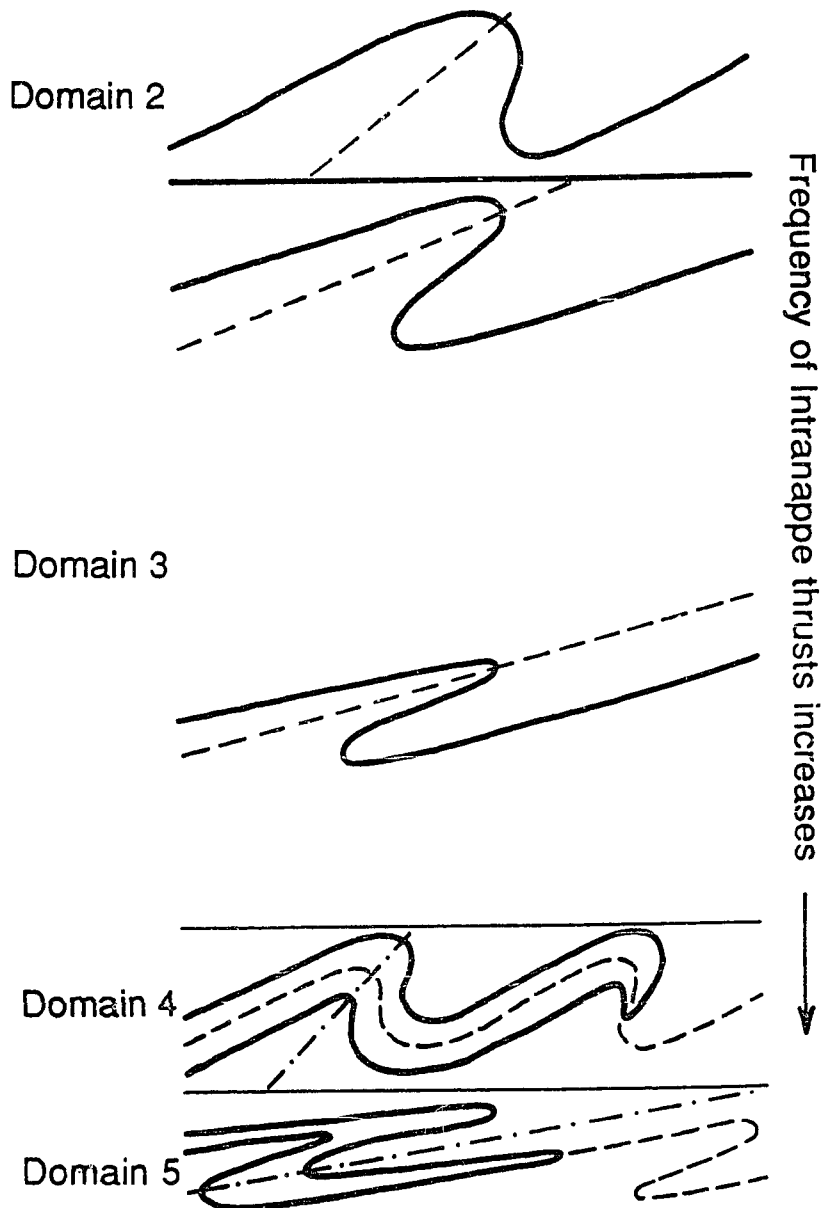


Figure 2.14 - Schematic vertical section through the southern nappe of the Endicott Mountains allochthon showing the progressive change in fold style and increase in intraformational thrust frequency with depth.

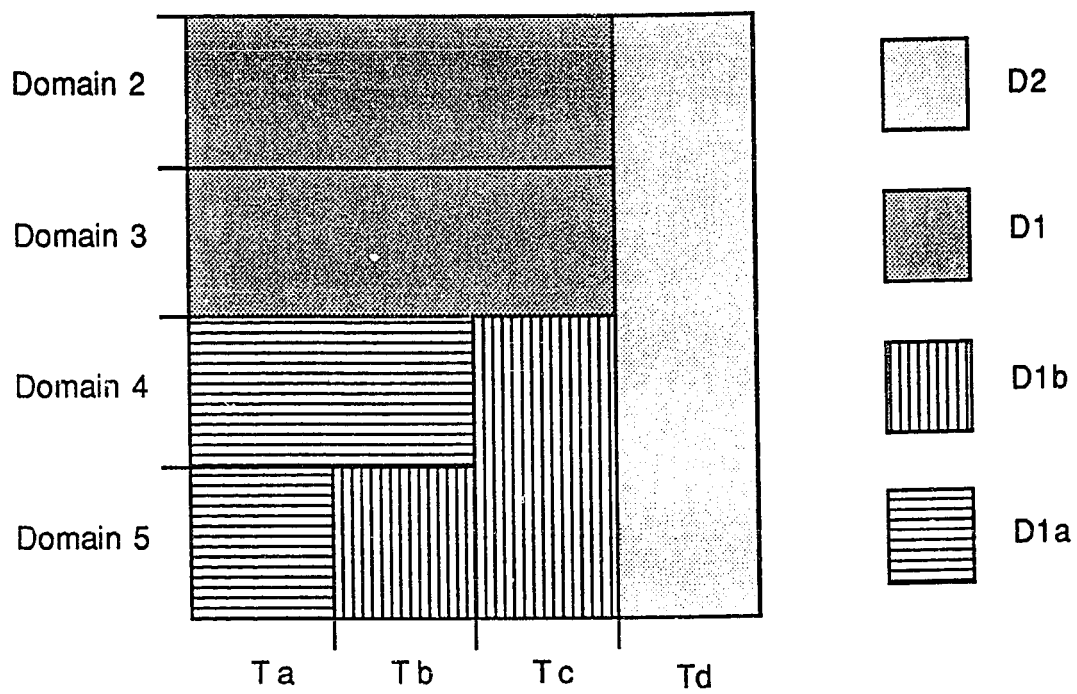


Figure 2.15 - Spatial and temporal relationships of deformational phases in the Endicott Mountains allochthon.

the total pure and simple shear components. In addition, the measured strains only reflect ductile deformation between intranappe detachments.

Progressive rotation and tightening of D1 and D1a folds in domains 3 through 5 and progressive development and rotation of D1b folds in domains 4 and 5 indicate that deformation was essentially continuous despite the presence of numerous intranappe detachments (Fig. 2.14). This implies that D1 folds in domain 3 formed during the same time interval as D1a and D1b folds in domain 5 (Fig. 2.15). Synchronous development of systematically changing polyphase folds within a single thrust nappe also implies that all of the necessary deformation processes occurred in a specific, incremental sequence (i.e. layer parallel shortening, followed by layer parallel shear, followed by layer normal shortening, etc.) or that the processes occurred concurrently. Since synchronous layer parallel shortening and layer normal shortening is mechanically difficult to explain, it is assumed that deformation of the southern Endicott Mountains allochthon was facilitated by a sequence in which layer parallel shortening plus simple shear was followed by layer normal collapse of the shear zone (Fig. 2.12b).

DISCUSSION

Fold reorientation and strain

Asymmetric intranappe folding can be the product of simple shear (Ramsay et al., 1983), a combination of simple shear and layer parallel shortening (Sanderson, 1982), or a combination of simple shear, layer parallel shortening, and layer normal collapse of the shear zone. Although fold orientation is often the most conspicuous indicator of intranappe strain, it does not provide direct information about the strain history or the amount of strain. Finite strain markers supply information about the total strain at any given point but, in folded rocks, are the product of inhomogeneous strain and, thus, do not define the mechanisms of folding (Ramsay, 1967, p.343). Fold axis reorientation is potentially the most accurate strain indicator, but it too is generic since both pure shear and

simple shear cause arcuation of fold axes.

Individually, or as a group, fold orientation, measured finite strain, and fold axis arcuation do not provide enough information to resolve the mechanics of fold formation unless cutoff relations can be used to define the style of deformation (banded vs. inclined in the direction of tectonic transport) and the sequence of deformation can be approximated. In the southern Endicott Mountains allochthon, formations are in normal stratigraphic order and formation contacts are approximately parallel to the Amawk thrust, indicating banded deformation. Progressive reorientation of D1 folds, superposition of D1b folds on D1a folds, and reorientation of D1b folds defines an incremental strain history involving both layer parallel shortening and simple shear. Given these boundary conditions, fold and strain marker orientations can be used to factor strain into pure and simple shear components (Fig. 2.13).

The absolute proportions of pure and simple shear necessary to produce observed fold styles and orientations are difficult to resolve, especially in polyphase terranes. If strain markers are present they can be used to approximate of the relative proportions of pure and simple shear, and the orientation of the pure shear component. These relative values can then be used in conjunction with field observations about the sequence of folding, fold orientation, and the style of deformation to model fold development and rotation (Fig. 2.12). Strains necessary to produce the observed fold orientation and arcuation can then be calculated and the required pure and simple shear components reevaluated (Fig. 2.13).

Implications for cross section balancing

Balanced cross-sections are one of the most useful tools available for the analysis of fold-thrust belts and, in recent years, the principles outlined by Dahlstrom (1969) have become more mathematically rigorous (Woodward et al., 1985; Kligfield et al., 1986; DePaor, 1988; etc.). The importance of including intranappe strain during the construction of balanced cross sections is primarily a function of scale. Mesoscopic

intranappe strain is often ignored during construction of regional balanced cross sections (e.g. Bally et al., 1966; Oldow et al., 1987) because the amount of mesoscopic shortening is unknown or the observed amount of mesoscopic shortening is very small relative to the macroscopic shortening. In larger scale balanced sections, however, it may be necessary to incorporate mesoscopic intranappe strain. Strain variation in the southern Endicott Mountains allochthon presents a problem for cross section balancing and, although it may be impractical to quantitatively incorporate into a balanced section, recognition of this and similar problems may improve the accuracy of the section.

The structural complexity and stratigraphic ambiguity of domains 3, 4, and 5 preclude any realistic attempt to balance the Hunt Fork and Beaucoup. Neither the original stratigraphic thicknesses nor the amount of structural thickening are known; the hangingwall cutoff is not preserved and the footwall cutoff is not exposed. Within the limits of the data, however, the strain profile (Fig. 2.13) for the southern nappe can be used to model the bulk strain that must be removed during section restoration. The final strain state is analogous to a stack of parallelograms which must be restored to unit squares with the same areas during balancing (Fig. 2.16). This requires heterogeneous changes in line lengths and formation thicknesses within the same thrust sheet (Fig. 2.16). The impact of these changes is relaxed through area balancing, but the change from layer parallel shortening in the upper layer (domain 2) to layer parallel lengthening in the lower layers (domains 3, 4, and 5) dictates that the southern Endicott Mountains allochthon must be balanced as at least two separate layers. The upper layer, which was shortened during deformation, will increase in length and decrease in thickness during balancing. The lower layer, which was lengthened during deformation, will decrease in length and increase in thickness during balancing.

The deformed state profile (Fig. 2.16) also implies that intranappe slip increases upward within the sheet (Elliott, 1976) and invalidates the use of local pin lines during

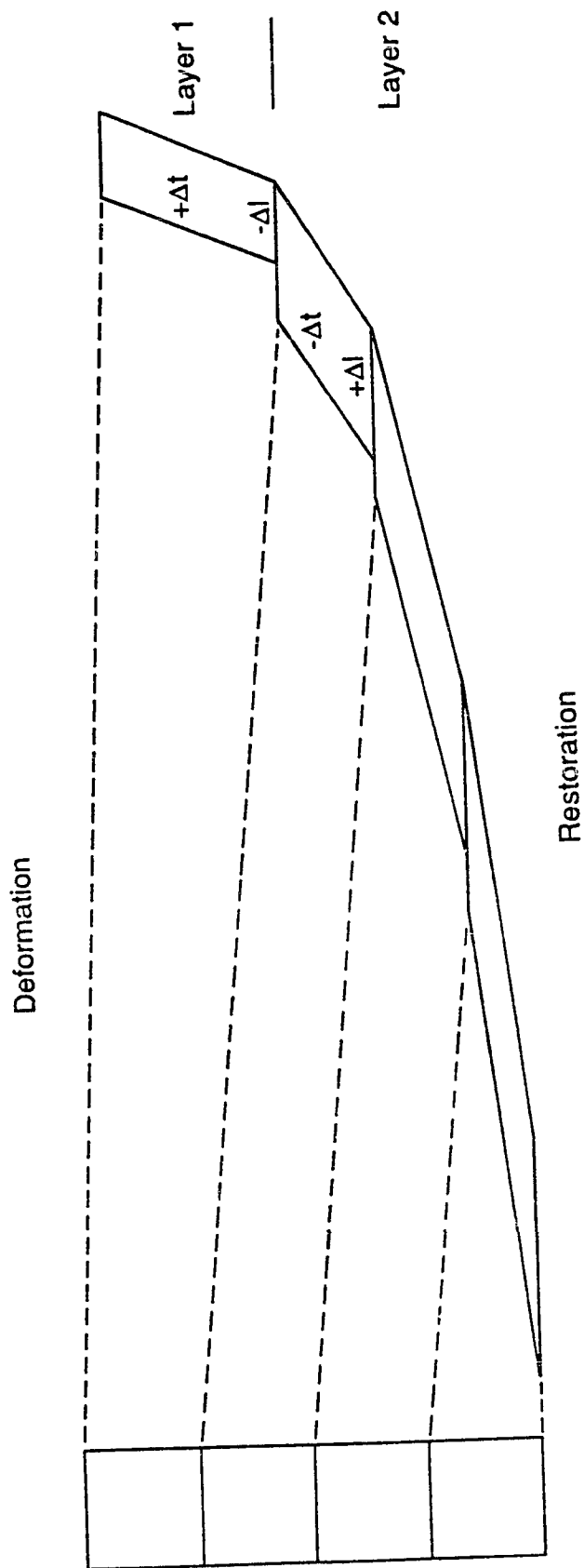


Figure 2.16 - Deformation by a combination of simple shear and pure shear changes line length, unit thicknesses, and the relative angles between units. Layer 1 is shortened parallel to the direction of transport during deformation. Layer 2 is lengthened parallel to the direction of tectonic transport during deformation.

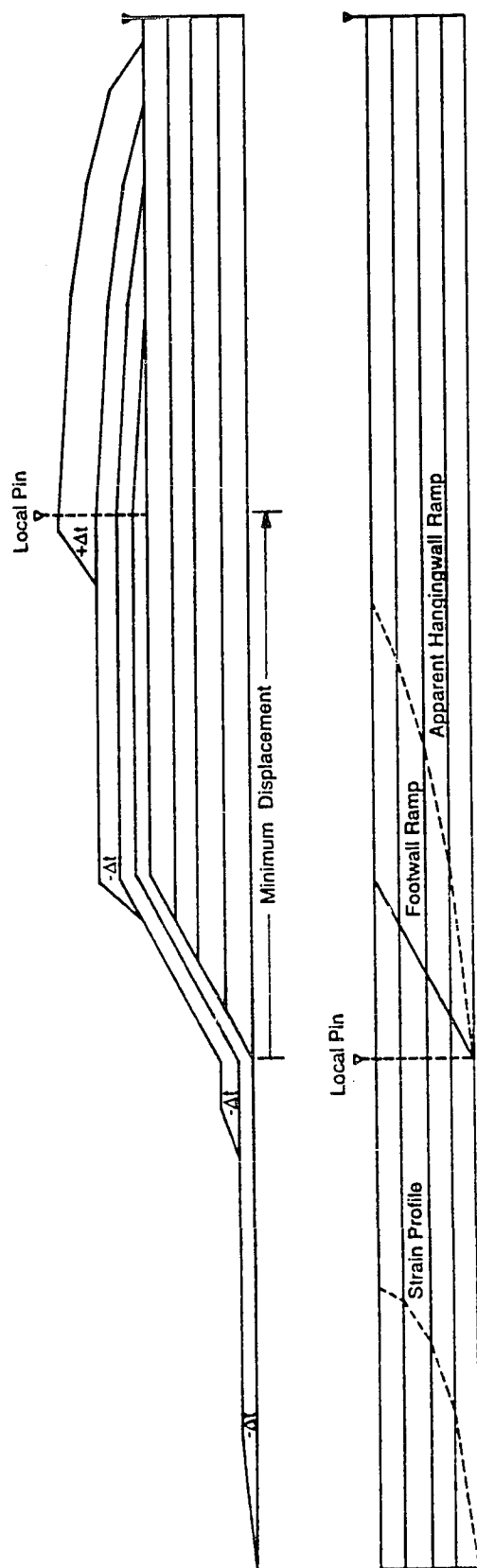


Figure 2.17 - Fault trajectory mismatch created by the use of local pin lines during balancing of an internally strained thrust sheet. a) deformed state cross section created by the strain profile in Figure 2.16 and an initial ramp angle of 30° . b) difference in the true (footwall) ramp and the apparent hangingwall ramp when the section is balanced using a local pin line in the middle of the allocthonous sheet.

section balancing (Woodward et al., 1985, p.91). If local pin lines are used during balancing, intranappe strain can cause a mismatch of fault cutoffs in the balanced section even if hangingwall cutoffs are preserved in the deformed state (Fig. 2.17). Incorporation of strain data into a balanced cross section can, thus, improve the accuracy of the section (Fig. 1.2b). Conversely, fault trajectory mismatches in balanced cross sections with well constrained footwall and hangingwall cutoffs can be used to define intranappe strain profiles (Fig. 2.17).

Strain within a thrust sheet also has implications for displacement of the thrust sheet. If intranappe strain is the product of simple shear alone, or a combination of layer parallel shortening and simple shear, the amount of displacement increases upward in the sheet (Elliott, 1976). If intranappe deformation is the product of simple shear plus bulk layer parallel lengthening, as in domains 3, 4, and 5 of the Endicott Mountains allochthon the strain profile implies a minimum displacement (Fig. 2.17). In addition, lengthening in the southern Endicott Mountains allochthon may partially explain why the lower Hunt Fork and Beaucoup are present beneath much of the Skagit allochthon (Fig. 1.2b).

Lateral strain variations

Two types of lateral strain gradients are present in the Endicott Mountains allochthon. The first is evidenced by a change from open north-vergent folds in domain 1, to heterogeneous intranappe folding in domains 2 through 5. D1 folds in domain 1 involve the Hunt Fork Shale, Kanayut Conglomerate, Kayak Shale, and Lisburne Limestone. These units are usually folded together into large, open, north-vergent folds, or separated by interformational thrusts. D1 folds in the Hunt Fork dip consistently toward the south and fold axes parallel the strikes of the axial planes (Fig. 2.3). Structural continuity across the Kanayut-Hunt Fork contact and the absence of D1 fold reorientation reflects relatively shallow deformation and control of fold style by the Kanayut Conglomerate (Fig. 2.11). The abrupt change in structural style between domain 1 and the southern thrust nappe is

related to the distribution of the superjacent Skajit allochthon.

Heterogeneous intranappe deformation in domains 3 through 5 was produced as the Skajit allochthon was thrust over the southern Endicott Mountains allochthon, and the entire nappe pile (Endicott plus Skajit) was displaced northward along the Amawk thrust (Fig. 2.11). Differential shortening across the Kanayut-Hunt Fork contact, estimated from layer parallel shortening in domain 2 and layer parallel lengthening in domain 3 (Fig. 2.13), suggests that the southernmost outcrops of Kanayut in domain 2 have been displaced a minimum of 10 km northward relative to the subjacent Hunt Fork. Northward displacement of the Kanayut is evidenced in the field by detachment of domain 2 from domain 3 and north-vergent folds and imbricate thrusts in domain 2. Synchronous northward displacement of the Kanayut over the Hunt Fork and layer parallel shortening in the Kanayut imply that the Skajit allochthon soled into the Kanayut-Hunt Fork contact and pushed the Kanayut northward. Synchronous layer parallel shortening, simple shear, and collapse of domains 3 through 5 (Fig. 2.18c) require simultaneous displacement of the Skajit allochthon over the Endicott Mountains allochthon and forward propagation of the Amawk thrust beneath the Endicott Mountains allochthon (Fig. 2.11).

The second lateral strain gradient is evidenced by a northward decrease in the intensity of D2 within the southern nappe and the absence of D2 in the Hunt Fork of domain 1. Seidensticker (1988; Seidensticker et al., 1987) cites the absence of D2 north of the leading edge of the Doonerak duplex and the general decrease in D2 on the north side of the duplex as evidence that D2 is related to latest stage of duplex emplacement.

CONCLUSIONS

The change in structural style from single-phase folds and imbricated thrust sheets in domain 1 to heterogeneous intranappe strain and progressive polyphase folding in domains 2 through 5 is the product of rheologic differences between the Kanayut Conglomerate, Hunt Fork Shale, and Beaucoup Formation, the original distribution of

sedimentary facies, and the depth of deformation. The greater thickness of Kanayut, its relative rigidity, and the lack of an overriding thrust sheet favored thrust imbrication in the north; whereas thicker Hunt Fork and Beaucoup shales and deformation beneath the Skajit allochthon favored formation of a strain gradient in the south.

Unlike strain gradients documented in the Helvetic Alps (Ramsay et al., 1983), the Apennines (Carmignani et al, 1973), and in the Moine Thrust Zone (Coward and Kim 1981), the net strain in the southern Endicott Mountains allochthon changes from simple shear plus layer parallel shortening in the upper part of the nappe to simple shear plus layer parallel extension in the lower part of the nappe. Strain ratios, fold orientations, and fold superposition in domains 4 and 5 suggest a complex deformation history involving layer parallel shortening, simple shear, and layer normal collapse of the shear zone.

References

- Abbott, J.G., 1986, Devonian extension and wrench tectonics near MacMillan Pass, Yukon Territory, Canada, *in* R.J.W. Turner and M.T.Einaudi, eds., The genesis of stratiform sediment hosted lead and zinc deposits, Conference proceedings: Stanford University Press, Stanford, California, p.85-89.
- Alvarez, W., T. Engelder, and P. A. Geiser, 1978, Classification of solution cleavage in pelagic limestones: *Geology*, v.6, p.263-266.
- Anderson, A.V., 1987, Provenance and petrofacies of the Endicott and Hammond terranes, Phillip Smith Mountains and Arctic quadrangles, Brooks Range, Alaska: *Geological Society of America Abstracts with Programs*, v. 19, p.354.
- Armstrong, A.K., 1974, Carboniferous carbonate depositional models, preliminary lithofacies and paleotectonic maps, Arctic Alaska: *American Association of Petroleum Geologists Bulletin*, v.58, p.621-645.
- Armstrong, A.K., and B.L. Mamet, 1978, Microfacies of the Carboniferous Lisburne Group, Endicott Mountains, arctic Alaska, *in* C.R. Stelck and B.D.E. Chatterton, eds., *Western and Arctic Canadian Biostratigraphy*: Geological Association of Canada, Special Paper 18, p.333-362.
- Armstrong, A.K., B.L. Mamet, W.P. Brosgé, and H.N. Reiser, 1976, Carboniferous section and unconformity at Mount Doonerak, Brooks Range, northern Alaska: *American Association of Petroleum Geologists Bulletin*, v.60, p.962-972.
- Armstrong, A.K., B.L. Mamet, and J.T. Dutro, Jr., 1970, Foraminiferal zonation and carbonate facies of the Mississippian and Pennsylvanian Lisburne Group, central and eastern Brooks Range, Alaska: *American Association of Petroleum Geologists Bulletin*, v.54, p.687-698.
- Bally, A.W., P.L. Gordy, and G.A. Stewart, 1966, Structure, seismic data, and orogenic evolution of the southern Canadian Rocky Mountains: *Bulletin Canadian Petroleum Geology*, v.14, p337-381.
- Barberi, F., R. Santacroce, and J. Varet, 1982, Chemical aspects of rift magmatism, in G. Palmason, ed., *Continental and oceanic rifts*: American Geophysical Union Geodynamics Series, v. 8, p.223-258.
- Basu, A., S.W. Young, L.J. Suttner, W.C. James, and G.H. Mack, 1975, Re-evaluation of the use of undulatory extinction and polycrystallinity in detrital quartz for provenance studies of sedimentary rocks: *Journal of Sedimentary Petrology*, v.45, p.873-882.
- Beaumont, C., C.E. Keen, and R. Boutilier, 1982, A comparason of foreland and rift margin sedimentary basins: *Philosophical transactions of the Royal Society of London, Series A*, v.305, p.295-317.

- Bowsher, A.L., and J.T. Dutro Jr., 1957, The Paleozoic section in the Shainin Lake area, central Brooks Range, Alaska: U.S. Geological Survey Professional Paper 303-A, p.1-39.
- Brosgé, W.P., J.T. Dutro Jr., M.D. Mangus, and H.N. Reiser, 1962, Paleozoic sequence in eastern Brooks Range, Alaska: American Association of Petroleum Geologists Bulletin, v.46, p.2174-2198.
- Brosgé, W.P., H.N. Reiser, J.T. Dutro Jr., and R.L. Detterman, 1979, Bedrock geologic map of the Phillip Smith Mountains quadrangle, Alaska. U.S. Geological Survey Miscellaneous Field Studies Map MF-879B, 2 sheets, 1:250,000.
- Cant, D.J., 1978, Development of a facies model for sandy braided river sedimentation: Comparison of the south Saskatchewan River and the Battery Point Formation, *in* A.D. Miall, ed., *Fluvial Sedimentology*: Canadian Society of Petroleum Geologists Memoir 5, p.627-640.
- Carlson, R., and K.F. Watts, 1987, Shallowing upward cycles in the Wahoo Limestone, eastern Sadlerochit Mountains, ANWR, NE Brooks Range, Alaska: Geological Society of America Abstracts with Programs, v. 19, p.364.
- Carmignani, L., G. Giglia, and R. Kligfield, 1978, Structural evolution of the Apuane Alps: An example of continental margin deformation in the northern Apennines, Italy: *Journal of Geology*, v.86, p.487-504.
- Chamberlain, C.K., 1978, Trace fossil ichnofacies of an american flysch, *in* C.K. Chamberlain, ed., *A guidebook to the trace fossils and paleoecology of the Ouachita geosyncline*: Society of Economic Paleontologists and Mineralogists, Tulsa, Oklahoma, p.23-37.
- Chan, M.A., and Dott, R.H. Jr., 1986, Depositional facies and progradational sequences in Eocene wave-dominated deltaic complexes, southwestern Oregon: American Association of Petroleum Geologists Bulletin, v.70, p.415-429.
- Chapman, R.M., R.L. Detterman, and M.D. Mangus, 1964, Geology of the Killik - Etivluk Rivers region, Alaska: U.S. Geological Survey Professional Paper 303-F, p.325-407.
- Churkin, M., Jr., W.J. Nockleberg, and C. Huie, 1979, Collision deformed Paleozoic continental margin, western Brooks Range, Alaska: *Geology*, v.7, p.379-383.
- Cook, T.D., and A.W. Bally, eds., 1975, *Stratigraphic atlas of North and Central America*: Princeton University Press, Princeton, New Jersey, 272p.
- Coward, M.P., 1980, The analysis of flow profiles in a basaltic dyke using strained vesicles: *Journal Geological Society London*, v. 137, p.605-615.
- Coward, M.P., and J.H. Kim, 1981, Strain within thrust sheets: *in* K. McClay and N.J. Price, eds., *Thrust and nappe tectonics*, Geological Society London, Special Publication, p.275-292.

- Crimes, T.P., 1975, The stratigraphic significance of trace fossils, *in* R.W. Frey, ed., *The study of trace fossils*: Springer-Verlag, New York, p.109-130.
- Dahlstrom, C.D.A., 1970, Balanced cross sections: *Canadian Journal Earth Science*, v.6, p.743-757.
- DePaor, D.G., 1988, Balanced section in thrust belts. Part 1: Construction: *American Association of Petroleum Geologists Bulletin*, v.72, p.73-90.
- Dickinson, W.R., and C.A. Suczek, 1979, Plate tectonics and sandstone composition: *American Association of Petroleum Geologists Bulletin*, v.63, p.2164-2182.
- Dillon, J.T., W.P. Brosgé, and J.T. Dutro Jr., 1986, Generalized geologic map of the Wiseman quadrangle: U.S. Geological Survey Open-File Report 86-219, 1 sheet, 1:250,000.
- Dillon, J.T., A.G. Harris, J.T. Dutro Jr., 1987a, Preliminary description and correlation of lower Paleozoic fossil-bearing strata in the Snowden Mountain area of the south-central Brooks Range, Alaska, *in* I. Tailleux and P. Weimer, eds., *Alaskan North Slope geology: Society of Economic Paleontologists and Mineralogists*, Pacific Section, p.337-345.
- Dillon, J.T., G.H. Pessel, J.A. Chen, and N.C. Veatch, 1980, Mid Paleozoic magmatism and orogenesis in the Brooks Range, Alaska: *Geology*, v.8, p.338-343.
- Dillon, J.T., G.R. Tilton, J. Decker, and M.J. Kelly, 1987b, Resource implications of magmatic and metamorphic ages for Devonian igneous rocks in the Brooks Range, *in* I. Tailleux and P. Weimer, eds., *Alaskan North Slope geology: Society of Economic Paleontologists and Mineralogists*, Pacific Section, p.713-723.
- Durney, D.W., 1972, Solution-transfer, an important geological deformation mechanism: *Nature*, v.235, p.315-316.
- Dutro, J.T. Jr., W.P. Brosgé, M.A. Lanphere, and H.N. Reiser, 1976, Geologic significance of the Doonerak structural high, central Brooks Range, Alaska: *American Association of Petroleum Geologists Bulletin*, v.60, p.952-961.
- Dutro, J.T. Jr., W.P. Brosgé, H.N. Reiser, and R.L. Detterman, 1979, Beaucoup Formation, a new Upper Devonian stratigraphic unit in the central Brooks Range, northern Alaska: *U.S. Geological Survey Bulletin*, 1482-A, p.A63-A69.
- Dutro, J.T. Jr., A.R. Palmer, J.E. Repetski, and W.P. Brosgé, 1984, Middle Cambrian fossils from the Doonerak anticlinorium, central Brooks Range, Alaska: *Journal of Paleontology*, v.58, p.1364-1371.
- Elliott, D., 1976, The energy balance and deformation mechanisms of thrust sheets: *Philosophical transactions of the Royal Society of London, Series A*, v.283, p.289-312.
- Escher, A., and J. Watterson, 1974, Stretching fabrics, folds and crustal shortening: *Tectonophysics*, v.22, p.223-231.

- Fleuty, M.J., 1964, The description of folds: Geological Association Proceedings v.75, p.461-492.
- Folk, R.F., 1980, Petrology of sedimentary rocks: Hemphill Publishing Company, Austin, Texas, 182p.
- Frey, R.W., and S.G. Pemberton, 1984, Trace fossil facies models, *in* R.G. Walker, ed., Facies Models: Geological Association of Canada, Geoscience Canada Reprint Series 1, p. 189-208.
- Galloway, W.E., 1975, Process framework for describing the morphologic and stratigraphic evolution of deltaic systems, *in* M.L. Broussard, ed., Deltas: Houston Geological Society, Houston, Texas, p.87-98.
- Gehrels, G.E., and M.T. Smith, 1987, "Antler" allochthon in the Kootenay arc?: Geology, v.15, p.769-770.
- Gordey, S.P., J.G. Abbott, D.J. Tempelman-Kluit, and H. Gabrielse, 1987, "Antler clastics in the Canadian Cordillera: Geology, v.15, p.103-107.
- Graham, S.A., R.B. Tolson, P.G. DeCelles, R.V. Ingersoll, E. Barger, M. Caldwell, W. Cavazza, D.P. Edwards, M.F. Follo, J.W. Handschy, L. Lemke, I. Moxon, R. Rice, G.A. Smith, and J. White, 1986, Lithology of source terranes as a determinant in styles of foreland sedimentation, *in* D.A. Allen and P. Homewood, eds., Foreland Basins: International Association of Sedimentologists Special Publication 8, p.425-436.
- Gray, D.R., 1978, Cleavages in deformed psammitic rocks from southeastern Australia: Their nature and origin: Geological Society of America Bulletin, v.89, p.577-590.
- Handschy, J.W., J.S. Oldow, J.C. Phelps, and H.G. Avé Lallemant, 1987, Stratigraphy and facies relationships of the Endicott Group between Atigun Pass and the eastern Doonerak window, central Brooks Range, Alaska: Geological Society of America Abstracts with Programs, v. 19, p.386.
- Hein, F.J., and R.G. Walker, 1977, Bar evolution and development of stratification in the gravelly, braided Kicking Horse River, B.C.: Canadian Journal of Earth Science, v.14, p.562-570.
- Ingersoll, R.V., W. Cavazza, S.A. Graham, and Indiana University Graduate Field Seminar Participants, 1987, Provenance of impure calcilithites in the Laramide foreland of southwestern Montana: Journal of Sedimentary Petrology, v.57, p.995-1003.
- Ingersoll, R.V., and C.A. Suczek, 1979, Petrology and provenance of Neogene sand from Nicobar and Bengal fans, DSDP sites 211 and 218: Journal of Sedimentary Petrology, v.49, p.1217-1228.
- Johnson, J.G., G. Klapper, and C.A. Sandberg, 1985, Devonian eustatic fluctuations in Euramerica: Geological Society of America Bulletin, v. 96, p.567-587.

- Julian, F.E., 1986, Stratigraphy and tectonic provenance of lower Paleozoic rocks, Doonerak structural high, Brooks Range, Alaska: Geological Society of America Abstracts with Programs, v.18, p.123.
- Julian, F.E., J.S. Phelps, C.M. Seidensticker, J.S. Oldow, and H.G. Avé Lallemant, 1984, Structural history of the Doonerak window, central Brooks Range, Alaska: Geological Society of America Abstracts with Programs, v.16, p.291.
- Klepacki, D.W., and J.O. Wheeler, 1985, Stratigraphic and structural relations of the Milford, Kaslo, and Slocan Groups, Goat Range, Lardeau and Nelson map areas, British Columbia: Geological Survey of Canada Paper 85-1, p.277-286.
- Kligfield, R., L. Carmignani, and W.H. Owens, 1981, Strain analysis of a Northern Appenine shear zone using deformed marble breccias: *Journal of Structural Geology*, v.3, p.421-436.
- Kligfield, R., P. Geiser, and J. Geiser, 1986, Construction of geologic cross-sections using microcomputer systems: *Geobyte*, v.1, p.60-66.
- Krebs, W., 1979, Devonian basinal facies: Paleontological Association of London Special Papers, no. 23, p.125-139.
- Little, T.A., 1987, Stratigraphy and structure of metamorphosed upper Paleozoic rocks near Mountain City, Nevada: Geological Society of America Bulletin, v.98, p.1-17.
- Mack, G.H., 1978, Survivability of labile light-mineral fluvial, eolian, and littoral marine environments: the Permian Cutler and Cedar Mesa Formations: *Sedimentology*, v.25, p.587-604.
- Mack, G.H., 1984, Exceptions to the relationship between plate tectonics and sandstone composition: *Journal of Sedimentary Petrology*, v.54, p.212-220.
- Mauch, E.A., 1985, A seismic stratigraphic and structural interpretation of the middle Paleozoic Ikpikpuk-Umiat basin, National Petroleum Reserve, Alaska: unpublished M.A. thesis, Rice University, Houston, Texas.
- McPherson, J.G., G. Shanmugam, and R.J. Moiola, 1987, Fan-deltas and braid deltas: Varieties of coarse-grained deltas: Geological Society of America Bulletin, v. 99, p. 331-340.
- Miall, A.D., 1977, A review of the braided river depositional environment: *Earth Science Reviews*, v.13, p.1-62.
- Miall, A.D., 1978, Lithofacies types and vertical profile models in braided rivers: a summary, *in* A.D. Miall, ed., *Fluvial Sedimentology*: Canadian Society Petroleum Geologists Memoir 5, p.597-604.
- Miall, A.D., 1981, Analysis of fluvial depositional systems: American Association of Petroleum Geologists, Educational Course Notes No. 20, 75p.

- Miller, E.L., B.K. Holdsworth, W.B. Whiteford, and D. Rodgers, 1984, Stratigraphy and structure of the Schoonover sequence, northeastern Nevada: Implications for Paleozoic plate margin tectonics: *Geological Society of America Bulletin*, v.95 1063-1076.
- Mitra, G., and D. Elliott, 1980, Deformation of basement in the Blue Ridge and the development of the South Mountain cleavage: in D.R. Wones, ed., *The Caledonides in the U.S.A.*, Virginia Polytech. Inst./ State University, Memoir 2, p.307-311.
- Moore, R.C., ed., 1953, *Treatise on Invertebrate Paleontology, Part G, Bryozoa*: Geological Society of America, University of Kansas Press, Lawrence, 253p.
- Moore, R.C., ed., 1956, *Treatise on Invertebrate Paleontology, Part F, Coelenterata*: Geological Society of America, University of Kansas Press, Lawrence, 498p.
- Moore, R.C., ed., 1956, *Treatise on Invertebrate Paleontology, Part H, Brachiopoda 2*: Geological Society of America, University of Kansas Press, Lawrence, 404p.
- Moore, R.C., C.G. Lalicker, and A.G. Fisher, 1952, *Invertebrate fossils*: McGraw-Hill, New York, 766p.
- Moore, T.E., 1986, Stratigraphic framework and tectonic implications of pre-Mississippian rocks, northern Alaska: *Geological Society of America Abstracts with Programs*, v.18, p.159.
- Moore, T.E., and M.Churkin, Jr., 1984, Ordovician and Silurian graptolite discoveries from the Neurokpuik Formation (*sensu lato*), northeastern and central Brooks Range, Alaska: *Paleozoic Geology of Alaska and Northwestern Canada Newsletter*, no.1, p.21-23.
- Moore, T.E., and T.H. Nilsen, 1984, Regional variations in the fluvial Upper Devonian and Lower Mississippian(?) Kanayut Conglomerate, Brooks Range, Alaska: *Sedimentary Geology*, v.38, p.465-497.
- Mull, G.C., 1982, Tectonic evolution and structural style of the Brooks Range, northern Alaska: An illustrated summary: in R.B. Blake (Ed.), *Geologic studies of the Cordilleran thrust belt*: Rocky Mountain Association Geologists, Denver, p.1-45.
- Mull, C.G., K.E. Adams, and J.T. Dillon, 1987, Stratigraphy and structure of the Doonerak fenster and Endicott Mountains allochthon, central Brooks Range, Alaska, in I. Tailleux and P. Weimer, eds., *Alaskan North Slope geology*: Society of Economic Paleontologists and Mineralogists, Pacific Section, p.663-679.
- Nilsen, T.H., 1981, Upper Devonian and Lower Mississippian redbeds, Brooks Range, Alaska, in A.D. Miall, ed., *Sedimentation and tectonics in alluvial basins*: Geological Association of Canada Special Paper 23, p.187-219.
- Nilsen, T.H., 1984, Tectonic reconstruction of the Devonian redbeds of the Brooks Range, Alaska: *Geological Society of America Abstracts with Programs*, v. 16, p.326

- Nilsen, T.H., W.P. Brosgé, J.T. Dutro Jr., and T.E. Moore, 1981a, Depositional model for the fluvial Upper Devonian Kanayut Conglomerate, Brooks Range, Alaska: U.S. Geological Survey Circular 823-B, p.B20-B21.
- Nilsen, T.H., and T.E. Moore, 1982a, Sedimentology and stratigraphy of the Kanayut Conglomerate, central and western Brooks Range, Alaska - Report of the 1981 field season: U.S. Geological Survey Open-File Report 82-674, 64p.
- Nilsen, T.H., and T.E. Moore, 1982b, Fluvial facies model for the Upper Devonian and Lower Mississippian(?) Kanayut Conglomerate, Alaska, *in* A.F. Embry and H.R. Balkwill, eds., Arctic Geology and Geophysics: Canadian Society of Petroleum Geologists, Memoir 8, p.1-12.
- Nilsen, T.H., and T.E. Moore, 1984, Stratigraphic nomenclature for the Upper Devonian and Lower Mississippian(?) Kanayut Conglomerate, Brooks Range, Alaska: U.S. Geological Survey Bulletin, 1529-A, p.A1-A64.
- Nilsen, T.H., T.E. Moore, D.F. Balin, and S.Y. Johnson, 1982, Sedimentology and stratigraphy of the Kanayut Conglomerate, central Brooks Range, Alaska - Report of the 1980 field season: U.S. Geological Survey Open-File Report 82-199, 81p.
- Nilsen, T.H., T.E. Moore, and W.P. Brosgé, 1980a, Paleocurrent maps for the Upper Devonian and Lower Mississippian Endicott Group, Brooks Range, Alaska: U.S. Geological Survey Open-File Report 80-1066, 1:1,000,000.
- Nilsen, T.H., T.E. Moore, J.T. Dutro Jr., W.P. Brosgé, and D.M. Orchard, 1980b, Sedimentology and stratigraphy of the Kanayut Conglomerate, central and eastern Brooks Range, Alaska - Report of the 1978 field season: U.S. Geological Survey Open-File Report 80-888, 40 p.
- Nilsen, T.H., T.E. Moore, W.P. Brosgé, and J.T. Dutro Jr., 1981b, Sedimentology and stratigraphy of the Kanayut Conglomerate and associated units Brooks Range, Alaska - Report of the 1979 field season: U.S. Geological Survey Open-File Report 81-506, 37p.
- Norris, D.K., and Yorath, C.J., 1981, The North American plate from the Arctic archipelago to the Romanzof Mountains, *in* A.E.M. Narin, M. Churkin Jr., and F.G. Stehli, eds., The ocean basins and margins, Volume 5, The Arctic Ocean: Plenum Press, New York, p.37-103.
- Oldow, J.S., H.G. Avé Lallemant, F.E. Julian, C.M. Seidensticker, and J.C. Phelps, 1984, The Doonerak window duplex: Regional implications: Geological Society of America Abstracts with Programs, v.16, p.326.
- Oldow, J.S., M. Seidensticker, J.C. Phelps, F.E. Julian, R.R. Gottschalk, K.W. Boler, J.W. Handschy, and H.G. Avé Lallemant, 1987, Balanced cross sections through the central Brooks Range, Alaska: American Association of Petroleum Geologists Special Paper, 19p., 8 plates.
- Okulitch, A.V., 1985, Paleozoic plutonism in southeastern British Columbia: Canadian Journal of Earth Sciences, v.22, p.2813-2857.

- Palmer, A.R., J.T. Dillon, and J.T. Dutro, Jr., 1984, Middle cambrian trilobites with Siberian affinities from the central Brooks Range, northern Alaska: *Geology of Alaska and Northwestern Canada Newsletter*, no.1, p.29-30.
- Patton, W.W., 1973, Reconnaissance geology of the northern Yukon-Koyukuk province, Alaska: U.S. Geological Survey Professional Paper 774-A, 17p.
- Phelps, J.C., 1987, Stratigraphy and structure of the northeastern Doonerak window area, central Brooks Range, northern Alaska: unpublished Ph.D. thesis, Rice University, Houston, Texas, 171p.
- Phelps, J.C., H.G. Avé Lallemant, C.M. Seidensticker, F.E. Julian, and J.S. Oldow, 1987, Late-stage high-angle faulting, eastern Doonerak window, central Brooks Range, Alaska: in I. TAILLEUR and P. WEIMER, eds., *Alaskan North Slope geology*, Society Economic Paleontologists Mineralogists, Pacific Section, p.685-690.
- Postma, G., 1984, Slumps and their deposits in fan-delta front and slope: *Geology*, v.12, p.27-30.
- Potter, P.E., 1978, Significance and origin of big rivers: *Journal of Geology*, v. 86, p.13-33.
- Ramberg, I.B., and P. Morgan, 1984, Physical characteristics and evolutionary trends of continental rifts: *Tectonics*, v.7, p.165-216.
- Ramberg, H., 1975, Superposition of homogeneous strain and progressive deformation in rocks: *Bulletin Geologic Institute University Uppsala, Sweden*, v.6, p.35-67.
- Ramsay, J.G., 1967, *Folding and fracturing of rocks*: New York, McGraw-Hill, 568pp.
- Ramsay, J.G., and R.H. Graham, 1970, Strain variation in shear belts: *Canadian Journal of Earth Sciences*, v. 7, p.786-813.
- Ramsay, J.G., and M.I. Huber, 1983, *The techniques of modern structural geology Volume 1: Strain analysis*: London, Academic Press, p.1-307.
- Ramsay, J.G., M. Casey, and R. Kligfield, 1983, Role of shear in development of the Helvetic fold-thrust belt of Switzerland: *Geology*, v.11, p.439-442.
- Ramsay, J.G., and D.S. Wood, 1973, The geometric effects of volume change during deformation processes: *Tectonophysics*, v.16, p.263-277.
- Roberts, R.J., P.E. Hotz, J. Gilluly, and H.G. Ferguson, 1958, Paleozoic rocks of north-central Nevada: *American Association of Petroleum Geologists Bulletin*, v.42, p.2813-2857.
- Roeder, D., and C.G. Mull, 1978, Tectonics of Brooks Range ophiolites, Alaska: *American Association of Petroleum Geologists Bulletin*, v.62, p.1696-1713.
- Rust, B.R., 1972, Structure and process in braided river: *Sedimentology*, v.18, p.221-245.

- Rust, B.R., 1978, Depositional models for braided alluvium, *in* A.D. Miall, ed., *Fluvial Sedimentology*: Canadian Society of Petroleum Geologists Memoir 5, p.605-625.
- Sanderson, D.J., 1979, The transition from upright to recumbent folding in the Variscan fold belt of southwest England: a model based on the kinematics of simple shear: *Journal of Structural Geology*, v.1, p.171-180.
- Sanderson, D.J., 1982, Models of strain variation in nappes and thrust sheets-a review: *Tectonophysics*, v.88, p.201-233.
- Seidensticker, C.M., 1986, Structural development at the northern margin of the Doonerak duplex, Brooks Range, Alaska: *Geological Society of America Abstracts with Programs*, v.18, p.182.
- Seidensticker, C.M., F.E. Julian, J.S. Oldow, and H.G. Avé Lallemant, 1987, Kinematic significance of antithetic structures in the central Brooks Range, Alaska: *Geological Society of America Abstracts with Programs*, v.19, p.449.
- Seidensticker, C.M., F.E. Julian, J.C. Phelps, J.S. Oldow, and H.G. Avé Lallemant, 1987, Lateral continuity of the Blarney Creek thrust, Doonerak window, central Brooks Range, Alaska, *in* I. Tailleir and P. Weimer, eds., *Alaskan North Slope geology*: Society of Economic Paleontologists and Mineralogists, Pacific Section, p.681-683.
- Shimer, H.W., and R.R. Shrock, 1944, *Index fossils of North America*: John Wiley and Sons, New York, 837p.
- Silberling, N.J., and D.L. Jones, 1984, Lithotectonic terrane map of the North American cordillera: U.S. Geological Survey Open-File Report 84-523, p.A1-A12.
- Smith, N.D., 1974, Sedimentology and bar formation in the upper Kicking Horse River, a braided outwash stream: *Journal of Geology*, v.82, p.205-224.
- Speed, R.C., 1979, Collided Paleozoic platelet in the western U.S.: *Journal of Geology*, v.87, p.279-292.
- Speed, R.C., and N.H. Sleep, 1982, Antler orogeny and foreland basin: A model: *Geological Society of America Bulletin*, v.93, p.815-828.
- Suczek, C.A., 1987, Accreted terranes and sandstone composition: *Geological Society of America Abstracts with Programs*, v. 19, p.455.
- Tailleir, I.L., W.P. Brosgé, and H.N. Reiser, 1967, Palinspastic analysis of Devonian rocks in northwestern Alaska, *in* D.H. Oswald, ed., *International symposium on the Devonian system*: Alberta Society of Petroleum Geologists, Calgary, Canada, p.1345-1361.
- Tasch, P., 1980, *Paleobiology of the invertebrates*: John Wiley and Sons, New York, 975p.

- Templeman-Kluit, D.J., 1979, Transported cataclasite, ophiolite, and granodiorite in Yukon: Evidence of an arc-continent collision: Geological Survey of Canada Paper 79-14, 27p.
- Waldron, H.M., and M. Sandiford, 1988, Deformation volume and cleavage development in metasedimentary rocks from the Ballarat slate belt: *Journal Structural Geology*, v.10, p.53-62.
- Warren, P.S., and C.R. Stelck, 1956, Devonian faunas of western Canada: Geological Association of Canada Special Paper, no.1, 73p.
- Williams, P.F., and B.R. Rust, 1969, The sedimentology of a braided river: *Journal of Sedimentary Petrology*, v.39, p.649-679.
- Wirth, K.R., D.J. Harding, A.E. Blythe, and J.M. Bird, 1976, Brooks Range ophiolite crystallization and emplacement ages from $^{40}\text{Ar}/^{39}\text{Ar}$ data: Geological Society of America Abstracts with Programs, v.18, p.792.
- Woodcock, N.H., 1977, Specification of fabric shapes using an eigenvalue method: Geological Society of America Bulletin, v.88, p.1231-1236.
- Woodward, N.B., S.E. Boyer, and J. Suppe, 1985, An outline of balanced cross-sections: University of Tennessee, Studies in Geology No. 11, Knoxville, TN, USA, 170pp.
- Young, S.W., 1976, Petrographic textures of detrital polycrystalline quartz as a aid to determining crystalline source rocks: *Journal of Sedimentary Petrology*, v.46, p.595-603.
-

Appendix 1 - Measured stratigraphic sections

Stratigraphy of the Kayak Shale, southern Endicott Mountains allochthon
(SE 1/4, sec. 19, T. 15 S., R. 11 E., Phillip Smith Mtns. A-5 quadrangle, Alaska)

Description Thickness	Interval thickness	
	(meters)	(meters)
present erosion surface		
Thinly laminated, black (N1) shale with occasional mottled yellowish gray (5 Y 7/2) bioturbated intervals.	5.0	39.5
Interbedded black (N1) shale and medium- (N5) to dark- (N3) gray argillaceous limestone. Shales are thinly laminated and occasionally burrowed. Limestone beds are 5 cm to 40 cm thick and composed of fossiliferous wackestone and/or packstone. Fossils: solitary and colonial Rugose corals; crinoid fragments	7.5	34.5
Thinly laminated, black (N1) shale. Bioturbation is common near the base of this interval.	22.5	27.0
Interbedded black (N1) shale, mottled yellowish gray (5 Y 7/2) shale, grayish orange (10 YR 7/4) siltstone, and very fine- to fine-grained grayish yellow (5 Y 8/4) quartz arenite. Shales are frequently bioturbated.	2.5	4.5
Thinly bedded (<20 cm), well sorted, fine-grained pale grayish yellow (5 Y 8/4) quartz arenite. Most beds are massive or horizontally laminated. Some beds are ripple cross-laminated. Discontinuous, poorly sorted coarse- to medium- grained, pebbly quartz-chert arenite lenses are locally present at the base of this interval.	2.0	2.0
Top of Kanayut Conglomerate		0.0

Stratigraphy of the Kanayut Conglomerate, southern Endicott Mountains allochthon
(secs. 19 and 30, T. 15 S., R. 11 E., Phillip Smith Mtns. A-5 quadrangle, Alaska)

Note: Lithofacies codes are defined in Table 2.2 on page 83.

Description Thickness	Interval thickness	
	(meters)	(meters)

Base of Kayak Shale (see previous page)

Grayish yellow (5 Y 8/4) to grayish orange (10 YR 7/4) pebbly sandstone and pebble conglomerate. Bedding thickness varies from 30 cm to 1.7 m. Beds are amalgamated or separated by thin (<20 cm) poorly-cemented, fine- to medium-grained quartzose sandstone. Individual beds are trough cross-stratified, massive, and/or horizontally stratified. Most beds normally graded. Maximum clast size is 4 cm. Clasts are composed of black, gray, red, green, and white chert, gray quartzite, and brown mudstone. Sandstone/conglomerate ratio \approx 3/1.
Lithofacies: Gt, Gm, St, Sp, Sh, Fm.

75.0 1015.0

Grayish orange (10 YR 7/4), grayish yellow (5 Y 8/4) and medium gray (N5) pebble conglomerate and pebbly sandstone. Bedding thickness varies from 20 cm to 2.0 m. Beds are amalgamated or, more rarely, separated by thin (<20 cm) fine- medium grained sandstone. Individual beds are massive or trough cross-stratified. Most beds are normally graded. Maximum clast size is 5 cm. Clasts are composed of black, gray, red, green, and white chert, light gray quartzite, brown mudstone, and brown to orange calcareous mudstone. Sand fraction is composed of chert and quartz grains. Sandstone/conglomerate ratio \approx 3/2.
Lithofacies: Gm, Gt, St.

122.0 940.0

Grayish orange (10 YR 7/4), grayish yellow (5 Y 8/4) and light olive gray (5 Y 6/1) pebble conglomerate and pebbly sandstone. Bedding thickness varies from 20 cm to 2.0 m. Beds are amalgamated. Individual beds are trough cross-stratified, massive, horizontally stratified, or planar cross-stratified. Most beds are normally graded. Maximum clast size is 5 cm. Clasts are composed of black, gray, red, green, and white chert, light gray quartzite, and brownish orange calcareous mudstone. Sand fraction is composed of chert and quartz grains. Sandstone/conglomerate ratio \approx 3/2.
Lithofacies: Gt, Gm, Gp, St, Sh.

41.0 818.0

Yellowish gray (5 Y 7/2), moderate yellowish brown (10 YR 5/4), and medium gray (N5) pebble conglomerate and pebbly sandstone. Bedding thickness varies from 30 cm to 1.9 m. Beds are amalgamated or, less frequently, separated by fine- to coarse-grained sandstone. Individual beds are trough cross-stratified or massive. Most beds are normally graded. Maximum clast size is 5 cm. Clasts are

composed of black, gray, red, green, and brown chert, light gray quartzite, and brown mudstone. Sand fraction is composed of chert and quartz grains. Sandstone/conglomerate ratio $\approx 1/1$.

Lithofacies: Gt, Gm, St.

171.0

777.0

Moderate yellowish brown (10 YR 5/4), grayish orange (10 YR 7/4), light gray (N7), and grayish yellow (5 Y 8/4) pebble conglomerate and pebbly sandstone. Bedding thickness varies from 30 cm to 1.9 m. Beds are amalgamated. Individual beds are trough cross-stratified, massive, or horizontally stratified. Most beds are normally graded. Maximum clast size is 6 cm. Clasts are composed of black, light gray, medium gray, greenish gray, reddish brown, and mottled chert, light gray quartzite, and brownish orange calcareous mudstone. Sand fraction is composed of fine- to coarse-grained chert and quartz.

Sandstone/conglomerate ratio $\approx 2/3$.

Lithofacies: Gt, Gm, St.

87.0

606.0

Grayish orange (10 YR 7/4), medium gray (N5), and light olive gray (5 Y 6/1) pebble conglomerate. Bedding thickness varies from 70 cm to 2.5 m. Beds are amalgamated. Individual beds are trough cross-stratified or massive. Both normal and reverse graded beds are present. Maximum clast size is 8 cm. Clasts are composed of black, light gray, white, medium gray, greenish gray, reddish brown, red, green, and mottled chert, light gray quartzite, brown mudstone, dark gray mudstone/slate, and brownish orange calcareous mudstone. Sand fraction is composed of fine- to coarse-grained chert and quartz.

Sandstone/conglomerate ratio $\approx 1/4$.

Lithofacies: Gt, Gm.

205.0

519.0

Light olive gray (5 Y 6/1) and grayish yellow (5 Y 8/4) pebble conglomerate and pebbly sandstone. Bedding thickness varies from 20 cm to 2.0 m. Beds are amalgamated or separated by thin (<20 cm) coarse- to fine-grained sandstone. Individual beds are trough cross-stratified, horizontally stratified, planar cross-stratified, or massive. Some beds are normally graded. Maximum clast size is 6 cm. Clasts are composed of dark gray, medium gray, greenish gray, brown, red, and mottled chert, light gray quartzite, brown mudstone, and dark gray mudstone/slate. Sand fraction is composed of fine- to coarse-grained chert and quartz. Sandstone/conglomerate ratio $\approx 1/3$.

Lithofacies: Gt, Gm, Gp, St.

112.0

314.0

Light olive gray (5 Y 6/1), light gray (N7), and grayish yellow (5 Y 8/4) pebble conglomerate and pebbly sandstone. Bedding thickness varies from 40 cm to 2.0 m. Beds are amalgamated or separated by thin (<20 cm) coarse- to fine-grained sandstone. Individual beds are trough cross-stratified or massive. Some beds are normally graded. Maximum clast size is 6 cm. Clasts are composed of black, medium gray, greenish gray, reddish brown, white, and mottled chert, light gray quartzite, brown mudstone, dark

gray mudstone/slate, and brownish orange calcareous mudstone.
 Sand fraction is composed of fine- to coarse-grained chert and quartz.
 Sandstone/conglomerate ratio $\approx 2/3$.
 Lithofacies: Gt, Gm, St.

145.0 202.0

Light gray (N7), grayish orange (10 YR 7/4), and grayish yellow (5 Y 8/4) pebble conglomerate and pebbly sandstone. Bedding thickness varies from 20 cm to 2.0 m. Beds are amalgamated or separated by thin (<20 cm) coarse- to fine-grained sandstone. Individual beds are trough cross-stratified, massive, horizontally stratified, or planar cross stratified. Some beds are normally graded. Maximum clast size is 5 cm. Clasts are composed of black, medium gray, light gray, brown, and mottled chert, light gray quartzite, brown mudstone, dark gray mudstone/slate, and brownish orange calcareous mudstone. Sand fraction is composed of fine- to coarse-grained chert and quartz. Sandstone/conglomerate ratio $\approx 3/2$.
 Lithofacies: Gt, Gm, Gp, St.

26.0 57.0

Light grayish orange (10 YR 7/4) and grayish yellow (5 Y 8/4) pebbly fine- to coarse-grained sandstone. Bedding thickness varies from 10 cm to 2.0 m. Beds are amalgamated. Individual beds are trough cross-stratified, planar cross-stratified, or massive. Maximum clast size is 3 cm. Clasts are composed of black, medium gray, greenish gray, reddish brown, white, and mottled chert, light gray quartzite, and gray mudstone.
 Lithofacies: St, Sp, Fm.

31.0 31.0

Top of Hunt Fork Shale

0.0

Stratigraphy of the upper Hunt Fork Shale, southern Endicott Mountains allochthon (N 1/2, sec. 27, and S 1/2, sec. 22, T. 15 S., R. 11 E., Phillip Smith Mtns. A-5 quadrangle, Alaska)

Description Thickness	Interval thickness	
	(meters)	(meters)
Base of Kanayut Conglomerate		
Interbedded very fine-grained grayish yellow (5 Y 8/4) sandstone, light olive gray (5 Y 6/1) to grayish orange (10 YR 7/4) siltstone, and thinly laminated greenish gray (5 GY 6/1) to black (N1) shale. Individual beds are 0.5 cm to 7.0 cm thick. Some sandstone beds are ripple cross stratified. Symmetrical ripples are preserved on the tops of some sandstone beds. Mudcracks are occasionally preserved in yellowish orange siltstone intervals. Sandstone and siltstone layers frequently contain vertical burrows. Sandstone/shale ratio \approx 1/2.	12.0	248.0
Interbedded very fine-grained grayish yellow (5 Y 8/4) sandstone and light olive gray (5 Y 6/1) siltstone. Individual sandstone and siltstone beds are 1.0 cm to 10.0 cm thick. Sandstone and siltstone beds are amalgamated or separated by very thin (< 1 cm) dark greenish gray (5 GY 4/1) shale intervals. Some sandstone beds are ripple cross stratified. Sandstone and siltstone layers frequently contain vertical burrows. Sandstone/shale ratio \approx 6/1.	5.0	236.0
Interbedded very fine-grained grayish yellow (5 Y 8/4) sandstone, light olive gray (5 Y 6/1) siltstone, grayish orange (10 YR 7/4) calcareous mudstone and thinly laminated olive gray (5 Y 4/1) to black (N1) shale. Individual sandstone and siltstone beds are 0.5 cm to 20.0 cm thick. Most sandstone beds are massive; some are ripple cross-stratified. Ripple marks are preserved on the tops of some sandstone beds. Mudcracks, wrinkle marks, algal mats, and oncolites are occasionally preserved in calcareous mudstones. Sandstone and siltstone layers occasionally contain vertical burrows. This part of the section also contains medium gray (N5) to olive gray (5 Y 4/1) channelized fine- to coarse-grained sandstone and pebbly sandstone. Channels are between 1.0 and 12.0 m wide and between 10 cm and 5 m deep. Internally the channels are trough cross-stratified, massive, and/or normally graded. Pebbles are composed of medium gray, black, reddish brown, and light gray chert, and mudstone rip-up clasts. Maximum clast size is 4 cm. Sand fraction is composed of chert and quartz grains. Sandstone/shale ratio \approx 1/3. Fossils: Terebratulid brachiopods, algal mats, oncolites, woody plant impressions.	131.0	231.0
Olive gray (5 Y 4/1) to grayish yellow (5 Y 8/4) fine- to medium-grained quartzose sandstone. Internally trough cross-stratified to massive.	3.5	100.0

Interbedded very fine-grained light olive gray (5 Y 6/1) sandstone, and thinly laminated olive gray (5 Y 4/1) to olive black (5 Y 2/1) shale. Individual beds are 0.5 cm to 10.0 cm thick. Some sandstone beds are ripple cross-stratified. Sandstone layers occasionally contain vertical burrows; some shale beds contain <i>Chondrites</i> trace fossils. Sandstone/shale ratio $\approx 1/2$.	30.0	96.5
Grayish orange (10 YR 7/4) argillaceous limestone. Fossils: Terebratulid brachiopods, algal mats, oncolites. Laterally discontinuous.	1.5	66.5
Interbedded very fine-grained olive gray (5 Y 4/1) sandstone and thinly laminated olive gray (5 Y 4/1) to black (N1) shale. Individual sandstone beds are 0.5 cm to 10.0 cm thick. Most sandstone beds are massive; some are ripple cross-stratified. Wrinkle marks, algal mats, and oncolites are occasionally preserved in shales. Sandstone layers occasionally contain vertical burrows. This part of the section also contains medium gray (N5) to olive gray (5 Y 4/1) channelized fine-grained sandstone and pebbly sandstone. Channels are between 1.0 and 7.0 m wide and between 10 cm and 2.0 m deep. Internally the channels are trough cross-stratified or massive. Pebbles are composed of medium gray, black, and light gray chert, and mudstone rip-up clasts. Maximum clast size is 4 cm. Sand fraction is composed mostly of quartz grains. Sandstone/shale ratio $\approx 1/5$. Fossils: Spirifer brachiopods, crinoid fragments, gastropods, algal mats, oncolites.	65.0	65.0
Base of undeformed section		0.0

Stratigraphy of the middle Hunt Fork Shale, southern Endicott Mountains allochthon
(E 1/2, sec. 5, T. 16 S., R. 11 E., Phillip Smith Mtns. A-5 quadrangle, Alaska)

Description Thickness	Interval thickness	
	(meters)	(meters)
Top of undeformed section		
Interbedded very fine-grained olive gray (5 Y 4/1) quartzose sandstone and thinly laminated dark greenish gray (5 GY 4/1) to black (N1) shale. Individual sandstone beds are 0.5 cm to 20.0 cm thick. Most sandstone beds are massive; some are ripple cross-stratified. Sandstone layers occasionally contain vertical burrows; some shale beds contain <i>Chondrites</i> trace fossils. Sandstone/shale ratio $\approx 1/4$.	5.0	44.0
Thinly bedded grayish yellow (5 Y 8/4) fine-grained quartzose sandstone. Internally, beds are trough cross-stratified or massive. Laterally discontinuous, lenticular geometry.	2.0	39.0
Interbedded fine-grained olive gray (5 Y 4/1) quartzose sandstone and thinly laminated olive gray (5 Y 4/1) to black (N1) shale. Individual sandstone beds are 0.5 cm to 10.0 cm thick. Most sandstone beds are massive, some are trough cross-stratified, others are ripple cross-stratified. Shales frequently contain thin (1 cm to 4 cm) graded beds which are composed of silt and very fine-grained sand at the base and grade upward to clay shale. This part of the section also contains discontinuous grayish orange (10 YR 7/4) calcareous breccia beds composed of algal mat fragments, oncolites, fossil fragments, and mudstone rip-up clasts. Sandstone layers occasionally contain vertical burrows. Sandstone/shale ratio $\approx 1/4$. Fossils: <i>Spirifer</i> brachiopods, crinoid fragments, Rugose coral fragments, gastropods, Tabulate coral fragments, bryozoan fragments, Terebratulid brachiopods, algal mat fragments, oncolites.	9.5	37.0
Hummocky cross-stratified, fine- to very fine-grained yellowish gray (5 Y 8/1) quartzose sandstone. Individual hummocks are 1.0 m to 2.5 m wide and 5 cm to 70 cm deep.	2.5	27.5
Interbedded grayish yellow (5 Y 8/4) siltstone and very fine-grained sandstone, and thinly laminated dark greenish gray (5 GY 4/1) to olive black (5 Y 2/1) shale. Individual sandstone beds are 0.5 cm to 1.5 cm thick. Sandstone beds are massive or contain abundant vertical burrows. Sandstone/shale ratio $\approx 1/1$.	2.0	25.0
Interbedded fine-grained light olive gray (5 Y 6/1) quartzose sandstone and thinly laminated olive gray (5 Y 4/1) to olive black (5 Y 2/1) shale. Individual sandstone beds are 0.5 cm to 4.0 cm thick. Sandstone beds are massive or contain vertical burrows. Shales occasionally contain <i>Chondrites</i> trace fossils. Shales frequently contain thin (1 cm to 4 cm) graded beds which are composed of silt and very		

fine-grained sand at the base and grade upward to clay shale.		
This part of the section also contains discontinuous yellowish orange (10 YR 7/4) calcareous breccia beds composed of algal mat fragments, oncolites, fossil fragments, mudstone rip-up clasts, and chert pebbles. Sandstone/shale ratio \approx 1/6.		
Fossils: Spirifer brachiopods, crinoid fragments, bryozoan fragments, algal mat fragments.	16.0	23.0
Hummocky cross-stratified, fine- to very fine-grained yellowish gray (5 Y 8/4) quartzose sandstone. Individual hummocks are 1.0 m to 2.0 m wide and 5 cm to 50 cm deep.		
	2.0	7.0
Dark gray (N3) rip-up clast and fossil breccia. Laterally discontinuous. Fossils: Rugose corals, crinoid fragments, Terebratulid brachiopods, oncolites.		
	1.0	6.0
Interbedded fine-grained light olive gray (5 Y 6/1) quartzose sandstone and thinly laminated olive gray (5 Y 4/1) to olive black (5 Y 2/1) shale. Individual sandstone beds are 0.5 cm to 4.0 cm thick. Shales frequently contain thin (1 cm to 4 cm) graded beds which are composed of silt and very fine-grained sand at the base and grade upward to clay shale. Sandstone/shale ratio \approx 1/6.		
	5.0	5.0
Base of undeformed section		0.0

Stratigraphy of the lower Hunt Fork Shale, southern Endicott Mountains allochthon
(sec. 30, T. 16 S., R. 10 E., Phillip Smith Mtns. A-5 quadrangle, Alaska)

Description Thickness	Interval thickness	
	(meters)	(meters)
Top of undeformed section		
Interbedded fine-grained light olive gray (5 Y 6/1) quartzose sandstone and thinly laminated dark greenish gray (5 GY 4/1) to black (N1) shale. Individual sandstone beds are 0.5 cm to 4.0 cm thick. Shaley intervals are composed of thin (1 cm to 4 cm) graded beds which grade upward from silt and very fine-grained sand to clay shale. Sandstone/shale ratio < 1/10.	8.0	73.0
Laterally continuous, massive fine-grained light olive gray (5 Y 6/1) quartzose sandstone.	0.8	65.0
Interbedded fine-grained light olive gray (5 Y 6/1) quartzose sandstone and thinly laminated dark greenish gray (5 GY 4/1) to black (N1) shale. Individual sandstone beds are 0.5 cm to 4.0 cm thick. Shaley intervals are composed of thin (1 cm to 4 cm) graded beds which grade upward from silt and very fine-grained sand to clay shale. Sandstone/shale ratio < 1/10.	7.0	64.2
Channel-fill, trough cross-stratified, medium gray (N5) to greenish gray (5 GY 6/1) sandstone containing shale rip-up clasts. Rip-up clasts are concentrated in the bottom 20 cm of the channel.	1.5	57.2
Interbedded fine-grained light olive gray (5 Y 6/1) quartzose sandstone and thinly laminated dark greenish gray (5 GY 4/1) to olive black (5 Y 2/1) shale. Individual sandstone beds are 0.5 cm to 4.0 cm thick. Shaley intervals are composed of thin (1 cm to 4 cm) graded beds which grade upward from silt and very fine-grained sand to clay shale. Sandstone/shale ratio < 1/10.	50.0	55.7
Channel-fill, trough cross-stratified, medium gray (N5) to greenish gray (5 GY 6/1) sandstone containing shale rip-up clasts. Rip-up clasts are concentrated in the bottom 10 cm of the channel.	1.2	5.7
Interbedded fine-grained light olive gray (5 Y 6/1) quartzose sandstone and thinly laminated dark greenish gray (5 GY 4/1) to olive black (5 Y 2/1) shale. Individual sandstone beds are 0.5 cm to 4.0 cm thick. Shaley intervals are composed of thin (1 cm to 4 cm) graded beds which grade upward from silt and very fine-grained sand to clay shale. Sandstone/shale ratio < 1/10.	4.5	4.5
Bottom of undeformed section		0.0

Stratigraphy of the Beaucoup Formation, southern Endicott Mountains allochthon
(S 1/2, sec. 2, W 1/2 sec. 11, and sec. 10, T. 36 S., R. 10 W., Chandalar D-6
quadrangle, Alaska)

Note: Shales in this section are intensely deformed, thus, the measured thickness probably does not represent true stratigraphic thickness. In addition, unrecognized intraformational thrust faults may internally disrupt the section

Description Thickness	Interval thickness	
	(meters)	(meters)
Lower Hunt Fork Shale. Tightly folded dark greenish gray (5 GY 4/1) to black (N1) shale. The basal ± 5.0 m of Hunt Fork Shale at this locality is composed of thinly laminated clay shale and thin (1.0 cm to 5.0 cm) graded beds.		
Medium dark gray (N4) fossiliferous limestone. Corals in the middle of this unit are in upright (growth) position. In the basal part of the unit, the shale content increases and fossils are sheared from upright approximately 1.0 m above the basal contact to bedding parallel along the basal contact. Fossils: Colonial and solitary Rugose corals, colonial Tabulate corals, bryozoans.	5.0	347.0
Intensely deformed, yellowish gray (5 Y 7/2), olive gray (5 Y 4/1), and dark gray (N3) to olive black (5 Y 2/1) shale.	8.0	342.0
Medium dark gray (N4) fossiliferous limestone. Corals in the middle of this unit are in upright (growth) position. In the basal part of the unit, the shale content increases and fossils are sheared from upright approximately 1.2 m above the basal contact to bedding parallel along the basal contact. Fossils: Colonial and solitary Rugose corals, colonial Tabulate corals, bryozoans, crinoids.	4.0	334.0
Intensely deformed, olive gray (5 Y 4/1) to olive black (5 Y 2/1) shale, medium gray (N5) to yellowish gray (5 Y 7/2) calcareous silt-shale, and mottled grayish red (10 R 4/2) to greenish gray (5 GY 6/1) silt-shale.	20.0	330.0
Massive, grayish yellow (5 Y 8/4) to medium gray (N5), silica-cemented, chert and quartz granule conglomerate, pebbly sandstone, and coarse-grained sandstone.	2.0	310.0
Mostly covered, intensely deformed, olive gray (5 Y 4/1) to black (N1) shale, and light gray (N7) to yellowish gray (5 Y 7/2) silt-shale and calcareous silt-shale.	276.0	308.0
Pale grayish yellow (5 Y 8/4), massive, fine-grained quartz arenite.	1.2	32.0
Laterally discontinuous, massive, medium light gray (N6) chert pebble		

		131
conglomerate. Maximum (deformed) clast size is 14 cm; Rs≈5.0, Ri≈1.0, estimated undeformed maximum clast size ≈6.5 cm.	0.5	30.8
Laterally discontinuous, dark reddish brown (10 R 3/4) silicified volcaniclastic breccia. Maximum clast size (deformed) is 9 cm.	0.3	30.3
Mostly covered, intensely deformed, olive gray (5 Y 4/1) to olive black (5 Y 2/1) shale, and light gray (N7) to yellowish gray (5 Y 7/2) silt-shale and calcareous silt-shale.	30.0	30.0
Fault contact: Hunt Fork Shale		0.0

Stratigraphy of the Fortress Mountain Formation
(E 1/2, sec. 13, T. 11 S., R. 11 E., and W 1/2, sec. 18, T. 11 S., R. 12 E.,
Phillip Smith Mtns. B-5 quadrangle, Alaska)

Description Thickness	Interval thickness	
	(meters)	(meters)
Top of measured section at top of ridge.		
Amalgamated channel-fill clast supported conglomerate. Internally, most channels are massive or trough cross-stratified; some are normally graded. Maximum clast size is 19 cm. Clasts: grayish green chert (17%), black chert (14%), brownish gray chert (12%), mottled chert (11%), green chert (5%), medium gray chert (3%), laminated gray and black chert (2%), white chert (1%), red chert (1%), light gray fine-grained quartzite (14%), light gray medium-grained chert and quartz arenite (11%), dark gray fine-grained quartzose sandstone (5%), pale red quartz arenite (3%), and milky quartz (1%). Lithofacies: Gm, Gt	10.0	430.0
Partially covered, trough cross-stratified fine- to medium-grained sandstone, pebbly sandstone, and mudstone. Sandstone/conglomerate ratio > 10/1. Maximum clast size is 2.0 cm. Clast compositions similar to adjacent units. Lithofacies: St, Ss, Gt, Fm	27.5	420.0
Amalgamated channel-fill clast supported conglomerate. Internally, most channels are massive or trough cross-stratified; some are normally graded. Maximum clast size is 8 cm. Clasts: black chert (15%), brownish gray chert (14%), mottled chert (14%), grayish green chert (12%), medium gray chert (5%), red chert (1%), light gray medium-grained chert and quartz arenite (15%), dark gray fine-grained quartzose sandstone (10%), light gray fine-grained quartzite (6%), and pale red quartz arenite (3%). Lithofacies: Gm, Gt	52.0	392.5
Partially covered, trough cross-stratified fine- to coarse-grained sandstone, pebbly sandstone, pebble conglomerate, and mudstone. Sandstone/conglomerate ratio > 10/1. Maximum clast size is 3.0 cm. Clast compositions similar adjacent units. Lithofacies: St, Ss, Gt, Fm	30.5	340.5
Amalgamated channel-fill clast supported conglomerate. Internally, most channels are massive or normally graded. Maximum clast size is 8 cm. Clasts: black chert (15%), brownish gray chert (14%), mottled chert (11%), grayish green chert (7%), red chert (5%), medium gray chert (3%), green chert (2%), light gray medium-grained chert and quartz arenite (22%), dark gray fine-grained quartzose sandstone (11%), light gray fine-grained quartzite (5%), pale red quartz arenite (3%), milky quartz (1%), pale pinkish gray gneiss (1%). Lithofacies: Gm	3.0	310.0

Partially covered, trough cross-stratified fine- to coarse-grained sandstone, pebbly sandstone, pebble conglomerate, and mudstone. Sandstone/conglomerate ratio > 10/1. Maximum clast size is 3.0 cm. Clast compositions similar to next lower unit.

Lithofacies: St, Ss, Gt, Fm 24.5 307.0

Amalgamated channel-fill clast supported conglomerate. Internally, most channels are massive or normally graded. Maximum clast size is 18 cm. Clasts: black chert (15%), brownish gray chert (14%), mottled chert (11%), grayish green chert (7%), red chert (5%), medium gray chert (3%), green chert (2%), light gray medium-grained chert and quartz arenite (22%), dark gray fine-grained quartzose sandstone (11%), light gray fine-grained quartzite (5%), pale red quartz arenite (3%), milky quartz (1%), pale pinkish gray graine (1%).

Lithofacies: Gm 18.0 282.5

Three thick (≈ 14 m) fining-upward cycles composed of amalgamated channel-fill clast supported conglomerate and pebbly sandstone.

Internally, channels are trough cross-stratified or massive.

Sandstone/conglomerate ratio $\approx 1/3$. Maximum clast size is 9 cm.

Clasts: black chert (20%), grayish green chert (16%), mottled chert (11%), brownish gray chert (7%), green chert (5%), white chert (4%), laminated gray and black chert (3%), red chert (2%), dark gray fine-grained sandstone and siltstone (15%), light gray medium- to coarse-grained chert and quartz arenite (15%), milky quartz (2%).

Lithofacies: Gt, Gm, St. 42.5 264.5

Partially covered, trough cross-stratified fine- to coarse-grained sandstone, pebbly sandstone, pebble conglomerate, and mudstone.

Sandstone/conglomerate ratio > 10/1. Maximum clast size is 3.0 cm.

Clast compositions similar to next lower unit.

Lithofacies: St, Ss, Gt, Fm 27.5 222.0

Trough cross-stratified to massive clast supported conglomerate and pebbly sandstone. Divided into three 6.0 m thick fining-upward cycles. Sandstone/conglomerate ratio $\approx 1/3$. Maximum clast size is 14 cm. Clasts: black chert (15%), brownish gray chert (10%), grayish green chert (10%), mottled chert (8%), laminated gray and black chert (7%), red chert (5%), green chert (5%), white chert (2%), medium gray chert (1%), light gray medium-grained chert and quartz arenite (16%), dark gray fine-grained sandstone (14%), pale yellowish gray quartzite (5%), and chert pebble conglomerate (2%).

Lithofacies: Gt, Gm, St 18.0 194.5

Trough cross-stratified, 1.5 m thick fining-upward cycles composed of clast supported conglomerate and coarse- to fine-grained sandstone. Sandstone/conglomerate ratio $\approx 1/1$. Maximum clast size is 3.0 cm. Clasts: black chert (19%), mottled chert (15%),

brownish gray chert (12%), medium gray chert (12%), white chert (6%), grayish green chert (5%), green chert (2%), red chert (2%), light gray chert and quartz arenite (15%), dark gray fine-grained sandstone (8%), and chert pebble conglomerate (3%). Lithofacies: St, Gt	55.0	176.5
Partially covered, trough cross-stratified fine- to coarse-grained sandstone, pebbly sandstone, pebble conglomerate, and mudstone. Sandstone/conglomerate ratio > 10/1. Maximum clast size is 3.0 cm. Clast compositions similar to next lower unit. Lithofacies: St, Ss, Gt, Fm	75.0	121.5
Massive clast supported conglomerate. Maximum clast size is 12 cm. Clasts: brownish gray chert (24%), black chert (15%), grayish green chert (10%), mottled chert (8%), medium gray chert (7%), green chert (5%), white chert (4%), dk. gray fine-grained sandstone (22%), and chert pebble conglomerate (5%). Lithofacies: Gm	1.0	46.5
Trough cross-stratified fine- to coarse-grained sandstone, pebbly sandstone, and pebble conglomerate. Sandstone/conglomerate ratio \approx 8/1. Maximum clast size is 1.5 cm. Clast compositions similar to next lower unit. Lithofacies: Gt, St	37.5	45.5
Massive clast supported conglomerate. Maximum clast size is 5 cm. Clasts: black chert (28%), white chert (20%), brownish gray chert (8%), mottled chert (10%), medium gray chert (11%), green chert (8%), maroon fine-grained quartzite (10%), and milky quartz (5%). Lithofacies: Gm	2.0	8.0
Amalgamated channel-fill clast supported conglomerate. Internally trough cross-stratified to massive. Maximum clast size is 11 cm. Clasts: black chert (30%), brownish gray chert (15%), mottled chert (13%), medium gray chert (12%), green chert (7%), white chert (2%), maroon fine-grained quartzite (12%), chert pebble conglomerate (6%), milky quartz (2%), and light gray granite (1%). Lithofacies: Gm, Gt	6.0	6.0
Tundra covered slope		0.0

Appendix 2 - Point Count Data

Mono Qtz - # monocrystalline quartz grains, Poly Qtz - # polycrystalline quartz grains,
 Chert - # chert grains, MudRF - # mudrock fragments, Carb - # carbonate rock fragments,
 PRF - # plutonic rock fragments, MeteRF - # metamorphic rock fragments,
 VRF - # volcanic rock fragments, Plag - # plagioclase feldspar grains,
 K-spar - # potassium feldspar grains.

Grain parameters (percentages):

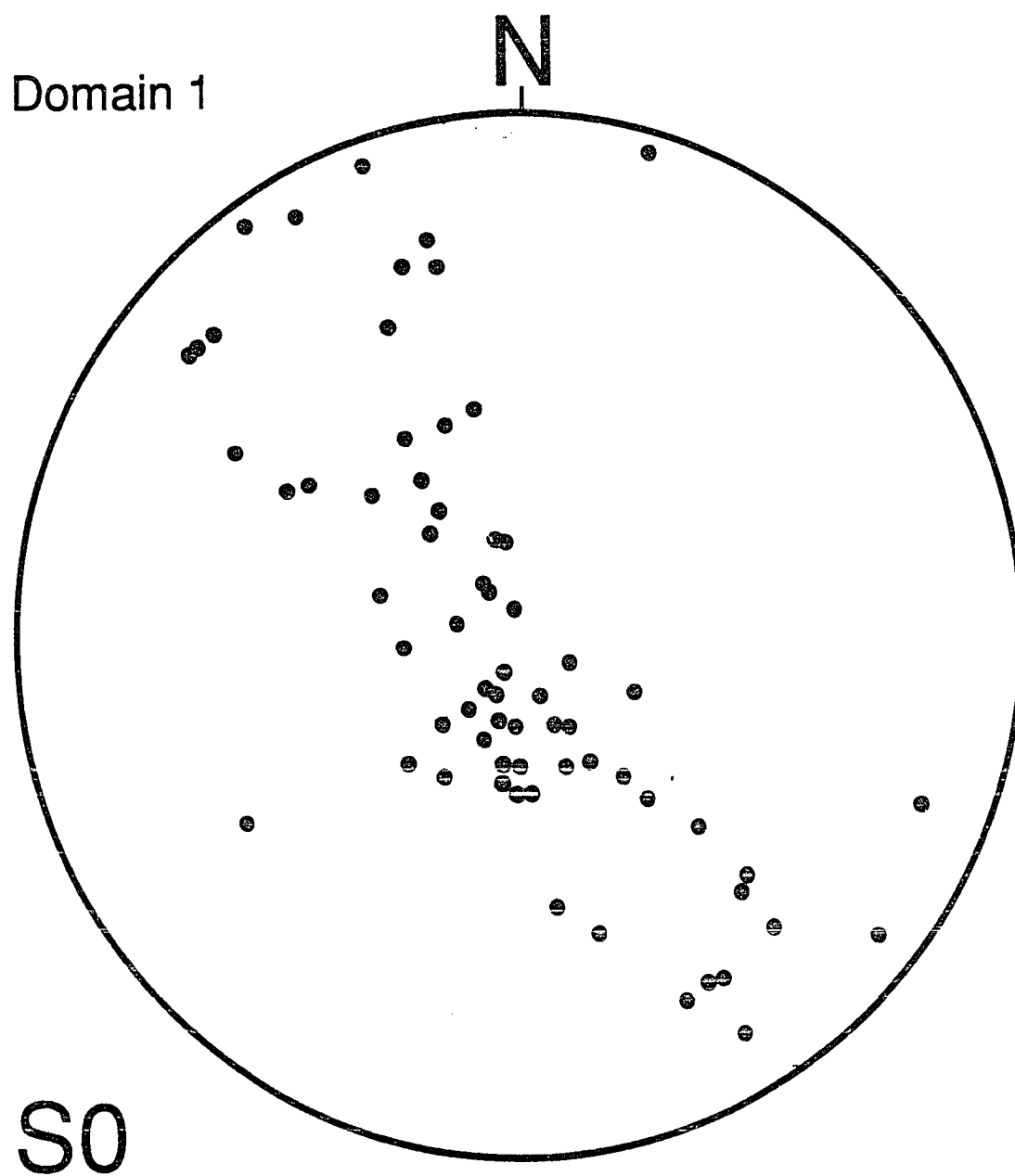
$Q = Q_m + Q_p$	where	<p>Q = total quartzose grains Q_m = monocrystalline quartz grains Q_p = polycrystalline quartz and chert grains</p>
$F = P + K$	where	<p>F = total feldspar grains P = plagioclase feldspar grains K = potassium-feldspar grains</p>
$L = L_m + L_v + L_s$	where	<p>L = total lithic grains (exclusive of chert and polycrystalline quartz) L_m = metamorphic rock fragments L_v = volcanic rock fragments L_s = sedimentary rock fragments</p>
$L = L_{vm} + L_{sm}$ fragments	where	<p>L_{vm} = volcanic and metavolcanic rock L_{sm} = sedimentary and metasedimentary rock fragments</p>
$L_t = L + Q_p$		

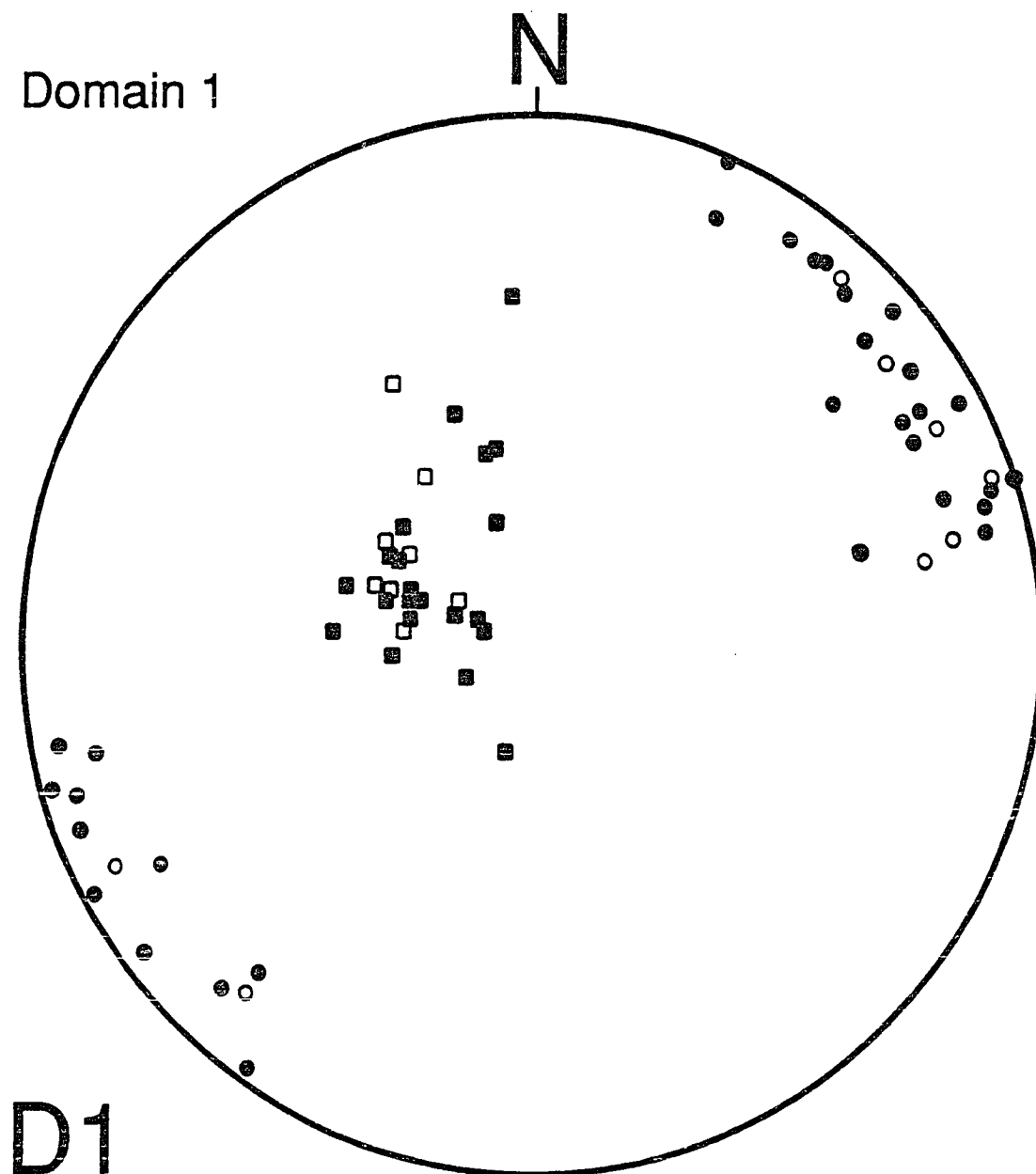
Sample	Formation	Om	Lt	F	Q _t	L	SRF%RF	MRF%RF	VRF%RF	Qp	Lvm	Lsm
686-28	Kanayut	35	64	0	81	18	95	5	0	72	0	28
686-28A	Kanayut	41	58	0	87	12	92	8	0	80	0	20
686-28B	Kanayut	41	58	2	90	9	80	20	0	83	0	17
686-AP	Kanayut	51	48	1	92	8	100	0	0	83	1	16
686-AP2	Kanayut	49	51	0	78	22	100	0	0	58	0	42
887-7	Kanayut	38	60	2	73	25	93	7	0	56	3	41
887-7B	Kanayut	42	57	1	75	24	96	4	0	58	2	41
887-8	Kanayut	42	58	0	71	29	97	3	0	50	0	50
887-8A	Kanayut	57	43	0	76	24	97	3	0	45	0	55
887-8B	Kanayut	38	62	0	69	31	97	3	0	51	0	49
887-19	Kanayut	47	51	2	75	23	100	0	0	52	0	48
887-20	Kanayut	39	60	1	75	24	95	5	0	59	0	41
887-21	Kanayut	44	56	0	72	28	100	0	0	49	0	51
686-1	Hunt Fork	70	28	2	89	9	75	25	0	65	0	35
686-26	Hunt Fork	76	24	0	96	4	100	0	0	83	0	17
686-30	Hunt Fork	71	29	0	98	2	100	0	0	95	0	5
686-44	Hunt Fork	65	35	0	87	13	92	8	0	64	0	36
687-3	Hunt Fork	38	62	0	73	27	97	3	0	56	0	44
687-15	Hunt Fork	55	45	0	80	20	73	27	0	56	0	44
786-123	Hunt Fork	76	24	0	100	0	0	100	0	100	0	0
786-83	Hunt Fork	69	31	0	99	1	0	0	0	97	0	3
787-6	Hunt Fork	31	66	3	56	41	98	2	0	36	4	60
787-8	Hunt Fork	60	40	0	93	7	100	0	0	82	0	18
787-12	Hunt Fork	34	64	0	62	36	97	3	0	44	0	56
787-124	Hunt Fork	41	66	2	81	26	91	3	6	60	5	36
787-124A	Hunt Fork	63	32	0	86	9	100	0	0	73	0	27
787-23	Hunt Fork	47	52	0	76	24	100	0	0	55	0	45
787-27	Hunt Fork	45	55	0	81	19	100	0	0	68	0	34
787-27	Hunt Fork	39	60	0	74	25	100	0	0	58	0	42
787-41	Hunt Fork	45	48	4	61	33	100	0	0	30	7	63
787-41	Hunt Fork	44	54	3	71	27	100	0	0	48	6	46
887-1	Hunt Fork	46	54	0	82	18	80	20	0	66	0	34
887-1B	Hunt Fork	32	63	4	56	39	59	37	4	35	6	58
887-4	Hunt Fork	50	47	3	74	22	54	46	0	48	2	50
887-4B	Hunt Fork	44	55	1	67	32	83	17	0	41	0	59
887-6	Hunt Fork	41	55	4	76	19	87	13	0	60	7	33
686-7	Beaucoup	64	34	3	96	1	0	100	0	90	8	3
686-33	Beaucoup	72	28	0	95	5	100	0	0	83	0	17
687-7	Beaucoup	24	76	1	68	32	76	24	0	58	0	42
787-118	Beaucoup	62	36	2	81	16	91	0	9	51	9	40
787-41A	Beaucoup	19	76	7	54	41	71	0	29	42	23	35
787-55A	Beaucoup	5	78	17	7	76	27	0	73	3	73	24
787-55B	Beaucoup	3	90	7	4	90	7	4	88	1	88	11
787-55C	Beaucoup	17	83	0	83	17	82	18	0	79	0	21
787-55D	Beaucoup	47	48	4	83	13	14	86	0	69	7	24
787-59	Beaucoup	14	82	4	64	32	46	21	33	58	17	25
Sample	Formation	Om	Lt	F	Q _t	L	SRF%RF	MRF%RF	VRF%RF	Qp	Lvm	Lsm

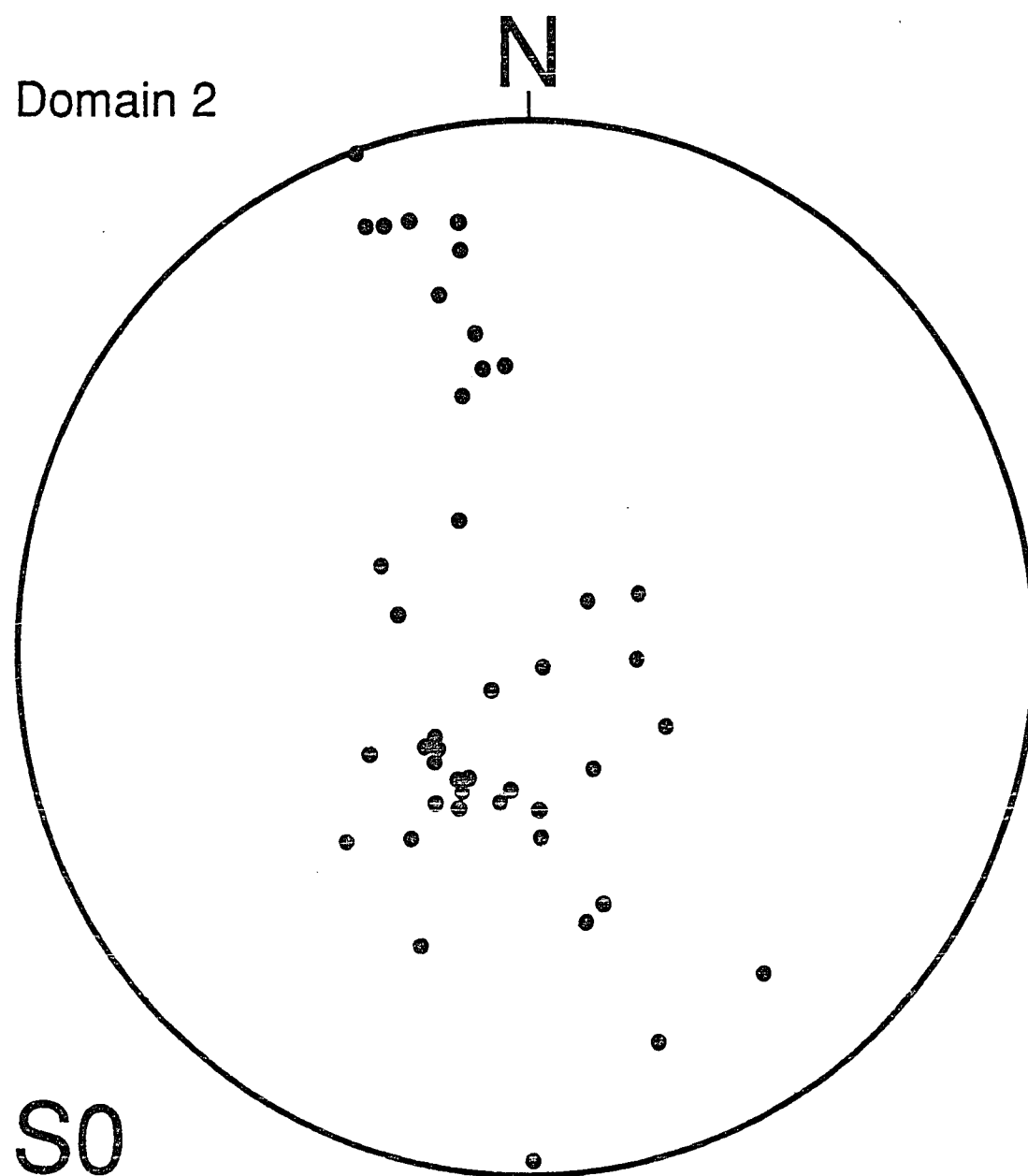
Sample	Formation	Points	Mono Qtz	Poly Qtz	Chert	MudRF	CarbRF	PRF	MetaRF	VRF	Plag	K-Spar
686-28	Kanayut	124	44	18	39	20	1	0	1	0	0	0
686-28A	Kanayut	111	46	9	42	9	1	0	1	0	0	0
686-28B	Kanayut	116	47	10	47	6	2	2	2	0	0	2
686-AP	Kanayut	154	79	18	44	5	7	0	0	0	1	0
686-AP2	Kanayut	115	56	9	25	24	1	0	0	0	0	0
887-7	Kanayut	115	44	17	23	27	0	0	2	0	2	0
887-7B	Kanayut	114	48	17	21	26	0	0	1	0	1	0
887-8	Kanayut	110	46	8	24	29	2	0	1	0	0	0
887-8A	Kanayut	131	75	14	11	30	0	0	1	0	0	0
887-8B	Kanayut	118	45	14	23	35	0	0	1	0	0	0
887-19	Kanayut	115	54	9	23	27	0	2	0	0	0	2
887-20	Kanayut	155	60	24	32	34	1	2	2	0	0	2
887-21	Kanayut	171	76	10	37	48	0	0	0	0	0	0
686-1	Hunt Fork	141	98	8	20	9	0	3	3	0	0	3
686-26	Hunt Fork	123	94	3	21	5	0	0	0	0	0	0
686-30	Hunt Fork	131	93	5	31	2	0	0	0	0	0	0
686-44	Hunt Fork	103	67	5	18	12	0	0	1	0	0	0
687-3	Hunt Fork	113	43	30	9	26	4	0	1	0	0	0
687-15	Hunt Fork	110	60	13	15	16	0	0	6	0	0	0
786-123	Hunt Fork	105	80	0	25	0	0	0	1	0	0	0
786-83	Hunt Fork	115	79	3	32	0	0	0	1	0	0	0
787-6	Hunt Fork	112	35	19	9	41	4	0	1	0	3	0
787-8	Hunt Fork	121	72	1	39	9	0	0	0	0	0	0
787-12	Hunt Fork	106	36	10	20	35	2	0	0	0	0	0
787-124	Hunt Fork	125	51	37	13	27	2	0	1	2	0	0
787-124A	Hunt Fork	103	65	7	17	5	4	0	0	0	0	0
787-12A	Hunt Fork	123	58	6	29	10	19	0	0	0	0	0
787-23	Hunt Fork	113	51	25	16	15	6	0	0	0	0	0
787-27	Hunt Fork	104	41	23	13	26	0	0	0	0	0	0
787-41	Hunt Fork	128	58	10	10	34	8	0	0	0	5	0
787-41	Hunt Fork	147	64	17	23	35	4	0	0	0	5	0
887-1	Hunt Fork	109	50	4	35	16	0	0	4	0	0	0
887-1B	Hunt Fork	117	38	12	16	27	0	2	17	2	3	2
887-4	Hunt Fork	116	58	17	11	14	0	3	12	0	1	1
887-4B	Hunt Fork	109	48	15	10	29	0	1	6	0	0	0
887-6	Hunt Fork	118	48	22	20	20	0	0	3	0	5	0
686-7	Beaucoup	110	70	5	31	0	0	0	1	0	3	0
686-33	Beaucoup	126	91	2	27	5	1	0	0	0	0	0
687-7	Beaucoup	119	28	18	35	29	0	1	9	0	0	1
787-118	Beaucoup	140	87	7	20	20	1	0	0	2	3	0
787-41A	Beaucoup	68	13	12	12	14	6	0	0	8	5	0
787-55A	Beaucoup	83	4	2	0	15	2	0	0	46	12	2
787-55B	Beaucoup	105	3	1	0	6	1	0	0	83	7	0
787-55C	Beaucoup	98	17	8	56	14	0	0	3	0	0	0
787-55D	Beaucoup	112	53	21	19	2	0	0	12	0	4	0
787-59	Beaucoup	74	10	23	14	5	6	0	5	8	3	0
Sample	Formation	No. Points	Mono Qtz	Poly Qtz	Chert	MudRF	CarbRF	PRF	MetaRF	VRF	Plag	K-Spar

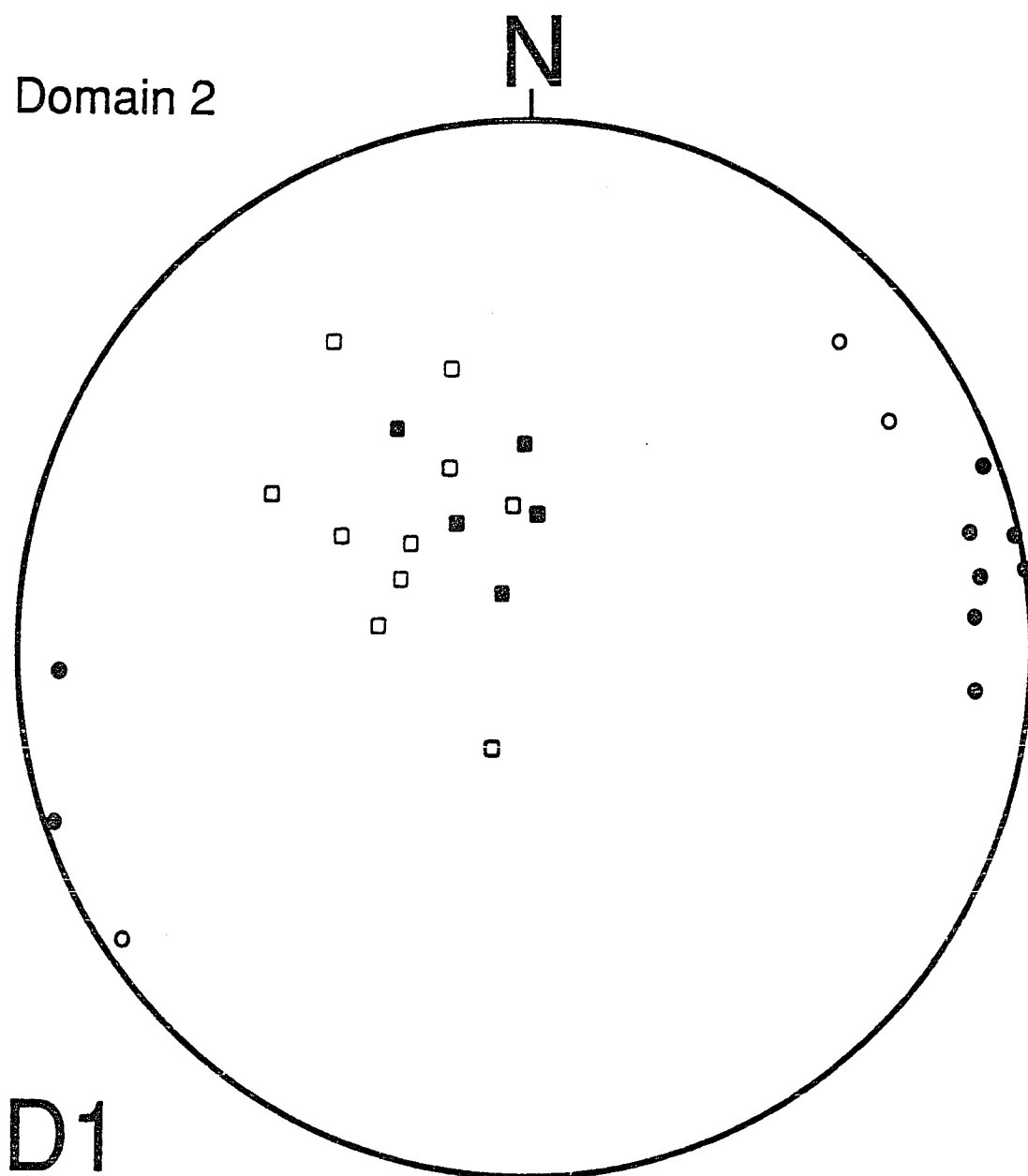
Appendix 3 - Lower hemisphere equal-area stereographic plots of structural data.

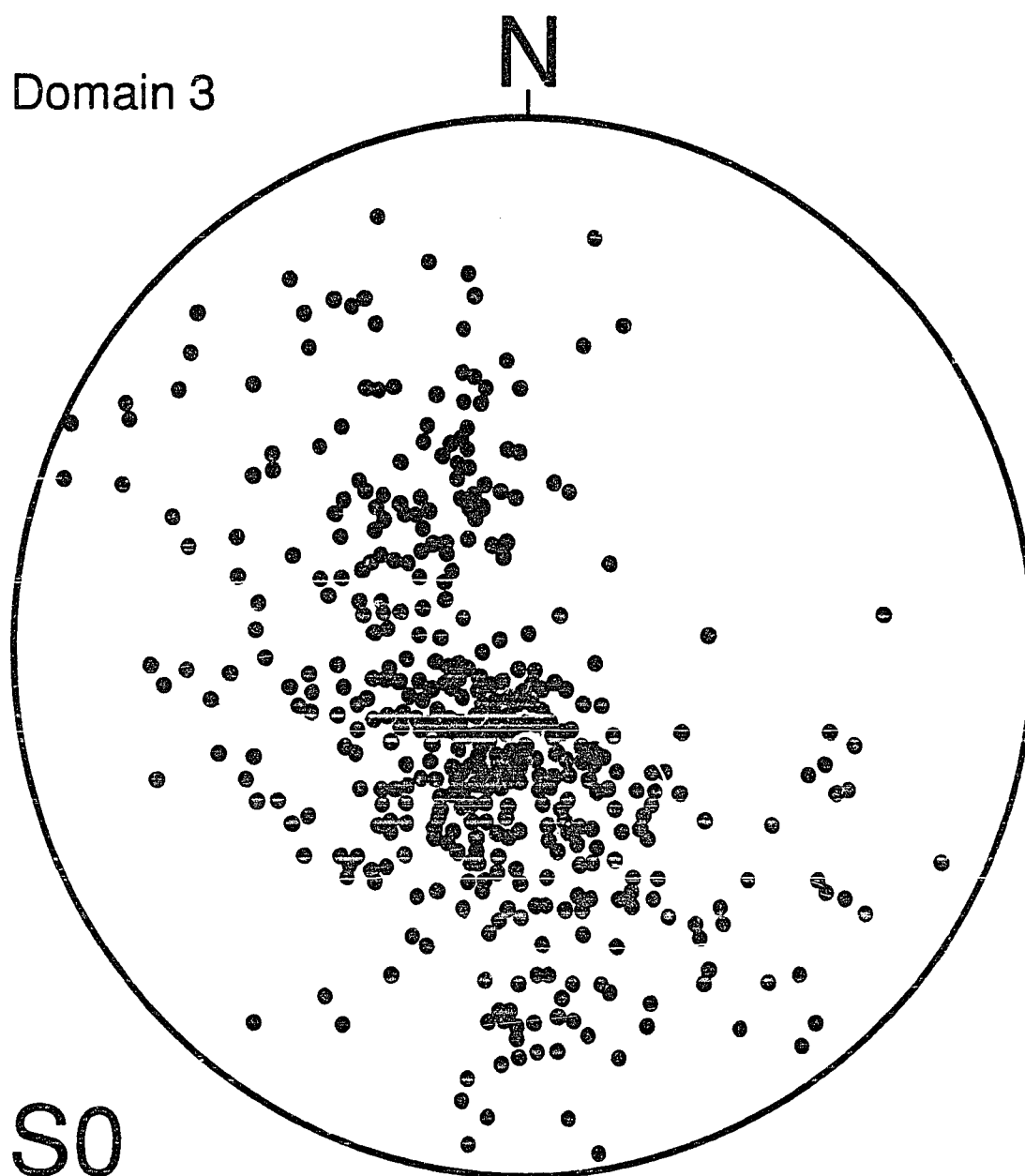
SO solid dots are poles to bedding. On all other stereonet solid dots are fold axes, open circles are intersection lineations, solid squares are poles to axial planes, and open squares are poles to cleavage planes.

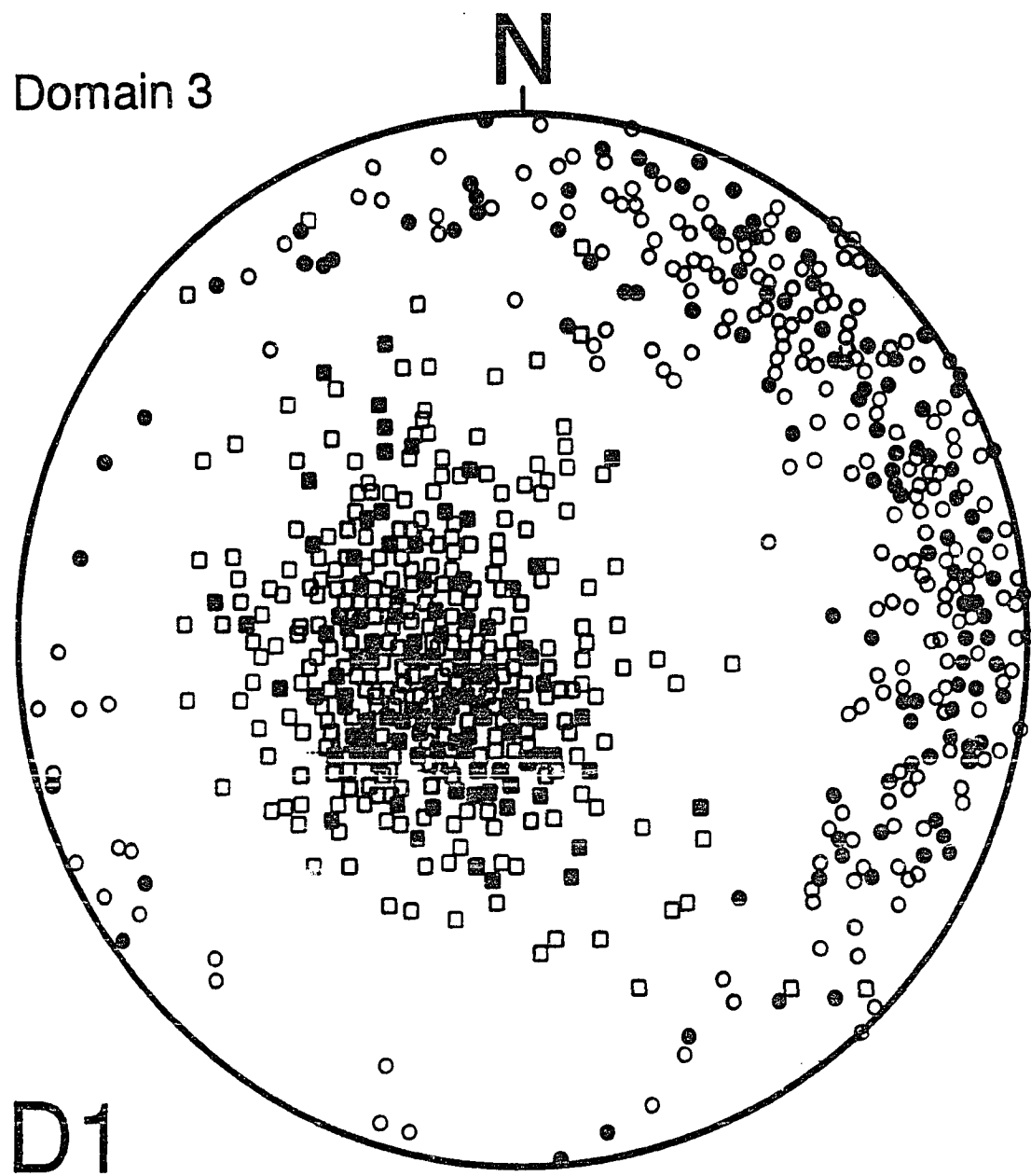


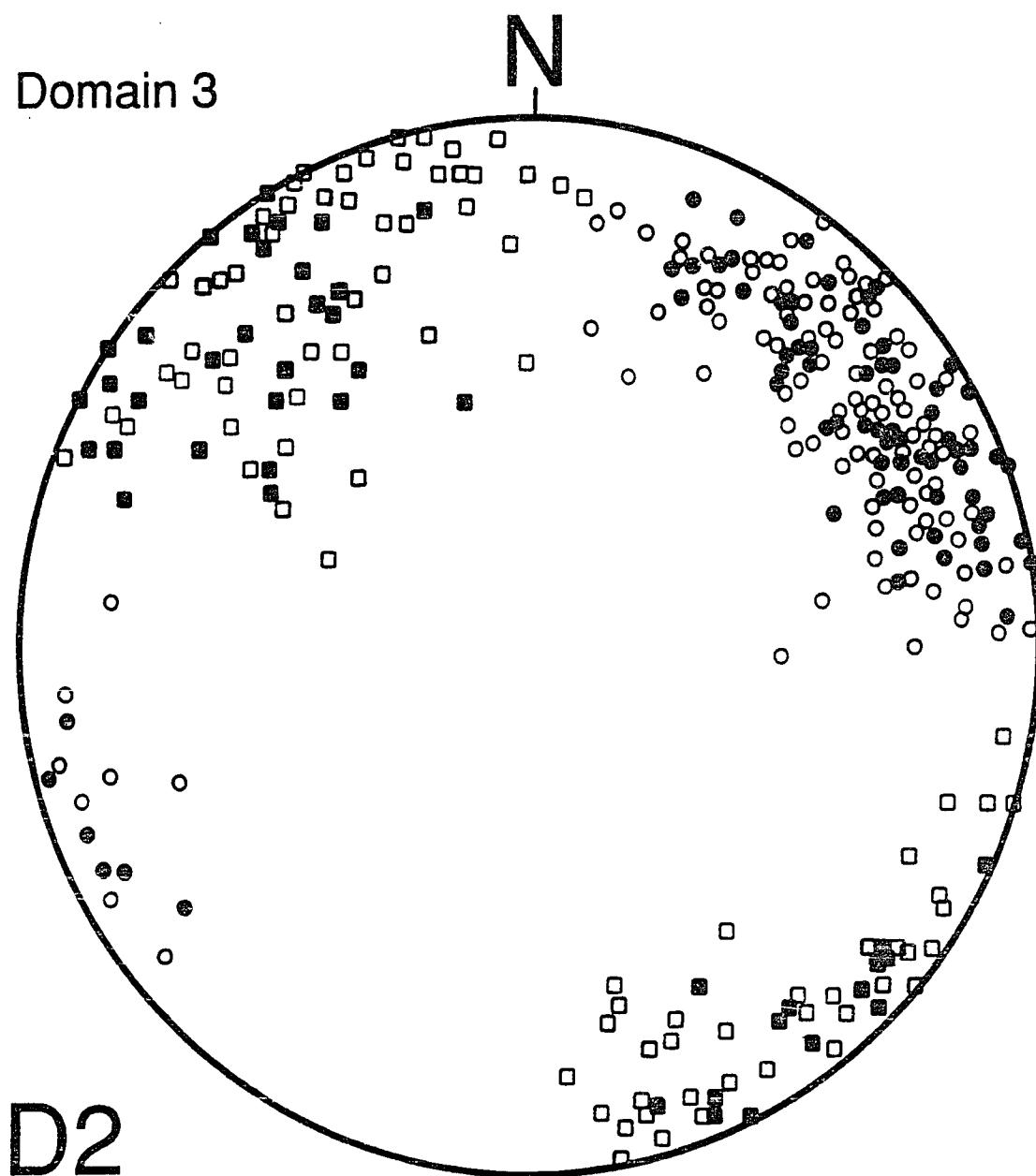


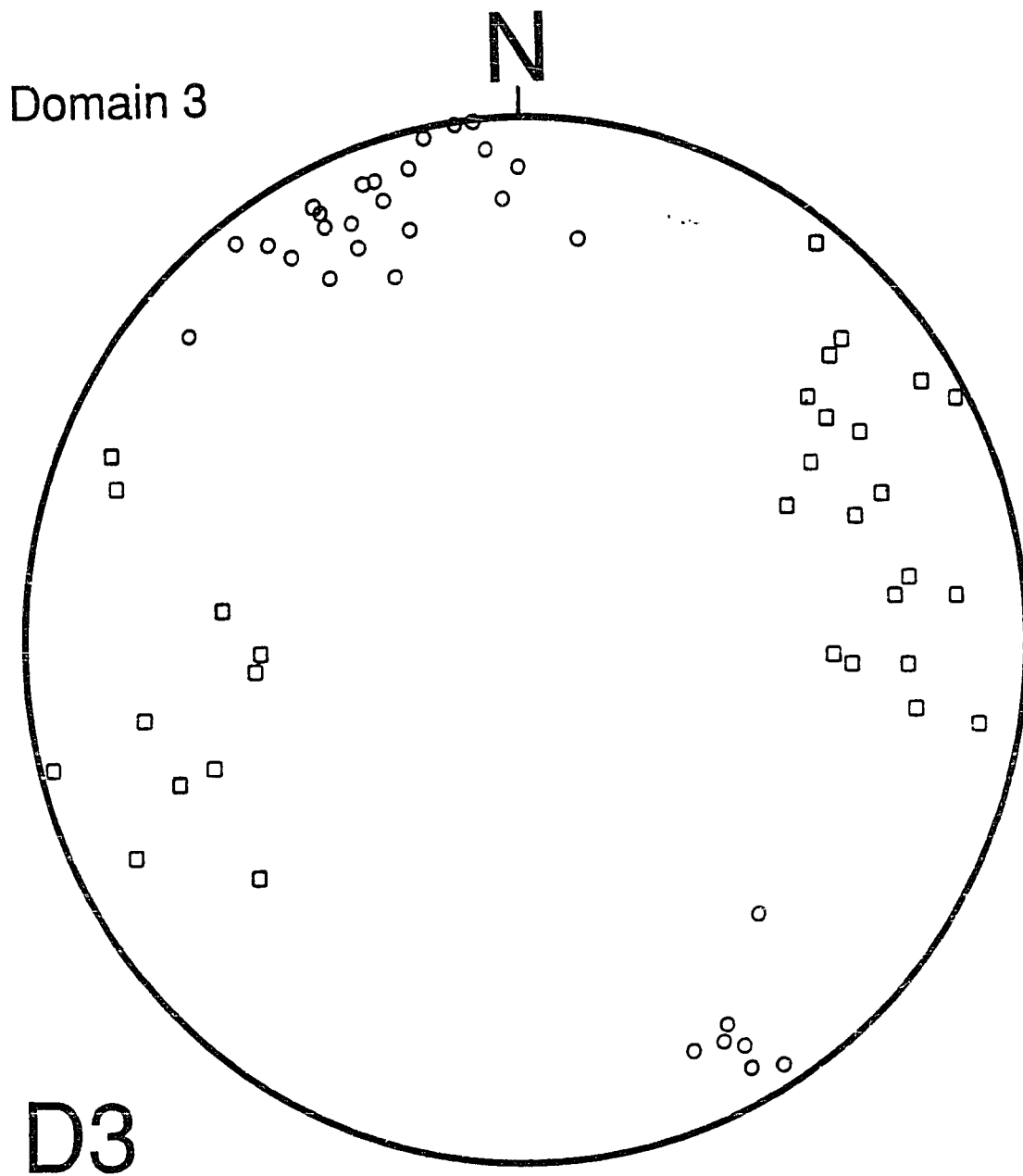


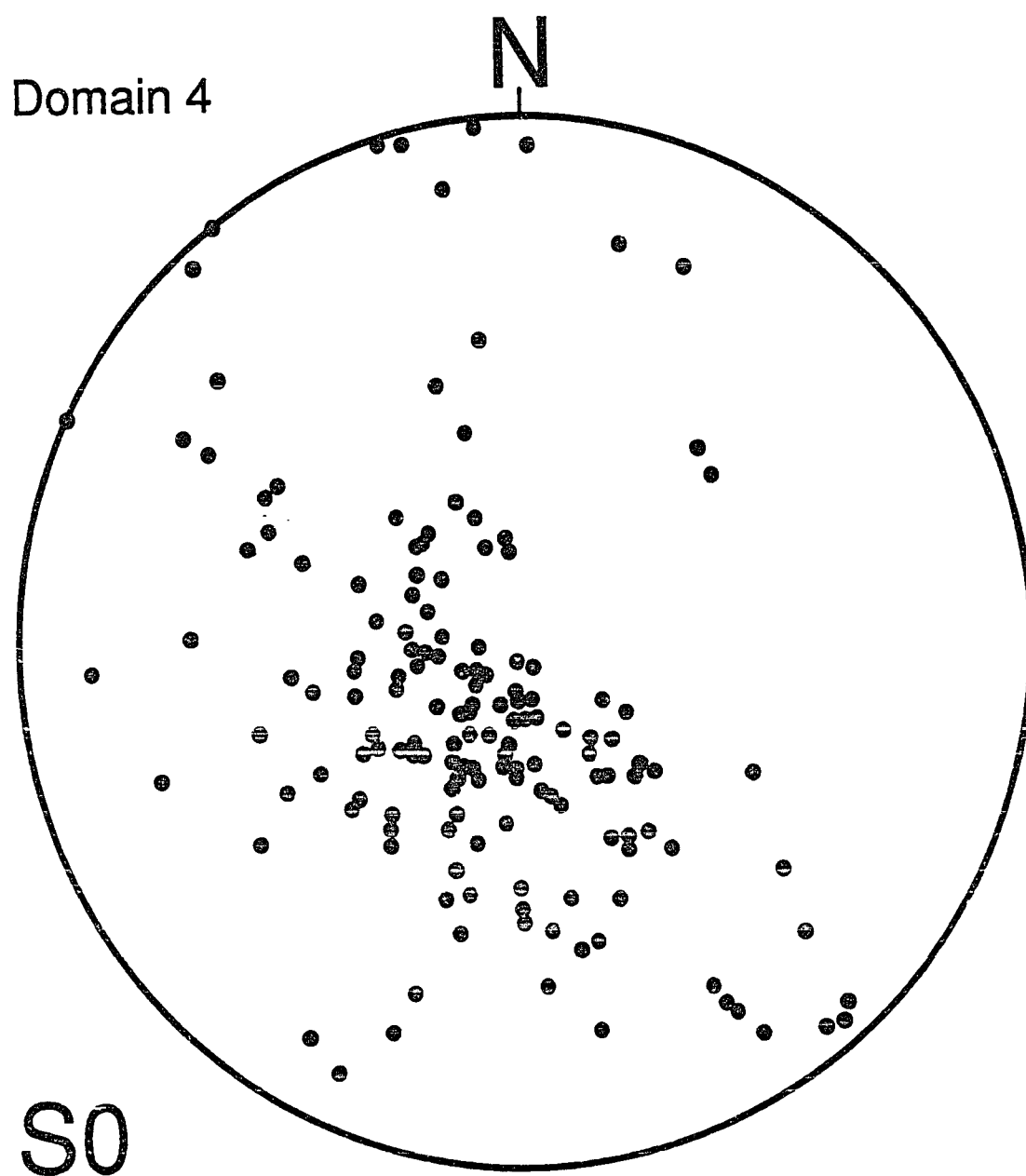


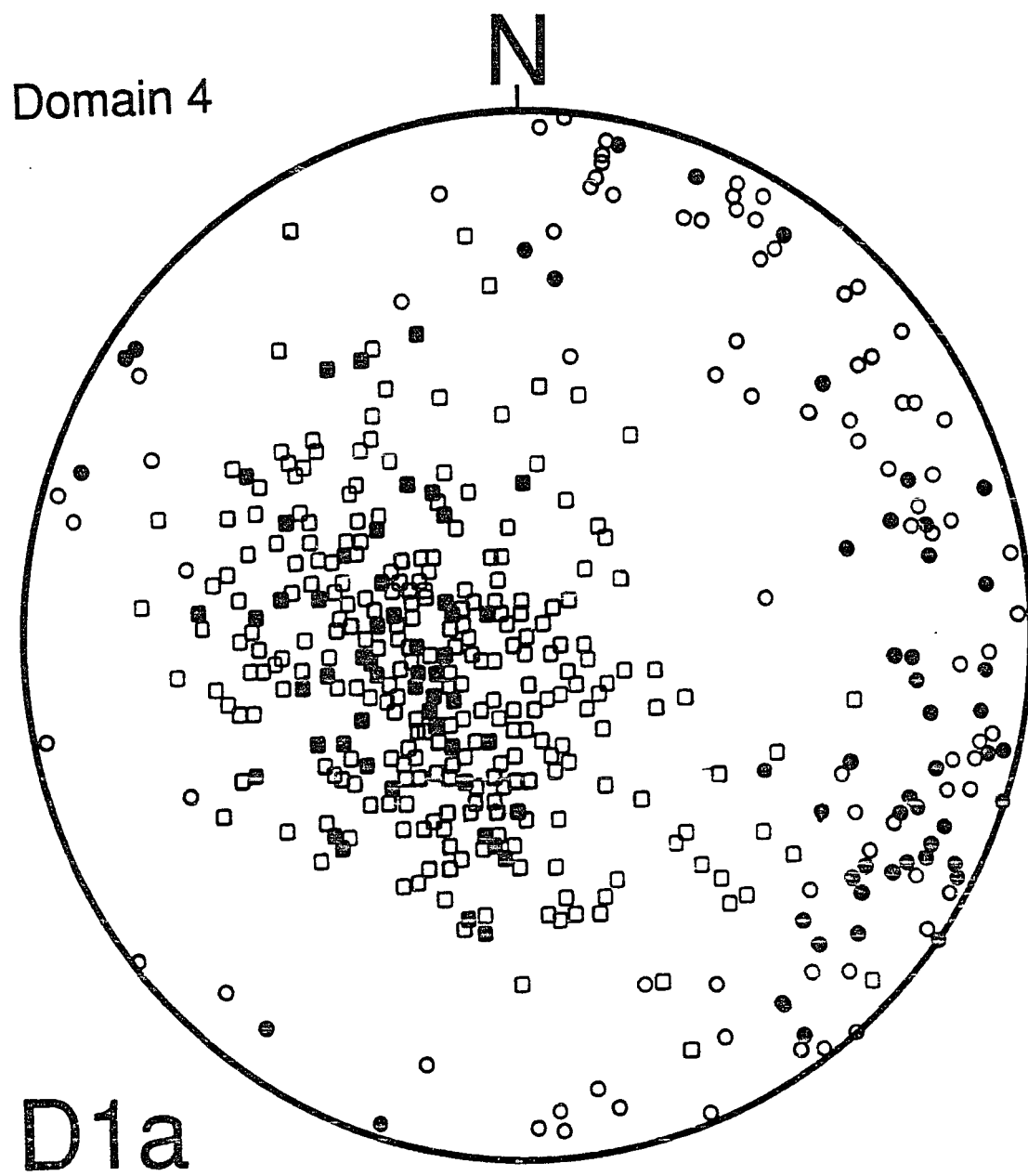


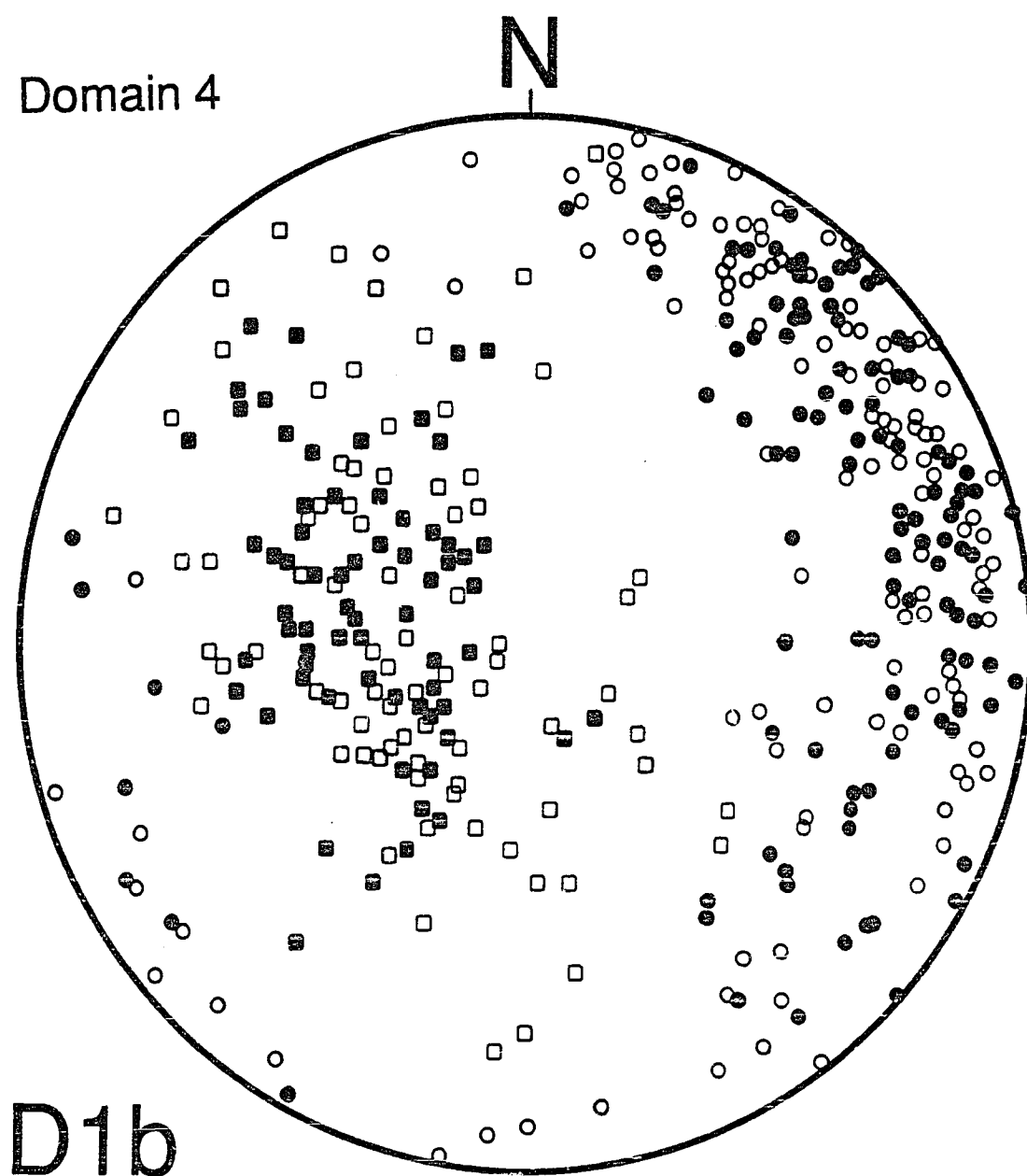


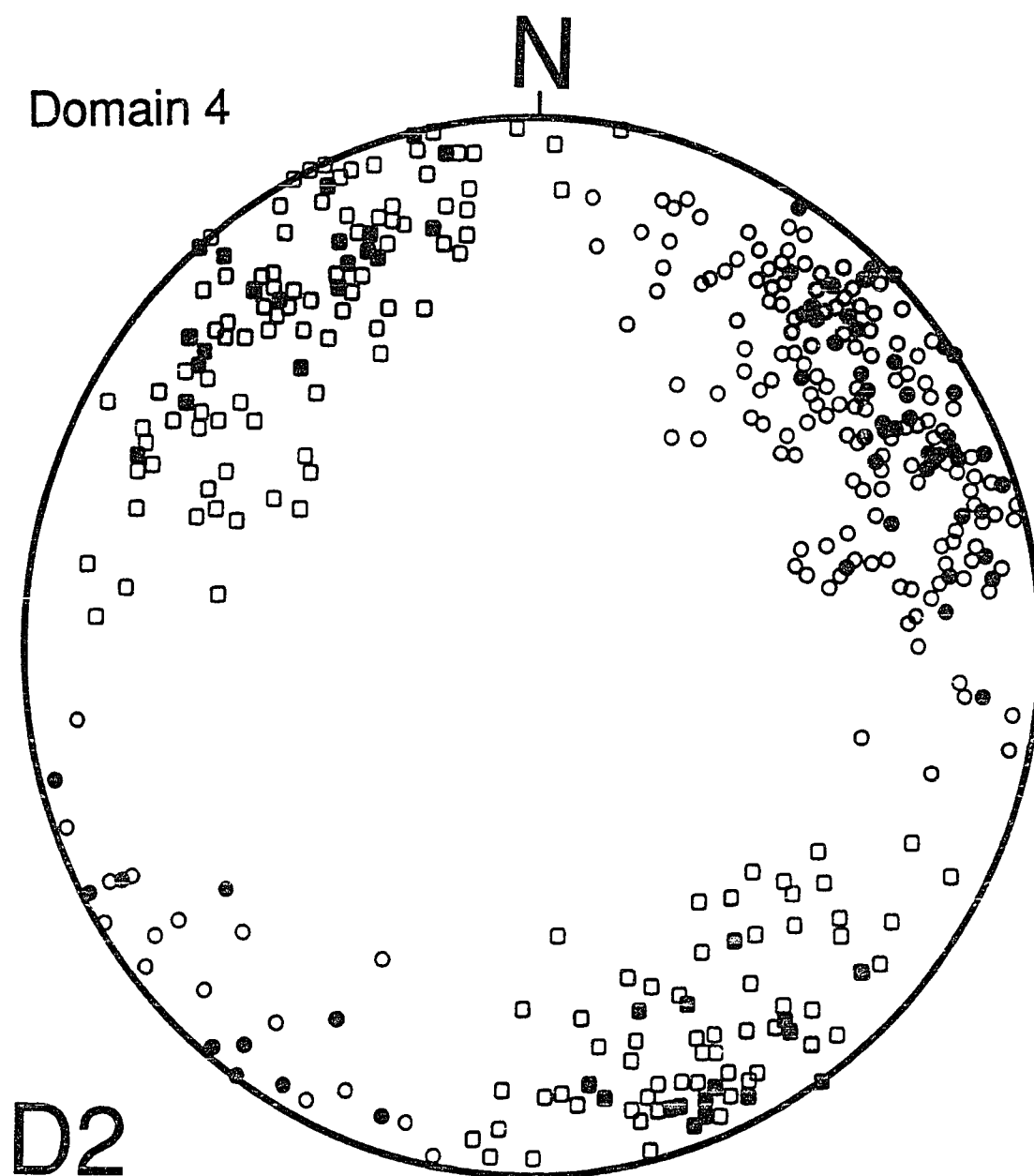


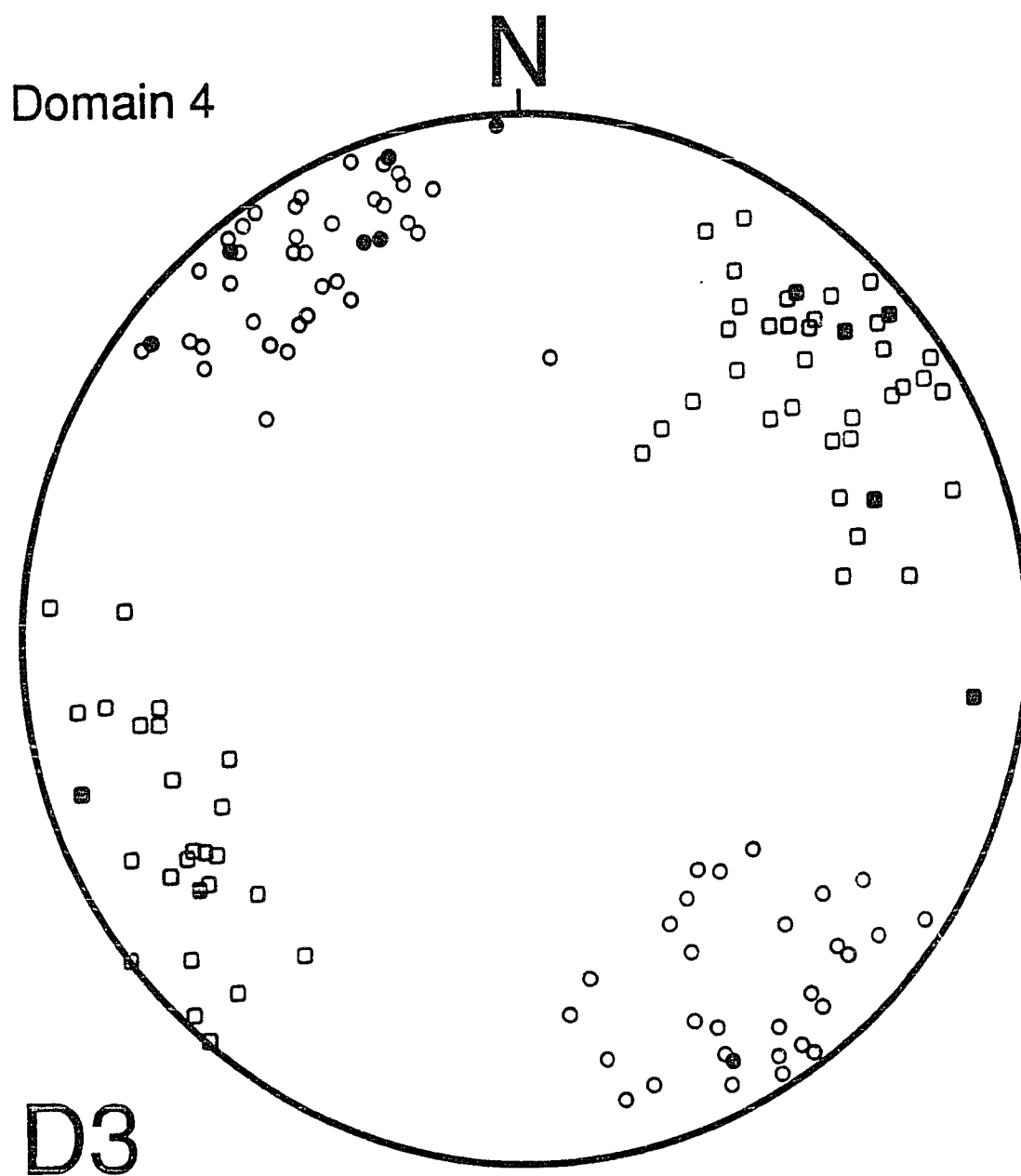


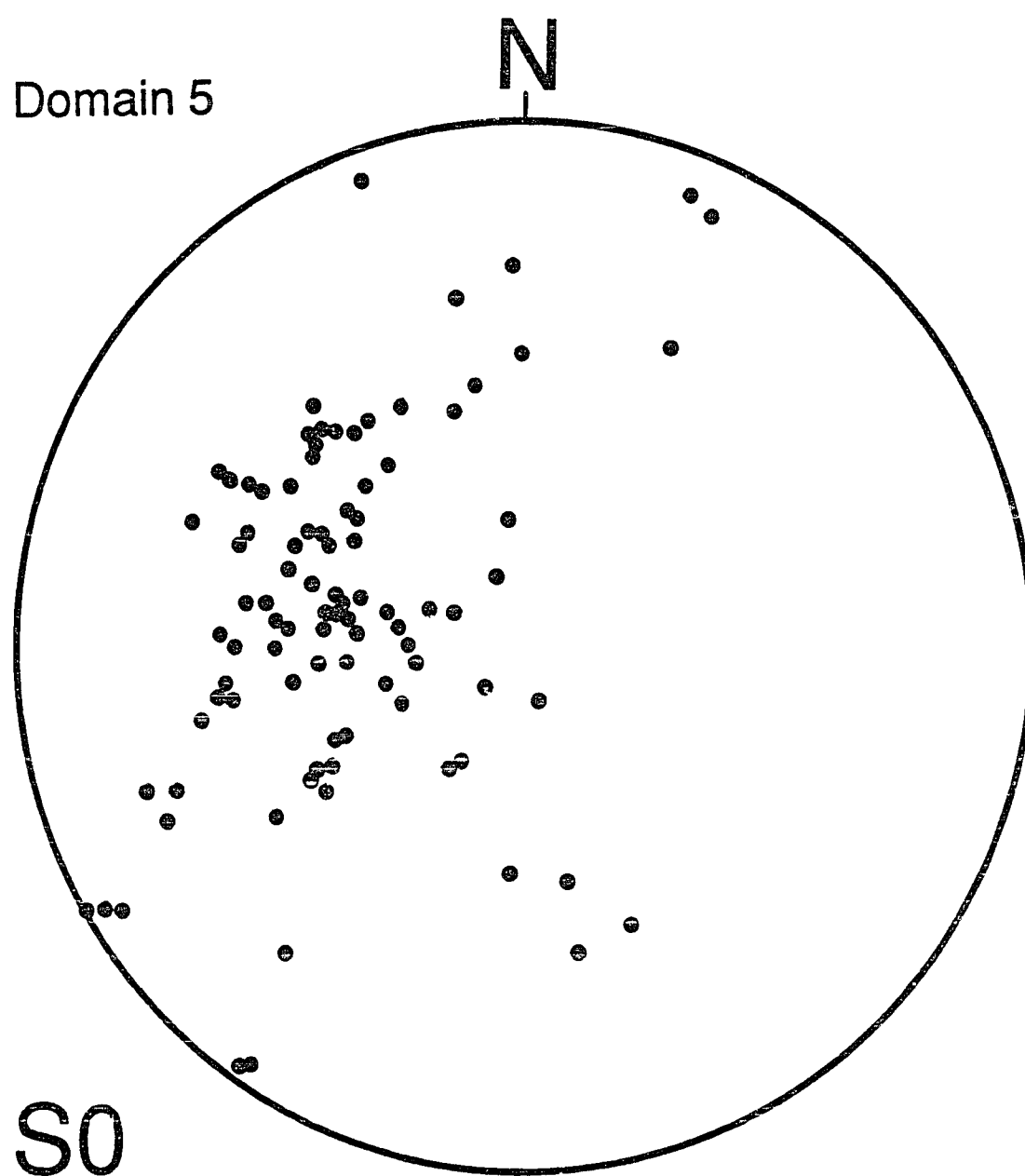


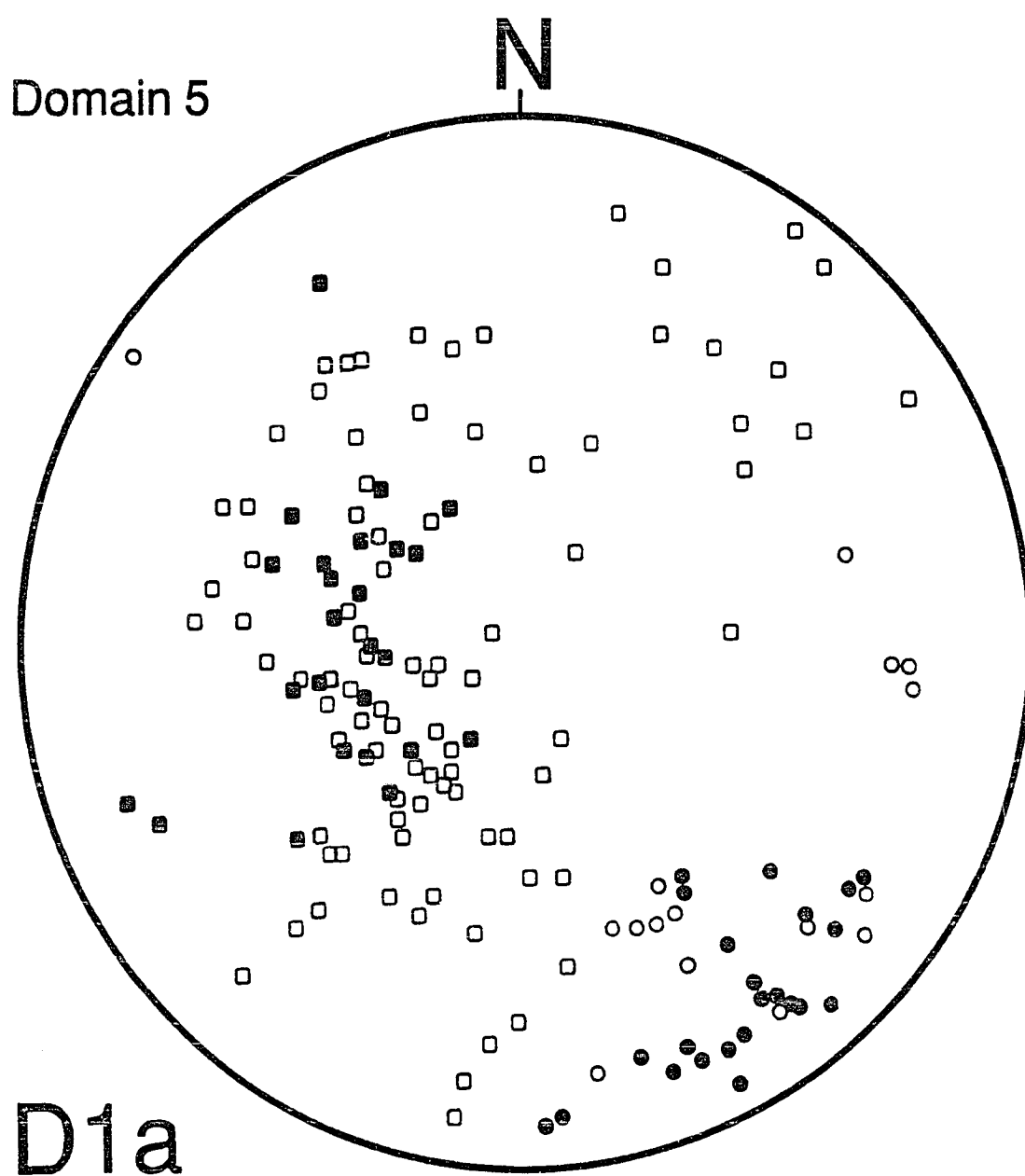


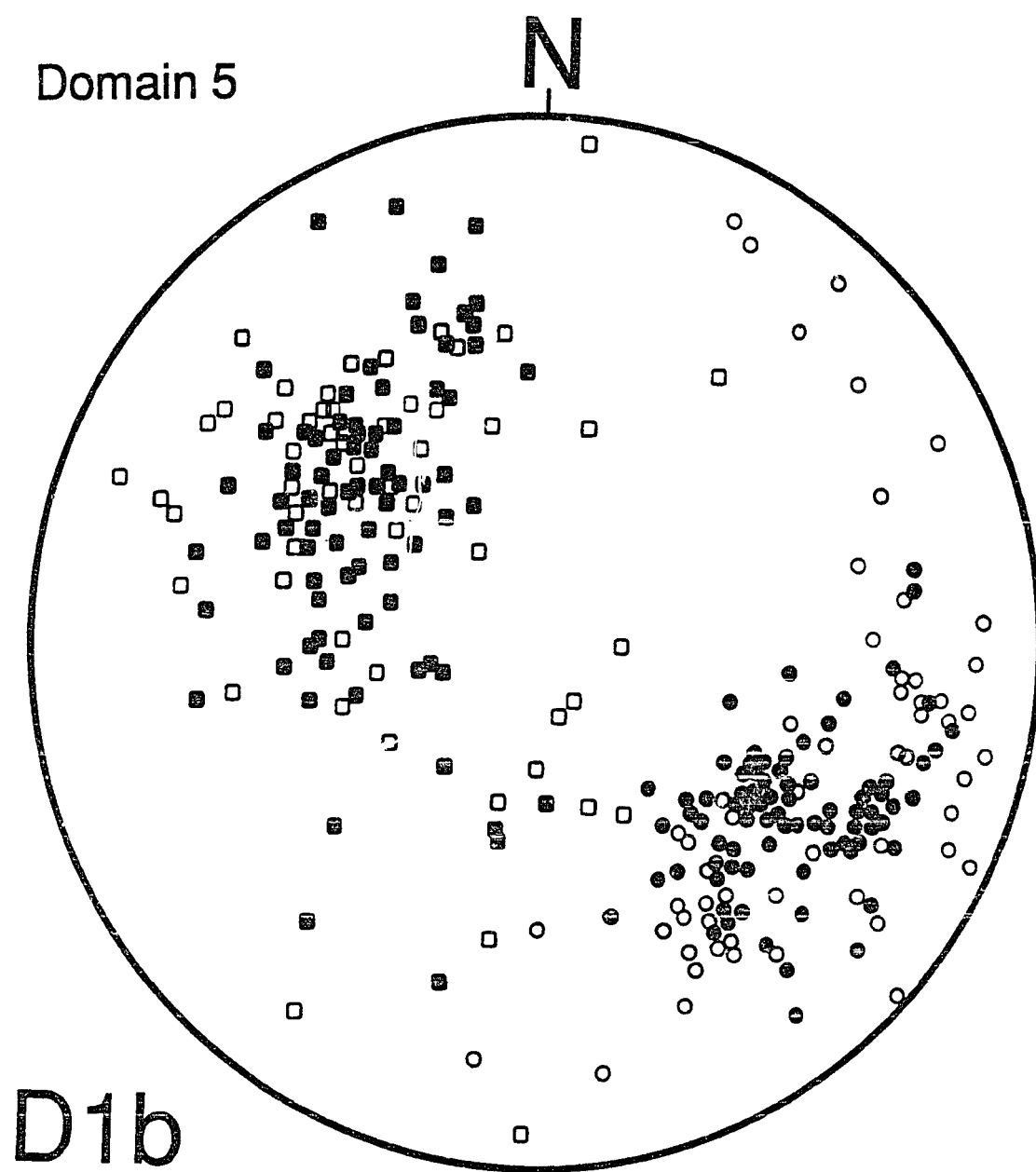


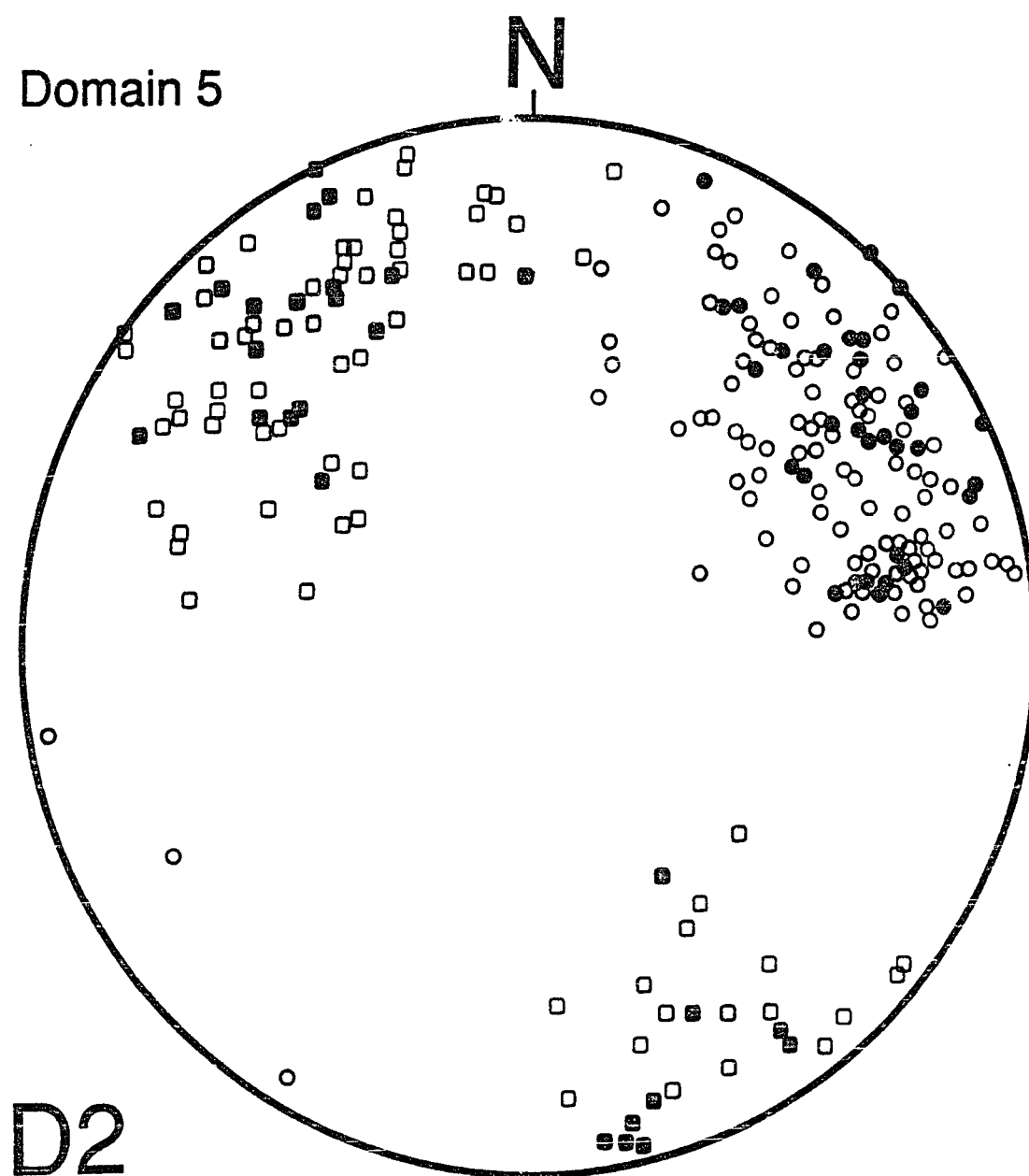


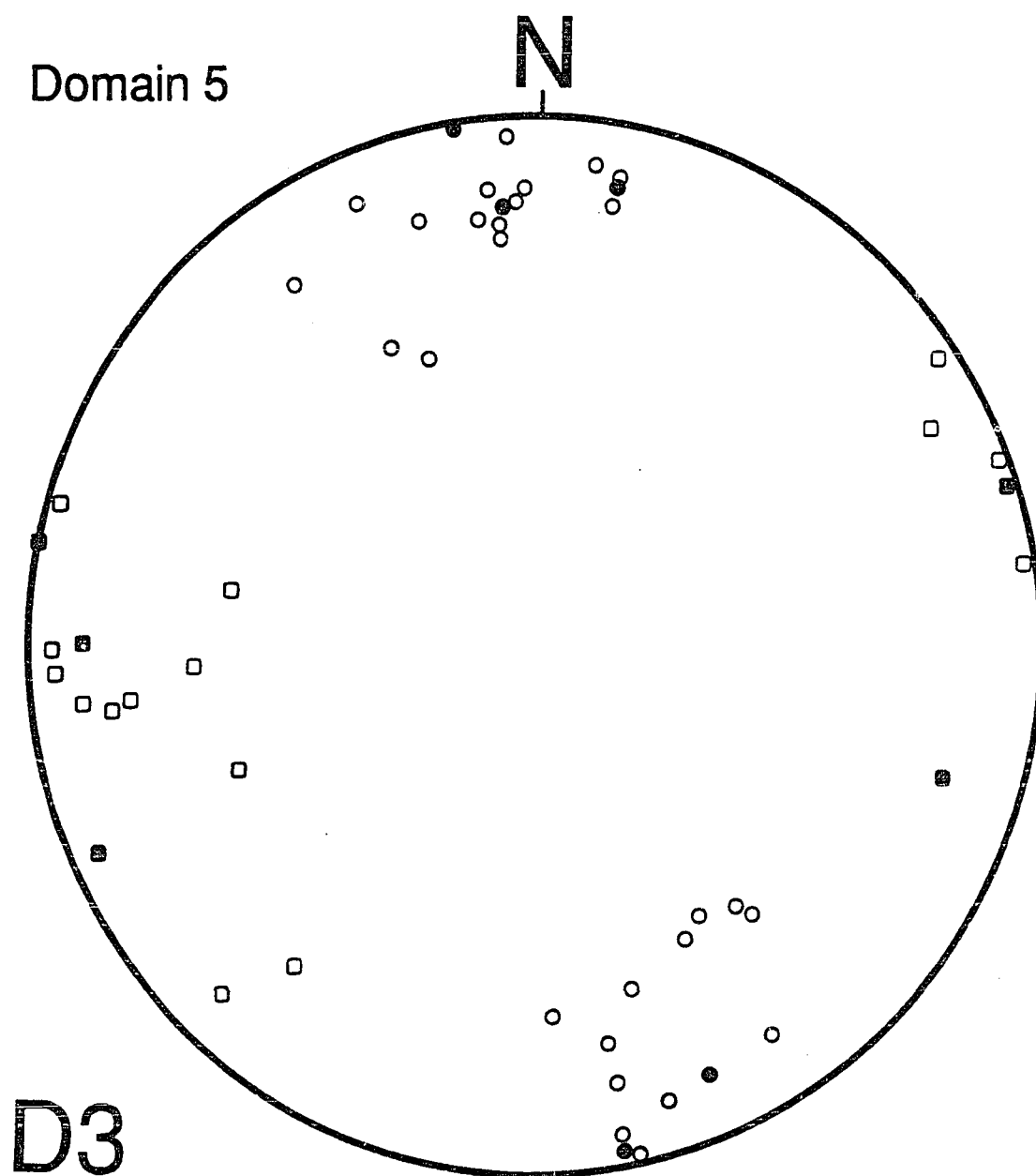












Appendix 4 - Strain analysis

Section 1 - Flinn and R_f/ϕ plots of stretched conglomerates and breccias.

Section 2 - Microfabric analysis of deformed mudrocks.

Section 3 - Derivation of α and γ isopleths for synchronous pure and simple shear.

Section 1 - Flinn and Rf/ϕ plots of stretched conglomerates and breccias

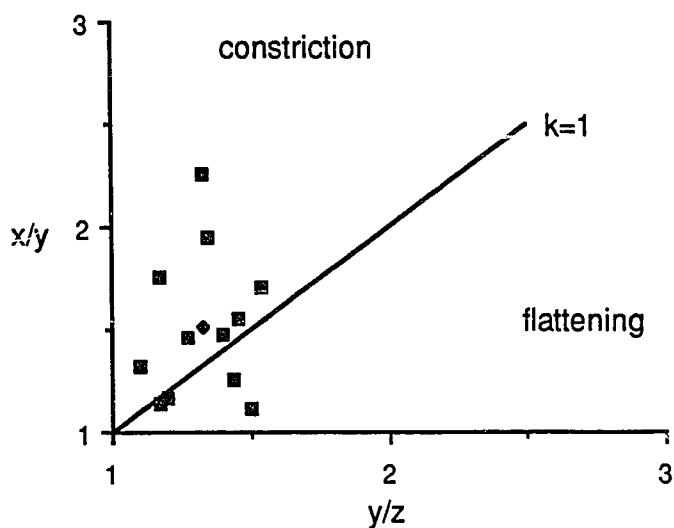
Stretched pebble conglomerate in the middle Hunt Fork Shale.

Location: Sec. 18, T.16 S., R.11 E., Phillip Smith Mountains A-5 quadrangle.

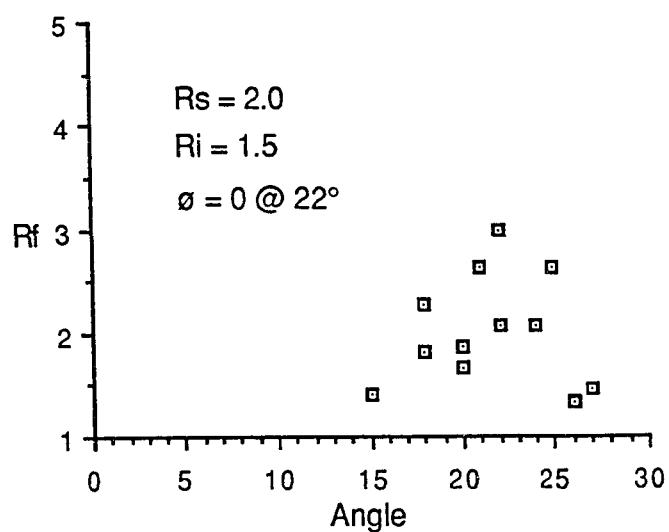
Estimated depth in allochthon: 1.8 km.

Stretching azimuth: 346°

A. Flinn plot (12 data points). Squares are data points; small diamond is the average of all data.



B. Rf/θ' plot for the same 12 data points. θ' measured with respect to a bedding parallel detachment surface along the base of the conglomerate bed.



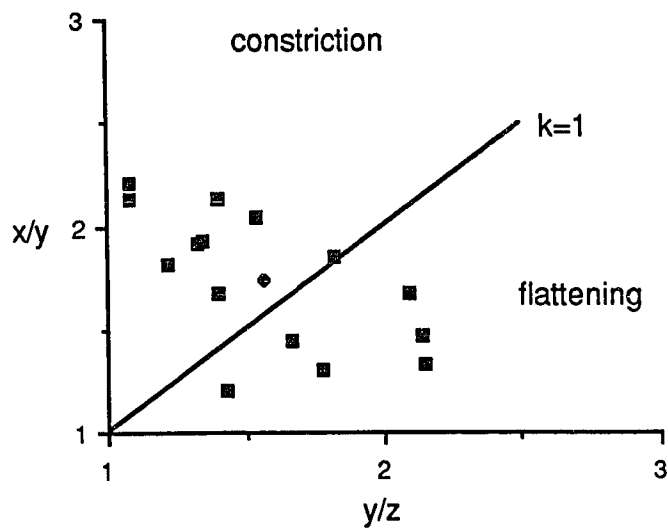
Stretched pebble conglomerate in the middle Hunt Fork Shale.

Location: Sec. 20, T.16 S., R.11 E., Phillip Smith Mountains A-5 quadrangle.

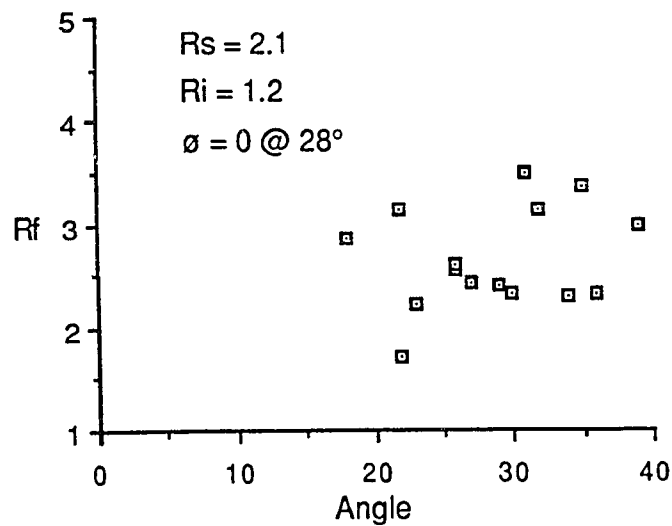
Estimated depth in allochthon: 2.1 km.

Stretching azimuth: 342°

A. Flinn plot (15 data points). Squares are data points; diamond is the average of all data.



B. R_f/θ' plot for the same 15 data points. θ' measured with respect to a bedding parallel detachment surface along the base of the conglomerate bed.



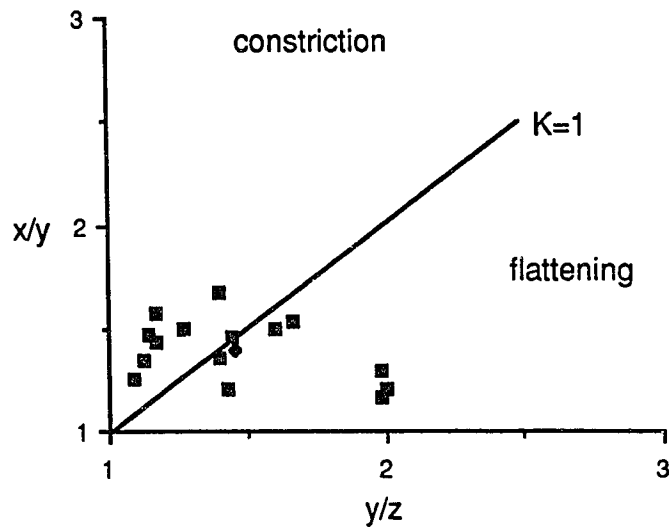
Stretched pebble conglomerate in the middle Hunt Fork Shale.

Location: Sec. 28, T.16 S., R.11 E., Phillip Smith Mountains A-5 quadrangle.

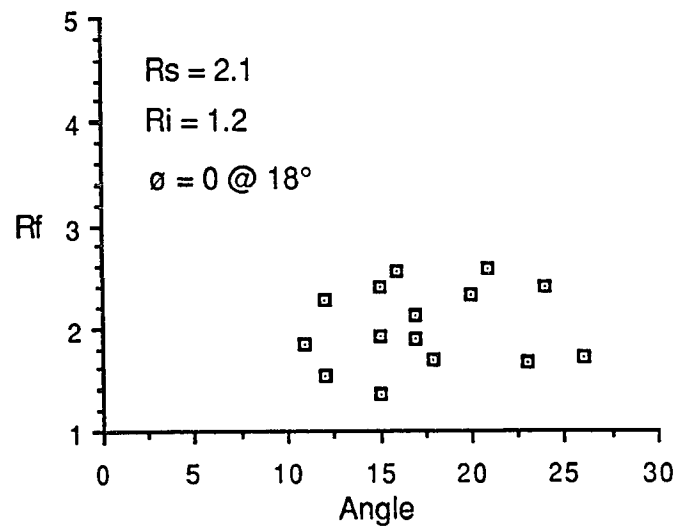
Estimated depth in allochthon: 2.1 km.

Stretching azimuth: 350°

A. Flinn plot (15 data points). Squares are data points; small diamond is the average of all data.



B. R_f/θ' plot for the same 15 data points. θ' measured with respect to a bedding parallel detachment surface along the base of the conglomerate bed.



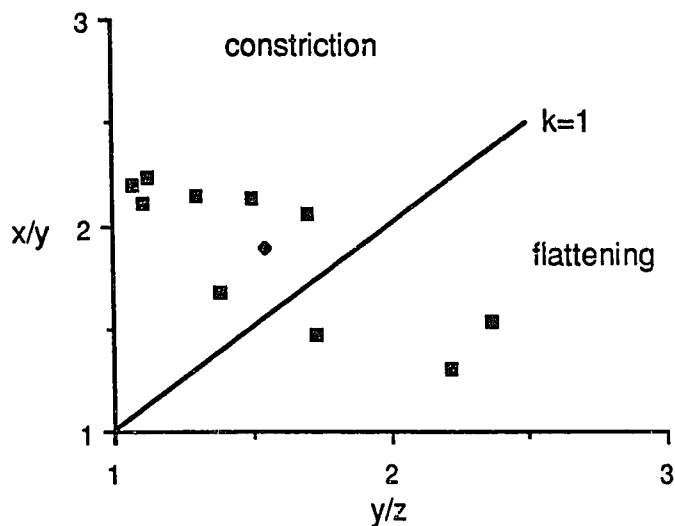
Stretched breccia clasts in purple and green sheared phyllitic breccia, lower and middle Hunt Fork Shale.

Location: Sec. 32, T376 N., R.9 W., Chandalar D-6 quadrangle.

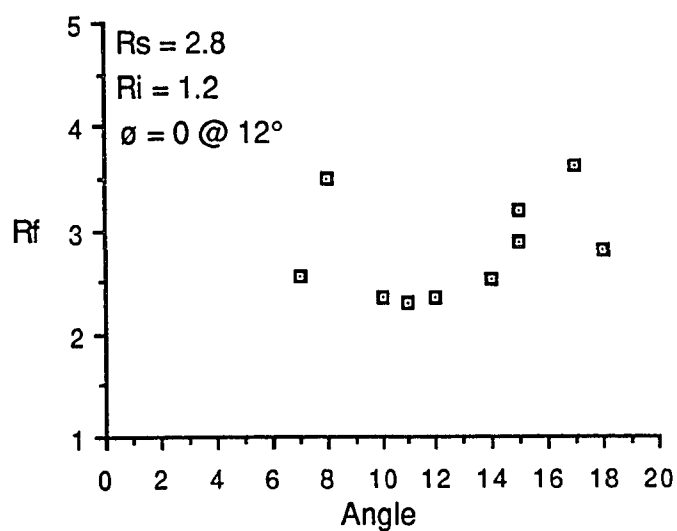
Estimated depth in allochthon: 6.1 km

Stretching azimuth: 152°

A. Flinn plot (10 data points). Squares are data points; small diamond is the average of all data.



B. R_f/θ' plot (10 data points). θ' measured with respect to a major intraformational thrust within this interval.



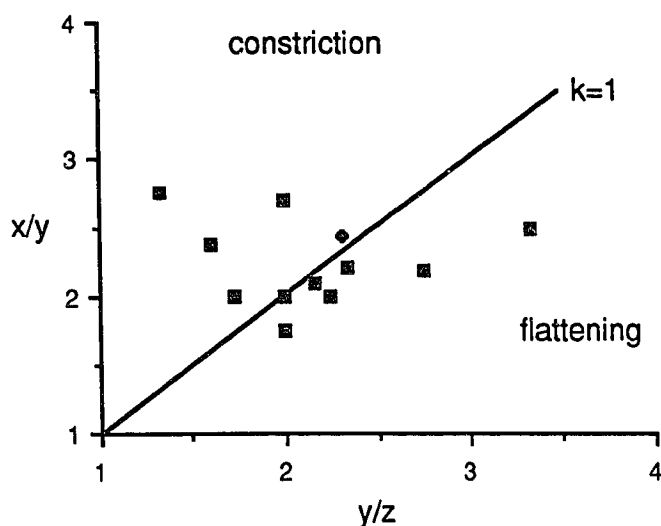
Stretched breccia clasts in purple and green sheared phyllitic breccia, lower and middle Hunt Fork Shale.

Location: Sec. 1, T.36 N., R.10 W., Chandalar D-6 quadrangle.

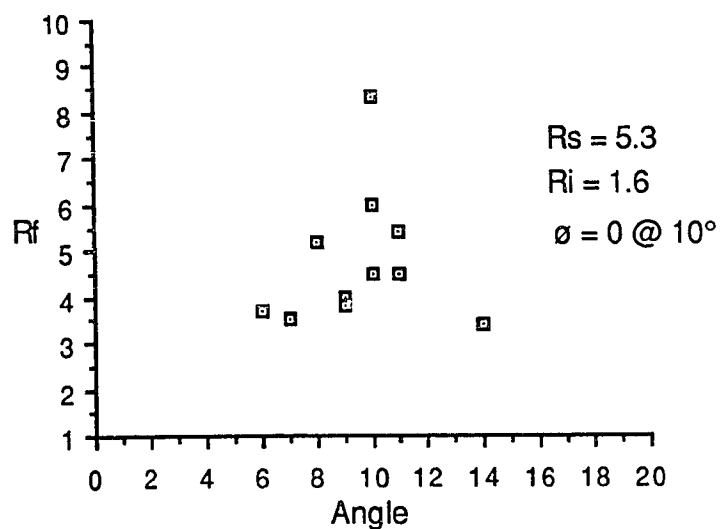
Estimated depth in allochthon: 6.4 km

Stretching azimuth: 157°

A. Flinn plot (12 data points). Squares are data points; diamond is the average of all data.



B. R_f/θ' plot (12 data points). θ' measured with respect to a major intraformational thrust within this interval.



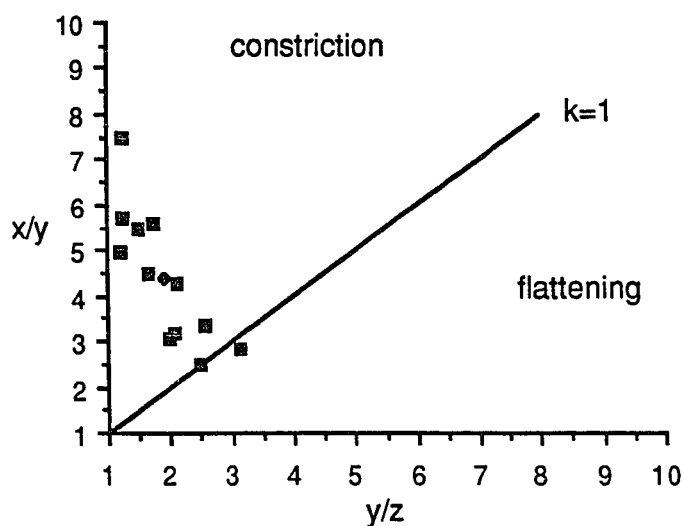
Stretched pebble conglomerate in the Beaucoup Formation.

Location: Sec. 11, T.36 N., R.10 W., Chandalar D-6 quadrangle.

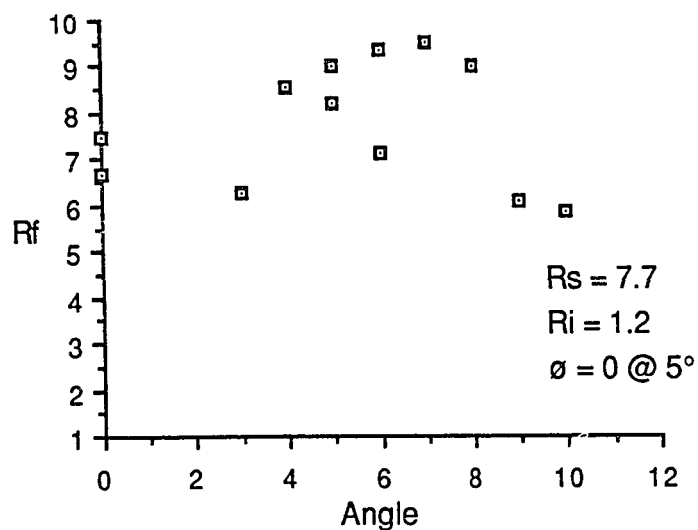
Estimated depth in allochthon: 7.1 km

Stretching azimuth: 160°

A. Flinn plot (12 data points). Squares are data points; small diamond is the average of all data.



B. R_f/θ' plot (12 data points). θ' measured with respect to a bedding parallel thrust beneath the conglomerate bed.



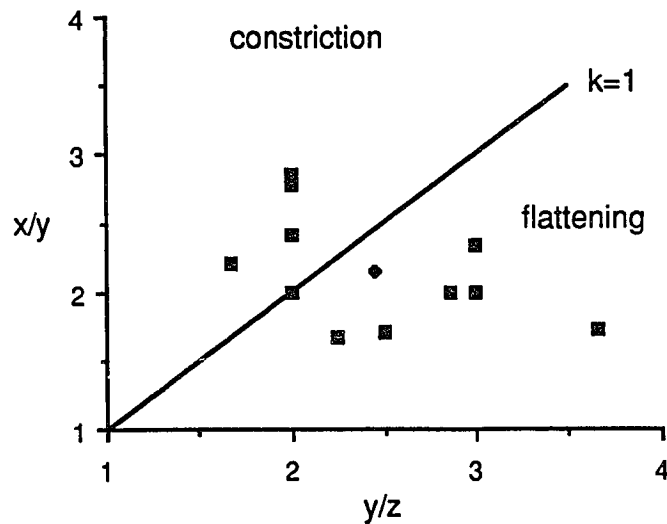
Stretched pebble conglomerate in the Beaucoup Formation.

Location: Sec. 10, T.36 N., R.10 W., Chandalar D-6 quadrangle.

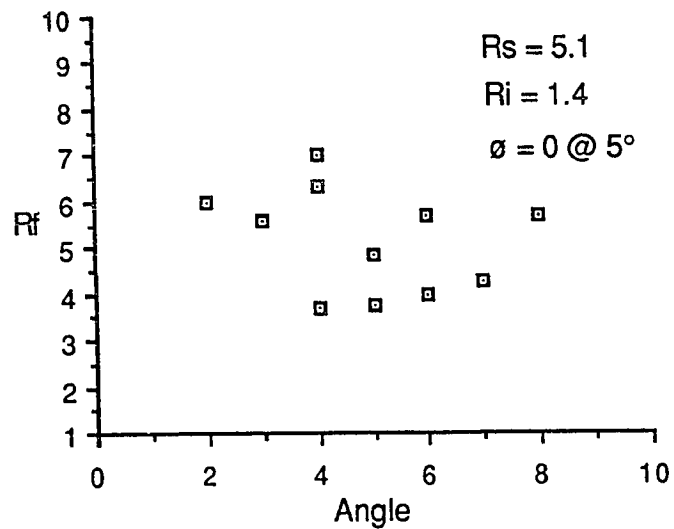
Estimated depth in allochthon: 7.5 km

Stretching azimuth: 148°

A. Flinn plot (11 data points). Squares are data points; small diamond is the average of all data.



B. R_f/θ' plot (11 data points). θ' measured with respect to a bedding parallel thrust beneath the conglomerate bed.



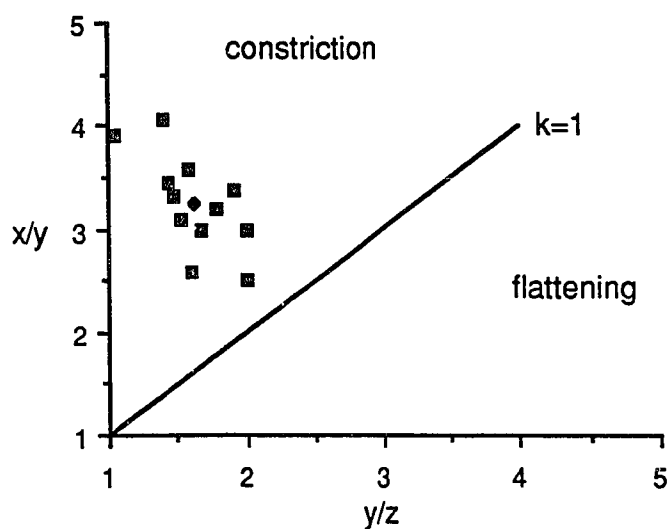
Stretched pebble conglomerate in the Beaucoup Formation.

Location: Sec. 9, T.36 N., R.10 W., Chandalar D-6 quadrangle.

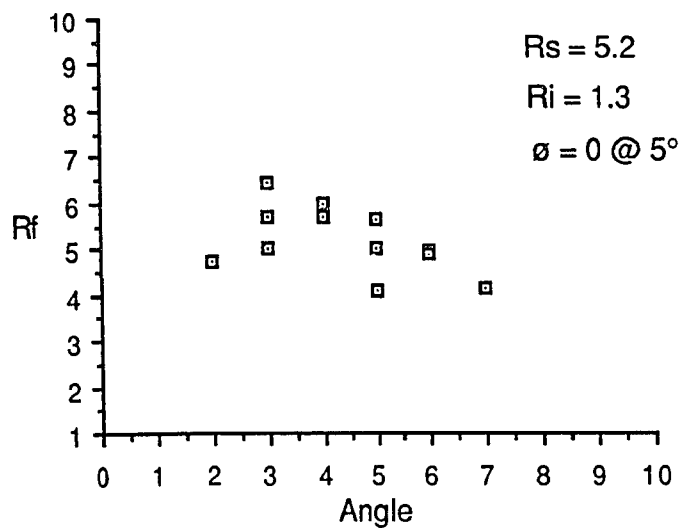
Estimated depth in allochthon: 7.5 km

Stretching azimuth: 143°

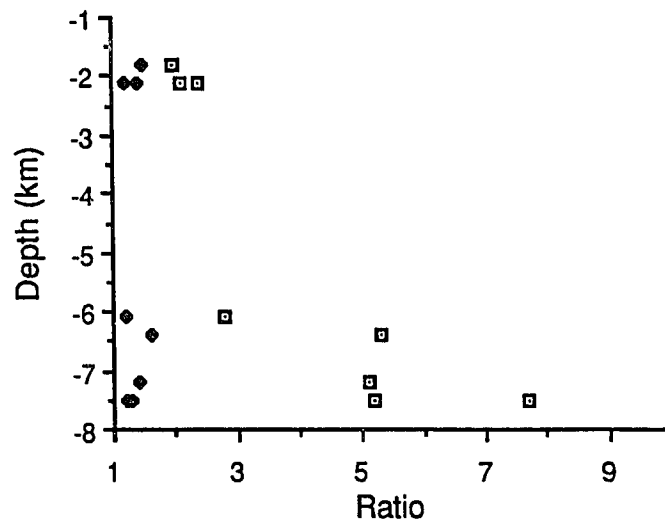
A. Flinn plot (12 data points). Squares are data points; small diamond is the average of all data.



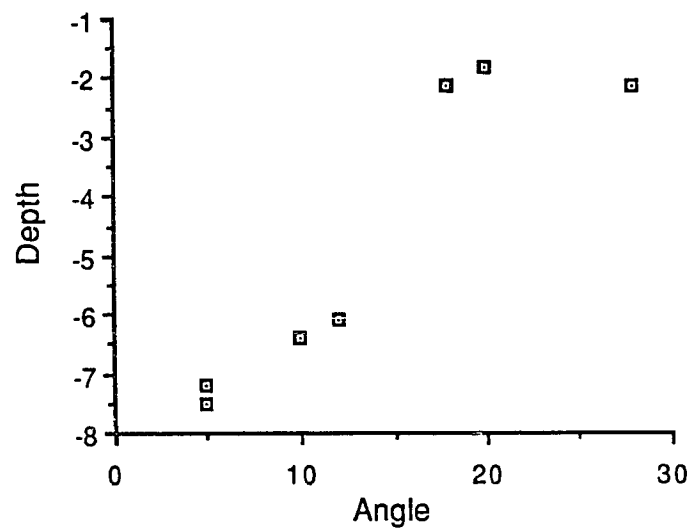
B. R_f/θ' plot (12 data points). θ' measured with respect to a bedding parallel thrust beneath the conglomerate bed.



Relationship between depth, initial axial ratio, and strain ratio for the seven stretched pebble/breccia clast data sets. Diamonds are initial ratios (R_i). Squares are strain ratios (R_s).



Relationship between depth and θ' at $\phi=0$.



Section 2 - Microfabric analysis of deformed mudrocks

Table of microfabric measurements in deformed mudrocks. Fry indicates Fry analysis; e1 was determined from Fry strain ratios using Figure 4.2.1. Ps indicates pressure shadows.

Formation	Depth (km)	Rs (Fry)	e1 (PS)	e1 (from Fry)
Hunt Fork	-1.4	1.1	0.2	.03
Hunt Fork	-3.5	1.5	0.7	.15
Hunt Fork	-4.1	1.7	1.0	.20
Hunt Fork	-5.2	2.5	1.0	.32
Hunt Fork	-5.8	1.8	1.5	.22
Hunt Fork	-6.5	1.6	1.1	.17
Beaucoup	-7.3	1.9	1.0	.24
Beaucoup	-7.4	2.8	0.8	.38
Beaucoup	-7.5	1.3	2.0	.10

Figure 4.2.1 - Plot of the relationship between e1 and strain ratio (Rs) assuming constant volume deformation.

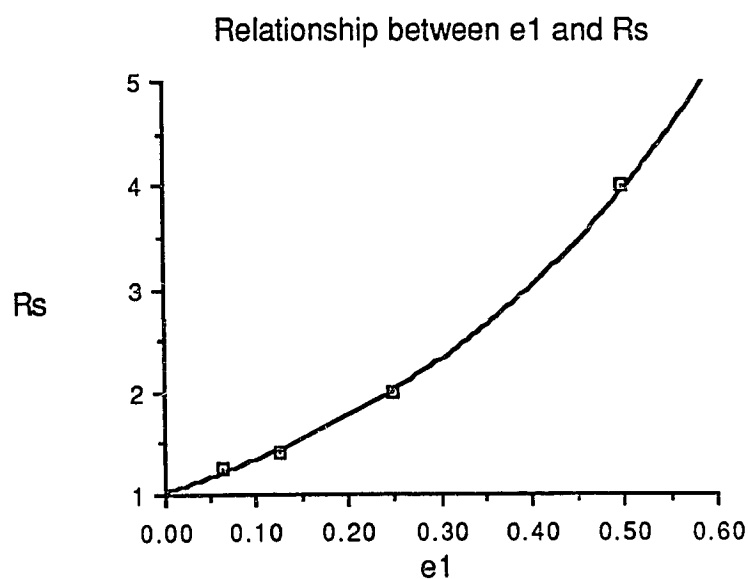


Figure 4.2.2 - Plot of e_1 depth relations. Squares are e_1 values from pressure shadows. Solid circles are e_1 values from Fry strain ratios.

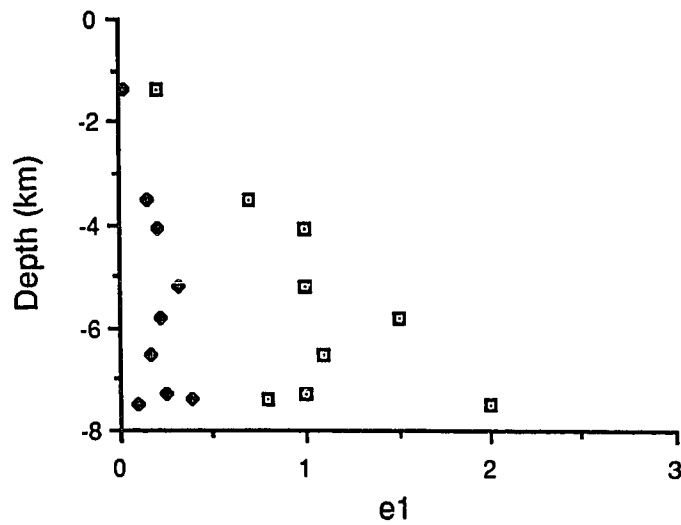
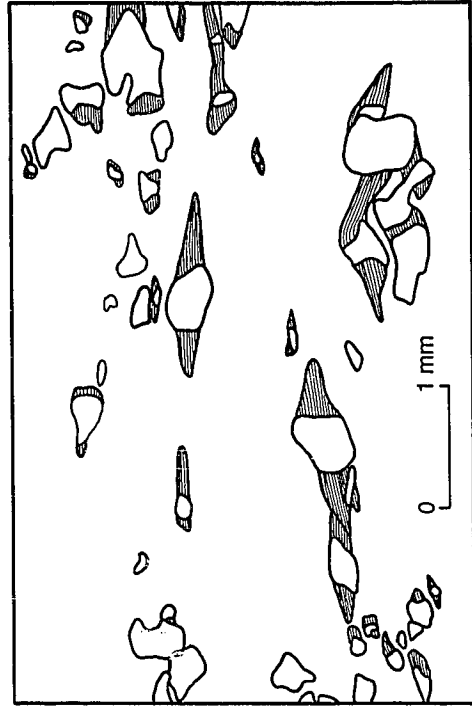
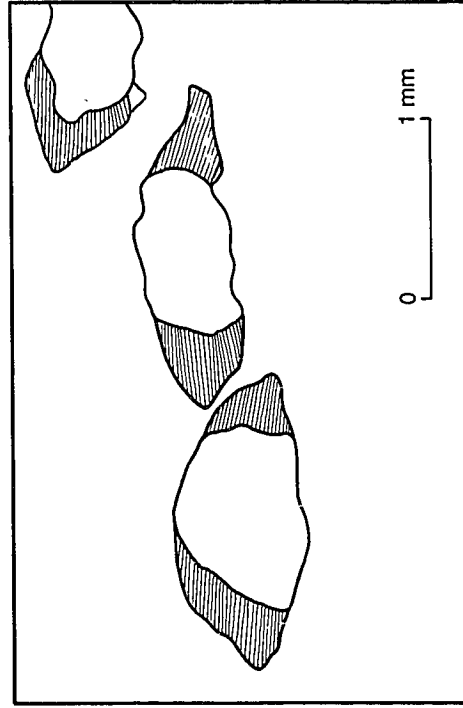


Figure 4.2.3 (next page) - Photomicrographs and sketches of representative pressure shadows and grain distributions in the Beaucoup (a) and the Hunt Fork (b). Note that pressure shadows are not consistently well developed and that grain distribution is not uniform.

A Sample 686-6



B Sample 687-24



Section 3 - Derivation of α and γ isopleths for synchronous pure and simple shear.

From Ramberg (1975), values for simultaneous pure and simple shear during constant volume deformation can be solved for using the deformation gradient tensor:

$$\begin{array}{cc} \epsilon & \gamma \\ 0 & -\epsilon \end{array}$$

which, assuming constant deformation rates gives:

$$\begin{array}{cc} \exp(\epsilon t) & \gamma/2\epsilon (\exp(\epsilon t) - \exp(-\epsilon t)) \\ 0 & \exp(-\epsilon t) \end{array}$$

where, $\epsilon t = \epsilon = \ln \alpha$, $\gamma t = \gamma$, α = pure shear, and γ = simple shear (also from Ramberg, 1975).

Which simplifies to:

$$\begin{array}{cc} \alpha & \gamma(\alpha - 1/\alpha)/2\ln\alpha \\ 0 & 1/\alpha \end{array}$$

at $\alpha=1$ the equation must be evaluated using l'Hôpital's rule, which yields:

$$d((\alpha - 1/\alpha)/\ln\alpha) = 1$$

For a matrix in the form:

$$\begin{matrix} a & b \\ c & d \end{matrix}$$

The values of the principal strains can be determined by using the equations:

$$\tan 2\theta' = 2(ab+cd)/(a^2-b^2+c^2-d^2)$$

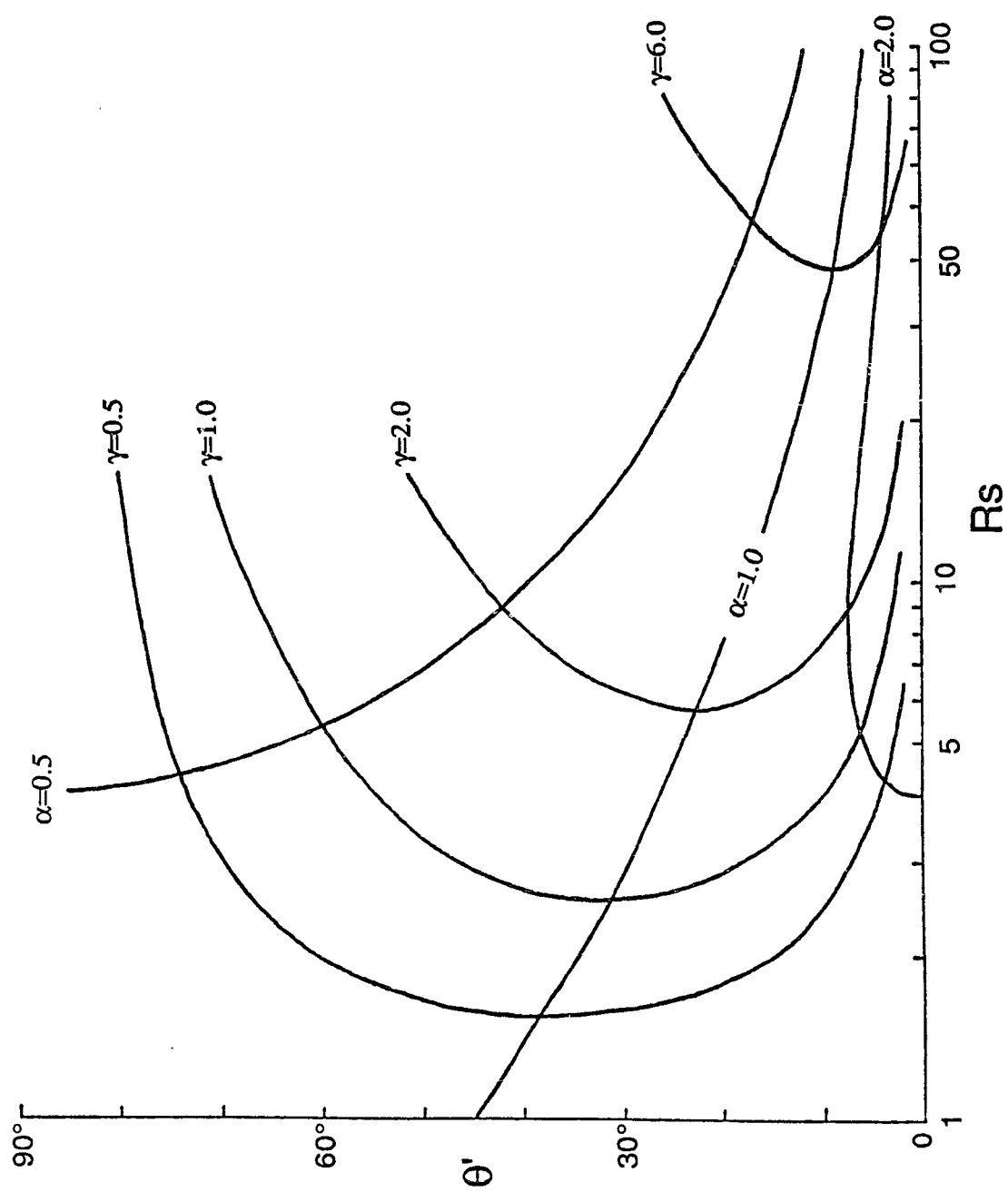
$$\lambda_1 = (a^2+b^2+c^2+d^2)/2 + [(a^2+b^2+c^2+d^2)^2 - 4(ad-bc)^2]^{1/2}/2$$

$$\lambda_2 = (a^2+b^2+c^2+d^2)/2 - [(a^2+b^2+c^2+d^2)^2 - 4(ad-bc)^2]^{1/2}/2$$

$$Rs = (\lambda_1/\lambda_2)^{1/2}$$

where, λ_1 = long axis of the strain ellipse, λ_2 = short axis of the strain ellipse, and θ' = the angle between λ_1 and the shear direction (Ramsay and Huber, 1983).

Figure 4.3.1 (next page) - Rs/θ' diagram (semi-log) with α and γ isopleths for simultaneous pure and simple shear.



PLEASE NOTE:

Oversize maps and charts are filmed in sections in the following manner:

LEFT TO RIGHT, TOP TO BOTTOM, WITH SMALL OVERLAPS

The following map or chart has been refilmed in its entirety at the end of this dissertation (not available on microfiche). A xerographic reproduction has been provided for paper copies and is inserted into the inside of the back cover.

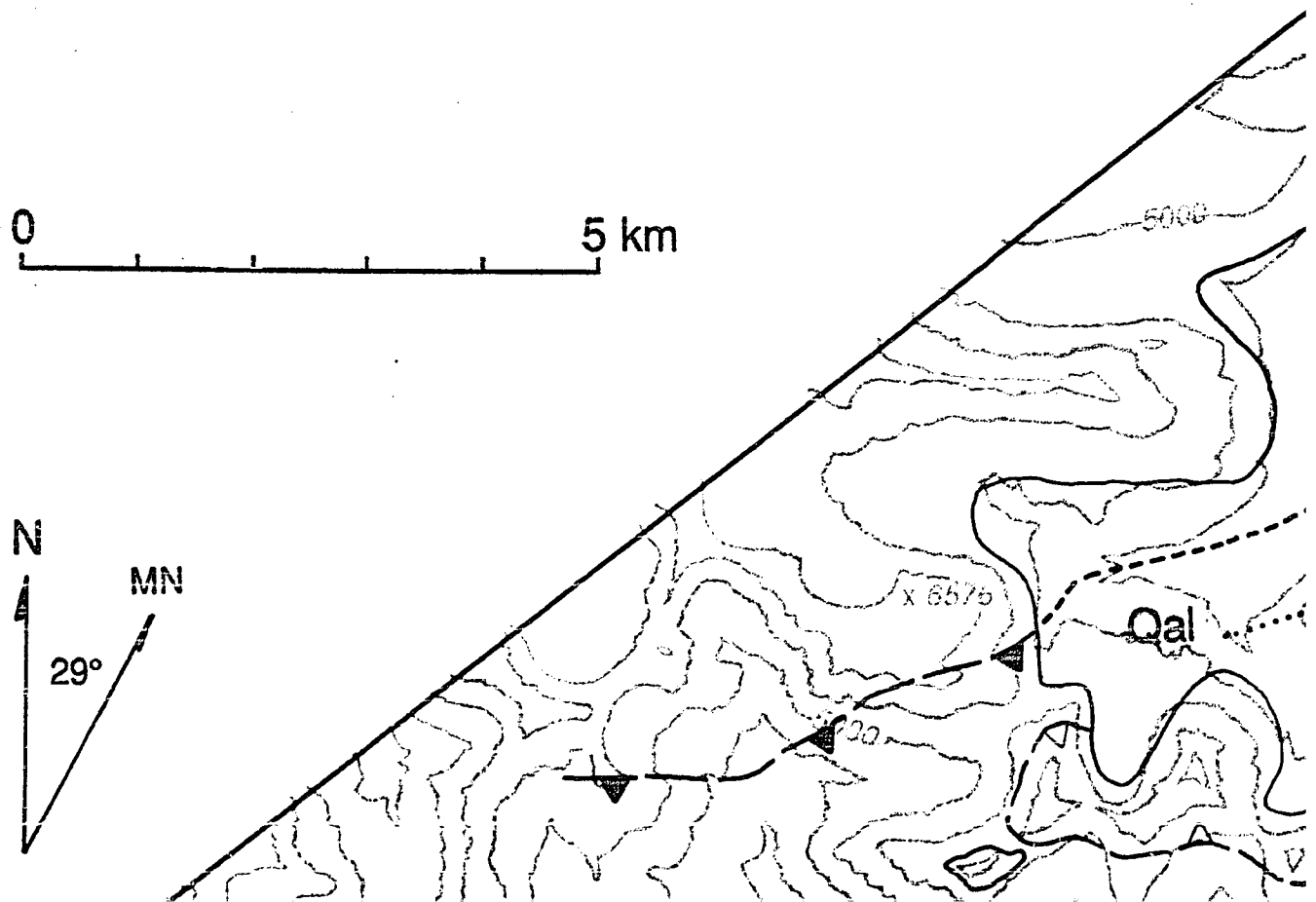
Standard 35mm slides or 17" x 23" black and white photographic prints are available for an additional charge.

U·M·I

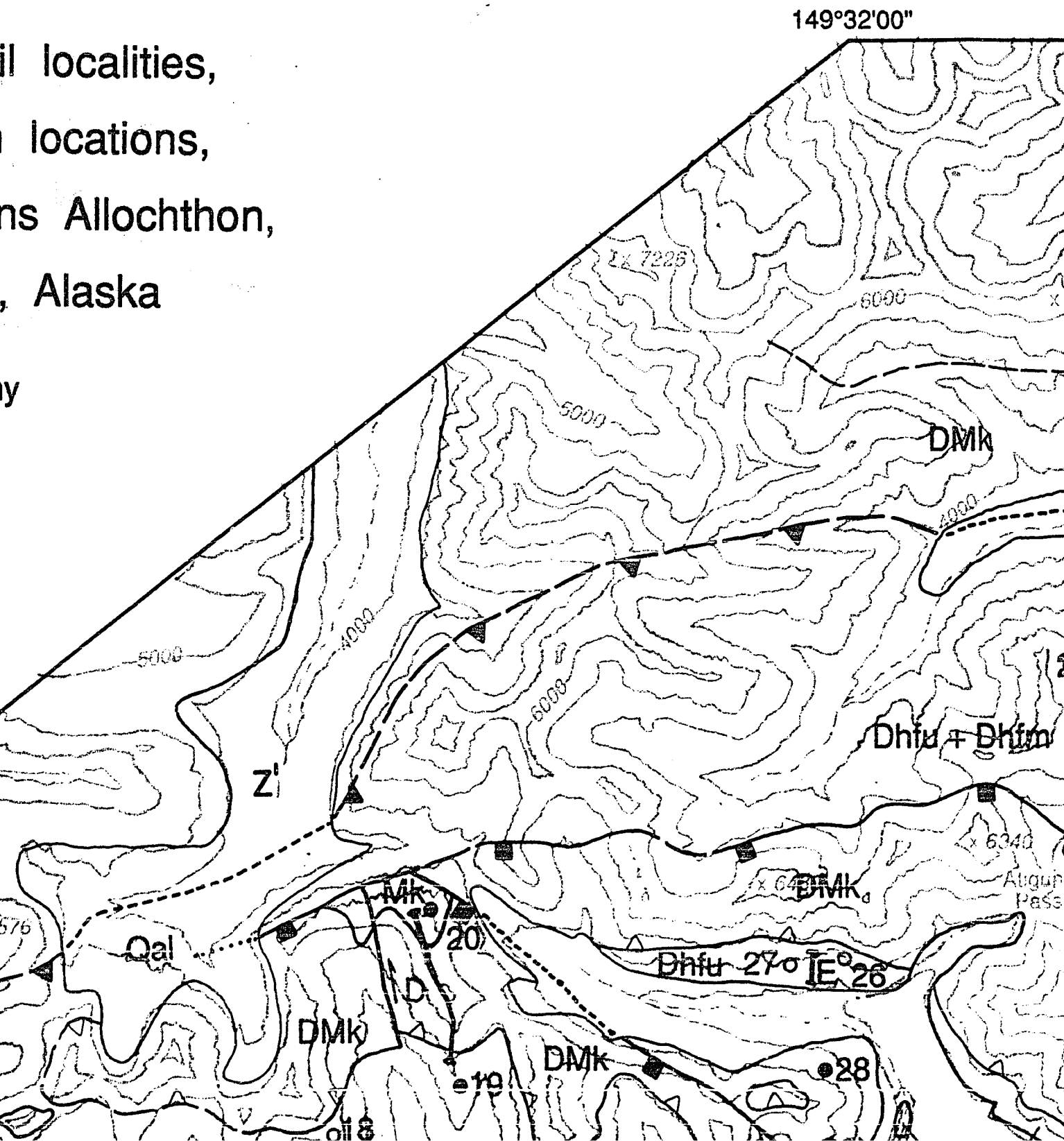
Plate 1

Sedimentary facies, fossil localities, and stratigraphic section locations, southern Endicott Mountains Allochthon central Brooks Range, Alaska

James W. Handschy
Rice University

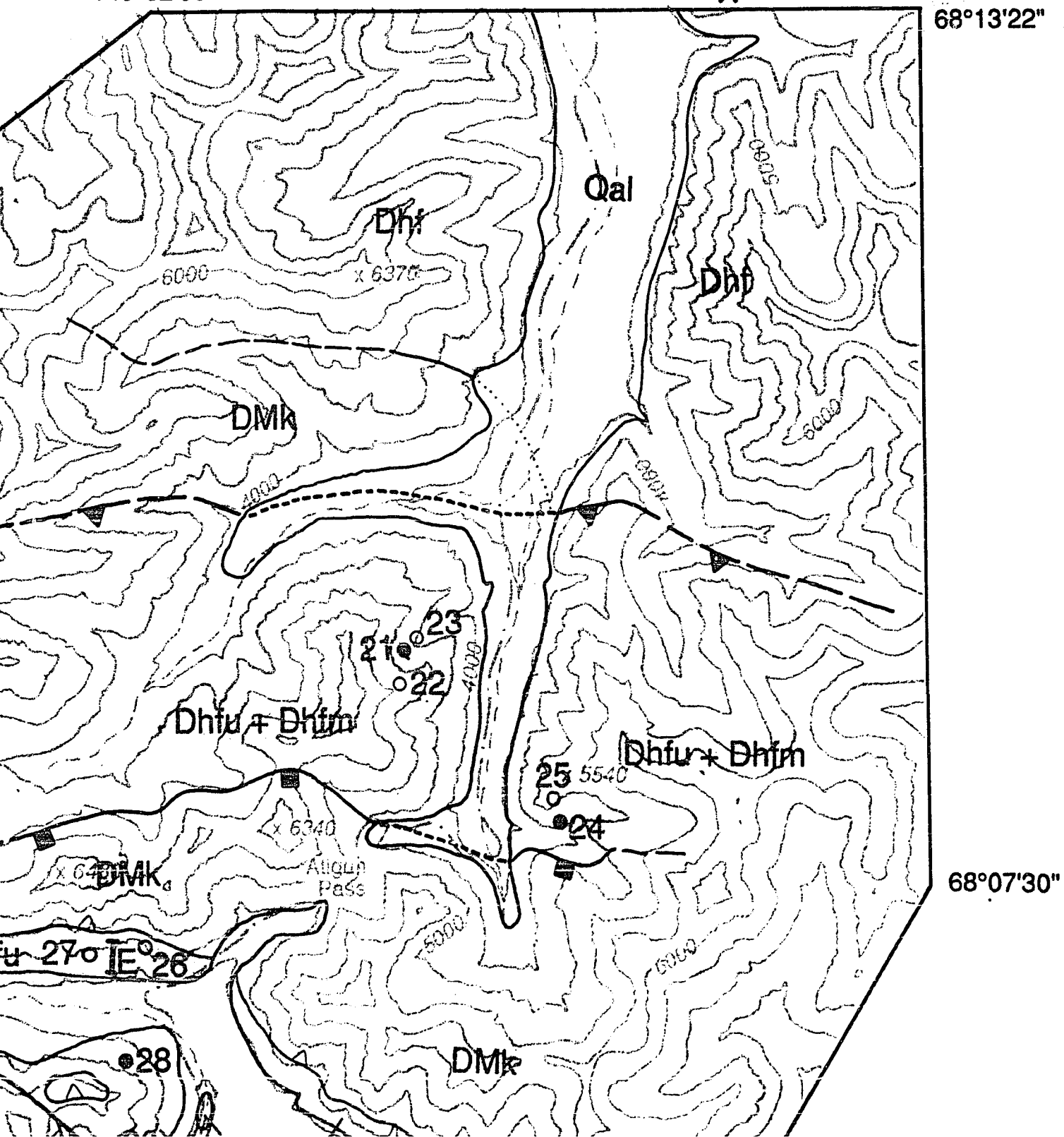


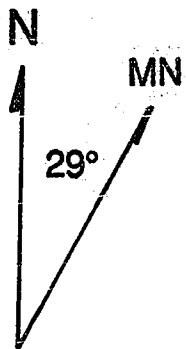
y



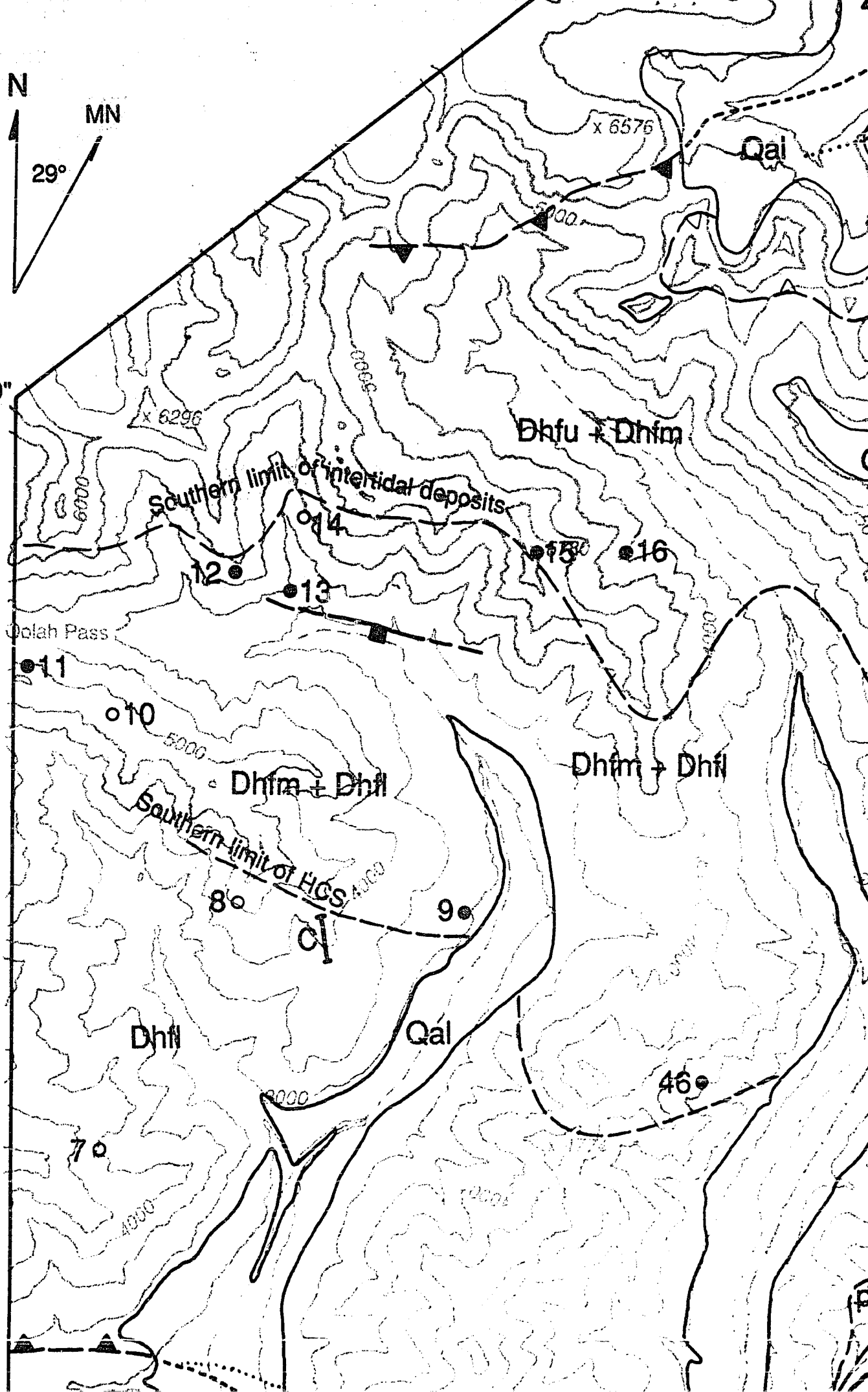
X

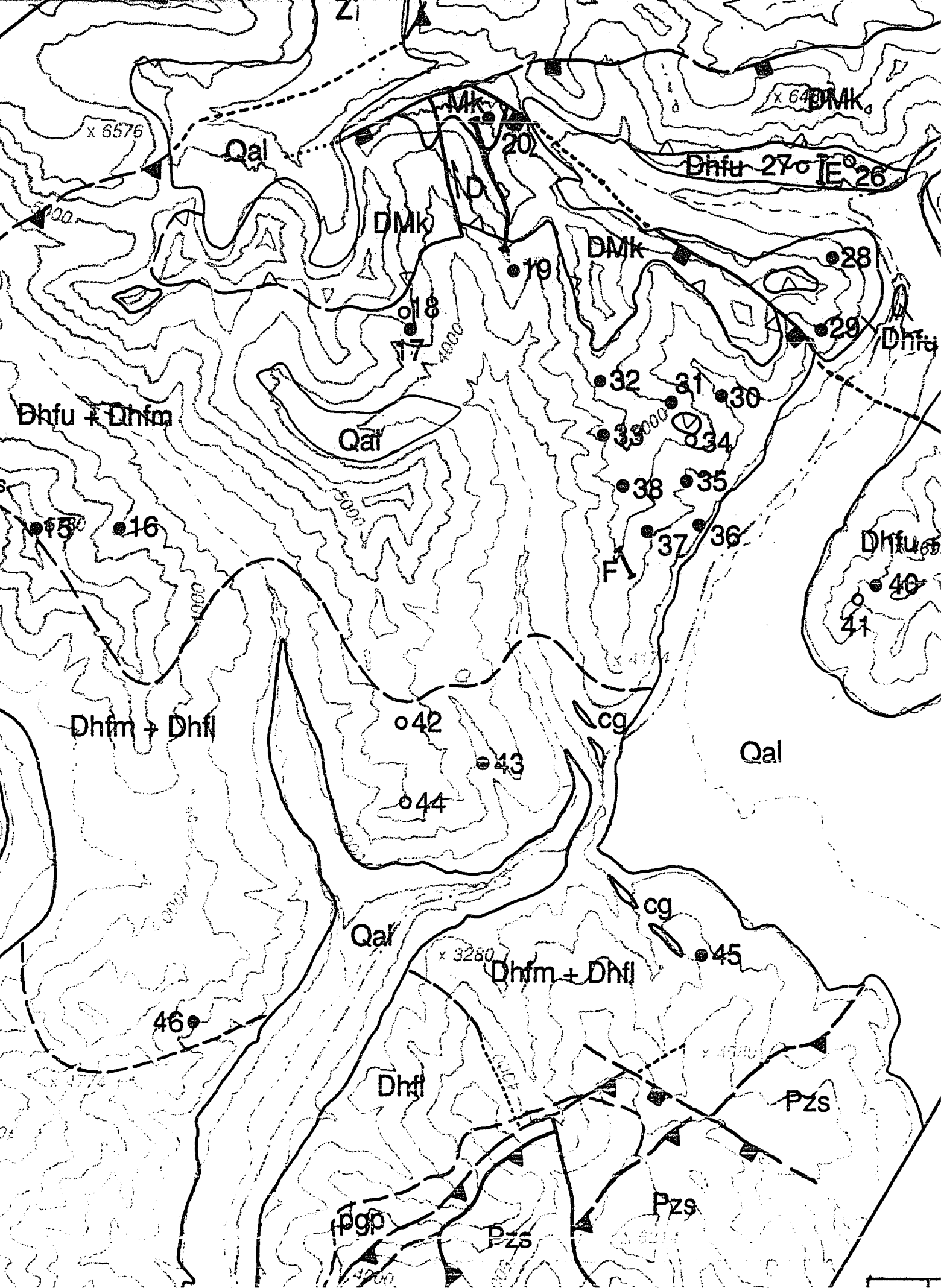
68°13'22"

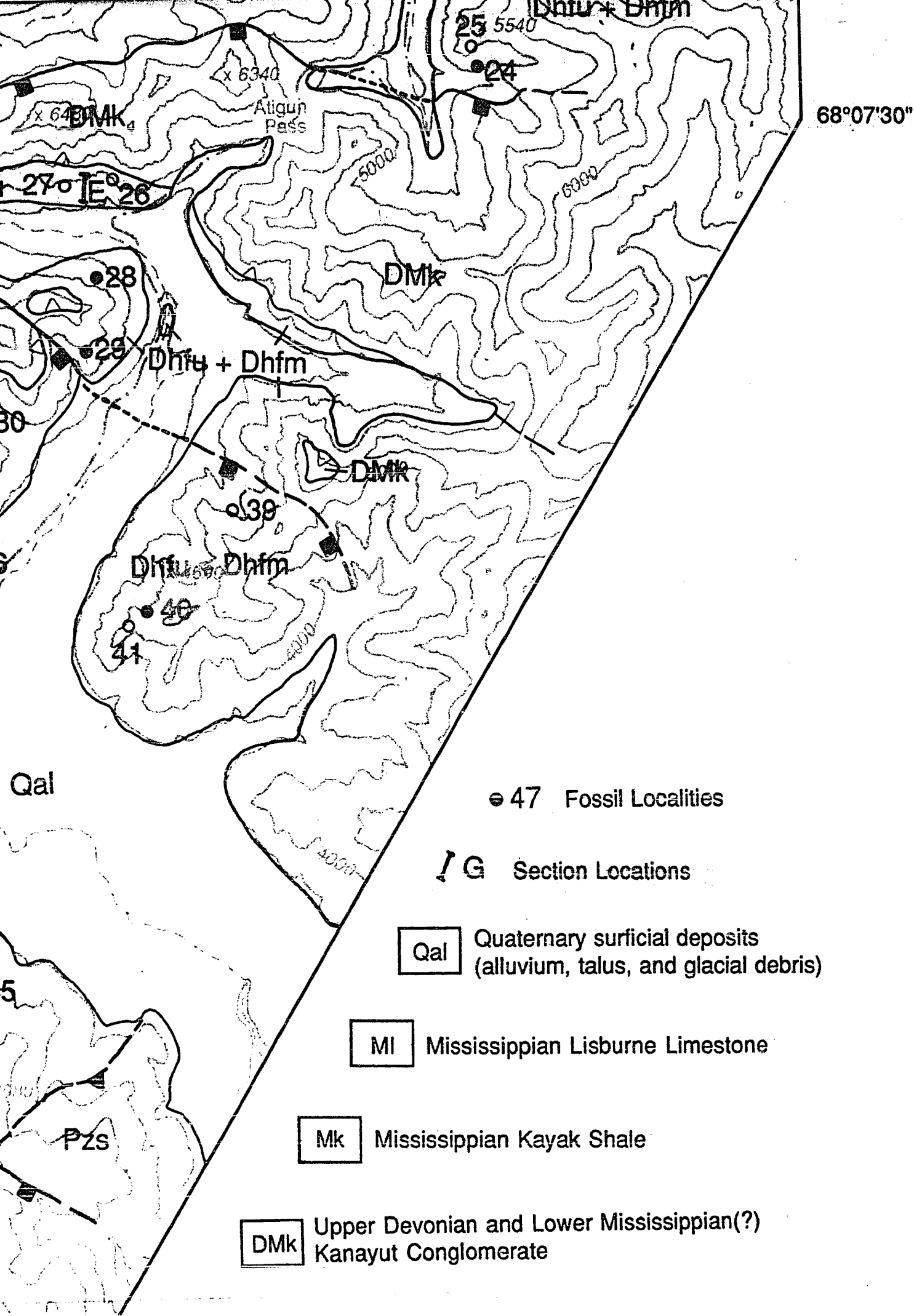




68°05'30"







● 47 Fossil Localities

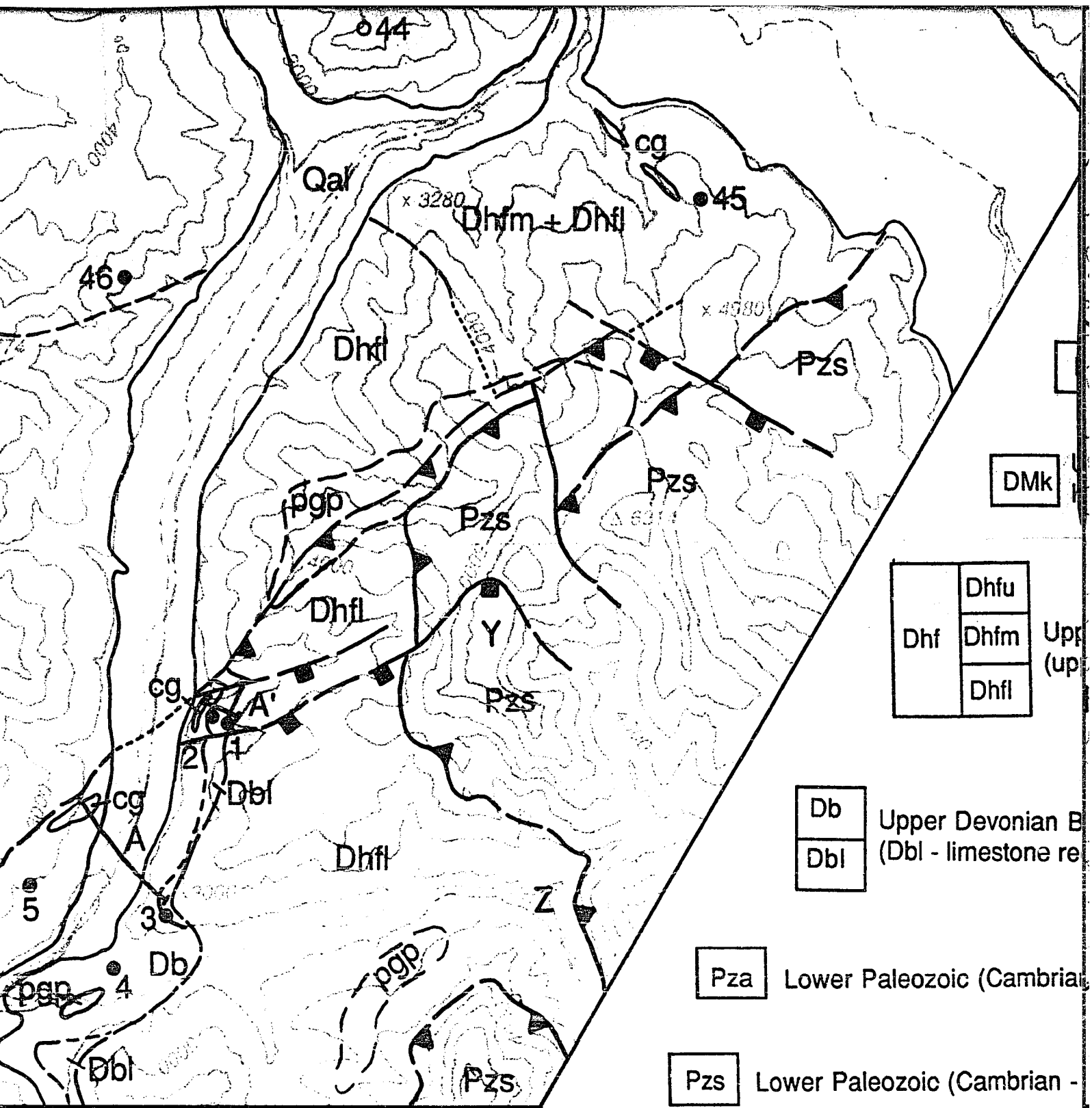
— G Section Locations

Qal Quaternary surficial deposits
(alluvium, talus, and glacial debris)

MI Mississippian Lisburne Limestone

Mk Mississippian Kayak Shale

DMk Upper Devonian and Lower Mississippian(?)
Kanayut Conglomerate

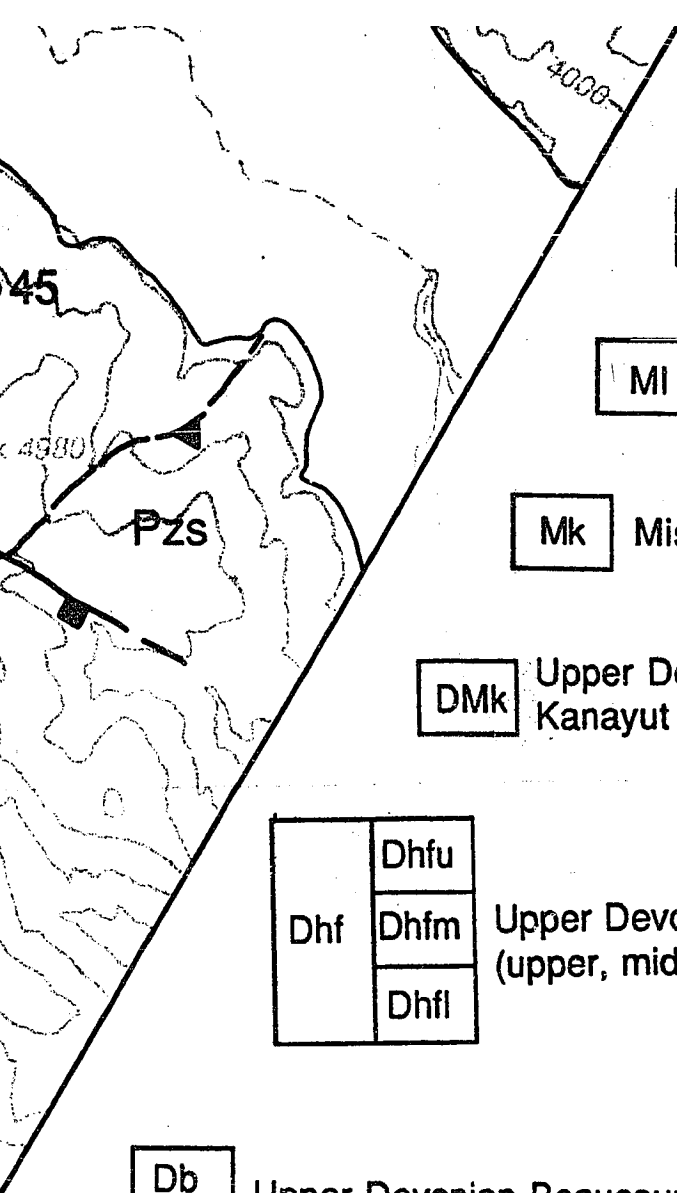


149°39'00"

pgp - purple and green phyllite

 Thrust Fault

 Normal Fault



I G Section Locations

Qal Quaternary surficial deposits
(alluvium, talus, and glacial debris)

MI Mississippian Lisburne Limestone

Mk Mississippian Kayak Shale

DMk Upper Devonian and Lower Mississippian(?)
Kanayut Conglomerate

Dhf	Dhfu	Upper Devonian Hunt Fork Shale (upper, middle, and lower members)
	Dhfm	
	Dhfl	

Db	Upper Devonian Beaucoup Formation (Dbl - limestone reefs)
Dbl	

Pza Lower Paleozoic (Cambrian - Silurian) Apoon Assemblage

Pzs Lower Paleozoic (Cambrian - Middle Devonian) Skajit allochthon

O - purple and green phyllite

cg - conglomerate

PLEASE NOTE:

Oversize maps and charts are filmed in sections in the following manner:

LEFT TO RIGHT, TOP TO BOTTOM, WITH SMALL OVERLAPS

The following map or chart has been refilmed in its entirety at the end of this dissertation (not available on microfiche). A xerographic reproduction has been provided for paper copies and is inserted into the inside of the back cover.

Standard 35mm slides or 17" x 23" black and white photographic prints are available for an additional charge.

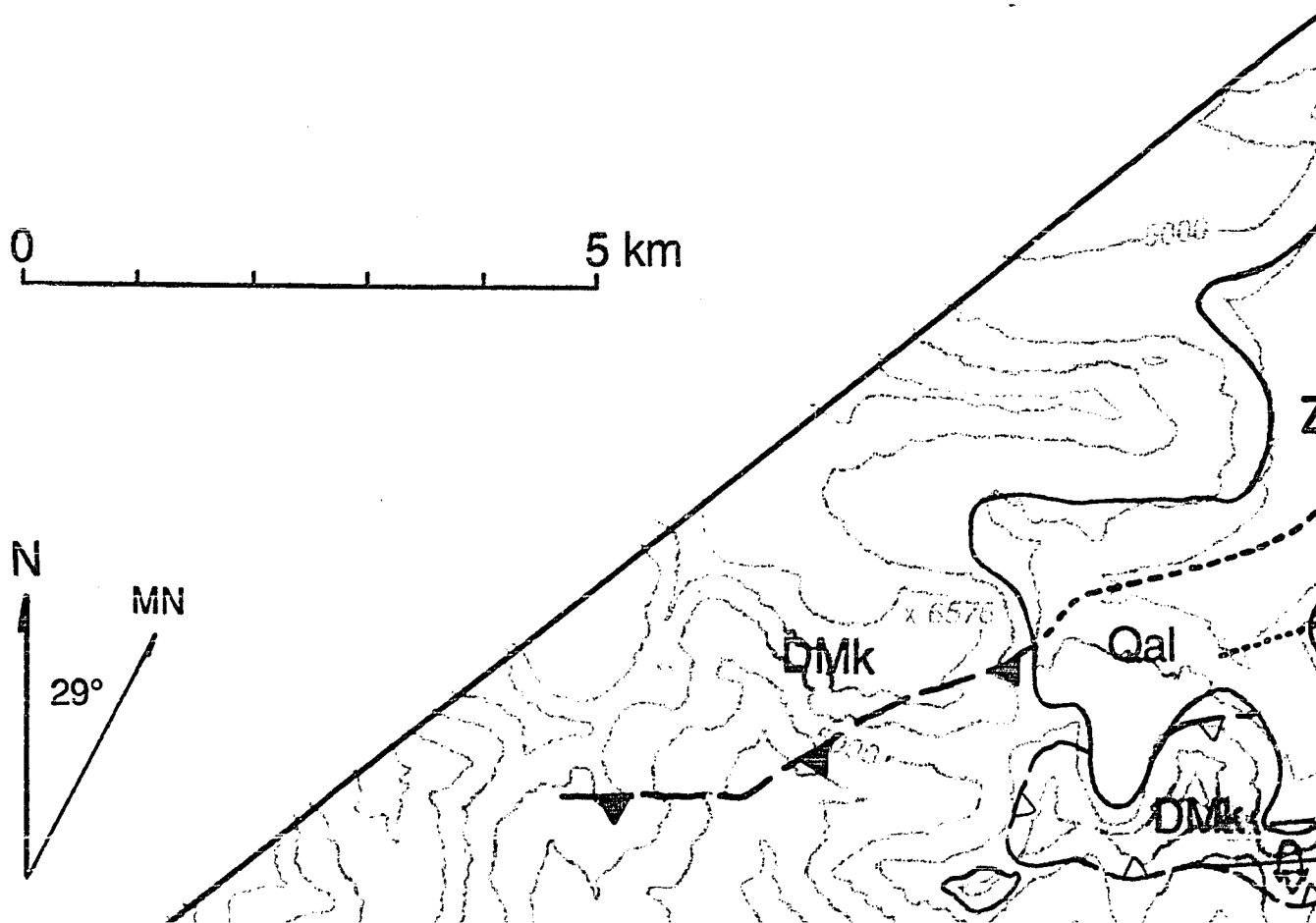
U·M·I

Plate 2

Geology of the southern Endicott Mountains Allochthon, central Brooks Range, Alaska

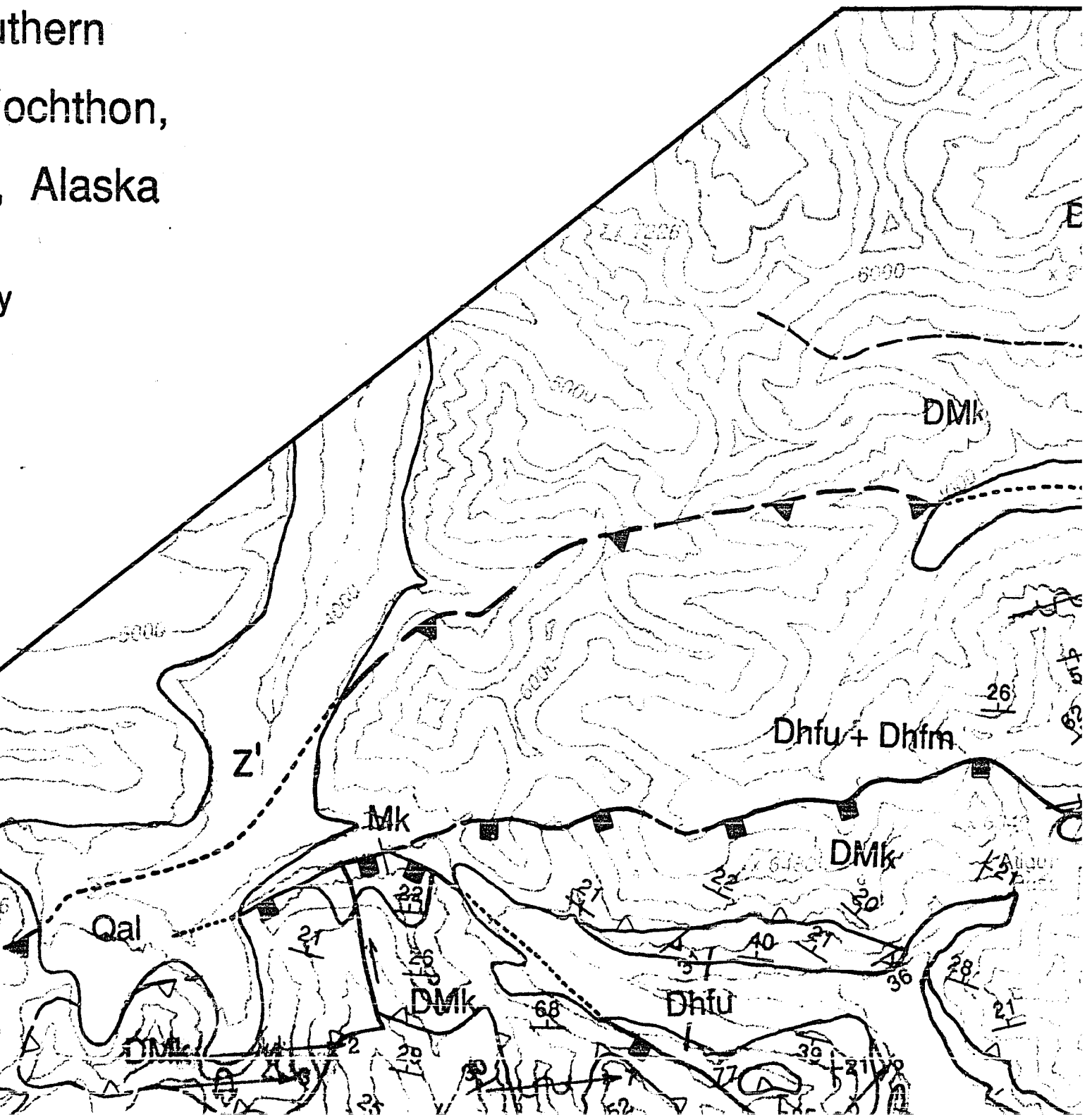
James W. Handschy

Rice University



thern
ochthon,
Alaska

149°32'00"

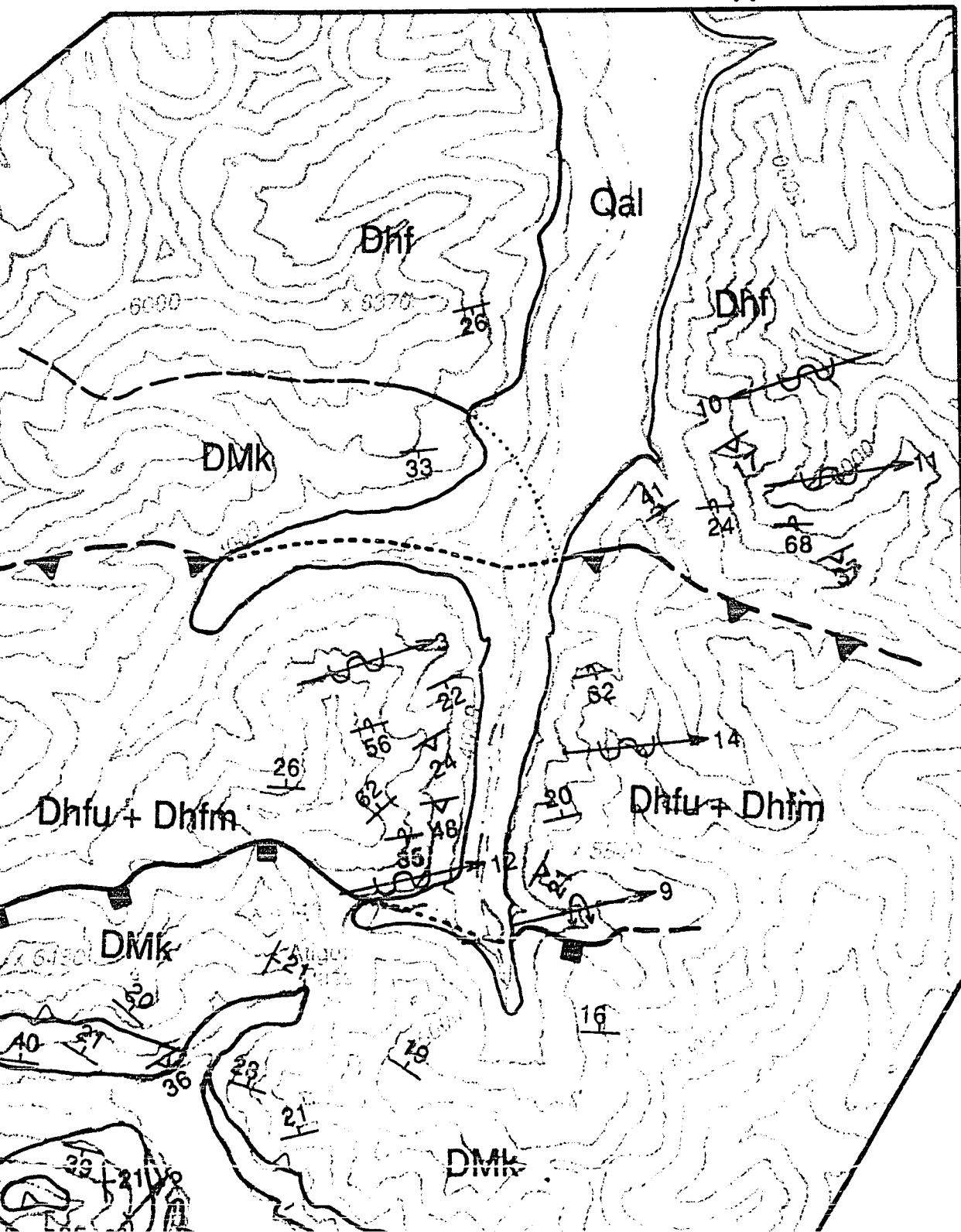


149°32'00"

X'

149°18'30"

68°13'22"

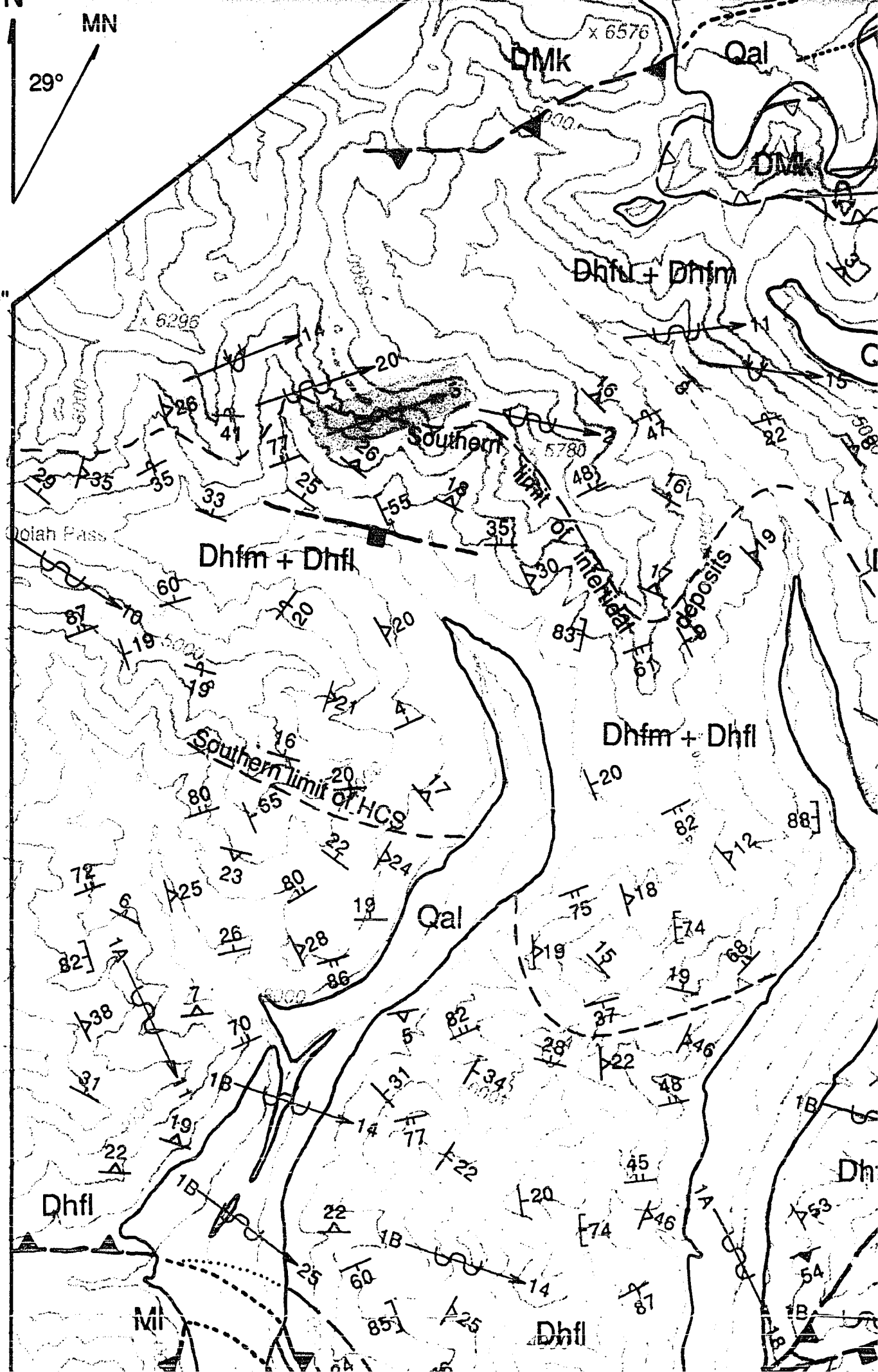


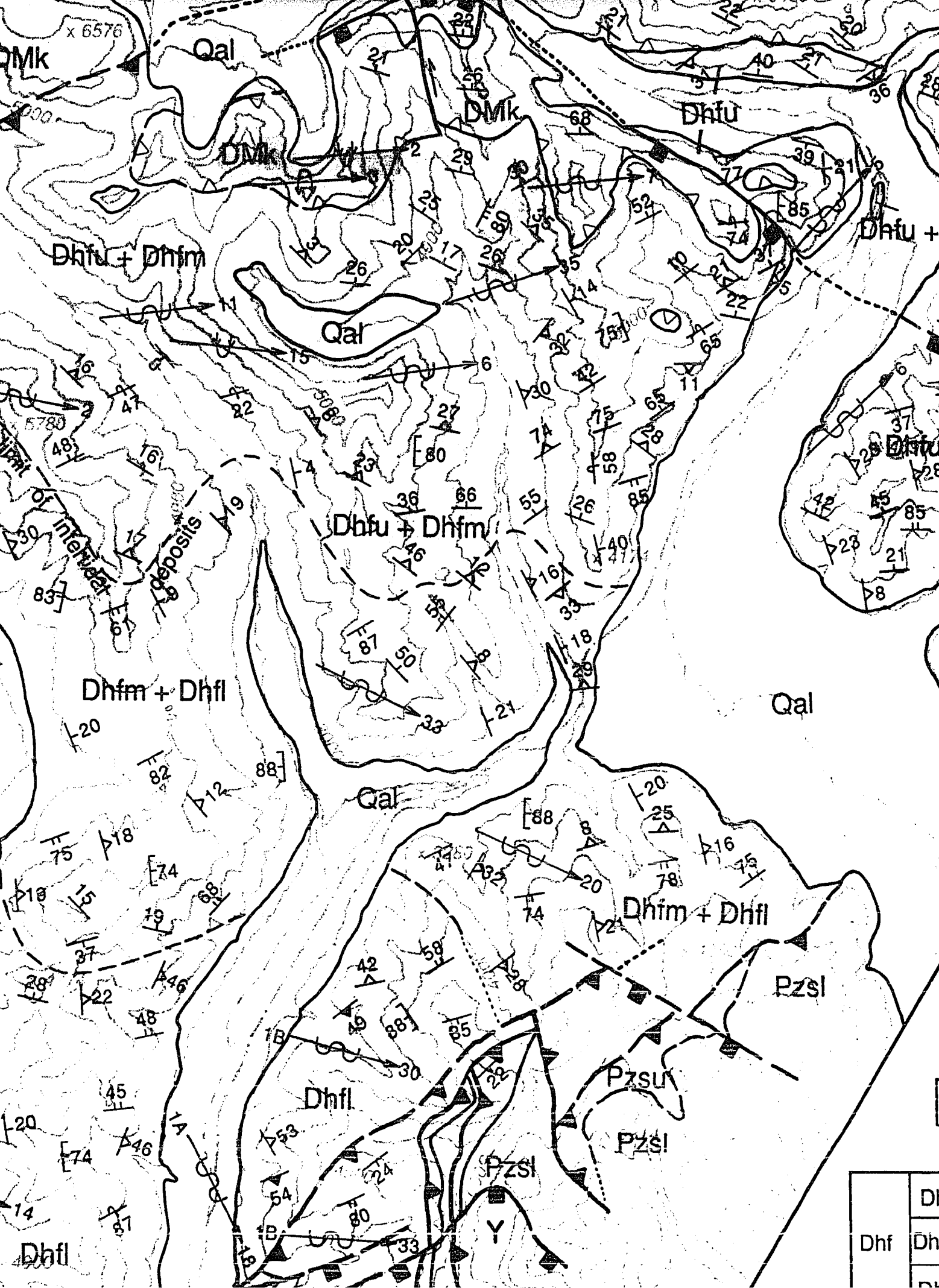
68°07'30"

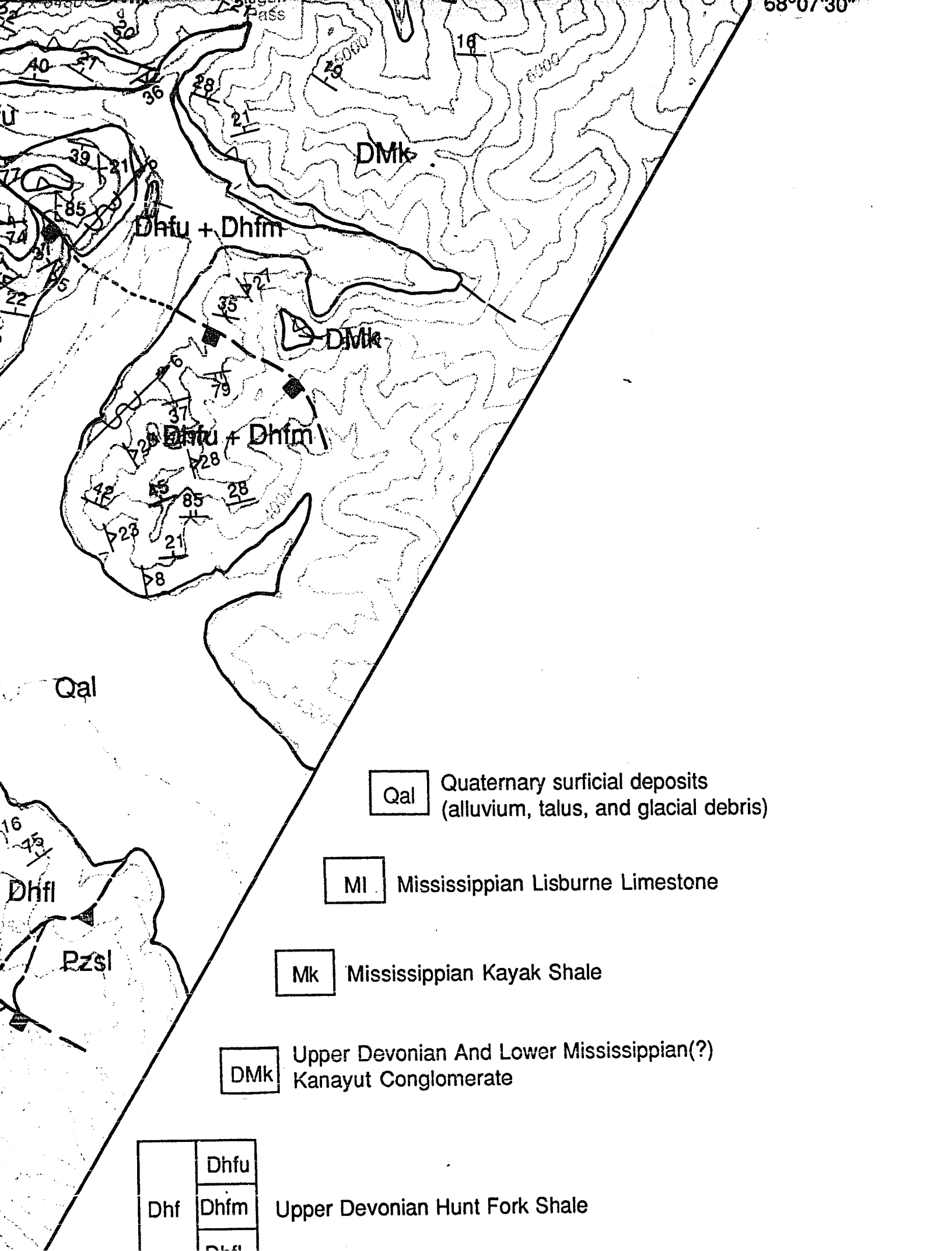
MN

29°

68°05'30"







Qal Quaternary surficial deposits
(alluvium, talus, and glacial debris)

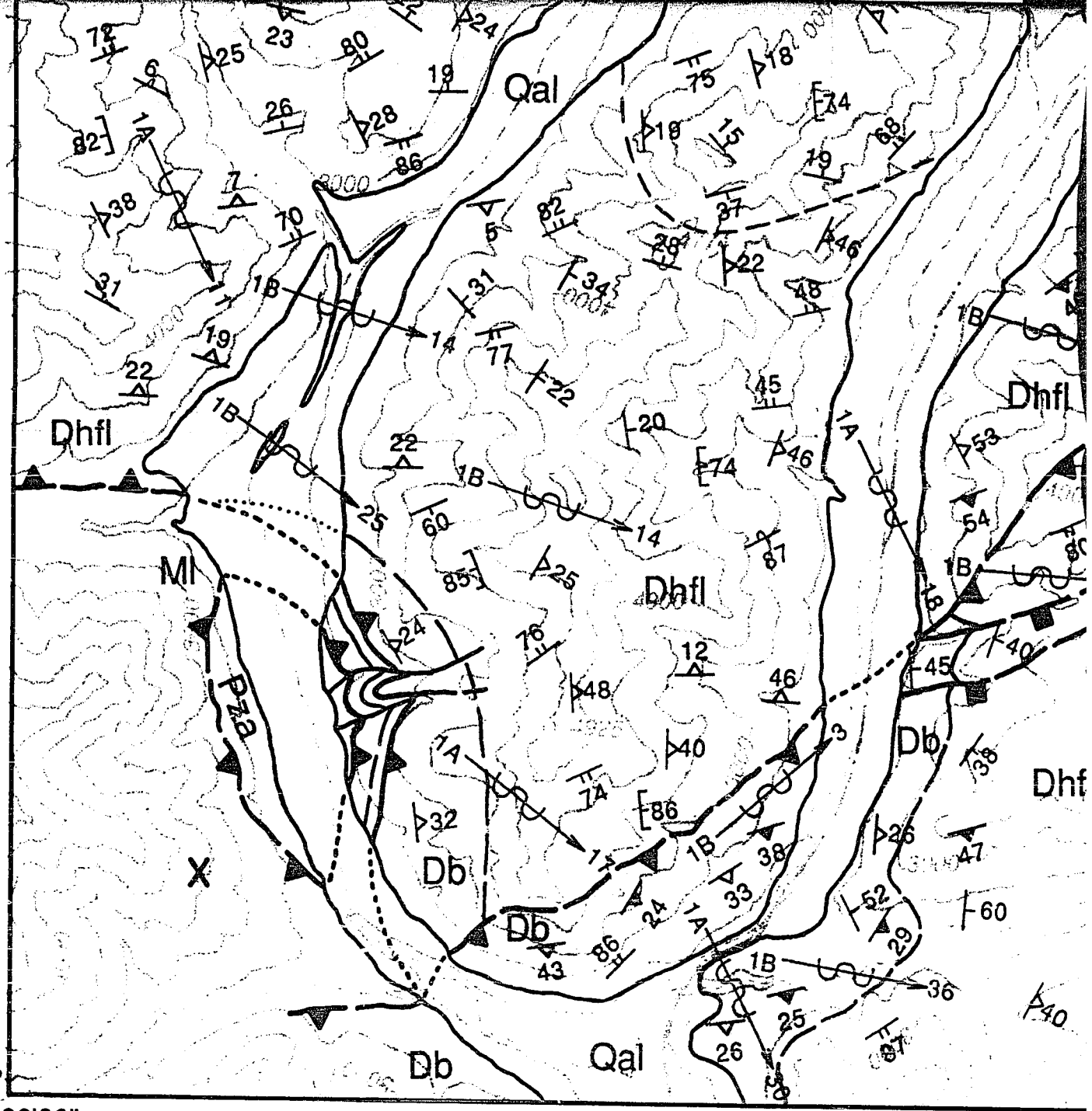
MI Mississippian Lisburne Limestone

Mk Mississippian Kayak Shale

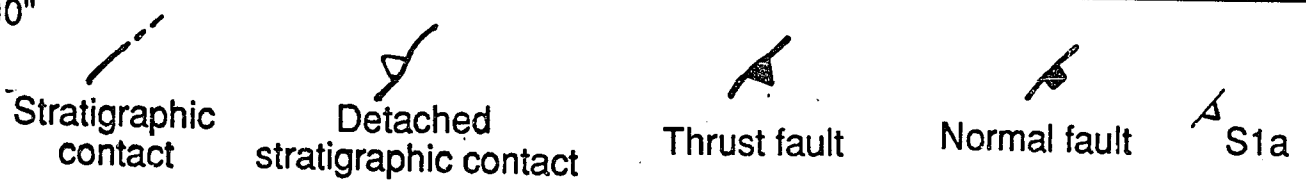
DMk Upper Devonian And Lower Mississippian(?)
Kanayut Conglomerate

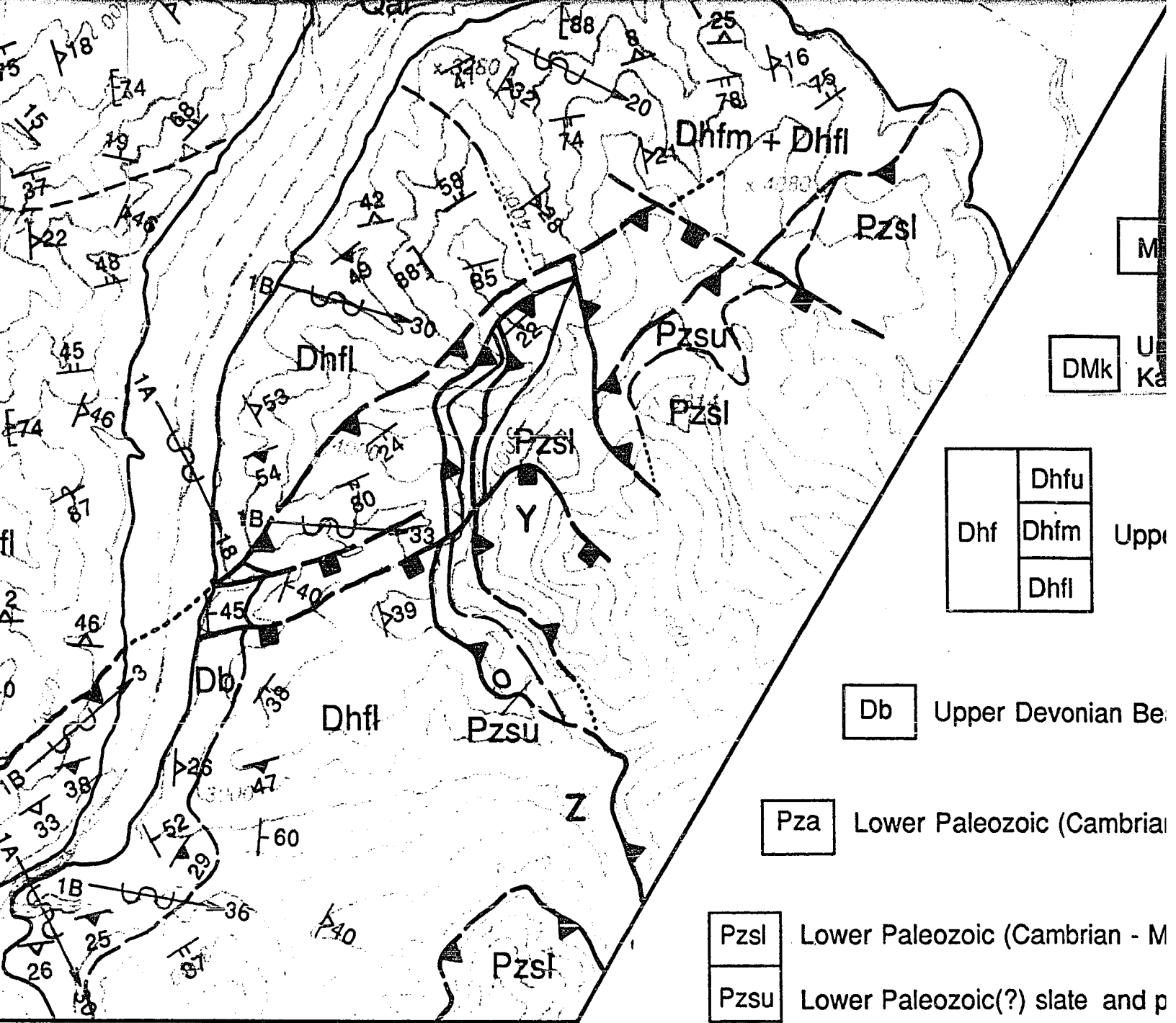
	Dhfu
Dhf	Dhfm
	Dhfl

Upper Devonian Hunt Fork Shale

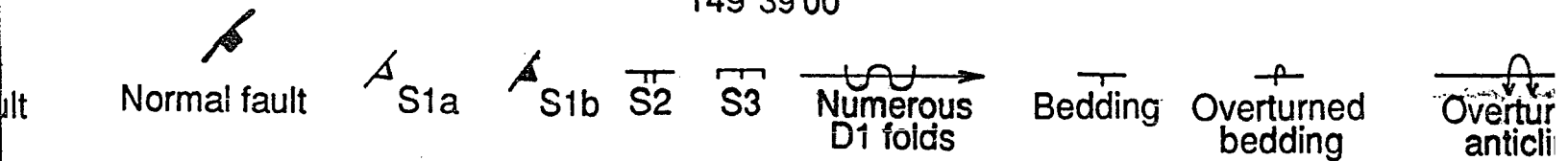


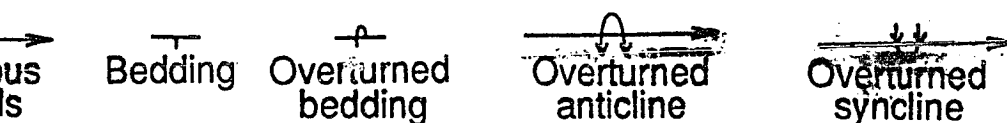
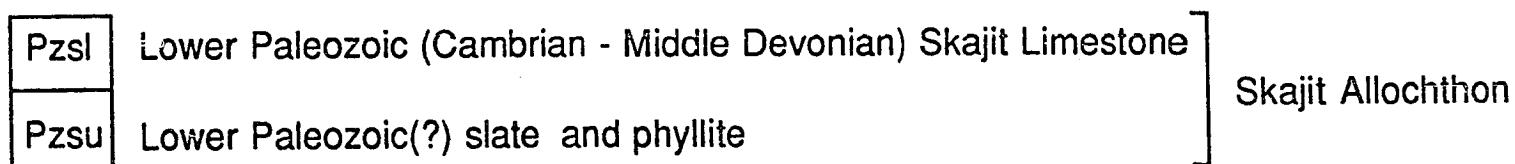
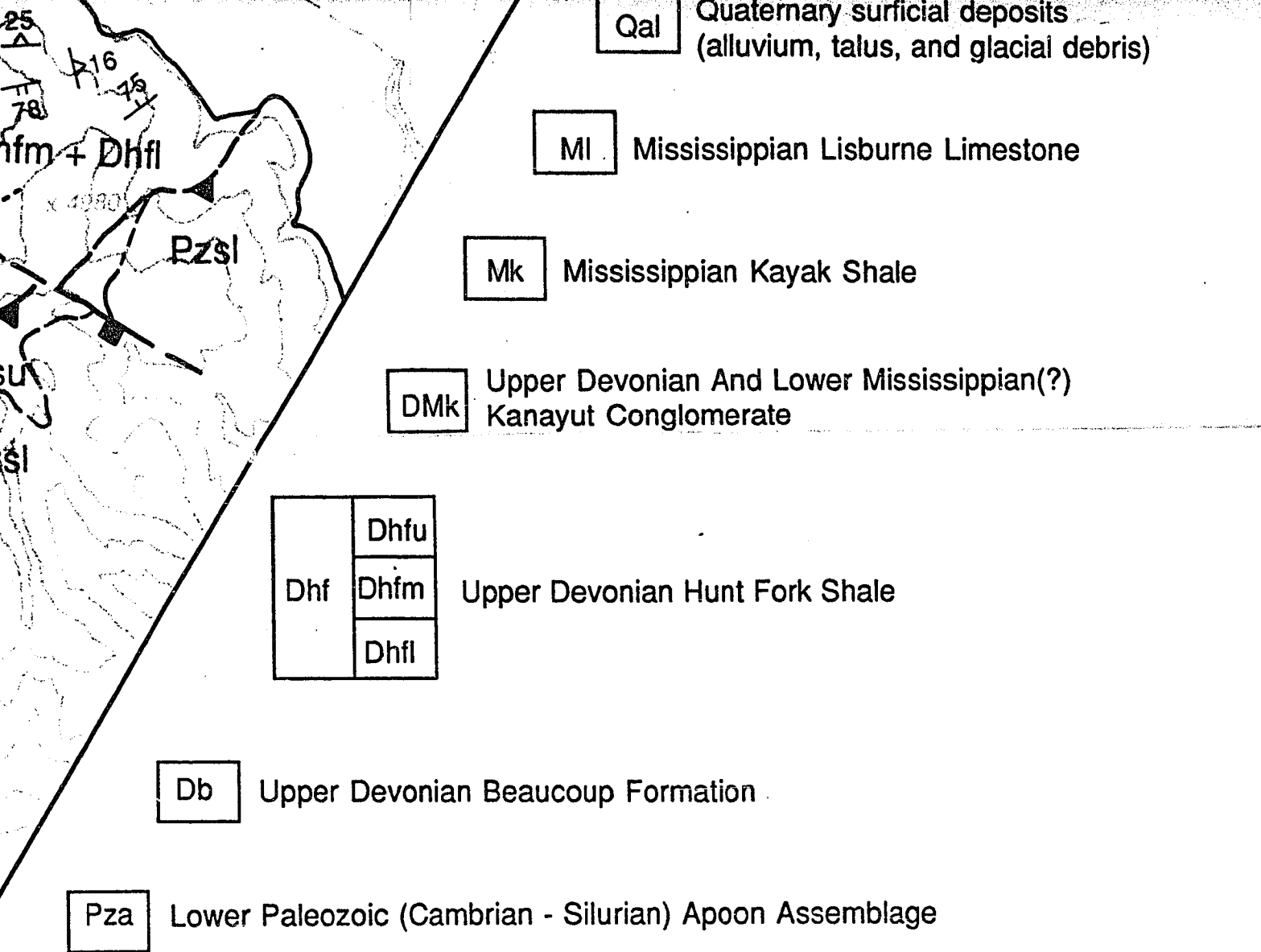
67°55'30"
150°00'00"





149°39'00"





PLEASE NOTE:

Oversize maps and charts are filmed in sections in the following manner:

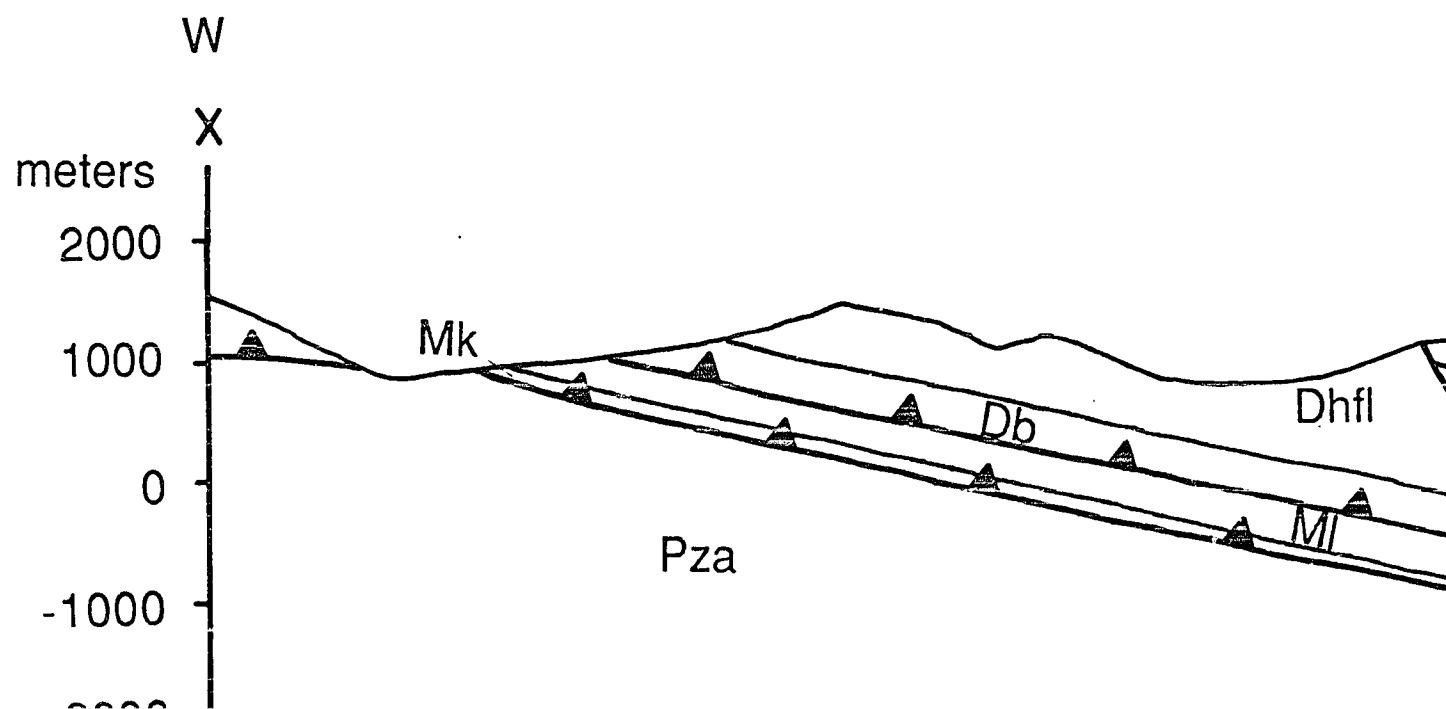
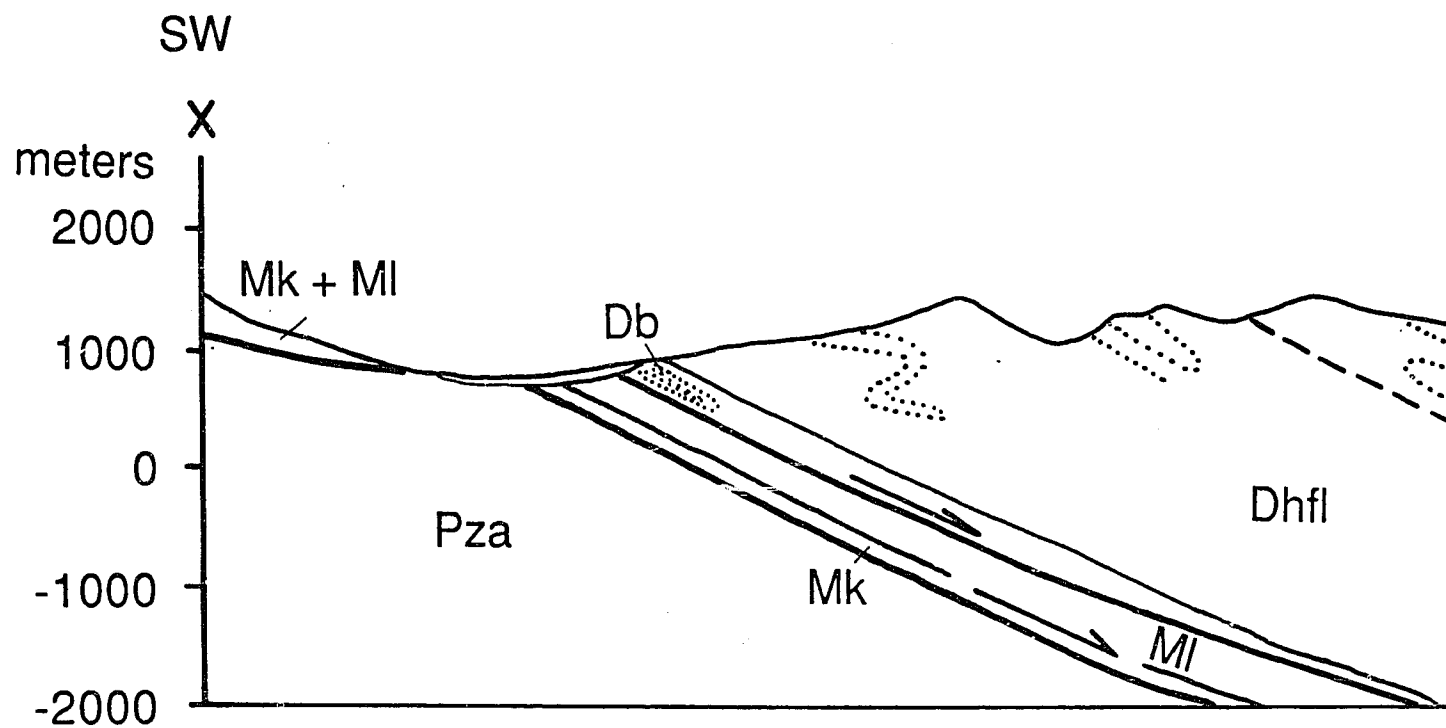
LEFT TO RIGHT, TOP TO BOTTOM, WITH SMALL OVERLAPS

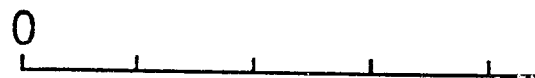
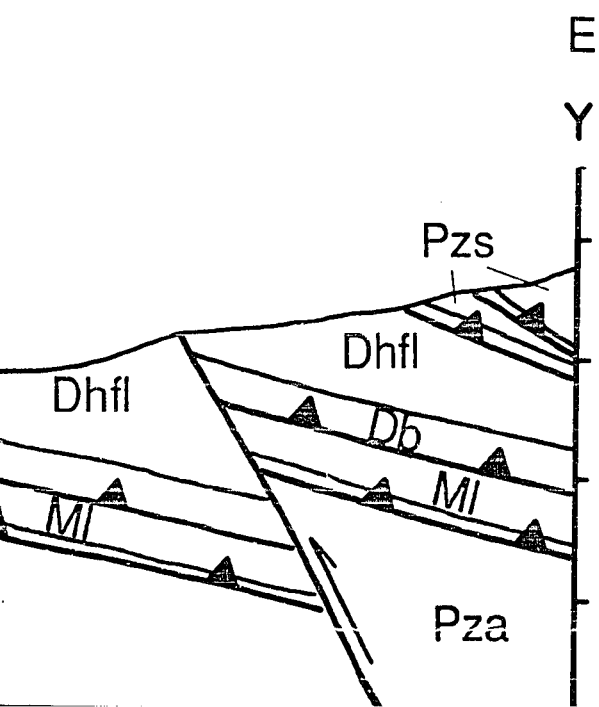
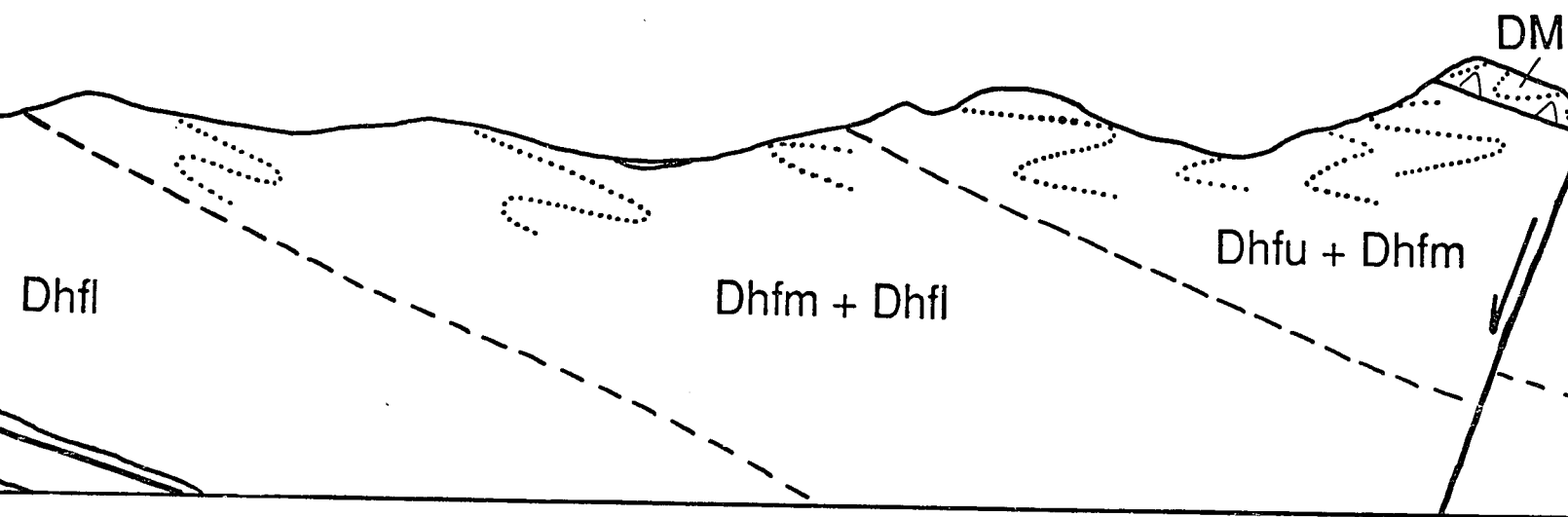
The following map or chart has been refilmed in its entirety at the end of this dissertation (not available on microfiche). A xerographic reproduction has been provided for paper copies and is inserted into the inside of the back cover.

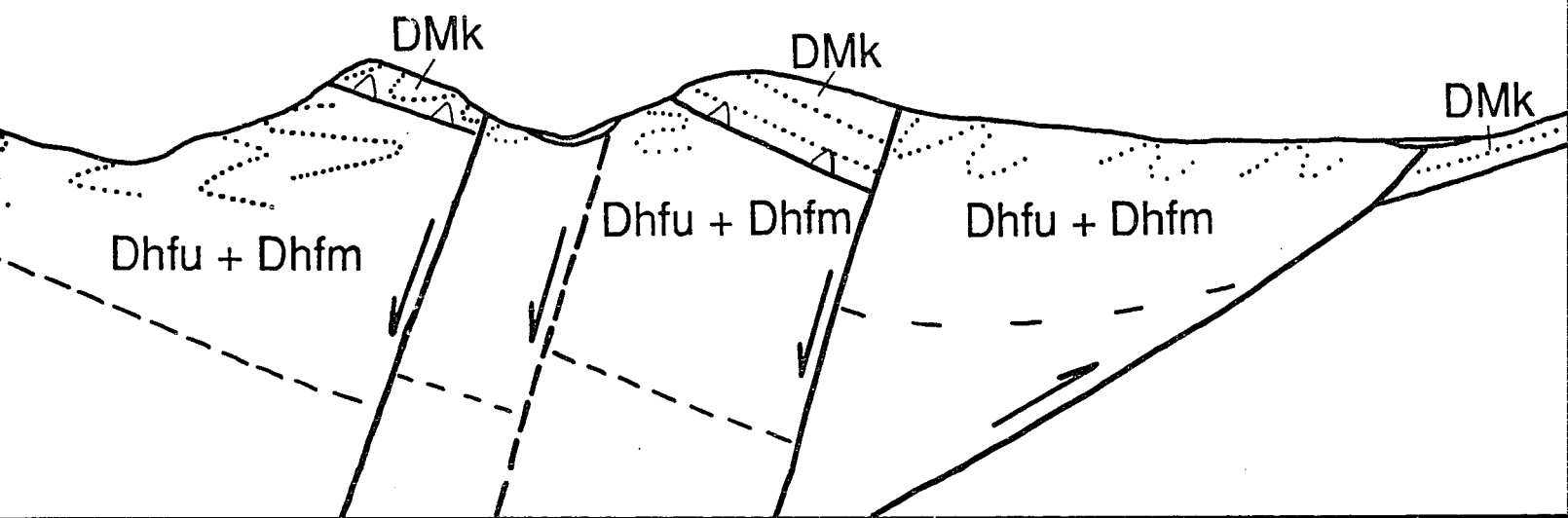
Standard 35mm slides or 17" x 23" black and white photographic prints are available for an additional charge.

U·M·I

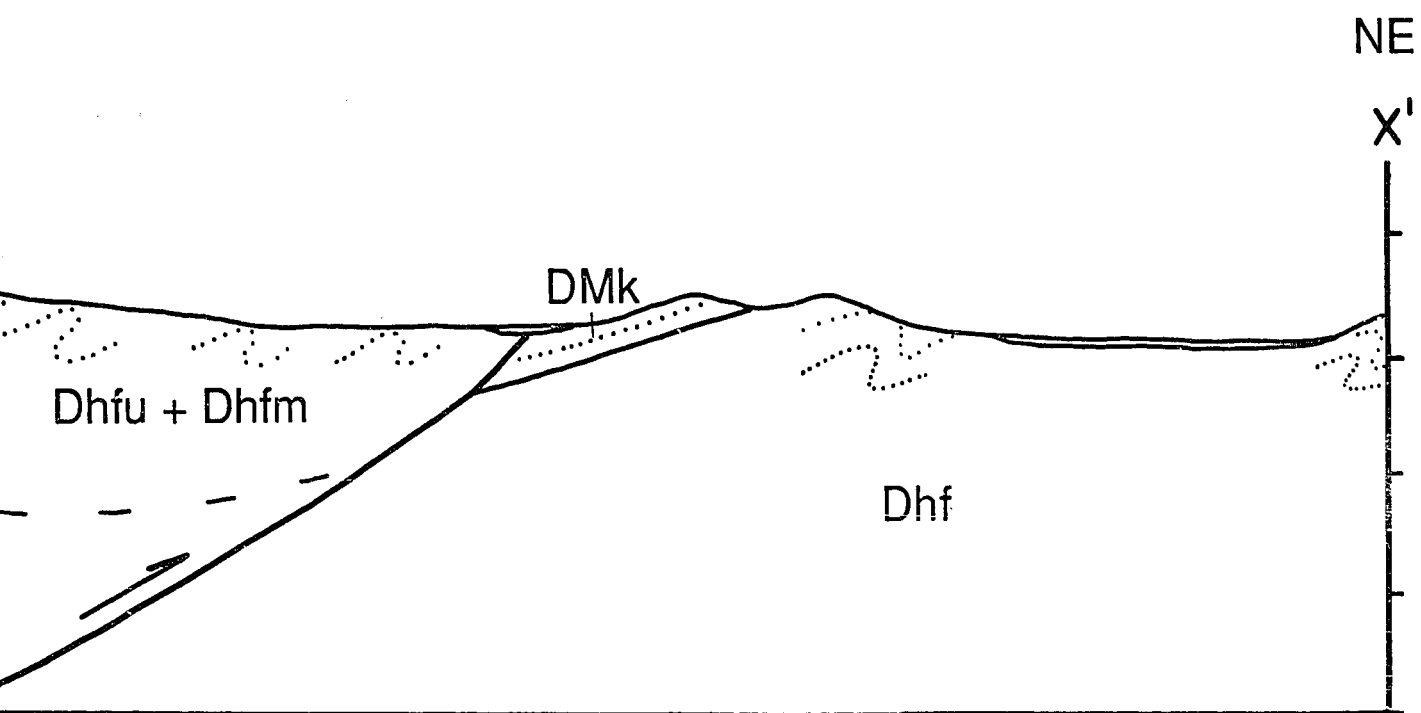
Plate 3

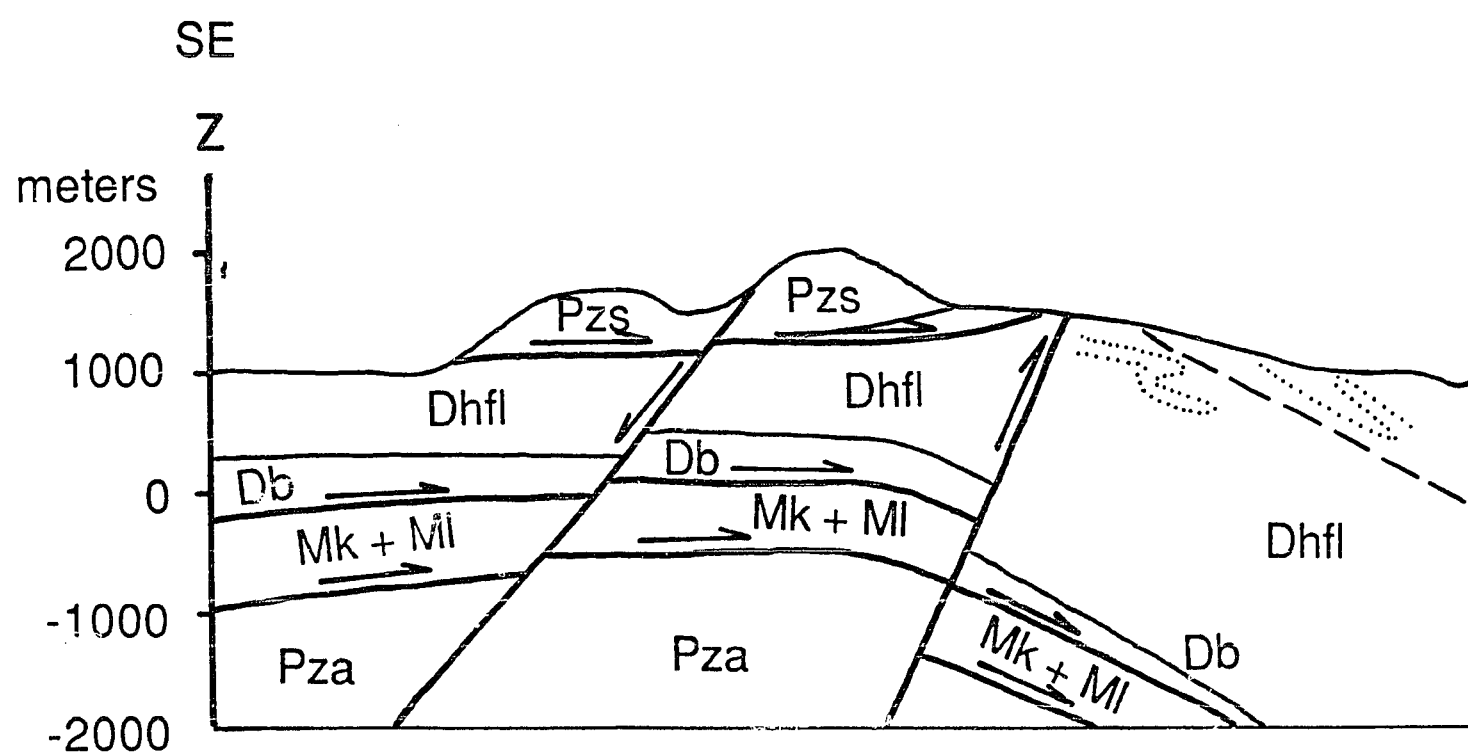
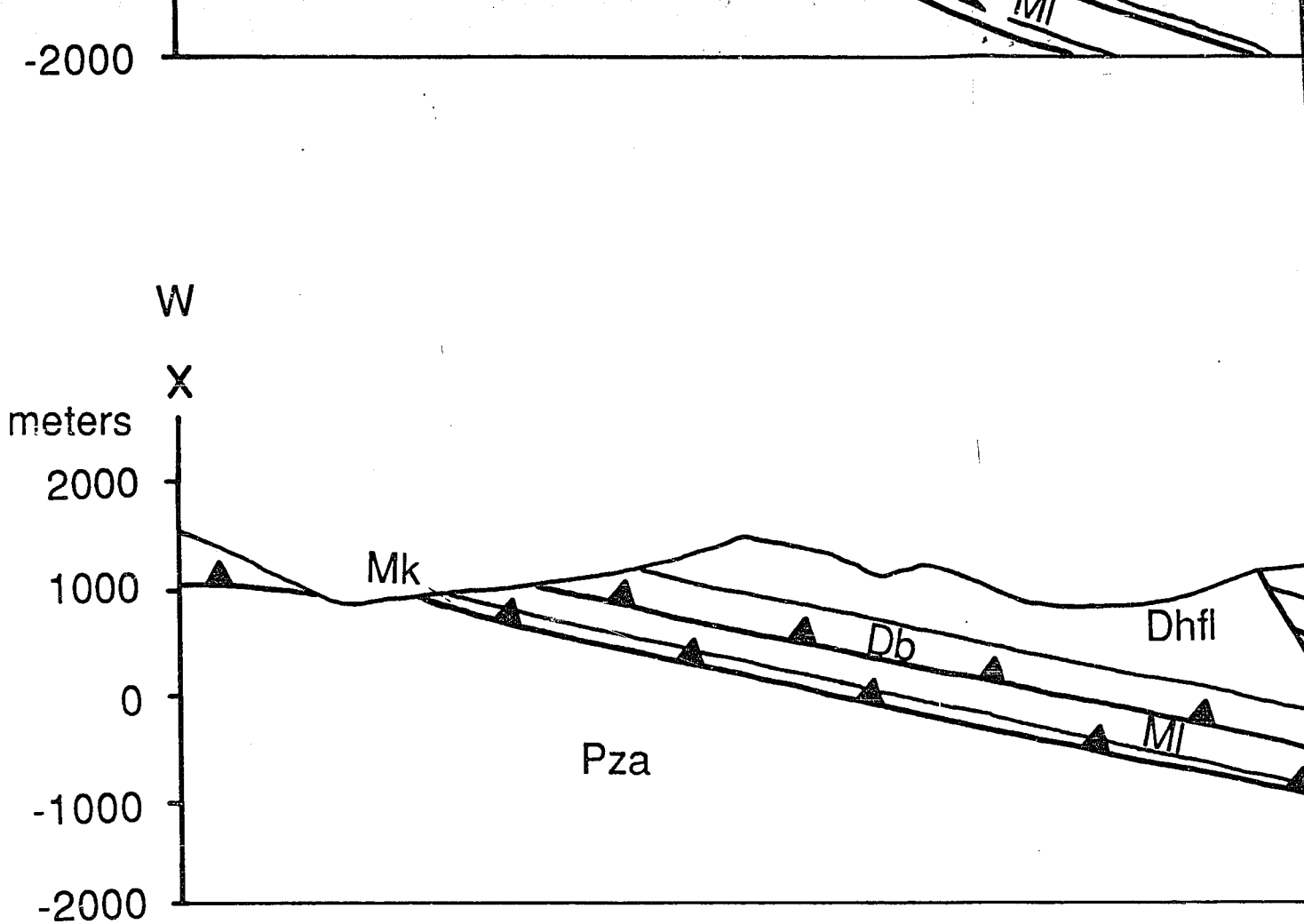


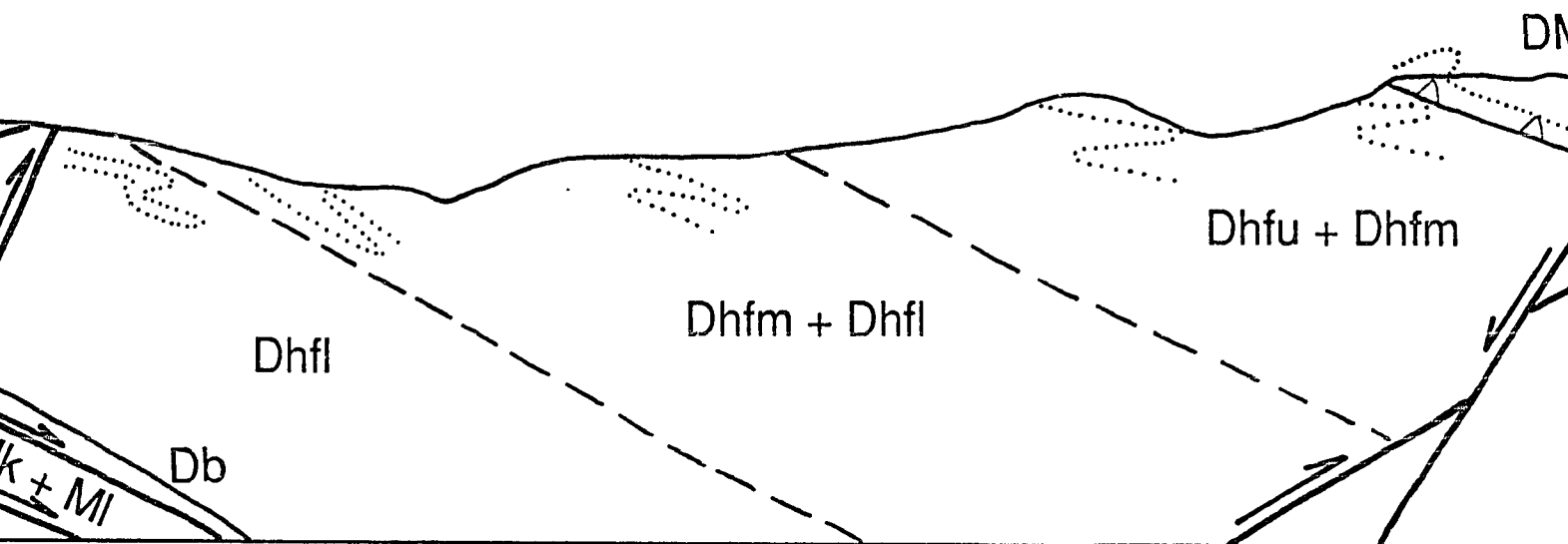
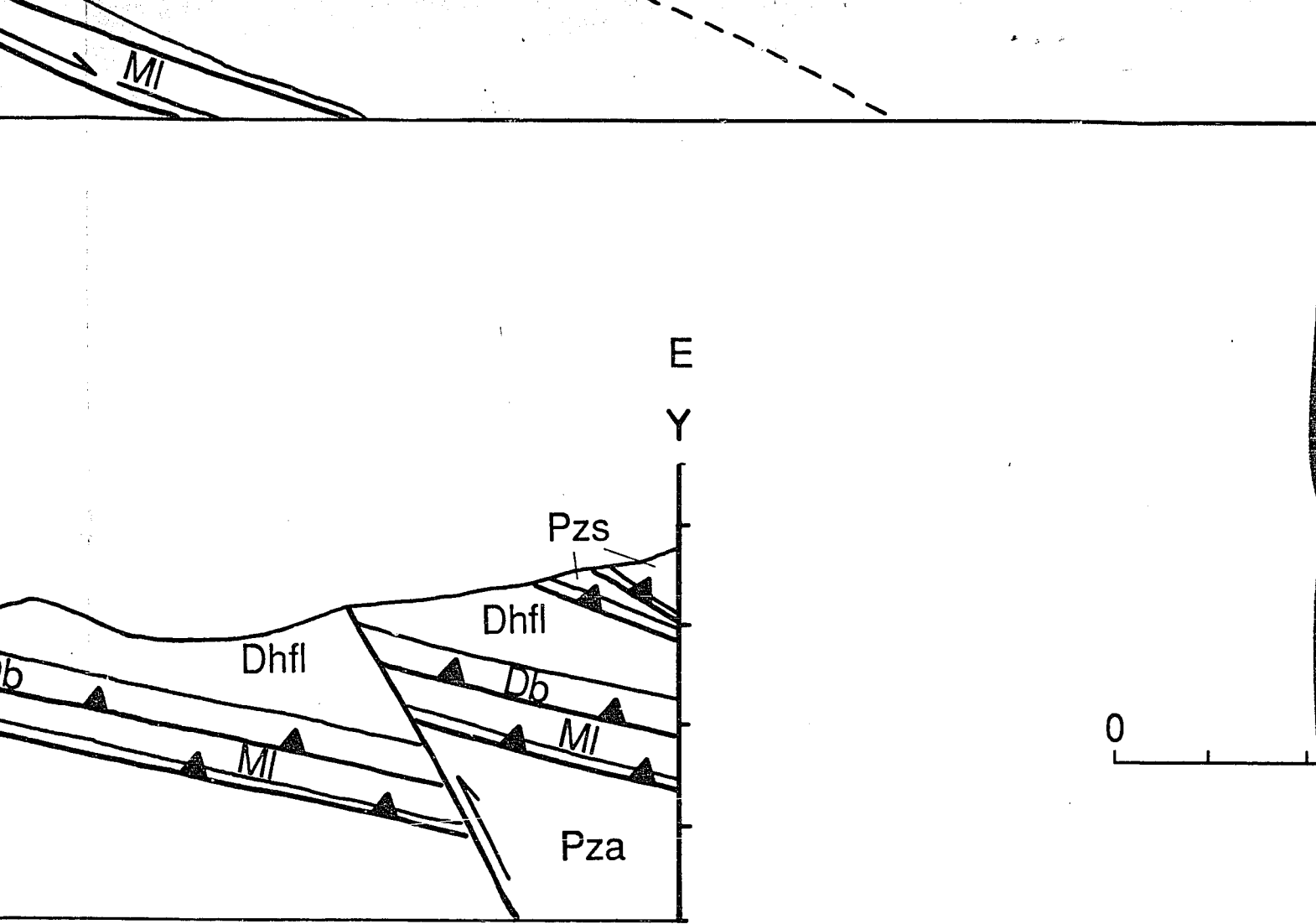


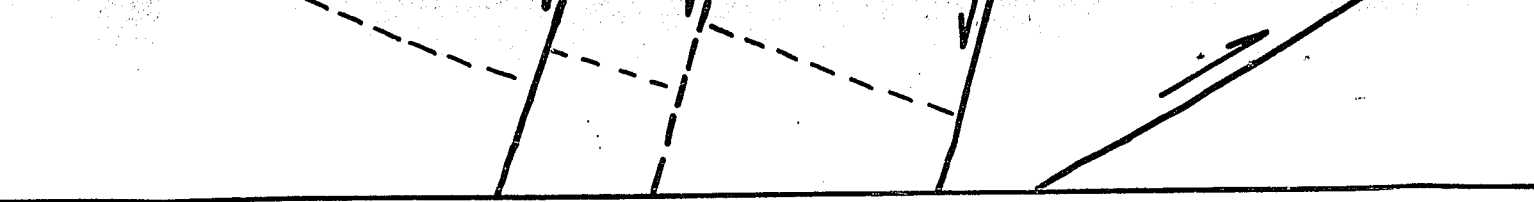


5 km

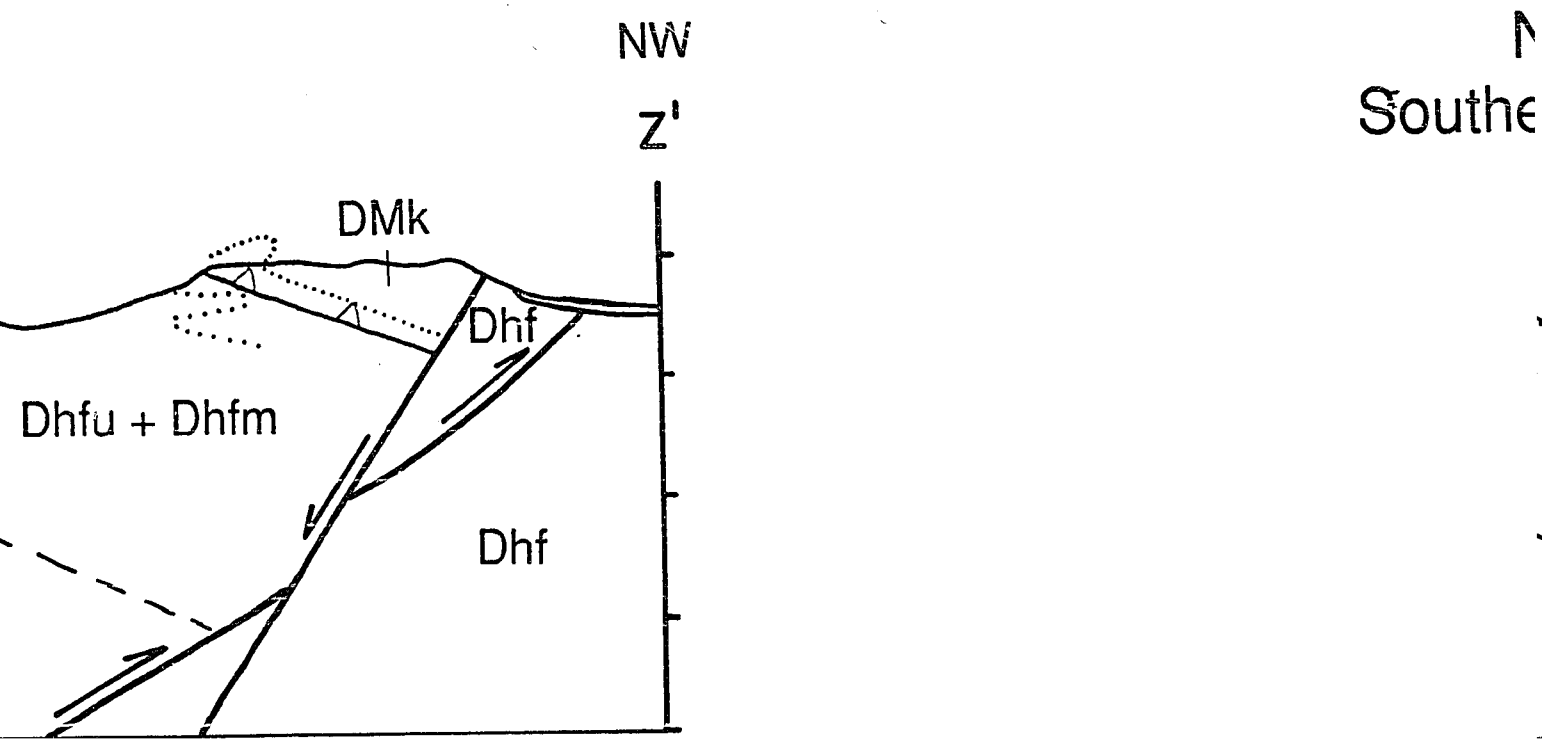








0 5 km





Dhf

Near-Surface Cross Sections Southern Endicott Mountains Allochthon

James W. Handschy

Rice University

PLEASE NOTE:

Oversize maps and charts are filmed in sections in the following manner:

LEFT TO RIGHT, TOP TO BOTTOM, WITH SMALL OVERLAPS

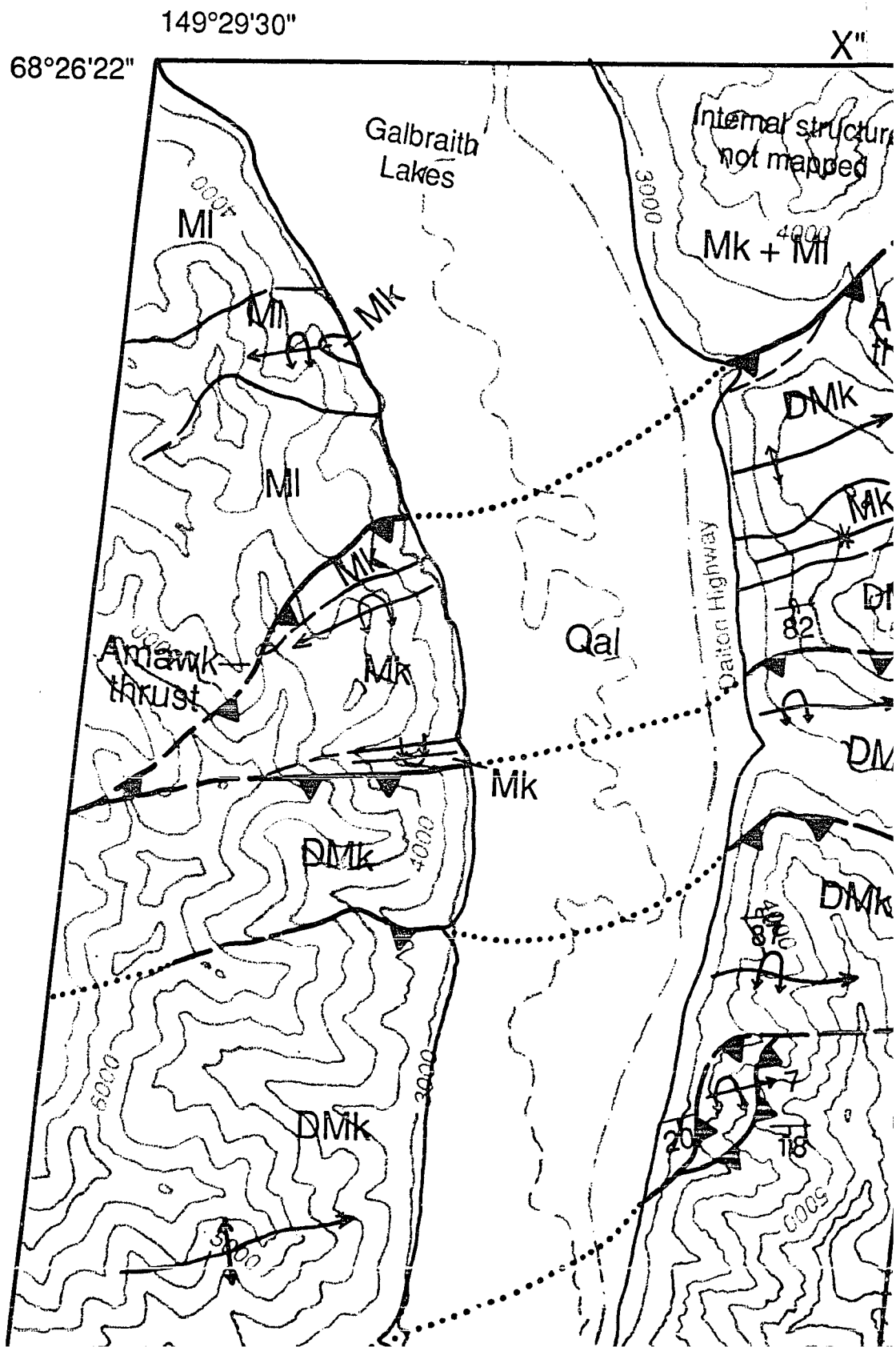
The following map or chart has been refilmed in its entirety at the end of this dissertation (not available on microfiche). A xerographic reproduction has been provided for paper copies and is inserted into the inside of the back cover.

Standard 35mm slides or 17" x 23" black and white photographic prints are available for an additional charge.

U·M·I

Plate 4

Geologic map and northern Endico Brooks Jam



James W. Handschy

